Hyperspectral Remote Sensing of Rice Agriculture for Field Scale Variability Mapping

Thesis submitted in partial fulfillment of the requirements for the degree of

Doctor of Philosophy

in

Civil Engineering

by

Shreedevi Moharana

Under the supervision of

Dr. Subashisa Dutta

Professor

Department of Civil Engineering
Indian Institute of Technology Guwahati
Guwahati – 781039, Assam, India
December, 2018

Dedicated to

My beloved
Parents
&
Grandparents

For their support, encouragement, love and laughter …

Acknowledgements

Pursuing a Ph.D. pogramme is just like climbing a high peak, step by step, accompanied with faith, encouragement, bitterness, hardships and with so many people's generous support. Today is the day: writing this note of thanks is the finishing touch on my dissertation. Though simple words will not be enough to express my gratitude to all those people who have supported and helped me so much throughout this endeavor. But in true spirit, I take this opportunity to remember and express my feelings of gratitude to those, whom I love, revere, and admire.Firstly, this journey would not have been possible, without the unconditional love, wholehearted support and profound encouragement of my mother, my father, my grandparents and above all my eternal cheerleaders – my beloved sisters, Lucky and Bugu. They shaped my vision and taught me the good things that really matter in life. Their relentless love, care, patience and sacrifice has always been my strength and inspiration.I extend my deepest gratitude to my supervisor Prof. Subashisa Dutta, Head of the Department of Civil Engineering, Indian Institute of Technology Guwahati, for being the guiding force behind my doctoral work. He provided me with every guidance, assistance, constructive suggestion, expertise and patience that I needed throughout this journey. He provided me intellectual freedom in my endeavors, and encouraged me to be innovative and creative. I simply cannot imagine a better adviser and mentor like him. Besides my advisor, I owe a deep sense of gratitude to the Chairman of my Doctoral Committee Dr. Bimlesh Kumar, Associate Professor, Department of Civil Engineering, Indian Institute of Technology Guwahati, for his constant encouragement and indelible inspiration throughout the study. Furthermore, I would like to express my gratefulness to the members of my doctoral committee Dr. Manish Kumar Goyal, Assistant Professor, Department of Civil Engineering, Indian Institute of Technology Guwahati and Dr. Vinayak Kulkarni, Associate Professor, Department of Mechanical Engineering, Indian Institute of Technology Guwahati, for their insightful ideas, feedback and suggestions at various stages of the study. This helped me a lot to improve myself. Most importantly, this thesis would not have been possible without the constant help, assistance and

support of my dear labmates working in Geoinformatics laboratory, Department of Civil Engineering, Indian Institute of Technology Guwahati. They always listened to me, cheered me up and provided all possible help at the time of difficulties. A special thanks to Mr. L.N.V. Satish for his immense help and support throughout this period in conducting field experiments, handling of geospatial softwares and compilation of the thesis. I am very much thankful to Mr. Suman who responded so promptly to solve my difficulties in programming language and ArcGIS. A special thanks to my junior Mr. A. Anjaneyulu, for his fruitful assistance during weekly field visits, data collection and help at any time I needed during this study. I especially thank Mr. Vinay Chembolu for his valuable suggestions and directions. I would also like to thank Mr. Chandan Pradhan for his friendly cooperation and support. My sincere thanks to Dr. Amit Kumar Dubey, Mr. Arpit Chouksey, Mr. Md. Ikram and all other research scholars of Geoinformatics lab. Next, I would like to thank Mr. Bazal Hoque for helping me in my experimentation work, during field visits and data collection. Completing this work would have been all the more difficult were it not for the support and friendship provided by my close friends, Lipika, Sunita, Madhu, Geeti, Rupasree, Piya, Soumya, Jayanta, Suchismita, Pramit, Surya, Dr. Deepak and Dr. Prem Kumar. I express my gratitude for their unconditional friendship, love, care, support and patience throughout these years. I would like to acknowledge the love and support of my lovely brothers Bablu, Sonu, Rocky, Rishi, Omm and Gudu for their constant motivation. I am also deeply grateful to mother, father and Situ from my in-laws family for their love, affection and support. Last but not the least, a special thanks to my better half for his indefinite love and care. Above all, I owe it all to the Almighty for granting me the health, wisdom and strength to undertake this research task and enabling me to its completion.

December 04, 2018 Shreedevi Moharana

Declaration

I, Shreedevi Moharana, declare that this Ph.D. thesis entitled "Hyperspectral Remote Sensing of Rice Agriculture for Field Scale Variability Mapping" is carried out by me under the guidance of my supervisor.

I certify that:

1. This thesis is a presentation of my own original research work.
2. Any part of this thesis has not been submitted for any degree or diploma or any other qualification either in this institute or in any other university.
3. Whenever I have referred any published things or quotas from other resources, every effort has been clearly accredited by citing them in the text of the thesis work.
4. Wherever contributions of others are involved, I have acknowledged to indicate this clearly.
5. I confirm that the present thesis is free from plagiarism to the best of my knowledge and I take the whole responsibility if any complaint arises.
6. I also affirm that my supervisor is not in a position to check for any possible instance of plagiarism within this submitted work

Signature: ……

Date: ……

Department of Civil Engineering
Indian Institute of Technology Guwahati
Guwahati-781039, Assam, India

Prof. Subashisa Dutta
email: subashisa@iitg.ac.in
phone: +91-361-258 2415

Certificate

This is to certify that the thesis entitled **"Hyperspectral Remote Sensing of Rice Agriculture for Field Scale Variability Mapping"** submitted by **Shreedevi Moharana,** in partial fulfilment of the requirements for the award of the degree of Doctor of Philosophy, to the Indian Institute of Technology Guwahati, Assam, India, is a record of the original bonafide research work carried out by her under my supervision and guidance at the Department of Civil Engineering, Indian Institute of Technology Guwahati, Assam, India. The thesis work, in my opinion is worthy of consideration for the award of the degree of Doctor of Philosophy in Civil Engineering of the Institute. The work presented in this thesis have not been submitted in part or full to any other university or institute for award of any degree/diploma.

Date: December 04, 2018
Place: Guwahati

Prof. Subashisa Dutta

Abstract

Rice, a staple food for majority of world's population, is extensively cultivated in Asia. India is the world's second largest rice producing country after China and occupies the largest area of cultivation in the world. Though demand for rice is increasing with ever growing population in the country, its production is decreasing due to resource crunch like land, water and labor. Thus, food security in India as well as the world is at stake. Therefore, requirement of advanced farming practices like precision agriculture (PA) and site specific crop management (SSCM) in rice fields in India and other countries is a necessity. PA and SSCM offers potential solution for increased rice production in an efficient and cost-effective manner along with low environmental impact. PA and SSCM means managing the crop field on a spatial basis where there is a need to improve the nutrient requirement, reduce water stress, and manage crop failure due to insect and pest infestation. Advancement in remote sensing provides insights of these spatial variability in the field, thus farmers could avoid scouting and manage the rice fields where it is exactly needed using the help from global navigation satellite system (GNSS) and geographic information system (GIS).

In this study, an improved methodology is proposed to investigate crop growth under different nitrogen fertilizer treatments in an Indian rice agriculture system. *In-situ* measurements using a portable spectroradiometer were made from rice vegetation canopy in 72 plots, comprising of eight rice varieties under three nitrogen applications, i.e., 3 plots each x 8 varieties of rice x 3 different fertilizer application rate. Spectrometer reading at specific wavelengths could find essential information on chlorophyll amount difference being able to detect water stress. The effect of nitrogen application and varietal crop growth were found to be significant at critical wavelengths: $\rho_{550}, \rho_{560}, \rho_{655}, \rho_{750}, \rho_{755}, \rho_{780}, \rho_{810}, \rho_{840}, \rho_{900}, \rho_{920}, \rho_{1000}, \rho_{1010}, \rho_{1020}$. Using the significant bands (wavelengths), the vegetation indices were developed to discriminate crop vigor so that we would be able to determine spatial variability in water stress, nutrient deficiency, and pest/insect infestation. It was found that the developed vegetation indices, VI_1 and VI_2, performed well in discriminating the nutrient availability based on variable rate nitrogen treatments for most of the varieties as compared to universally used vegetation

indices like Normalized Difference Vegetation Index (NDVI) and Green Ratio Index (GRI).

From yield point of view, fundamental knowledge on intra-species variability and unique discrimination among vegetation species plays a major role in implementing crop fertilizer and irrigation management schemes. It is to be noted that different varieties of rice species (cultivars) yield differently, requires different amount of nutrients and water, and above all, they mature at different time. Thus, we hypothesized that remote sensing hyperspectral wavebands may not be able to detect the chlorophyll content in each variety of rice at the same significant wavelengths. To prove our hypothesis, we developed an advanced method-waveform classification followed by hierarchical agglomerative clustering technique to develop a pure spectral library for paddy crop with various species. It was found that waveform classification technique is able to capture the embedded noise in the collection of field hyperspectral data. By eliminating noise, a better spectral library for the rice genotypes for varying nitrogen applications was achieved. It was observed that the rice varieties got segregated from each other in most cases, except in few cases, where the varieties could not be distinguished.

Hyperspectral satellite imaging provides vital information for crop biophysical parameters estimation at specific significant wavebands. The spatial variability of paddy crop biophysical parameters (total chlorophyll and nitrogen content) at field scale is investigated using EO-1 Hyperion image from space platform. Chemical analysis was performed in the laboratory to quantify the chlorophyll, nitrogen and leaf relative water content. By exploiting the ground based measurements from 24 rice varieties, regression models were developed using chlorophyll and nitrogen as inputs and the corresponding vegetation index based digital values (DV). It was observed that our rice leaf nitrogen concentration (LNC) and the corresponding simple ratio (SR) DV based linear and nonlinear correlation results were completely different from the one published in Tian et al. (2011). At crop field level, the rice nitrogen content varied widely from 1-4% and only 2-3% by using present modified index models and Tian et al. (2011) respectively. The modified LNC index model performed better than the established Tian et al. (2011) model as far as the estimated nitrogen content from Hyperion imagery is concerned.

We have developed various indices, such as LNC, OSAVI, Gitelson, mSR and MTCI and correlated with the observed LNC and found good correlation, which explained the spatial variability of chlorophyll content in rice through the use of Hyperion imagery. In Indian agro climatic conditions, to understand the field scale seasonal variability of water stress for summer (rabi) and winter (kharif) rice, narrow band index models were developed by using temporal hyperspectral imagery during pre-monsoon and monsoon periods, respectively. It was found that spatial distribution of the leaf relative water content (LRWC), retrieved from NDWI-2, MSI, SRWI, NDII, SAWI-1, WI-Hyperion index regression models at the reproductive phase for summer rice agriculture system, is in close agreement with the *in-situ* LRWC variation. Whereas, NDWI-1, NDWI-2, NDII, SAWI-1, SAWI-2 index models performed well in mapping of LRWC with a wide variation in winter rice agriculture system.

To overcome the limitations of Hyperion data, we introduced a new methodology to incorporate critical hyperspectral narrow bands into multispectral high spatial resolution LISS IV data through index-based fusion approach. This study demonstrated that the proposed methodology was efficient to differentiate chlorophyll and nitrogen content variability at spatial (plot) scale within the rice field using hyperspectral images. Further, the synthetic hyperspectral critical/significant bands were derived by adopting band average and spectral shape function approaches. The critical bands are found significant from regression analysis between each of the critical bands and Hyperion bands lying in the broad band spectrum of the multispectral image with a high coefficient of determination ($R^2 > 0.95$). It is confirmed that, only those indices can be employed for the mapping of crop variability in which significant critical bands resulted from the above two approaches are implemented, rather than all the chlorophyll and nitrogen related vegetation indices. It is observed that the field heterogeneity is purely a function of field topography due to large-scale variations in soil moisture and water availability. It was concluded that the slope of the field controlled the variability attributed to small scale farming system in India.

Contents

List of Figures

List of Tables

List of Symbols

Symbols	Description
d	Distance between two entities
D_i	First derivative at i^{th} nm
D_j	First derivative at j^{th} nm
n	Number of observation
ND	Normalized difference
O_i	Observed value of i^{th} data
P_i	Predicted value of i^{th} data
p	Level of significance
R	Reflectance at certain wavelength
w	Weight of sample
w_i	Weighted value for the entity i
x_i	Group of entity i
x_j	Group of entity j
v	Volume of sample
ρ_i	Reflectance at i^{th} waveband
$\Delta\rho$	Spectral reflectance difference
ρ_{IH}	Broadband equivalent to integrated narrow band
ρ_C	Critical band of the spectrum
ρ_{min}	Lower minimum spectral band of the broad band
ρ_{max}	Lower maximum spectral band of the broad band
λ	Wavelength
α	Intercept of linear equation
β	Coefficient of linear equation

List of Abbreviations

Abbreviations	Full form
ADP	Aerial Digital Photography
ANN	Artificial Neural Network
ANOVA	Analysis of Variance
AVHRR	Advanced Very High Resolution Radiometer
AVIRIS	Airborne Visible InfraRed Imaging Spectrometer
AWiFS	Advanced Wide Field Sensor
BPNN	Back Propagation Neural Network
CAPE	Crop Acreage and Production Estimation
CASI	Compact Airborne Spectrographic Imager
CCI	Canopy Chlorophyll Index
CHRIS	Compact High Resolution Imaging Spectrometer
DAP	Days After Transplanting
DARs	Data Acquisition Requests
DB	Dry Biomass
DEM	Digital Elevation Model
DM	Dry Mass
DSS	Decision Making Support System
EGS	Ending Date of Growing Season
EMI	Electromagnetic Induction
EO-1	Earth Observation-1
EROS	Earth Resources Observation and Science
ETM	Enhanced Thematic Mapper
EVI	Enhanced Vegetation Index
EWT	Equivalent Water Thickness
FASAL	Forecasting Agricultural Output Using Space, Agrometeorology and Land Observations
FCCs	False Colour Composites
FLAASH	Fast Line-of-sight Atmospheric Analysis of Spectral Hypercubes

FM	Fresh Mass
fWBI	Floating-Position Water Band Index
GIS	Geographical Information System
GOBPC	GIS Object-Based Post Classification
GPS	Global Positioning System
GRI	Green Ratio Index
GVI	Green Vegetation Index
HSI	Hyperspectral Imaging Instrument
IoA	Index of Agreement
IR	Infrared
IRS	Indian Remote Sensing
ISRO	Indian Space Research Organization
K	Potassium
LAI	Leaf Area Index
LBV	Lower Brahmaputra Valley
LCC	Leaf and Canopy Chlorophyll Content
LISS	Linear Imaging Self-Scanning Sensor
LNC	Leaf Nitrogen Concentration
LRWC	Leaf Relative Water Content
LUE	Light Use Efficiency
LUT	Look-Up Table
LWC	Leaf Water Content
MAFF	Ministry of Agriculture, Forestry and Fisheries
MCARI	Modified Chlorophyll Absorption Ratio Index
MLR	Multiple Linear Regression
MNF	Minimum Noise Fraction
MNFT	Minimum Noise Fraction Transformation
MODIS	Moderate Resolution Imaging Spectroradiometer
MSI	Moisture Stress Index
MSL	Mean Sea Level
mSR	Modified Simple Ratio
MSS	MultiSpectral Scanner
MTCI	MERIS Terrestrial Chlorophyll Index
N	Nitrogen

NASA	National Aeronautics and Space Administration
NDI	Normalized Difference Index
NDII	Normalized Difference Infrared Index
NDSI	Normalized Difference Spectral Index
NDVI	Normalized Difference Vegetation Index
NDWI	Normalized Difference Water Index
NDWI-1	Normalized Difference Water Index-1240
NDWI-2	Normalized Difference Water Index-1640
NIR	Near Infrared
NMDI	Normalized Multiband Drought Index
NNI	Nitrogen Nutrition Index
NOAA	National Oceanic and Atmospheric Administration
Num Opt	Numerical Optimization
NWI-1	Normalized Water Index- 1
NWI-2	Normalized Water Index- 2
NWI-3	Normalized Water Index- 3
NWI-4	Normalized Water Index- 4
OBSSR	On-Board Solid Staterecorder
OMBVI	Optimum Multiple-Band Vegetation Indices
OSAVI	Optimised Soil Adjusted Vegetation Index
P	Phosphorous
PA	Precision Agriculture
PFS	Precision Farming System
PLS	Partial Least Square Regression
PRI	Photochemical Reflectance Index
PVI	Perpendicular Vegetation Index
QTL	Quantitative Trait Locus
QUEFTS	Quantitative Evaluation of the Fertility of Tropical Soils
RDACS	Real-Time Data Acquisition Camera System
RE	Mean Relative Error
REGFLEC	REGularized canopy reFLECtance
RMSE	Root Mean Square Error
RRLRRS	Regional Rainfed Lowland Rice Research Station
RS	Remote Sensing

RSI	Ratio Spectral Index
RVI	Ratio Vegetation Index
SAR	Synthetic Aperture Radar
SARVI	Soil and Atmosphere Resistant Vegetation Index
SAVI	Soil-Adjusted Vegetation Index
SAWI-1	Semi-Arid Water Index-1
SAWI-2	Semi-Arid Water Index-2
SGS	Starting Date of Growing Season
SNR	Signal-to-Noise Ratio
SPOT	Satellite Pour l'Observation de la Terre (Satellite for observation of Earth)
SPOT-VGT	SPOT Vegetation
SR	Simple Ratio
SRWI	Simple Ratio Water Index
SSCM	Site-Specific Crop Management
SSE	Sum of Squared Error
SSNM	Site-Specific Nutrient Management
SVIs	Spectral Vegetation Indices
SWIR	Shortwave Infrared
TBVI	Two-Band Vegetation Indices
TCARI	Transformed Chlorophyll Absorption Ratio Index
TGI	Triangular Greenness Index
TM	Turgid Mass
TW	Turgid Weight
UAS	Unmanned Aerial Systems
UAVs	Unmanned Aerial Vehicles
USGS	U.S. Geological Survey
VI	Vegetation Index
VIs	Vegetation Indices
VNIR	Visible Near Infrared Region
VWC	Vegetation Water Content
WBI	Water Band Index
WI	Water Index
WI-Hyperion	Water Index–Hyperion

1 Introduction

1.1 Overview

Food, cloth and shelter are the three basic needs of human beings. Among them, the immediate basic need is food. Cereal grains, obtained from plant families, form primary source of food for human beings and are grown worldwide. Rice is one of the principal cereal grains, which is most widely grown in many countries of the world, mostly in the equatorial climate zone or tropical climate zone with higher precipitation. It is the most prevalently consumed staple food grain for a large part of the world's population including India and China and most of the densely populated Asian countries. On a global scale, around 3.5 billion people depend on rice for more than 20% of their daily calorie requirement (Muthayya et al., 2014). Asia, alone, accounts for 87% of the world's total rice production with over 100 kg per capita consumption annually. Most importantly, India is the second largest producer of rice in the world only after China. Rice contributes a significant share towards the entire food grain production in India. India with the second largest population in the world, where a majority of its population is dependent on agriculture for their livelihood, productivity of rice cultivation can play an essential role in obtaining food security and ensuring sustainable development in long term. Population growth in India does not keep up with the resource availability for higher rice production – rather the land availability for its cultivation decreases every year. In this regard, enhancing rice productivity with efficient farming is need of the hour and has always been the key area of focus for farmers, agricultural researchers and crop management personnel. However, cultivation of rice in India is afflicted with several problems from the very beginning. Rice production is getting lower due to several factors, such as soil fertility degradation over the years due to excessive farming on a piece of land and much dependence

of fertilizer (Scherr & Yadav, 1995), pests and insect infestation due to climate change (Karuppaiah & Sujyanad, 2012; Kiritani, 2007; Rosenzweig et al., 2001), improper nutrient management (Dobermann, 2000), inappropriate use of inputs, lack of information on field variability, and low adoption rate of advanced technologies by the farmers (Feder et al., 1985). Therefore, adaptation of new and novel technologies, which can go a long way in addressing the problems of low productivity, are required in the present.

Precision agriculture is defined as the observation, impact assessment, and timely strategic response for detecting small variations in agricultural production and the implementation of subsequent remedial measures (Panda et al., 2010[b]). Along with advanced farm machinery usage in cultivation, precision agriculture alternately know as site specific crop management (SSCM) would improve the crop yield in a larger amount (Noori & Panda, 2016; Panda et al., 2010[a,c]; Panda et al., 2011). It has been used in a wide range of agricultural activities including field crop production, dairy farming, horticulture, and forest management. SSCM involves spatial referencing, remotely sensed monitoring, crop and climate monitoring, attribute mapping, decision support systems, and differential action to improve crop production (Panda et al., 2010[b]). SSCM is carried out with greater degree of precision with geospatial technology, a combination of four essential tools, such as remote sensing, geographic information systems (GIS), global positioning systems (GPS), and information technology or data management (Baez-Gonzalez et al., 2005; Casanova et al., 1998; Li et al., 2009; Lobell et al., 2005; Magri et al., 2005; Otter-Nacke et al., 1986; Panda, 2004).

Precision rice farming offers the promise of significantly increasing the rice production with optimal agricultural and fertilizer inputs, and minimal environmental damage from the inputs (Zhao et al., 2013). Precision rice farming for small-scale farms is a challenging task for the scientists and researchers in a developing country like India. Precision rice agriculture, which is a site- specific farming management concept, is based on the management of inter and intra field variability in crops. To implement precision farming, at first the variabilities associated with the field such as its nutrients availabilities in form of chlorophyll, nitrogen, and leaf water content need to be considered (Schmidhalter et al., 2008). Furthermore, by adopting suitable site-specific fertilizer management based on the field variability, crop growth can be improved both in small and large scale agricultural fields. Nitrogen (N), the paddy crop growth

enhancing and yield determining nutrient, needs to be supplied timely in adequate amount as per the plant requirement to sustain yield without impacting the environment (Liu et al., 2016; Zhang et al., 2017). For that purpose, remote sensing technologies, both ground and satellite based, have become more operational for capturing field level data for generating maps of crop growth, crop diseases, nutrient deficiency, water requirement and soil condition (Kokaly, 2001; Mutanga et al., 2004; Rumpf et al., 2010; Tilling et al., 2007). Ledgard (2001) completed a review study on low input legume-based agriculture in temperate legume/grass pastures under grazing by livestock. His study found nitrogen (N) flow mechanism in legume pastures and he suggested methods for improving efficiency of N cycling in legume-based cropping and legume/grass pasture systems, such as 1) timing of management practices for synchrony of N supply via mineralisation and crop N uptake; 2) impoved spatial return of excreta and uptake of excreta N by pastures through dietary manipulation and management strategies with grazing animals, 3) plant species selection and plant constituent modification to potentially increase N efficiency through greater conversion into animal production; and 4) improved N uptake from soil and manipulation of mineralisation/immobilisation/nitrification reactions for improved fodder growth (Lagard (2001). Similarly, nitrogen management in rice can be conducted once, the deficiency of it ascertained.

Hyperspectral remote sensing and advanced geo-spatial technologies have the potential of providing essential information on plant characteristics (Mulla, 2013; Zhang & Kovacs, 2012; Zhang et al., 2002). Hyperspectral imaging provide plant characteristics in terms of very fine narrow band electromagnetic spectrum, because of which identification of sensitive characteristics like rice canopy chlorophyll and vegetation moisture content at significant bands is now possible. The mapping of the biophysical and biochemical parameters like chlorophyll, nitrogen and leaf water content to determine field scale heterogeneity for a rice agriculture system is now hypothesized to be feasible with the use of hyperspectral remote sensing.

In this study, hyperspectral satellite images are used to map the crop parameters. Different narrow band index models are employed in two different rice crop seasons. Besides this, hyperspectral in-situ data are collected from different rice varieties. The data sets are being used to select the most sensitive bands for nitrogen treatment variation and also to build a

spectral library. The identified hyperspectral optimum narrow bands for paddy crop are used to evaluate chlorophyll and nitrogen status at plot scale by employing index based fusion approach for hyperspectral satellite image with multispectral image. The plot scale information produced at field level is also used to map the crop parameters to visualize the field variability from space platform. The field heterogeneity is also captured from hyperspectral satellite image. Slope maps are developed over the studied agriculture system and the field heterogeneity is validated with the field survey data. The narrow band index models are proposed to map the variability of chlorophyll, nitrogen and water content in an Indian agriculture system. The statistical analysis is carried out to evaluate the performance of different index models. This study has been conducted in an Indian rice agriculture system.

1.2 Role of Remote Sensing in Agricultural crop studies

Remote sensing has wide application in the area of agricultural crop studies. Due to availability of high temporal, spectral and spatial resolution satellite images, different agricultural activities and productivity assessment have become efficient and economic (Figure 1.1). Remote sensing methods are operated in three different modes: ground-based, airborne, and satellite (Panda et al., 2015). In ground-based remote sensing method, handheld remote sensing instruments are used which are mostly effective for monitoring small-scale operational crop fields. Airborne remote sensing method refers to usage of Unmanned Aerial Vehicles (UAVs) and aerial imaging. These are small aircrafts, remotely controlled from a ground station or flown at low altitude and are very effective in monitoring large operational crop fields. UAVs as low cost, lightweight and low airspeed aircrafts designed specifically to collect data from crop fields. From past few decades, satellite based remote sensing is being used extensively. It uses satellite images for crop type mapping, diseases and pests detection, crop health assessment, crop acreage estimation and crop yield forecasting. Remote sensing technology has proved itself strongly in non-destructive estimation of crop yield (Becker and Schmidhalter, 2017; Hauk et al., 2015), monitoring plant growth (Dwyer et al., 1991; Liang et al., 2017; Tackenberg, 2007), detection of various stresses (Balasundram et al., 2013; Schmitter et al., 2017; Zygielbaum et al., 2009).

Figure 1.1 : Potential of remote sensing in the field of agricultural studies (Panda et al., 2010)

The characteristics of detailed plant response to their local environment provides the suitability for site specific agricultural management approaches (Panda et al., 2010) to enhance the crop yield. Using AVHRR/NOAA images, Doraiswamy et al. (2004) developed a model to monitor the growth and estimate corn and soybean crops yield using Landsat and MODIS imagery. Swain and Zaman (2012) used an unmanned helicopter to obtain multispectral images to estimate rice (Oryza sativa L.) yield. By using MODIS sensor data at a regional scale with the help of artificial neural network (ANN) structure, yields of maize and soybean were estimated (Li et al., 2008). QuickBird satellite multi-spectral data have been used to capture within field spatial variability of nitrogen status of maize for seasonal nitrogen management (Bausch and Khosla, 2010).

However, in a small farming system coupled with mixed cropping practices, which is mostly seen in developing countries, the use of remote sensing technology is a very challenging task. Analysis of multispectral remote sensing data only would not be sufficient to interpret the crops grown in the region. It does not provide the exact crop phenology over a period of time in the field due to limited number of spectral bands. For this, thorough understanding of spectral responses of crop species (cultivars*) and crop growth changes during the developmental period is required. Crop spectral signatures serve as the best interpretation of crop behavior and tell many things about crop phenology. This can only be effectively achieved in the fine spectral channels of the electromagnetic spectrum. Under such circumstances, hyperspectral data would facilitate the best discrimination between spectral variation obtained from crop species and identification of crop species through their spectral signatures. The hundreds of narrow bands with very small widths accompanied with hyperspectral sensor has made it possible to interpret the characteristics of spectral response of an object effectively.

1.3 Advantage of Hyperspectral Remote Sensing over Multispectral Remote Sensing

A multispectral image generally contains very few bands like 3 to 10 bands, in which each band is obtained using a remote sensing radiometer or band filters (Das and Seshasai, 2015). Whereas, a hyperspectral image could contain hundreds or thousands of bands, each nanometer wavelength, as an individual band provides spectral information on the ground object. It is obtained from an imaging spectrometer and comprises of much narrower bands (10-20 nm) than a multispectral image. The main difference between multispectral and hyperspectral is with respect to the number of bands and narrowness of the bands (Figure 1.2). The unique feature of hyperspectral data is the spectral characteristics of its narrow bands that are rich and more detailed in information than multispectral data.

**Cultivar and Species are interchangeably used throughout the thesis so as not to confuse a biology investigator*

Several studies revealed significant advantages of hyperspectral remote sensing over broad-band remote sensing in identifying vegetation properties (Eklundh et al., 2001; Roberts et al., 1993; Thenkabail et al., 2000). Information on crop phenology at growth stage during different crop seasons is essential for implementing agriculture management schemes. This information can be derived from spectral reflectance measurements. The central objective of the present study is to explore the possibility of optimal solutions concerning hyperspectral remote sensing imagery for paddy crop parameters mapping at plot scale within the crop fields.

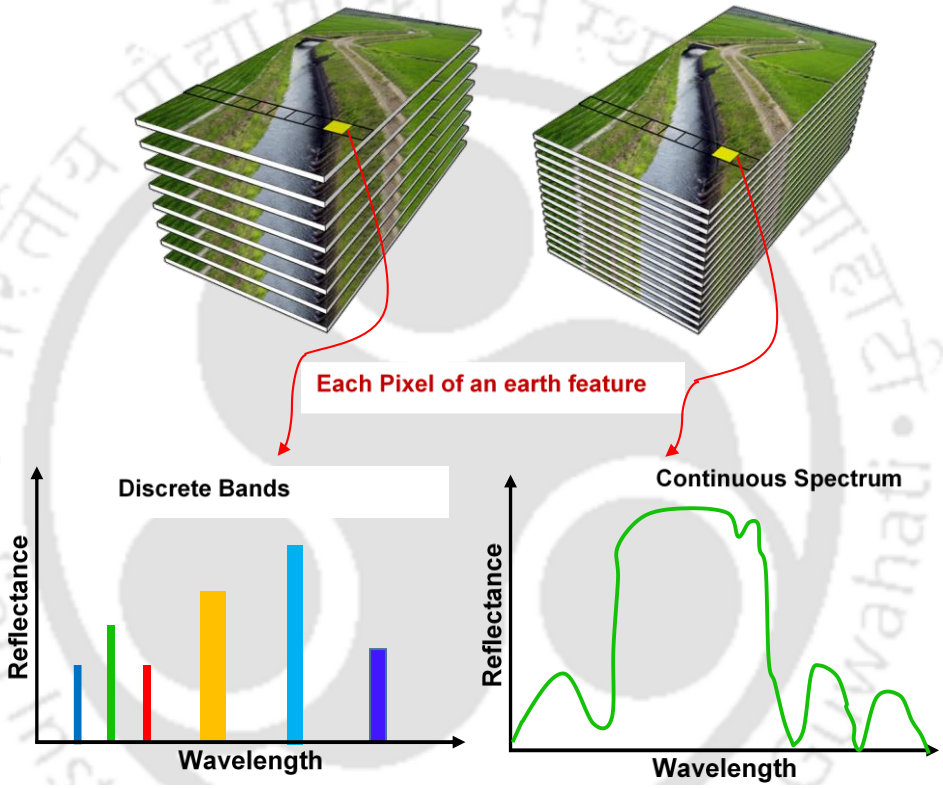

Figure 1.2 : Primary difference between multispectral and hyperspectral remote sensing

1.4 Field Scale Variability

Field scale variability knowledge can greatly enhance crop production through appropriate field scale inputs and crop field management. Field scale variability is very difficult to manage as it involves so many factors like soil fertility, soil moisture content, presence of pests, plant pigment, and fertilizer and irrigation requirements. Both inadequate and excess inputs supply hampers cropping management efficacy, crop health and its growth, ultimately leading to low crop production. Therefore, understanding the spatial and temporal variability of crop

parameters, topographic and hydrological conditions at field scale for agricultural inputs is the most important task in precision agriculture. An attempt has been made to map the crop parameters like total chlorophyll, nitrogen and water content at field scale for a rice agriculture system from spaceborne hyperspectral image. In addition to this, fusion of hyperspectral image with high spatial multispectral image has been employed to retrieve chlorophyll and nitrogen content at plot scale. Heterogeneity of paddy crop fields can also be captured from space platform so that site specific fertilizer management can be planned accordingly. Thus, there is a definite need of research to develop an optimized input system and fertilizer management system at field scale to enhance the crop yield through precision rice farming. The main goal of precision agriculture is to recognize within-field variation and implement suitable management of the crop field to address this variability (Schmidhalter et al., 2008). Cetin et al. (2005) examined the capability of hyperspectral Real-time Data Acquisition Camera System imagery (RDACS-3; 120 bands and 2/spl times/2m pixel resolution) to identify sensitive regions for detection of nitrogen deficiency in corn and improve fertilizer use efficiency consequently preserving the environment from excess nitrogen losses. The use of hyperspectral data analysis has revealed feasible solutions to estimate heterogeneous grassland canopy nitrogen with largely diversified plant species and canopy for better understanding of the function of natural and managed ecosystem (Ling et al., 2014). In the present study, *in-situ*, hyperspectral image and multispectral image are used to develop several models aiming to assess the crop variables at plot scale in a rice cultivation system. This will facilitate the employment of most effective management practices that will not only optimize nutrient and water use but also at same time minimize the usage of inputs with least impact on environment and human health.

1.5 Objectives of the Present Study

The main objectives of the present study are:

- To discriminate nitrogen treatments and varietal growth of paddy crop in Indian agro-climatic conditions by establishing an improved narrow band vegetation index.
- To develop a pure spectra of various Indian rice genotypes using ground-based hyperspectral data by incorporating waveform classification.

- To map crop growth parameters like nitrogen content and total chlorophyll (chlorophyll a and chlorophyll b) content from spaceborne hyperspectral data.
- To map variability of leaf water stress in a paddy crop calendar using temporal hyperspectral imagery.
- To develop a fusion technique of high spatial multispectral LISS IV image and hyperspectral Hyperion image to enhance spatial resolution to retrieve in-field variability of total chlorophyll and nitrogen content at small plot scale level.

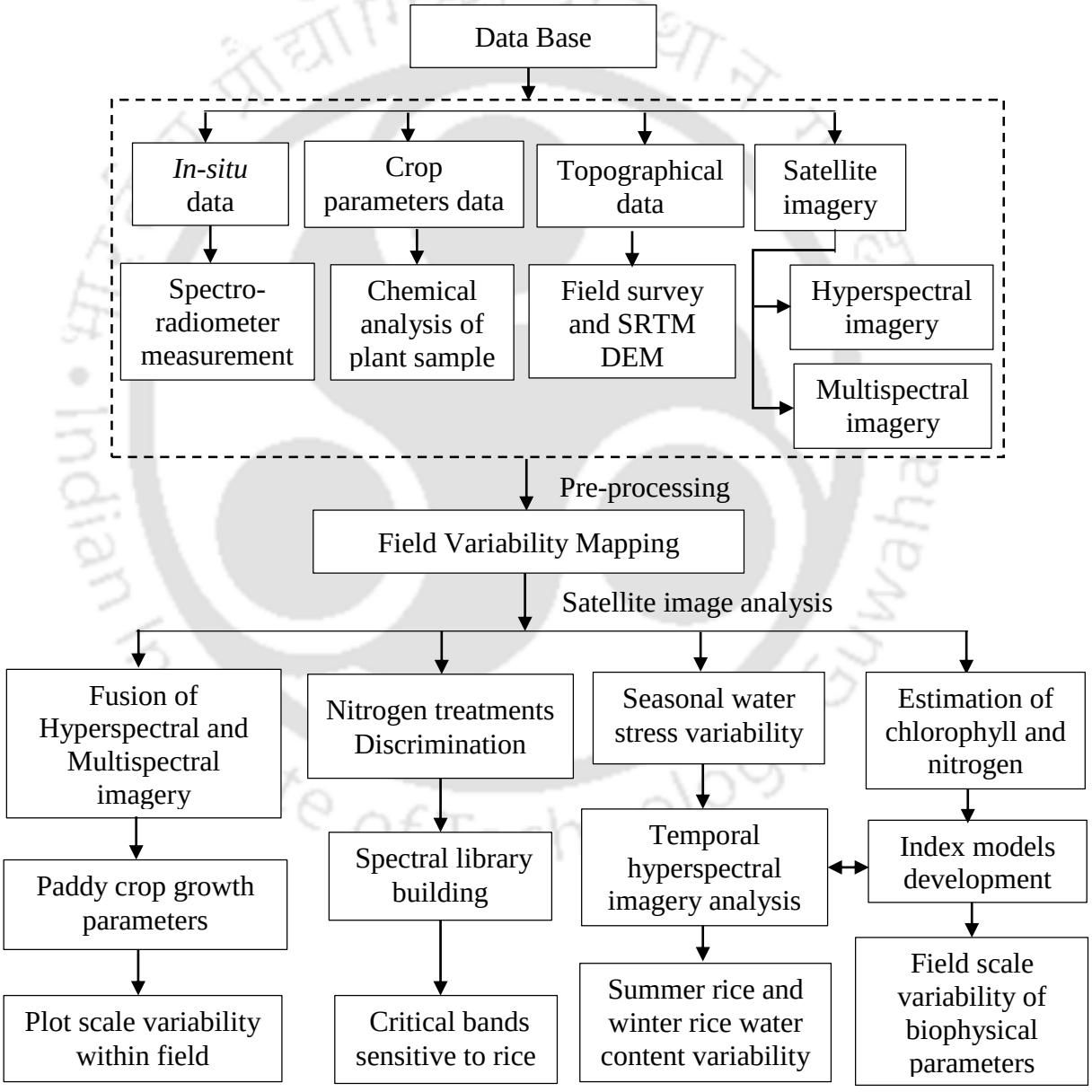

Figure 1.3 : Schematic diagram representing the objectives outlined in the thesis

1.6 Organization of the Thesis

The thesis comprises of nine chapters. The research work in this thesis deals with hyperspectral remote sensing of rice agriculture for field scale variability mapping (Figure 1.3). The thesis is organized in manner such that it covers the practicability of hyperspectral remote sensing technology in the field of rice agriculture research. Primarily, it addresses on critical bands sensitive to paddy crop specifically for nitrogen treatments and water stress. Secondly, it focuses on building a spectral library for paddy crop under different nitrogen applications. The subsequent chapters cover variability mapping of chlorophyll, nitrogen and water content in a rice agriculture system. Finally, hyperspectral data is fused with multispectral data to map the crop parameters variability at plot scale in the field level.

The chapter-wise brief description of the thesis is given below.

Chapter 1: This chapter includes an overview on advanced remote sensing technology application in precision agriculture and site specific crop management including nutrient management.

Chapter 2: This chapter discusses about relevant literatures concerning the present study.

Chapter 3: This chapter describes about the study sites for experiment and field survey, data collection, acquisition and processing of different satellites images for the study.

Chapter 4: This chapter describes the development of a novel technique to determine the sensitive spectral bands that explains the crop biophysical and chemical properties with clarity and proposes improved/new vegetation indices for discriminating nitrogen treatments as well as water stress for paddy crop.

Chapter 5: This chapter presents the development of a spectral library as well as the critical wave bands associated with discrimination of paddy crop species.

Chapter 6: This chapter provides details of the process associated with the estimation of crop parameters like total chlorophyll and nitrogen content from space platform and their spatial distribution in an Indian rice agriculture system.

Chapter 7: This chapter explains the processes associated with the estimation of Leaf relative water content and proposed index models to map its variability during different seasonal periods in a crop calendar.

Chapter 8: This chapter provides the methodology of the technology to create fusion of hyperspectral data and multispectral data is performed to find crop parameters variability at plot scale within the paddy crop field.

Chapter 9: The final chapter highlights the important findings of the study. Additionally, scope for the future research work is also presented at the section conclusion.

2 Review of Literature

2.1 Introduction

Rice is the single most important food crop in India that occupies 44.0 million hectares of agricultural land, the largest in the world by area. In India, the main rice grown is kharif, also known as winter rice as per the harvesting time. It is sown in June-July and harvested in November-December. Second form of rice is rabi rice or summer rice. It is sown during November to February and harvested during March to June. However, the time of sowing may slightly differ from state to state according to weather and rainfall pattern. The kharif season accounts for 88 percent, and rabi season accounts for 12 percent of the total production. Among the various cereals and crops produced in India, rice continues to lead. The crop is grown in very vast regions in the country due to its adaptability to a wide range of agro-climatic conditions. Thus, rice is the principal food grain of future and management of rice crop production has emerged as a key area of management in agriculture.

During the past few decades, a number of researchers all over the world have contributed to enhance rice productivity. A number of theoretical and modelling investigations as well as numerous field and laboratory experiments in different seasons with varying cultivation practices have been adopted towards the implementation of proper precision farming of agriculture. This chapter presents a brief discussion on the relevant research works carried out till date on precision farming specifically aimed at crop fertilizer management, species discrimination, crop biophysical parameters, crop field variation and field scale mapping of crop parameters.

2.2 Precision Agriculture

The concept of precision agriculture, which is an integrated information and production based system, is centred on two aspects, mainly the field spatial and temporal variations affecting crop production. Precision farming system (PFS) aims to increase agricultural crop productivity with minimum environmental impact through proper farm variability management. Site-specific crop management (SSCM) is about accurate, adequate and timely supply of crop inputs like water, fertilizers and pesticides in order to increase crop production and its yields through advanced farm mechanization (Srinivasan, 2006). Technologies like automatic yield recording system, automatic soil sensor, variability rate technology, advanced agronomy, advanced farm management, Global Positioning System (GPS), Geographical Information System (GIS), remote sensing, satellite navigation system, microwave sensing and hyperspectral sensing technology are employed to improve farm performance in mapping, getting the status of crops in the farm, and providing advice and support to farmers, the government, planners and the industries involved.

2.2.1 Precision rice farming: Global Developments

Research on rice precision farming has been going on in developed countries like US, Canada, Australia and Western European countries since early 1980s and also in developing country like India for the last couple of decades. Bailey et al. (2001) stated that the basic information needed for precision rice agriculture are crop biology, fertilizer application, soil moisture condition and soil type, which should be properly analyzed before growing the paddy crop. However, the rate of adoption of various technologies considerably differs from country to country, and region to region worldwide. In United States of America, the Midwest (heartland) and The Northern Great Plains regions are considered as most technology adopting sites for precision farming. Although, rice precision farming requires advanced technology, still spatial variability based site-specific fertilizer application has a significant role in precision agriculture (PA). Whelan et al. (1997) described there is no significant improvement towards rice PA in Australia, but the spatial variability of small-grain crop yield has shown a very good response in mapping and monitoring of spatial variability distribution of crop fields.

Japanese Precision Agriculture practices have faced some major issues related to agricultural workforce, farm mechanization structures, farmers' concerns and environment conservation leading to decline in rice production during the past two decades. Here, the agriculture system is intensively diversified in terms of crop field size, crop variety, elevation of the cropping area, water management practices, climate and soil types (Sasao and Shibusawa, 2000 and Shibusawa, 1998). Therefore, research teams of JAPAN Hokkaido University, Ministry of Agriculture, Forestry and Fisheries (MAFF), Kyoto University, and Tokyo University of Agriculture and Technology have come forward to provide a better solution to these serious problems. In this context, they have been working with a goal to develop soil nutrient sensor and mapping system, nitrogen sensor for rice plant, variable-rate fertilizer applicator, grain yield monitor and mapping system, and field robotics. In Germany, a group of researchers have been working on integrating both the map and sensor approaches with variable-rate technologies (VRT) for chemical applications on nitrogen fertilizer applicators (O'Neal et al., 2000). It focused on the establishment of a universal database for the sake of site-specific ecological fertilization management which requires spatial and temporal variability data of crop-specific nitrogen requirement, soil and plant water requirement, on-line sensing of nitrogen, real-time paddy crop data acquisition and transmission, and climate parameters like temperature and amount of intensive precipitation across fields (Pampolino et al., 2007). China accounts for 23% of the world's total area under rice cultivation. It ranks first in the world with highest yield per unit area and total rice production. It has shown a significant success in developing and implementing advanced precision agriculture technologies. Xie et al. (2003) has reported that the technologies adopted in China are GPS, geo-referenced data collection, farmland GIS, intelligence yield measurement system in the combine harvester, environmental, and economic assessment and development of an integrated decision making support system (DSS) for precision farming of rice (Figure 2.1). PA is widely accepted in other countries like Argentina, Australia, Bangladesh, Brazil, Canada, Chile, France, Indonesia, Italy, Korea, Netherlands, Russia, Saudi Arabia, Sri Lanka, Turkey, UK and Uruguay. By using the above emerging technologies, an artificial intelligence system was developed coupled with a combine harvester to evaluate real-time grain yield distribution map of paddy crop (Chung et al, 2002; Stott et al., 1993; Whelan and McBratney, 2002), which

has brought a great revolution in agriculture practices.

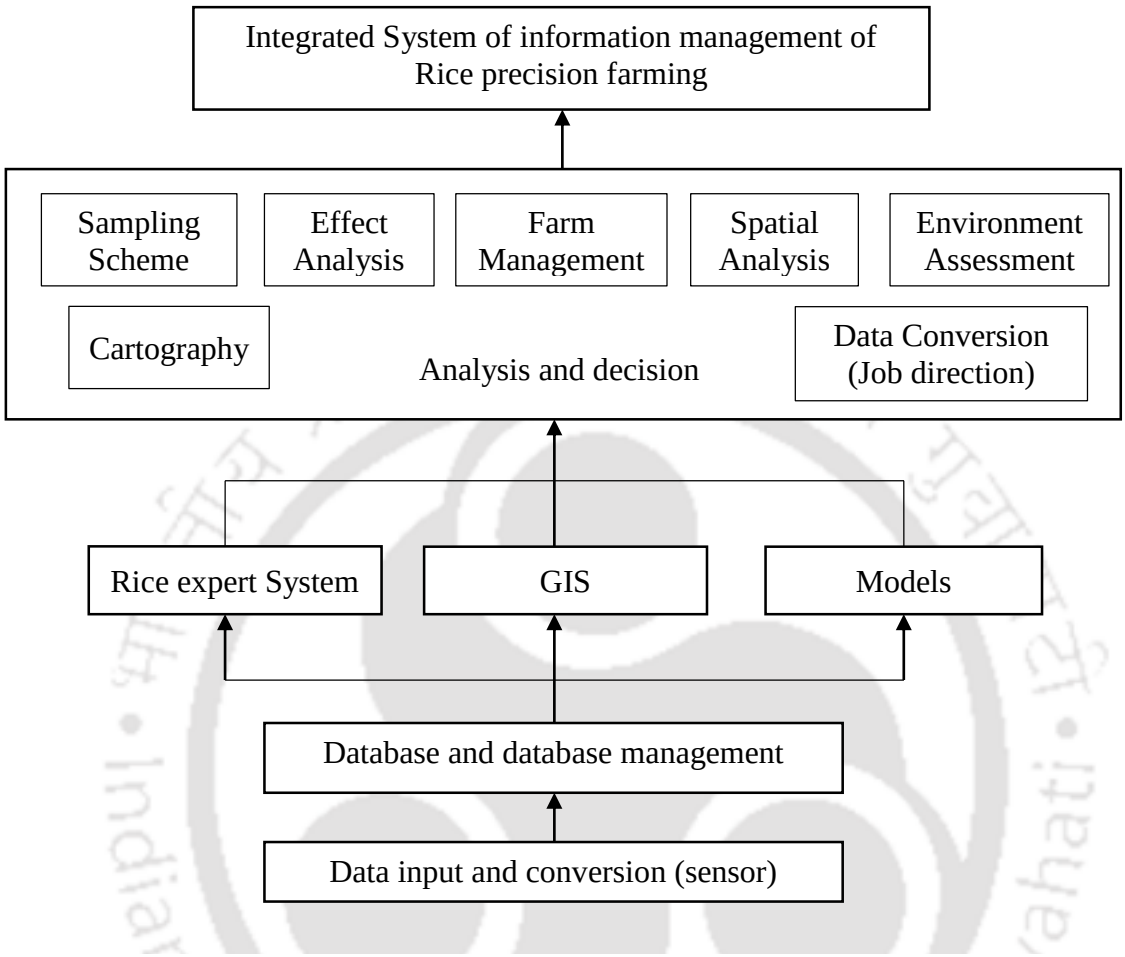

Figure 2.1 : Integrated system for information management of rice precision farming (Source: Xie et al., 2003)

Rapid socio-economic shifts in some developing countries like India are creating new strategies to adopt high-tech nature of PA in place of traditional technologies. The traditional strategies are solely based on visual interpretation of crop and soil, where management decisions are taken on experience and intuition, rather than on statistical and scientific analysis. Dadhwal (1986) reviewed that India like other countries have also started to use integration of advanced technologies like GIS, GPS, remote sensing, crop models, ground-based sensors and the internet as a part of agro informatics tools in increasing crop profitability. Under Crop Acreage and Production Estimation (CAPE) and Forecasting Agricultural Output Using Space, Agrometeorology and Land Observations (FASAL) project

schemes, advanced technologies have been developed to find out (i) crop forecast accuracy at district level, (ii) kharif crop inventory using microwave data, (iii) field data analysis using high resolution data, and (iv) linking crop growth models with remote sensing for improved yield estimation (Dadhwal 1999). In India, this is the only option left to realize farmers' goal to increase crop production by eliminating cost of production as well as environmental impacts.

2.2.2 Nutrient management in paddy cropping systems

Nutrient management is the most significant aspect of soil and crop management system. It is essential to keep track of nutrient requirements and the potential of the soil to provide them during all the stages of crop growth and understand nutrient treatment necessities for profitable crop production. Site-specific nutrient management (SSNM) implements this concept to a small area of field, which demands special treatment than in case of field average nutrient application. This SSNM concept for rice was first experimented in different parts of Asia to manage farm nutrient variability by Dobermann and White, (1999). He carried out some experiments on rice crop for two seasonal variations in a year in six Asian countries (China, Philippines, Thailand, South Vietnam, North Vietnam, Indonesia, and South India) to prove the hypothesis that rice yield, plant nutrient uptake, fertilizer efficiency and ultimately profit can be increased significantly by adopting field and cropping season specific nutrient management. He concluded that the concept helped the farmers to provide a systematic nutrient-based management of Nitrogen (N), Phosphorous (P) and Potassium (K) in rice which significantly indicated that the temporal variability in rice N status during crop developmental period and the status of soil P and K variability. Janssen et al. (1990) and Janssen (1998) found that the grain yield and nutrient requirements that can be expressed by using Quantitative Evaluation of the Fertility of Tropical Soils (QUEFTS) empirical modeling approach ,where grain yield is a function of three macronutrients N, P and K applications, significantly enhanced yield to 70-80% of the potential. Das et al. (2009) worked on paddy crop using SSNM in Eastern India by using QUEFTS model and confirmed that there was a significant improvement in site-specific and balanced fertilizer management in paddy crop. Application of N, P and K was adjusted to the location and season specific need of the rice.

Wang et al. (2007) demonstrated that the rice yield target responses to K have generally been lesser than that of the designed N and P (Liu et al., 2013). However, there has been a close association between the amount of N fertilizer applied to rice and the yield level. It has been reported that the yield obtained was approximately 20 kg more per kilogram of N applied (Chen et al, 2014). However, this will lead to inefficient nitrogen application and environment pollution. Hence, to protect the environment from excessive application of N fertilizer, the method of applying recommended N is most important to minimize N losses and achieve better nitrogen use efficiency in paddy crop. Many farmers do not use N fertilizer judiciously, whose application varies from upland to wetland rice, resulting in lower production even if high levels of N fertilizer was applied. The season of planting also influences the N requirement of rice (Bhuyan et al., 2012; Tian et al., 2017). Moreover, the rate of N management recommendations must change from single small scale farms to large scale farms. Usually, farmers grow high yielding rice varieties without following best soil-water-nutrient-crop management practices that significantly decreases the rice production and ultimately the economic returns. The use of computer and advanced satellite technology, in the management of N through SSNM, has performed very well resulting in more rice yield per unit fertilizer of N than the existing farmers' practices, without the help of special equipment and large farming operations. The advanced remote sensing technologies have positively amplified the status of rice agriculture system.

2.3 Remote Sensing and GIS applications for Agriculture

Real time assessment in agricultural applications is very crucial and use of remote sensing (RS) tools can provide a better solution to achieve this by overcoming the difficulties. Site specific crop management is being followed smartly to enhance crop production by implementing spatial referencing, crop and climate monitoring, crop area mapping, nutrient management, decision support system and preventive measures (Auernhammer, 2001; Campbell, 1996). GPS is being used to get the spatial variability of crop fields in crop production. Visible and near-infrared (NIR) regions of electromagnetic spectrum have performed well in monitoring photosynthetic radiation, nitrogen stress, soil moisture, crop health, crop growth, crop diseases, crop area, crop age and crop yield **(**Asner, 1998; Bausch,

1993; Clevers, 1989; Gallo et al., 1985). It is confirmed that RS sensor or the device gathers information from the radiation, transmission, absorption and reflection properties of leaves that can be used as indicators for plant parameters assessment. Chlorophyll reflects certain wavelengths of light within the visible light spectrum and absorbs the rest. It absorbs the blue and red lights and reflects green light thus making the plant appear green. The near infrared (NIR) wavelengths are reflected from the leaf's internal mesophyll structure (Curran, 1985). The NIR radiation enters through the topmost layer (Palisade tissue) of the leaf. Then after touching the mesophyll and the internal cavities of leaf, it is partly reflected upwards and partly transmitted downwards (Figure 2.2). The reflectance of visible spectrum is mainly a function of leaf pigments, whereas NIR reflectance is a function of leaf area index (LAI), cell turgor, leaf thickness, leaf internal air and water content (Campbell, 1996). Thus, healthy crops will show high NIR reflectance value and low reflectance in visible region.

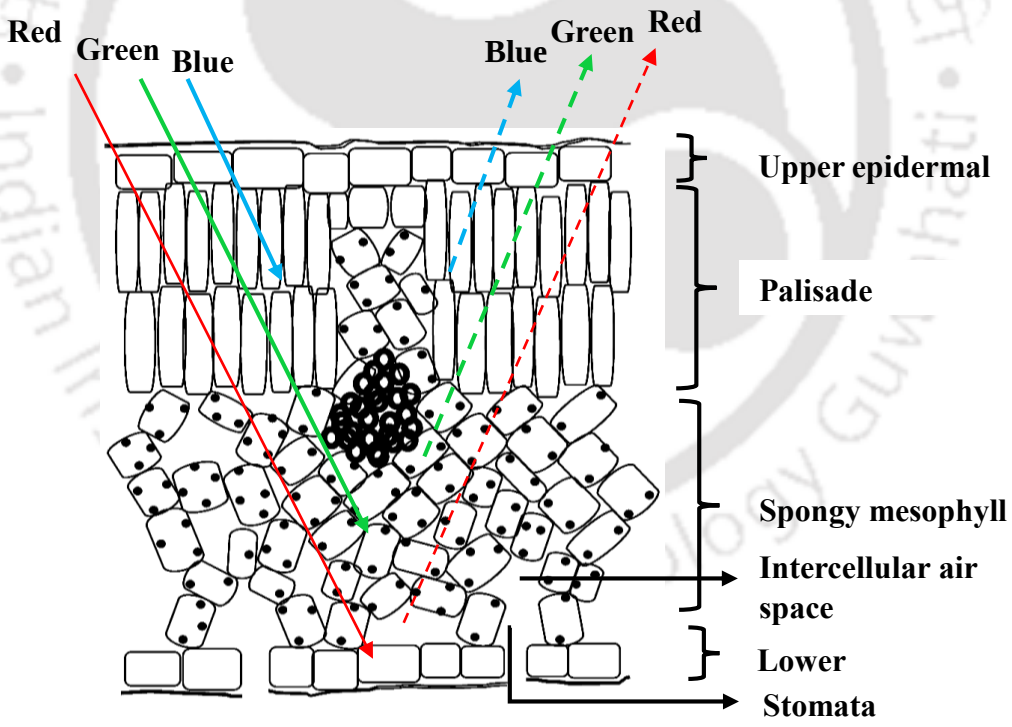

Figure 2.2 : The visible spectrum for monitoring plant health (Campbell, 1996)

Furthermore, RS has been widely used in PA to investigate field crop growth status and its variability. These include the use of ground-based remote sensors, satellite imagery and hand

held instruments. RS methods are categorized into passive and active remote sensing methods and similarly RS techniques are differentiated into multiple classes like panchromatic, multispectral and hyperspectral methods based on different standards like spatial, spectral and radiometric resolution. These RS classes have exhibited satisfactory results in various dimensions like detection of leaf pigment (Chappelle et al., 1992; Zhao et al., 2005), leaf water content (Hunt, 1991), plant nitrogen (Hansen, 2003; Serrano et al., 2000), potassium (Serrano et al., 2000) and phosphorous content (Osborne et al., 2002), deficiencies, pests, weed stress (Franz, 1991; Tian et al., 1999), salinity stress (Wiegand et al., 1994; Wiegand et al., 1996), LAI (Carlson, 1997), plant biomass production (Koetz et al., 2005), crop age estimation (Fang et al., 1998; Okamoto and Fukuhara, 1996; Tennakoon et al., 1992) and crop yield estimation (Dadhwal and Ray, 2000; Prasad et al., 2007). Previous studies have explored the ability of remote sensing platforms against various agricultural practices and management systems in different parts of the world. Rapid development of optical remote sensing system methods have offered a number of practical means for agricultural applications.

2.3.1 Optical remote sensing

Literatures reveal that researchers have dedicated significant efforts to estimate and forecast various crop yields using optical satellite images acquired from Landsat TM and ETM+, SPOT-VGT, NOAA/AVHRR, MODIS, IRS LISS-III etc. Tucker (1978) explored the potential of red and photographic infrared (IR) combination radiance values as well as of green and red combination. He declared that IR and red combination has an increased utility than green and red linear combination in estimating plant biomass, photosynthetic activity and nutrient deficiencies.

Bauer (1985) applied optical remote sensing for crop condition assessment by using multispectral reflectance and temperature data of crop canopies related to crop physiological processes like photosynthesis and evapotranspiration. Crop developmental stage and canopy parameters were found to be the most essential input to model crop growth, condition and yield. Optical remote sensing methods have demonstrated its potential worldwide in monitoring and mapping of rice crop. Rao and Rao (1987) identified different cropping patterns emphasizing Indian rice cultivation practices even from 80 m spatial resolution data

of LANDSAT MSS in form of False Colour Composites (FCCs). The results successfully identified 50% of the cropping patterns as paddy cultivated area with an accuracy of 90-94%. McCloy et al. (1987) proposed two classifiers i.e. maximum likelihood classifier and vector classifier to classify rice maps from Landsat MSS imagery. Using Landsat Thematic Mapper system with six bands, Tennakoon et al. (1992) analyzed to estimate rice yield and cultivated area from FCCs of 5R, 4G, 3B at the maturity stage of rice crop growth cycle. He tried to estimate actual crop grain yield from a fully ripened stage image of the crop. An interesting and important study has been carried out by Moran et al. (1997) where spatial and temporal information for the precision crop management were produced from aircraft and satellite based optical images, but with limitation of spectral, temporal and spatial resolution. Huete et al. (1997) investigated on vegetation indices (VIs) over desert, grassland, and forested biomes. He found that the normalized difference vegetation index (NDVI), which generally absorbed high red reflectance, was used to determine biophysical parameters to identify pure vegetation condition. It was more sensitive towards photosynthetic active radiation and greatly influenced by canopy background variations, but soil and atmosphere resistant vegetation index (SARVI) was highly responsive to NIR reflectance and sensitive to canopy structure and leaf morphology for evergreen needle leaf forest sites, deciduous broadleaf forests and drier, grassland, shrub sites. To improve the estimation of biophysical parameters by employing VIs, further studies have been carried out. By incorporating the visible and near-infrared wavelengths, optical–biophysical relationships have been derived for different canopy structures with a significant difference in foliage clumping, horizontal heterogeneity, and leaf types under agricultural, grassland, and forested canopies. It showed that the NDVI values were uniformly distributed for different canopy types but soil-adjusted vegetation index (SAVI), which showed significant values, were considerably different for broadleaf and cereal/needle leaf structural types (Gao et al., 2000). Furthermore, Huete et al. (2002) proposed two Moderate Resolution Imaging Spectroradiometer (MODIS) vegetation indices (VI) data, NDVI and enhanced vegetation index (EVI), to study vegetation variations, land cover variations and biophysical parameter variations for semi-arid grass/shrub, savanna and tropical forest biomes. This study concluded that the retrieval of biophysical parameters from VIs is not an easy task which requires a very good understanding of VI sensitivities across and within biomes, because VIs are integrative measures of vegetation photosynthetic activity

and other vegetation properties comprising of LAI, leaf optics, canopy structure, canopy crown cover, species composition and land cover type. Boegh et al. (2002) has made an effort to quantify the vegetation amount and variations in the physiological developmental age of agricultural vegetation in Denmark from airborne multispectral data acquired by the Compact Airborne Spectrographic Imager (CASI). From this data, they have derived spectral reflectance, vegetation indices and red edge positions, and compared them with the observed LAI, canopy nitrogen concentration data, and found no correlation between LAI and nitrogen. However, LAI exhibited correlation to NIR reflectance and photosynthesis exhibited linear correlation to transpiration, and Light Use Efficiency (LUE) was related to nitrogen concentrations. Colombo et al. (2003) have considered spectral and texture information to introduce Spectral Vegetation Indices (SVIs) from high resolution IKONOS satellite data to estimate LAI for different crops. They were able to find out within-field spatial variability of LAI that can also be useful for precision farming management practices and techniques. Chen et al. (2005) have taken the study to next level by evaluating the Vegetation Water Content (VWC) for growing period of corn and soybeans from MODIS satellite data by establishing VIs from combinations of the 7 MODIS bands. It revealed that the MODIS-derived indices such as Normalized Difference Vegetation Index (NDVI) and the Normalized Difference Water Index (NDWI) using SWIR (1640 nm or 2130 nm) performed well in estimating VWC. Besides this, the spatial and temporal large-scale mapping operations of green LAI, total chlorophyll content, and total VWC were retrieved using a numerical optimization method through combination of both vegetation index and physical approaches (Houborg et al., 2007). They explored the inversion of a canopy reflectance model from Terra and Aqua MODIS multi-spectral, multi-temporal and multi-angle reflectance data to investigate vegetation-specific physiological and structural canopy parameters. Further, VIs were proposed to be used in the development of sensors. Jiang et al. (2008) tried to develop a 2-band EVI without a blue band, which had a good correlation with 3-band EVI where the data quality was good with negligible atmospheric effects. It can be used as a sensor to detect the vegetation dynamics in a better way as compared to present AVHRR NDVI dataset. Panda et al. (2010) have carried out research to predict crop yield by adopting soft computing techniques like artificial neural network (ANN) for corn for a three-year period. They proposed back-propagation neural network (BPNN) models with four data sets and examined the efficiency

of four VIs i.e. red and near-infrared (NIR) based normalized difference vegetation index (NDVI), green and NIR based green vegetation index (GVI), red and NIR based soil-adjusted vegetation index (SAVI), and red and NIR based perpendicular vegetation index (PVI) to predict corn yields. Among the four indices, PVI provided overall prediction with an average accuracy of 93%. Wu et al. (2010) investigated on distinguishing the spatial patterns of phenology in croplands of China at a spatial resolution of 8 km and 15-d interval. NDVI time-series data were used to monitor crop phenological status. It showed that the starting date of growing season (SGS) and the ending date of growing season (EGS) for the first growing season, distributed widely over a large area with multiple cropping systems, exhibited significant improvement of SGS and EGS than the areas with single cropping patterns. These were influenced by the geophysical environmental factors. Wang et al. (2010) found the change in LAI at different stages of crop growth period from radiative transfer model. In his research, he concluded that time series of MODIS canopy reflectance has the ability to diminish the uncertainty of the inverted LAI values and crop growth model, in order to keep wheat crop water and nitrogen balances of the soil-vegetation-atmosphere system. Vohland et al. (2010) assessed LAI, canopy chlorophyll, water and dry matter contents for summer barley from airborne HyMap by using canopy reflectance model (PROSPECT + SAILH) in which three inversion techniques, numerical optimization (Num Opt), look-up table (LUT) and artificial neural network (ANN) approaches, were applied. In his research, the prediction accuracies decreased in the order of Num Opt > LUT > ANN. This was a result of increasing offset in the predicted state variable values. VIs were used to characterize crop characteristics in different phases of crops like corn, soybean, wheat, canola under different tillage and fertilizer management practices. VIs were found to be significantly different for a variety of corn and soybeans as they are very sensitive to the growing stage. This study implied appropriate VIs should be selected to best capture the agricultural crop characteristics (Hatfield and Prueger, 2010). Besides this, later Shiu et al. (2012) conducted research work to classify rice area in highly fragmented areas in Taiwan. However, they used advanced classification techniques - (i) geographic information system (GIS) object-based post classification (GOBPC) and (ii) pixel-based hybrid classification (i.e., both unsupervised and supervised) for FORMOSAT-2 images, and concluded that GOBPC classifier performed better than the others with a maximum accuracy level of 94%. Berjon et al. (2013) have put

efforts to retrieve vegetation parameters like LAI, average leaf angle, chlorophyll content and soil reflectance from high resolution QuickBird 2 imagery of agricultural field plots on two different dates using PROSPECT and SAILH models. Similarly, Hunt et al. (2013) proposed a spectral index namely Triangular Greenness Index (TGI) consisting of only visible wavelengths at 480, 550 and 670 nm to estimate chlorophyll content of Zea mays using remote sensing datasets of AVIRIS, Landsat TM and digital cameras. They confirmed that the index, TGI was only affected by leaf chlorophyll content, and it can be mounted on digital cameras or airborne spacecrafts to monitor crop nitrogen requirements. Now a days, non-destructive estimation of biophysical, biochemical and structural leaf properties such as LAI, Chl, N, leaf water content (LWC) and crop canopy development could be better assessed by using advanced remote sensing technologies with a higher accuracy level adding to more detailed vegetation information of crop plants.

2.3.2 Advanced remote sensing technologies

2.3.2.1 Microwave remote sensing applications for crop parameters studies

Optical remote sensing has been proved successful in retrieval of biophysical parameters of agricultural crops, but is only limited to cloud-free conditions. However, the wavelengths in the microwave region of the electromagnetic spectrum are unaffected by atmospheric conditions like cloud cover and are independent of sun illumination. Microwave sensor like Synthetic Aperture Radar (SAR) can capture earth observation images in a cloudy weather during night also. This encouraged researchers to investigate the application of SAR sensors for agriculture monitoring. SAR data is available from C-band satellite sensor like ERS-1, ERS-2, RADARSAT-1, Envisat-ASAR, RADARSAT-2, Sentinel-1, and from L-band satellite sensors JERS-1, ALOS-PALSAR, ALOS-2, PALSAR-2. Moran et al. (2002) demonstrated that SAR was very sensitive to recognize the field roughness (related to tillage), vegetation density, surface soil moisture and dry plant litter. They reached a conclusion that SAR image analysis would not be possible without optical images, and combined results of optical and SAR images can only differentiate soil moisture condition**.** Chakraborty et al. (2005) investigated on multi-temporal, multi-incidence angle Radarsat SAR data to derive crop heights and planting stage for a predominantly rice-growing region in West Bengal,

India. He observed that the obtained crop height from C band SAR was the height above water surface. Thus, the episodic events like flooding or draining could be determined from the change in backscatter value with respect to the difference in crop height. Jiao et al. (2009) found, there was a relationship between LAI and SAR parameters (HV backscatter, pedestal height, and volume-scattering parameter) derived for corn and soybean. The SAR responses changed as the crop canopy advanced and the LAI increased, which implied the potential of polarimetric SAR data as an indicator for monitoring crop productivity. Aubert et al. (2011) investigated to derive agriculture soil-surface moisture information such as roughness, moisture, composition and structure within field plots from TerraSAR-X data. They found greater backscattering signal implied presence of slaking crust and subsequently negligible backscattering value indicated soils out of crust. Later, LAI estimation was evaluated from X-band sensors using COSMO-SkyMed and TerraSAR-X data (Fontanelli et al., 2013). In case of wheat crop, they noticed a relatively high sensitivity of backscatter to LAI at both HH and VV polarizations. Moreover Claverie et al. (2012) analyzed optical and SAR (multi-polarized, multi-frequency, and multi-angular) data to estimate LAI and biomass of sunflower with an aim to evaluate evapotranspiration and crop grain yield. Vegetation water content of sunflower could be determined using X- and C-band data (Santi et al., 2012). There was a correlation between SAR data backscatter value and dry biomass (DB) of corn, canola, and soybean (Wiseman et al., 2014). Besides this, Yang et al. (2014) also succeeded in monitoring early seasons for the sowing of oilseed rape (Brassica napus L.) from SAR data of five consecutive Radarsat-2 images.

2.3.2.2 Hyperspectral remote sensing for the estimation of biophysical and biochemical variables of crops

Hyperspectral remote sensing can be categorized into three classes such as:

(i) *In-situ* hyperspectral RS
(ii) Airborne hyperspectral RS
(iii) Spaceborne hyperspectral RS

The hyperspectral data depends on sensor, bands used and direction of observation. The use of hyperspectral *in-situ* data has been used to estimate biophysical and biochemical parameters

of various crops. Some research studies reported that the spectral reflectance properties of narrow band indices derived from ground based hyperspectral data performed well in estimating crop variables. Hyperspectral data has improved the accuracy for LAI estimation of crops like potato, corn using spectral reflectance (Lee et al., 2004), vegetation ratio indices (Brown et al., 2000), principal component analysis (Pu and Gong, 2004), spectral derivative indices (Ray et al., 2006) and genetic algorithms (Fang et al., 2003). It is very important to identify the most suitable index among various band combinations that correlates to biophysical parameters. In case of LAI measurements, the indices (NDVI, SAVI, RVI) contributing reflectance properties at 680 and 780 nm exhibited high correlation with LAI (Ray et al., 2006). Thenkabail et al. (2000) studied on hyperspectral data comprised of field spectroradiometer and ground-truth observations collected from 196 sample locations where barley, wheat, lentil, cumin, chickpea and vetch were grown. They have tried to demarcate the optimal hyperspectral narrow bands for agricultural biophysical crop characteristics mainly LAI, plant nitrogen, plant height, canopy cover, dry biomass and wet biomass. The simple Two Band Vegetation Indices (TBVI) and the Optimum Multiple Band Vegetation Indices (OMBVI) models were proposed to evaluate the crop characteristics. However, wavebands at 550 nm (green reflectance maxima), 675 nm (red absorption maxima), 720 nm (mid portion of the red-edge), 905 nm (near-infrared reflection peak) and another 12 spectral bands were found dominant over agricultural biophysical crop characteristics.

Hyperspectral remote sensing has the potential for quick non-destructive estimation of chlorophyll, the indicator of plant growth and health, as well as nitrogen, the indicator of plant nutrient level. Ground based hyperspectral observations showed significant improvement in monitoring plant growth and nitrogen status, thus helping in proper fertilization management for efficient nitrogen use with minimum environmental pollution. Field measurements were conducted for rice and winter wheat cropping systems for the prediction of nitrogen concentrations. Using narrow spectral bands Normalized Difference Index (NDI) and two types of Nitrogen Nutrition Indices (NNI), mechanistic and semi-empirical methods were proposed to predict the nitrogen concentration of rice and wheat respectively by spectral resampling. The NDI and NNI semi-empirical methods were influenced to some extent by plant biomass, LAI and phenology, thus offering a valuable approach to identify crop nitrogen status (Stroppiana et al., 2006). Researchers highlighted that the visible (blue/green) region of

the spectrum is the most sensitive region to plant nitrogen concentration (Stroppiana et al., 2009), whereas Nguyen and Lee (2006) reported that the visible (355, 420, 524–534, 583 and 687 nm), red edge (707 nm) and near-infrared (>760 nm) regions of the spectrum derived from partial least square regression (PLS) model are critical towards rice growth and nutrient status prediction. Similar findings were also observed by Wang et al. (2012) in case of paddy and wheat from a new three-band vegetation index comprising central bands (423, 703 and 924 nm). Furthermore, it is very difficult to decide nitrogen fertilizer application for an irrigated crop field. Blackmer and Schepers (1995) did a research on the management of nitrogen fertilizer for an irrigated corn field by using a new instrument, SPAD 502 chlorophyll meter. They were successful in finding the change in nitrogen status during the seasonal period of the irrigated corn field. This will support better crop nitrogen supply management during the growing season. Besides this, Yi et al. (2007) used Multiple Linear Regression (MLR) and Artificial Neural Network (ANN) modelling methods to monitor crop nitrogen status. He concluded that combined application of ANN with PCA on hyperspectral reflectance data analysis may provide a worthwhile exploratory and predictive measure of nitrogen status rather than MLR model. Some of the laboratory findings from wheat crop nitrogen status estimation using a multi-spectral radiometer by the researchers highlighted that the crop variable is more sensitive to narrow and continuous spectral band for a specific crop thus providing an abundant laboratory of information.

Besides nitrogen, chlorophyll, which is treated as the driver of primary production, has always played an important role in vegetation studies. Wu et al. (2008) have investigated non-destructive chlorophyll estimation of maize using vegetation indices like normalized difference vegetation index (NDVI), modified simple ratio index (mSR), the modified chlorophyll absorption ratio indices (MCARI, TCARI) and the integrated forms (MCARI/OSAVI and TCARI/OSAVI) by using the PROSPECT and SAILH models. Crops with very different canopy architectures and leaf structures like corn and soyabean responded to their specific spectral ranges in estimation of chlorophyll (Gitelson, 2005). The details of the previous studies related to chlorophyll estimation from hyperspectral data sets are summarized in Tables 2.1-2.3.

Table 2.1 : Estimation of crop chlorophyll content using hyperspectral data (Ground- based measurement)

Study	Ground Measurements	Key Results
Thomas and Gausman (1977)	Spectrophotometer with a reflectance attachment.	Spectral reflectance of vegetation in the 400 to 700 nm region is primarily governed by the abundance of chlorophyll.
Collins (1978); Horler et al. (1983)	Spectral measurements	Declared the concept of the red-NIR wavelength transition for vegetation studies. Under stress condition, the position of red-edge alters with the shift of the slope towards shorter wavelengths.
Curran et al. (1990)	Spectroradiometer data over pine and forest cover	Chlorophyll estimation is very difficult. Thus, canopy chemical concentration can be derived as chemical amount per unit ground surface area from remote sensing data.
Daughtry et al. (2000)	Spectral reflectance measurements of corn and wheat	Found close link between leaf chlorophyll and leaf nitrogen concentration. Concluded that spectral channels near 550 nm, 715 nm and >750 nm are sensitive to leaf chlorophyll concentration.
Broge and Mortensen (2002)	Winter wheat Chlorophyll measurement using SPAD-502 chlorophyll meter	Observed that vegetation indices obtained by waveform analysis using narrow bands across the red edge improve the prediction of canopy chlorophyll density.
Haboudane et al. (2002)	Corn leaf reflectance and transmittance measurements using Li-Cor model coupled to a spectrometer (Ocean Optics model ST-1000), chlorophyll meter (Minolta SPAD 502)	Proposed (TCARI/OSAVI) and investigated chlorophyll variability that showed a strong correlation between estimated and field measured chlorophyll content data.

Study	Ground Measurements	Key Results
Gitelson et al. (2003)	Field reflectance measurement	Highlighted spectral range from 520 to 550 nm and 695 to 740 nm, which are closely related to non-destructive total chlorophyll estimation of maple, chestnut, wild vine and beech leaves.
Dash and Curran (2004)	*In-situ* Spectral reactance observations	Proposed MERIS terrestrial chlorophyll index, MTCI better index than the Red Edge Position, sensitive to a wider range of chlorophyll contents.
Le Maire et al. (2004)	Field reflectance measurements (400- 800 nm)	Wavelengths should be calibrated to determine the best wavelengths for each crop chlorophyll estimation in each index types.
Gitelson (2011); Le Maire et al. (2004)	*In-situ* reflectance measurements of various crop	Green and red-edge spectral bands are highly sensitive to changes in crop chlorophyll content.
Cho and Skidmore (2006)	Spectral reflectance at leaf scale for maize leaves and canopy scale for rye grass canopies	Proposed a new technique and obtained optimal band combinations, far-red (680 to 700 nm) and NIR (725 to 760 nm) for extracting the REP from hyperspectral data to estimate foliar chlorophyll or nitrogen content.
Darvishzadeh et al. (2008)	Reflectance measurements canopy using a GER 3700 spectroradiometer	Using multivariate techniques integrated with narrow band indices, leaf and canopy chlorophyll content (LCC) and canopy chlorophyll could be estimated for a heterogeneous Mediterranean grassland from field dominant in grass and herb species.
Haboudane et al. (2008)	Field campaigns were organized during the growing seasons of 2004 and 2005. Ground spectra and leaf chlorophyll content were collected	OSAVI, MSVI index combinations performed well as chlorophyll estimators resulted from PROSPECT-SAILH canopy simulated spectra and field-measured reflectances.
Zhang et al. (2008)	Ground reflectance measurements	Empirical relationships between chlorophyll content and spectral indices were established in prediction of leaf chlorophyll content.

Study	Ground Measurements	Key Results
Feret et al. (2011)	Large set of leaf reflectance data collected from all over the world	Accurate estimation of leaf chlorophyll content was obtained in the red-edge and near infrared regions of the spectrum.
Huang et al. (2011)	Canopy and BRDF reflectance spectrum	Chlorophyll-*a* and –*b* are indicators for crop nutrition status and photosynthetic capacity from canopy spectra.
Clevers and Kooistra (2012)	Field spectral measurements	Red-edge band (700–730 nm) was linearly related to the canopy maize chlorophyll content.
Peng and Gitelson (2012)	Hyperspectral radiometer reflectance.	Total crop chlorophyll content was evaluated in rainfed and irrigated maize and soybean crops.
Schlemmer et al. (2013)	Field spectral measurements	Observed Red-edge spectral bands were sensitive to chlorophyll and nitrogen estimation at canopy level.
Frazier et al. (2014)	Hyperspectral measurements for a broad range of vegetation types	Chlorophyll content is influenced by plant water, nitrogen, salinity content and leaf scattering properties and the observed visible near-infrared portion of the light spectrum is sensitive to it.
Guo and Guo (2016)	Spectral reflectance (400–760 nm)	Aimed to monitor growth status of water plants in urban wetland and found the key range as 550–750 nm, particularly 700–750 nm to estimate biochemical parameters.

Table 2.2 : Estimation of crop chlorophyll content using hyperspectral data (Air-borne measurement)

Study	Satellite Imagery	Key Results
Zarco-Tejada et al. (2001)	Field, laboratory measurements, and CASI imagery of 1-m spatial resolution	For Canadian forest canopies, Red edge optical indices (710 nm, 750 nm) performed better than single spectral reflectance channels from hyper-spectral airborne CASI data.
Haboudane et al. (2002)	Compact Airborne Spectrographic Imager (CASI) imagery	Proposed (TCARI/OSAVI), very sensitive to chlorophyll content variations, LAI and solar zenith angle. The index was validated over corn crops in three experimental farms from Ontario and Quebec, Canada.
Zarco-Tejada et al. (2004)	1m Resolution ROSIS data acquired from Hysens Campaign, Spain	MCARI/OSAVI well predicted chlorophyll content in open tree canopies using high spatial hyperspectral image than the published single ratio indices, the good indicator of chlorophyll.
Cho et al. (2007)	Field campaign for fresh green grass/herb biomass. Airborne HyMap data, 4th July, 2005	Partial least squares techniques incorporating hyperspectral indices improved grass/herb biomass estimation based on airborne hyperspectral imagery than univariate regression.
Houborg et al. (2009)	1m resolution aircraft and 10 m resolution SPOT-5 imagery	The REGularized canopy reFLECtance (REGFLEC) model retrieved a wide range in leaf chlorophyll content based on radiances in green, red and near-infrared wavelengths.
Jiao et al. (2014)	Spectroradiometer FieldSpec and airborne hyperspectral remote sensing imagery	Developed spectral linear mixture concept for winter wheat chlorophyll content estimation using ground spectra, airborne hyperspectral data and leaf chlorophyll content obtained from winter wheat fields.
Liang et al. (2016)	Compact High Resolution Imaging Spectrometer (CHRIS) datasets	Photochemical reflectance index (PRI) and canopy chlorophyll index (CCI) amongst fifty VIs were declared as optimal to map chlorophyll.

Table 2.3 : Estimation of crop chlorophyll content using hyperspectral data (Space-borne measurement)

Study	Satellite Imagery	Key Results
Wu et al. (2008)	Hyperion data for corn field	Concluded that establishing a unique relationship in estimating chlorophyll is very difficult and the indices depend on species, developmental stages, stress, and nutritional state. Predictive functions for wheat were also not reliable in the chlorophyll content estimation of corns with Hyperion data.
Croft et al. (2013)	Ground, CASI, Landsat TM 5 and MERIS reflectance data	High spatial resolution hyperspectral data has the capability to retrieve leaf chlorophyll content using narrow band indices.
Vyas et al. (2013)	Hyperion data for Teak and Bamboo forest	Simple ratio index (743/692) performed well in Teak and Bamboo chlorophyll content using satellite remote sensing data.
Navarro-Cerrillo et al. (2014)	AHS, CHRIS/Proba, Hyperion, Landsat and QuickBird data	Spectral mixing alters the characteristics of chlorophyll absorption features which controls the accuracy of leaf chlorophyll estimation using narrow band spectral indices.
Yang et al. (2015)	Hyperion data for a forest land	Estimated chlorophyll content quantitatively and confirmed spectral values at 480, 631, 735, 749 and 819 nm are highly correlated to it.

Leaf water content regulates the photosynthetic units of the leaf and the process of photosynthesis (Figure 2.3). Leaf chlorophyll pigment production depends on leaf water content. Thus, reduction in soil water leads to water stress causing chlorophyll pigment deficiency in leaves of rice crop. This results in lowering of net photosynthesis rate, affecting the leaf nitrogen content, paddy crop flowering, growth and development. Therefore, soil water below the crop water requirement level drastically reduces rice crop yield.

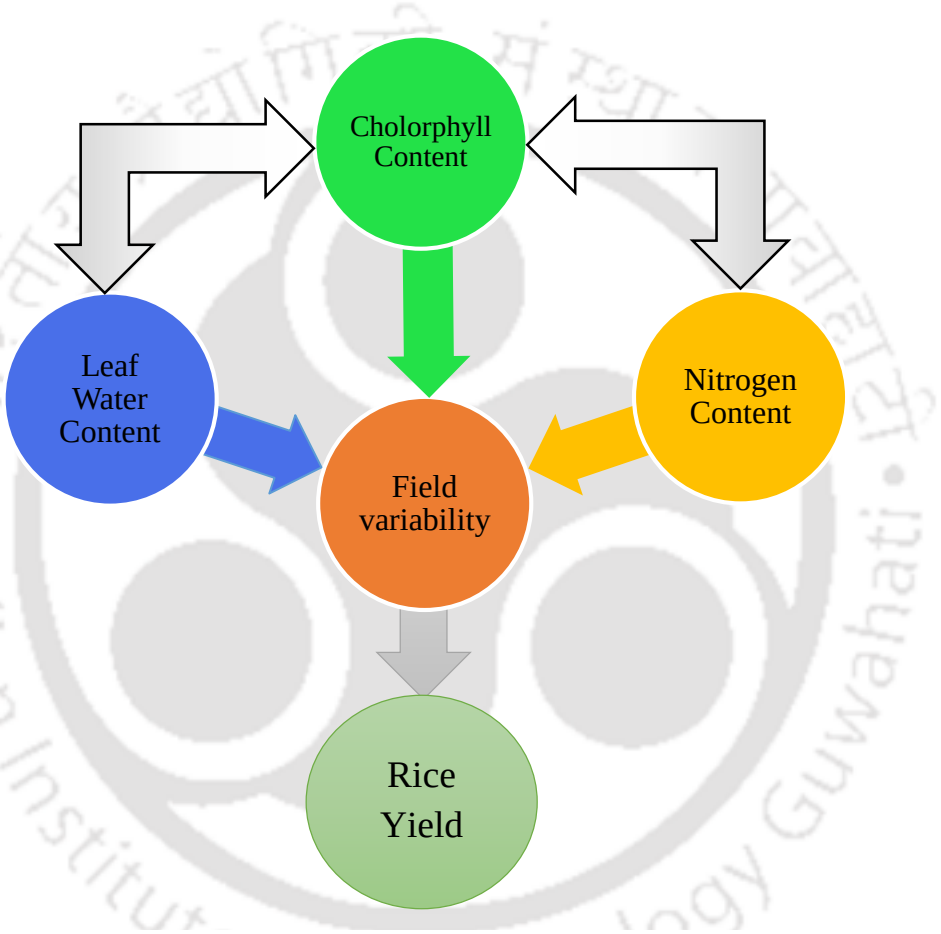

Figure 2.3 : Inter relationship of crop biophysical parameters, field variability and rice yield

To get maximum rice yield, it is very important to use water adequately in a timely manner for rice cultivation so that physiological processes and growth of the plant is not hampered. This is possible only when the leaf water content of rice species is known from time to time over a spatially distributed agriculture system. The present study focusses on mapping the leaf water content for an Indian agriculture system dominated by paddy crop cultivation. The

previous studies carried out by different researchers and scientists have helped to understand the physiological state in order to detect plant water status and provided technical support for leaf water content assessment quantitatively using remote sensing for rice crop.

Band combination from hyperspectral remote sensing technology is considered as an effective tool for rapid, non-destructive estimation of crop parameters and evaluating spatial variability across a crop field (Blackmer et al., 1994; Sankaran et al., 2010; Tucker et al., 1980; Zarco-Tejada et al., 2005). The most sensitive bands are found in the visible near infrared region (VNIR) and shortwave infrared region (SWIR) of the spectrum (Suarez et al., 2009; Suarez et al., 2010). However, the optimal sensitive bands differ from crop to crop, as the interaction of narrow wave bands is crop specific. Therefore, it is essential to calibrate the narrow bands for a specific crop for a particular crop parameter (Magney et al., 2016). Leaf water status has been identified by many researchers through water absorption bands for different crop species like winter wheat, summer wheat, maize, soybean, cotton, boxwood and so on (Chen et al., 2010; Kim et al., 2015; Xu et al., 2010). But, very few research studies have discussed on wave bands sensitive to paddy crop leaf water content (Carrijo et al., 2017), which is a very water demanding crop. Xu et al. (2007) used simple ratio index model, fixed-position Water Band Index (WBI) by considering reflectance at 900-970 nm in the near-infrared region for evaluating water content in bean leaves and established a strong relationship with water content. Strachan et al. (2002) continued to evaluate the water content and the findings suggested that the floating-position water band index (fWBI) has a correlation with area-weighted corn leaf water content. It is revealed from other researches that leaf water content index is not significantly different from relative water content of individual leaves or plants. Therefore, the average relative water content of canopies can be quantified from the leaf water content index (Hunt et al., 1987). According to their findings, the wavelengths 0.76 to 0.90 μm and 1.55 to 1.75 μm (Landsat Thematic Mapper Bands TM4 and TM5, respectively) were related to leaf relative water content. Their findings matched with Tucker (1980), who observed that the wavelength regions 1.55–1.75 μm and 0.7–2.5 μm of the spectrum were the best suited spectral channels to detect the plant canopy water status from satellite platform. Moreover, temperature, narrow-band VIS–NIR formulations, and chlorophyll fluorescence are best related to water stress at 747, 760, 762 and 780 nm wavebands (Zarco-Tejada et al., 2012). They confirmed these findings with the investigation of water stress in a citrus orchard

by taking images acquired from a thermal camera and a micro-hyperspectral imager. Cheng et al. (2006) retrieved equivalent water thickness (EWT) from hyperspectral AVIRIS images using synthetic spectra from three canopy reflectance models coupled to the PROSPECT leaf radiative transfer model. Many research studies have proposed various water stress based indices such as Water Index (WI) (Penuelas et al., 1997), Normalized Difference Water Index (NDWI) (Gao, 1996), Normalized Difference Infrared Index (NDII) (Hardisky et al., 1983) and Moisture Stress Index (MSI) (Hunt and Rock, 1989). These indices were derived using visible, NIR, SWIR bands of the spectrum, which employed multivariate analysis, partial least squares regression and PROSPECT leaf radiative transfer model to detect water stress in crop. Tian et al. (2004) developed a normalized difference index ($(R_{810} - R_{610})/ (R_{810} + R_{610})$) and a spectral water index ($R_{(610,560)}/ND_{(810,610)}$) to detect plant water status of wheat. Using ground-based spectroradiometric measurements, Ranjan et al. (2015) proposed that MSI, NDII, normalized difference water index-1640 (NDWI-2) and normalized multiband drought index (NMDI) are the most precise and accurate prediction models for leaf relative water content (LRWC) in wheat crop. Cheng et al. (2006) concluded that the quantification of EWT depends on canopy structure for which appropriate model should be adopted separately to evaluate different crop canopy or leaf water content. Thus, it can be concluded that there is still a general lack of research that employs empirical methods for the accurate prediction of plant water content by using hyperspectral image.

2.4 Field Scale Variability for Agricultural Crop Management

For the refinement of agricultural crop management practices, a strong understanding of the distribution of soil properties and crop parameters at a field scale is mandatory. It needs an estimation of variables associated with the soil properties. Field scale spatial variability is the outcome of interaction of biological, chemical and physical parameters with the soil properties**.** The continuum process is solely spatial, which is dependent on the topography of agricultural field. Furthermore, by considering the soil type and plant population density, crop yield variability within the field was measured (Basso et al., 2001). Electromagnetic induction (EMI), aerial digital photography (ADP) and radiometry technology could be implemented in mapping soil physical and chemical state, topography and the weed status of the fields

(Godwin and Miller, 2003). Using field observations, Scharf et al. (2005) reported spatial variability of nitrogen fertilizer needed for the production of corn**.** On the other hand, space platform image acquisition through small unmanned aerial systems (UAS) is described as an alternative to characterize within field variation and to decide different site-specific management schemes**.** There is a lack of research to identify the spatial variability of crop biophysical parameters at plot level from satellite imagery. Therefore, the present study emphasizes on the estimation of field variability at plot scale from space platform, which is pertinent to agricultural research. Hyperspectral imaging is a powerful tool for estimation of important plant biochemical properties such as nitrogen, pigments and trace minerals. Hence, to achieve both high spatial and spectral properties, fusion of hyperspectral and multispectral images is carried out to get the variability of crop parameters at plot scale within the field.

2.5 Conclusions

The literatures reviewed are concerned with estimation of crop biophysical and biochemical parameters, and field variability for precision agriculture using field and satellite based observations. Most of the literatures focused mainly on crops like wheat, maize, potato, barley by using spectroradiometer of various wavelength ranges. The number of research works on rice using hyperspectral data were very limited. Besides this, there was a lack of research to identify sensitive narrow bands meant for paddy crop characteristics and to monitor rice growth under different field conditions from space borne hyperspectral satellite imagery. Additionally, no specific studies addressed the basic knowledge of field scale spatial and temporal variability effect on nutrient, pigment and water content for rice varieties covering total crop developmental phase under Indian agro climatic conditions.

In current work, critical wavelengths responsible for the estimation of chlorophyll a, chlorophyll b, total chlorophyll, nitrogen and leaf water content of different rice species covering their total developmental age in Indian agro-climatic conditions are presented. Another important aspect i.e. the use of hyperspectral imagery acquired by Hyperion sensor to represent within field variability mapping of the essential growth parameters such as nitrogen, chlorophyll and water content of different rice varieties under different field conditions with different nitrogen and irrigation treatments is also portrayed. Further, fusion

of hyperspectral and high spatial resolution multispectral images is also carried out to provide plot scale information within the crop fields for precision agriculture that includes crop area, crop growth, crop health, crop stresses, crop nitrogen content and water requirement under different crop development stages.

3 Study Site and Data Acquisition

3.1 Introduction

This chapter provides a description of the study site considered for the present research work. Primarily, to understand the paddy crop characteristics, field observation is the most important requisite. Therefore, *in-situ* data was essential to be collected from rice crop fields for this study. Hence, field campaigns were carried out separately in two different parts of India during the pre-monsoon and monsoon seasonal periods of a paddy crop calendar. The field surveys were conducted to gather information about rice cultivation practices being adopted in India, basically with respect to agricultural inputs, fertilizer application, irrigation scheduling and crop yield. The ground based hyperspectral data were captured for the year 2009 and 2014 in order to obtain the most essential information necessary for precision rice farming. A portable spectroradiometer (FieldSpec-FR, ASD, India) is used to collect crop spectral measurements from paddy crop fields. Apart from *in-situ* data collection, satellite data using different platforms were also acquired from various sources such as hyperspectral satellite images for mapping of crop parameters (e.g. chlorophyll and nitrogen content) variability. Moreover, temporal satellite images acquired from Hyperion sensor were used for mapping of seasonal variability of rice leaf water content and multispectral satellite images from LISS IV were used for mapping of field scale variability of chlorophyll and nitrogen content of paddy crop at plot scale. Additionally, SRTM 30 m resolution Digital Elevation Model (DEM) data was acquired to understand the topographic characteristics of the paddy crop field in an Indian agriculture system. Besides, plant measurements for chlorophyll, nitrogen and leaf relative water content were obtained through chemical analyses in the laboratory using the leaves samples collected from study site.

3.2 Description of Study Sites

Constituting the major source of India's agricultural gross domestic product, rice plays a significant role in shaping the country's economy. The rice cultivating states in different parts of India are classified majorly as the western coastal strip, the eastern coastal strip, the deltas and the Assam plains. In India, rice is traditionally grown in two seasons as kharif (winter) rice and rabi (summer) rice during monsoon and pre-monsoon seasons respectively. Areas with hot and humid climate accompanied with heavy rainfall are mostly suitable for rice cultivation. States of Assam and Odisha, which experience a similar type of climate, prominently are engaged in rice cultivation. For the present study, two study sites were considered, one in Kamrup district of Assam (North East India) and the other in Cuttack district of Odisha (Eastern India).

3.2.1 Study Site 1: RRLRRS in Kamrup district of Assam

Assam constitutes a major share of rain fed rice production system in the eastern India. It accounts for around 9% of total rice production in India by area and 8% by quantity (Choudhury and Dayanandan, 2013).

The site, located at Gerua, Kamrup District of Assam (North East India), was chosen as one of the study sites for field experimental investigation. This is the experimental station of the Regional Rainfed Lowland Rice Research Station (RRLRRS), which was considered for winter rice cultivation in monsoon period. It is centred at latitude 26°15'18.84"N and longitude 91°33'50.68"E (Figure 3.1(b)). It experiences a subtropical hot summer climate with an average monthly temperature variation of 11.7°C and it receives an average annual precipitation of 1,722 mm. This area experiences temperatures as low as 25°C in winter to as high as 35°C in summer. The overall climate of this study area comes under Lower Brahmaputra Valley (LBV) Agro Climatic Zone. The soils of the Brahmaputra Valley are partly new and partly old. The variation in the mechanical composition of the soil is mainly due to the varying composition of the river borne materials deposited along the river bed over time under different conditions. The soil is rich in organic matters and nitrogen. The soil type of this area is classified as coarse-loamy. The total area of experimental site is 1.92 ha and it

is located at an average elevation of 56 m above the mean sea level (MSL). The selected site is an intensively rice cultivation agriculture area.

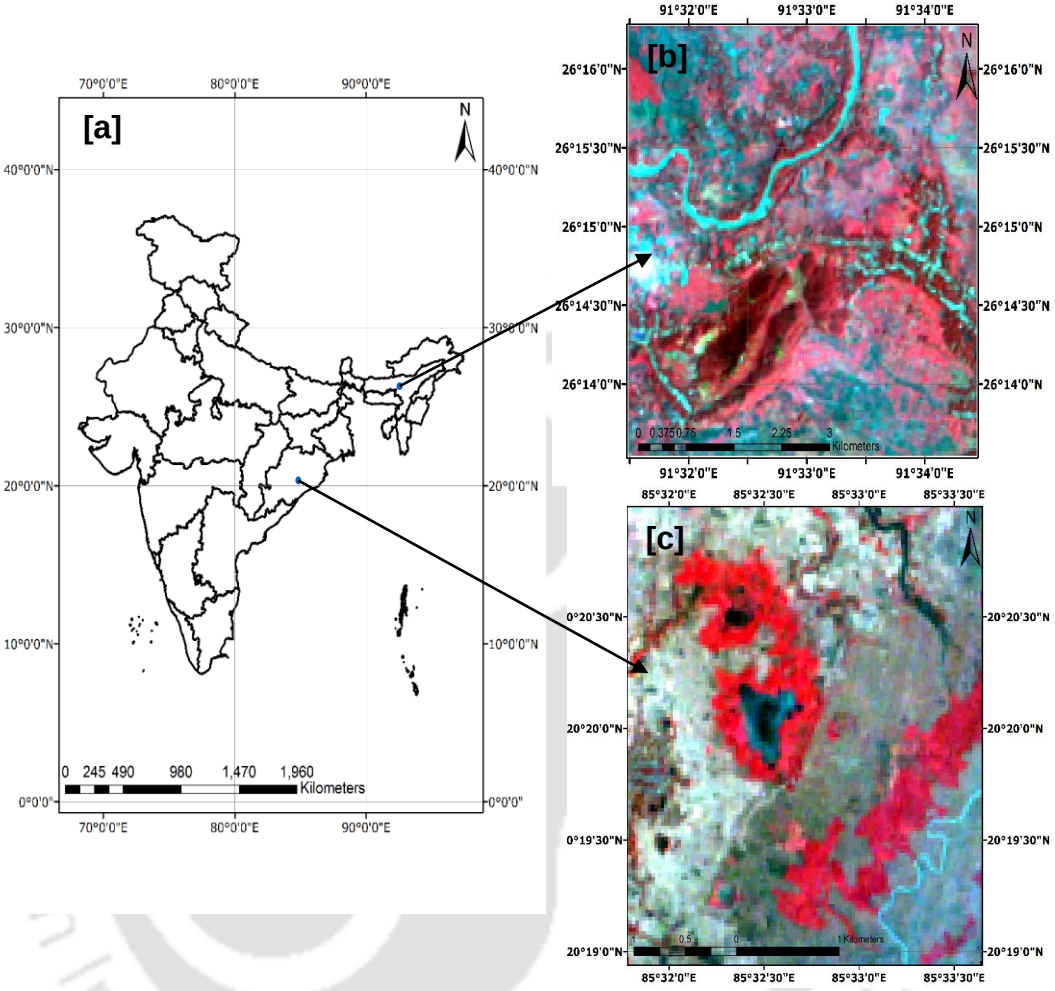

Figure 3.1 : (a) Map of India and satellite image of Hyperion for (b) Study site 1 - Kamrup, Assam: the study area showing winter rice agriculture system L1R FCC (RGB: Bands 51, 30, 20 displayed as red, green and blue respectively) and (c) Study site 2 - Cuttack, Odisha: the study area showing summer rice agriculture system and surrounding areas.

3.2.2 Study Site 2: Farmers' agricultural fields in Cuttack district of Odisha

While on the other hand, Odisha, which lies in the subtropical belt of eastern India, contributes more that 11% to the country's rice production. The mountain ranges of Eastern Ghats separates the eastern part of Odisha, a coastal belt with 482 km of coastline, from the western

part, an extensive plateau. The coastal belt has about 1.70 million hectares of rice land constituting about 38% of the total rice area of Odisha. This belt is generally prone to problems of serious waterlogging and flooding. In Odisha, rice is grown under diverse ecosystems and a wide range of climatic conditions. The immense diversity in growth conditions makes classification and characterization of the rice environments a challenging task. However, farmers follow their own method of classification for rice environments like uplands, medium lands, and lowlands, purely based on agriculture land topography and water regime. The farmers apply their experience-based knowledge to classify the land conditions and adopt appropriate agricultural management practices accordingly.

The farmers' agricultural farm fields in the district of Cuttack, Odisha, India (20°19'24.84"N, 85°32'41.94"E) with summer rice cultivation during pre-monsoon period was considered as another study site (Figure 3.1(c)). This is an extensively rice cultivated area. This area experiences a tropical wet and dry climate where temperatures may exceed 45°C in summer and may fall below 28°C in winter. Temperature is considerably lower during the rainy season, averaging around 30°C. Thunderstorms are common during summer. The average annual rainfall is around 1440 mm. It is situated at an average elevation of 34 m above the mean sea level (MSL). The soil is classified as typic tropaquepts as per the modern system of soil classification (Sahu and Mishra, 2005). The soil is acidic with pH varying from 4.77 – 5.33 with a mean of 4.95. The organic carbon content in the soil varies from 0.32 – 1.20% with a mean of 0.77%. Both kharif and rabi rice are grown in this area.

3.3 Developing Field Database

To understand the rice plant characteristics, crop parameters variability, crop varietal information, fertilizer application and irrigation scheduling, field experiments in rice fields were conducted. Field and laboratory measurements were made and field survey were carried out to build the necessary information for validating the achieved results. The field experiments were conducted in the Study Site 1 i.e. the experimental station of Regional Rainfed Lowland Rice Research Station (RRLRRS) using a hand held portable spectroradiometer (FieldSpec-FR, ASD).

Source: Field Photograph **Name:** 72 Rice plots, RRLRRS, Assam
Date: 14th March, 2009 **Location:** 26°15'18.84"N, 91°33'50.68"E

Figure 3.2 : Photograph showing the paddy crop with different nitrogen applications

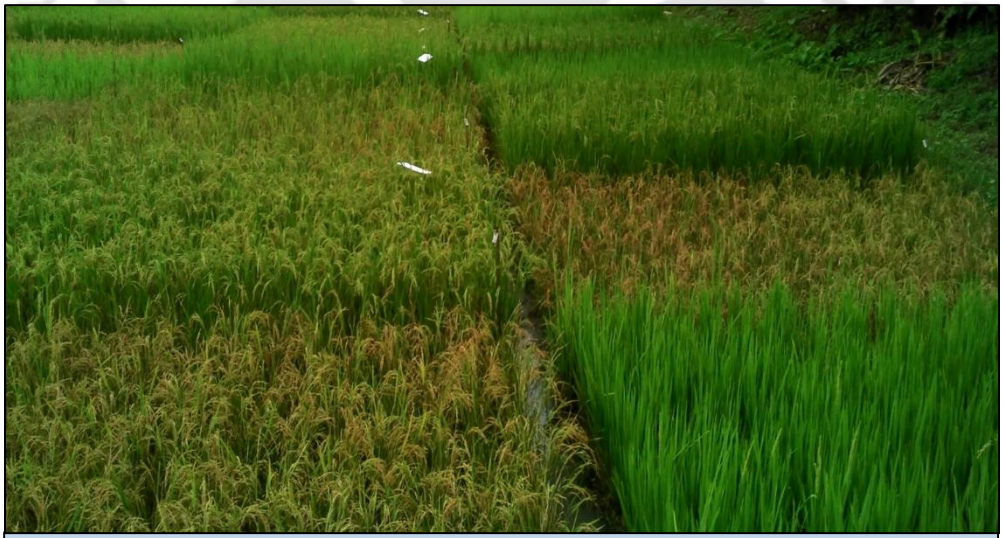

Source: Field Photograph **Name:** 24 Rice plots, RRLRRS, Assam
Date: 11th June, 2014 **Location:** 26°15'18.84"N, 91°33'50.68"E

Figure 3.3 : Photograph showing the paddy crop with different crop developmental age

3.3.1 Ground-based hyperspectral data collection

Paddy crop reflectance from rice canopy cover was retrieved from different rice plots comprising of different rice varieties. These selected paddy fields were made homogeneous for rice breeding and field management. Measurements were taken in an irrigated experimental paddy field of RRLRRS, Assam (Study site 1) in 2009. The field was under paddy cultivation already for several years prior to our study. The field was divided into 8 sets of 9 subplots each i.e. into 72 subplots in total. The size of each subplot was 3.3 m × 3.4 m. Each subplot had similar soil type, temperature and field conditions. In these subplots eight varieties of rice namely Gautam, IR-64, IET-18558, IET-19601, K.Hansa, Chandrama, IET-19600 and IET-20166 were grown (Figure 3.2), i.e. one rice variety in each set of 9 subplots. For each rice variety, three different levels of nitrogen treatments (50, 100, 150 kg/ha) were applied. Measurements were taken randomly from all the subplots with same irrigation, soil properties and at similar phenological stages, but with different levels of nitrogen fertilizer applications. Paddy crop was sown on 11th November, 2008 and fertilizer was applied as prilled urea in three splits after transplanting, $^{1}/_{2}$ as basal, ¼ at maximum tillering and ¼ at panicle initiation. Measurements of hyperspectral reflectance were collected during January, 2009 to May, 2009, starting from its transplanting stage to its harvesting stage at weekly intervals.

Furthermore, for the present work, different aged cropping rice species providing different yields for the estimation of chlorophyll and nitrogen content in Indian climatic condition were considered. In 2014, *in-situ* data were collected from an irrigated paddy field in RRLRRS, Assam (Study site 1) having 24 sub plots (Figure 3.3), each having a dimension of 3.3 m × 3.4 m, for 24 rice genotypes namely Jaya, Parijat, Luit, Abhishek, Chandrama, Shabhagi Dhan, Ranjit, Baismuthi, CR Dhan 601, Akshya Dhan, Chandan, Mahsuri, Tni, Nilanjana, Anjali, BPT5204, IR64, Tapaswini, Disang, Joymati, Vandana, Kolong, Naveen and No.15. The plots were prepared using conventional tillage methods and plantation was made in March, 2014. To satisfy fertilizer requirement at this site, urea was recommended to be applied in three splits i.e. half of nitrogen was suggested to be applied at the time of sowing and remaining in two equal splits. The crop was provided with adequate amount of water by establishing pumping irrigation throughout the growing period. Weed was totally controlled

in the rice plots.

Source: Field Photograph **Name:** RRLRRS, Assam
Date: 10th May, 2014 **Location:** 26°15'18.84"N, 91°33'50.68"E

Figure 3.4 : Photograph showing measurements with Spectroradiometer instrument

Table 3.1 : Field Observation of paddy crop in the year 2009 and 2014

Rice Genotypes	Date of Observations (2009)	Rice Genotypes	Date of Observations (2014)
Gautam, IR-64, IET-18558, IET-19601, K.Hansa, Chandrama, IET-19600 and IET-20166.	28/01/2009 06/02/2009 13/02/2009 20/02/2009 27/02/2009 06/03/2009 14/03/2009 20/0320/09 27/03/2009 03/04/2009 10/04/2009 17/04/2009 24/04/2009 08/05/2009 15/05/2009	Jaya, Parijat, Luit, Abhishek, Chandrama, Shabhagi Dhan, Ranjit, Baismuthi, CR Dhan 601, Akshya Dhan, Chandan, Mahsuri, Tni, Nilanjana, Anjali, BPT5204, IR64, Tapaswini, Disang, Joymati, Vandana, Kolong, Naveen and no.15.	17/04/2014 26/04/2014 03/05/2014 10/05/2014 15/05/2014 17/05/2014 21/05/2014 30/05/2014 11/06/2014 19/06/2014 09/07/2014

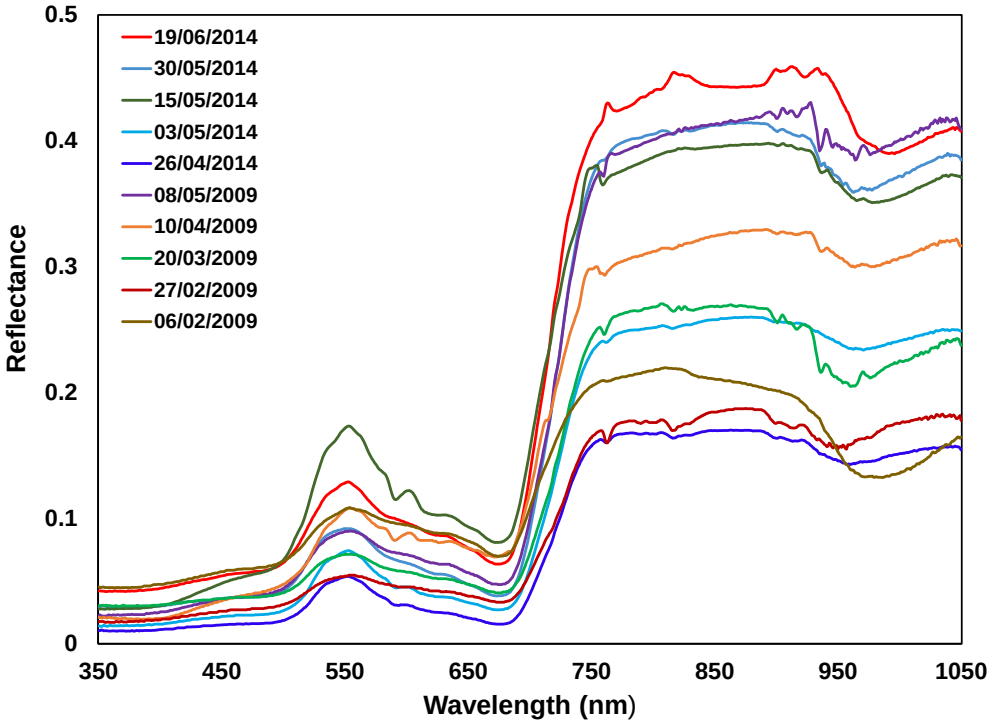

Figure 3.5 : Spectral signature of paddy crop observed in 2009 and 2014

Paddy crop canopy spectra were acquired under cloud free sky conditions around midday (10:00-13:00 LST) using a portable spectroradiometer (FieldSpec-FR, ASD, India). A spectroradiometer is a radiometer that measures the radiance in narrow spectral bands within the spectral range of the instrument. The spectral ranges of the sensors coupled with spectroradiometer were 350-1050 nm with a field of view of 25°. Spectral resolution was 2 nm for the region 350-1050 nm for the Field Spec-FR. Reflectance measurements were acquired at a nadir-looking angle from 90 cm above the canopy (Figure 3.4). Totally, spectral measurements with 95% canopy cover were taken for the rice varieties with different nitrogen fertilizer applications. The measurement of incident radiation is also quite complex because the target in the field is illuminated by various sources (Joseph, 2005). Therefore, more than 10 measurements were taken in every observation by moving over the canopy cover of each paddy field plot within one minute time interval, which enabled noise reduction by averaging the spectra (Muchovej et al., 2004). After the spectral observations were made, pre-processing of data is very much required. Hyperspectral measurements obtained from the spectro-radiometer were then processed by using RS^3 software. From the PC, the canopy reflectance

was derived in the range of 350-1050 nm. For every observation, the spectral reflectance values were averaged as the final spectral reflectance representing each paddy field of respective rice varieties on a particular date of observation (Figure 3.5). On repeating this procedure, sufficient reflectance data sets were prepared at weekly intervals from transplanting to the period of harvesting for each variety (Table 3.1) Spectral reflectance was computed as the ratio of reflected radiance to incident radiance estimated from a calibrated spectral on white reference (Milton and Rollin, 2006).

All the measurements were carried out in the experimental fields of Assam i.e. at RRLRRS (Study site 1) under controlled environmental conditions with certain agriculture management practices.

3.3.2 Field survey

Field campaigns were conducted to understand the field topography and obtain detailed information about agricultural inputs used by farmers for the rice agriculture systems of the study sites.

A survey was conducted in the experimental fields at RRLRRS, Assam (Study site 1) during the monsoon period of the year 2014 (Figure 3.6 and 3.7). Here in Assam, the farmers have not yet taken to mechanised cultivation and small holdings of farmers in general stand in the way of mechanised farming. Therefore, almost every farmer practices agriculture farming by manual labour mostly. The detailed information regarding cultivated rice varieties, application of fertilizers and method of irrigation were collected. Based on the topography, rice varieties like Shabhagi Dhan, Ranjit, Baismuthi, Anjali, BPT5204, IR64, Tapaswini, Joymati, Vandana, Luit and Naveen were grown in the rice agriculture system of the study site. Organic manure was applied as fertilizer before transplanting or at the time of final ploughing. Then, urea was applied in three splits, first 1/3rd at the time of final puddling, second (1/3rd) at tillering stage and third (1/3rd) at panicle initiation stage. The paddy crop cycle, here in Assam, was highly dependent on rainwater. Sometimes, the water pumped from the Brahmaputra riverbed, and other times, water from canal irrigation was used to maintain standing water to a depth of 2-3 cm during monsoon period in the paddy field.

Source: Field Photograph **Name:** Patani, Assam
Date: 10th Oct, 2014 **Location:** 26°15'30.02" N, 91°33'45.31" E

Figure 3.6 : Photograph showing farmer interaction for winter rice during the field campaign

Source: Field Photograph **Name:** Abhayapur, Assam
Date: 18th Nov, 2014 **Location:** 26°15'30.02"N,91°33'45.31"E

Figure 3.7 : Photograph showing winter rice field condition during the field survey

Source: Field photograph **Name:** Dhansarapatna, Odisha
Date: 25th August, 2016 **Location:** 20°19'5.45" N, 85°32'32.63" E

Figure 3.8 : Photograph showing summer rice field condition during the field survey

Another, field campaign was conducted in the farmers' agricultural fields at Cuttack, Odisha (Study site 2) during the pre-monsoon period of the year 2016 (Figure 3.8). In this campaign, detailed information were collected, through interaction with farmers, regarding summer paddy crop varieties, topographic conditions suited for summer rice cultivation, application of fertilizers and mode of irrigation used in the agricultural farmland. Rice genotypes such as Khandagiri, Konark, Lalata, Laxmisagar, Naveen, No 303, Purusotum, Pratikhya and Surendra were grown in this site with assured irrigation. Here, number of small holdings of farmers were less as compared to the site in Assam. Still the farmers were following mostly traditional method of cultivation, though mechanised cultivation methods were also adopted to some extent. The most important factor for summer rice production is availability of steady supply of water at early seedling stage with low temperature condition. Rice cultivation during the summer season is highly dependent on availability of water. The coastal belt rice lands generally suffer from serious water logging problems and are generally flood prone. Here, the soil type mostly is of deltaic alluvial and lateritic, these soils are generally fertile. The summer rice cultivation in Odisha is mainly controlled by the slope of the agricultural land according to which irrigation water is supplied. For adequate water supply throughout the cropping cycle

of paddy crop during pre-monsoon period, water from Rana river bed and also from bore wells were used for irrigation in the fields. Mostly, urea was applied as fertilizer in three splits in addition to organic farmyard manure in a similar way as mentioned for Study site 1.

3.4 Satellite Data Acquisition

Satellite data from different sensors were collected to study the field scale variability of paddy crop. Hyperspectral data from advanced hyperspectral satellite sensor i.e. Hyperion (EO-1) sensor and multispectral data from LISS IV (IRS-P6) satellite sensor were used for the purpose of the present research work.

3.4.1 Hyperspectral Satellite Data

Hyperspectral satellite data was acquired from Hyperion sensor, the first successful operational hyperspectral sensor (https://eo1.usgs.gov). It was launched in November 2000 on the NASA Earth Observation-1 (EO-1) satellite. It was the first mission in NASA's New Millennium Program. The primary objective of this mission was the validation of new technologies. The secondary objective of the mission is to extract useful information for a wide range of applications in the field of mining, geology, forestry, agriculture and environmental management. The Hyperion sensor delivers an advanced class of Earth observation data for improved Earth surface characterization through a fore-optics system designed with two separate grating image spectrometers in the Hyperspectral Imaging Instrument (HSI). The Hyperion has the potential to characterize the resolution of surface properties in terms of hundreds of spectral bands. Hyperion sensor on board the Earth Observing-1 (EO-1) mission is unique in the way that it maintains a high resolution hyperspectral imager capable of resolving wavelength range from 357 – 2576 nm, spanning the VIR/NIR and SWIR regions, into 220 contiguous unique spectral bands of 10 nm resolution each. Hyperion is a push-broom instrument that operates in a 705 km orbit around the earth. It can capture a surface area of 7.5 km by 100km in a single image at a spatial resolution of 30 m. The images acquired by EO-1 Hyperion sensor containing the spatial location of the scenes are periodically archived in the U.S. Geological Survey (USGS) Center for Earth Resources Observation and Science (EROS). Ready information on a temporal scene for a certain location is not available. It acquires data purely on the basis of customers' Data

Acquisition Requests (DARs). The Hyperion data enhanced land assets classification, better crop yield prediction, accurate remote mineral exploration and better containment mapping (Galloza and Crawford, 2011). Therefore, for the present study, Level 1 radiometrically corrected Hyperion satellite data were requested for the study sites in Assam (Study site 1) and Odisha (Study site 2) under DARs scheme and downloaded from (https://eo1.gsfc.nasa.gov/). Each of the data sets comes with a meta data file containing date and time of acquisition, latitude, and longitude. The details of the scene characteristics of the acquired Hyperion images of study sites in Assam and Odisha, which were used for field scale crop parameters variability mapping are listed in Table 3.2 and Table 3.3 respectively. As, Hyperion is a push broom sensor, it also captures noise during image acquisition. These images obtained from the Hyperion sensor have to be pre-processed carefully before analyzing them for any other application.

3.4.1.1 Hyperspectral data pre-processing

The radiometrically corrected image acquired from Hyperion sensor EO-1 satellite covering the experimental site required careful processing to nullify the sensor noise (https://eo1.usgs.gov). It was processed by using remote sensing (RS) image processing software ENVI 4.5. The hyperspectral imagery pre-processing includes rescaling, abnormal pixels stripping, cross-track illumination correction, elimination of non-calibrated, bad bands, destripping, Minimum Noise Fraction Transformation (MNFT) prior to atmospheric and geometric correction.

3.4.1.1.1 Bad band removal

This pre-processing not just eliminates sensor noise, but also reduces data dimensionality so as to reduce computational complexity. Bad band removal is the first major step for high dimensional data pre-processing. Hyperion level L1R data provides 242 contiguous spectral bands that cover a wide spectral range (400 - 2500 nm) with a narrow spectral resolution (10 nm). Amongst those bands, only 198 are non-zero, i.e. some of them are deliberately left unused (bands 1 to 7 and 225 to 242) and a few fall in the overlapping region of the two spectrometers (bands 58 to 76). Amongst the non-zero bands, four bands are still within the overlapping region of the two spectrometers (bands 56, 57 and 77, 78), and out of these bands

77 and 78 were eliminated due to presence of higher noise levels in those bands (Datt et al., 2003).

Table 3.2 : Hyperion scene characteristics of Study site 1 in Assam during monsoon period.

Data Attribute	Attribute Value	Data Attribute	Attribute Value
Entity ID	EO1H1370422014276110KF	Scene Start Time	2014 276 03:31:43
Acquisition Date	2014-10-03	Scene Stop Time	2014 276 03:36:03
Site coordinates	26°15'15.08"N, 91°33'50.88"E	Target Path	137
NW Corner	26°32'37.82"N, 91°33'58.49"E	Target Row	42
NE Corner	26°31'21.42"N, 91°39'37.53"E	Sun Azimuth	128.989086
SW Corner	25°38'33.70"N, 91°19'12.63"E	Sun Elevation	46.655598
SE Corner	25°37'17.99"N, 91°24'49.24"E	Satellite Inclination	97.93
Cloud Cover	10% to 19%	Look Angle	26.119

Table 3.3 : Hyperion scene characteristics of Study site 2 in Odisha during pre-monsoon period.

Data Attribute	Attribute Value	Data Attribute	Attribute Value
Entity ID	EO1H1400462016068110Pp	Scene Start Time	2016 068 02:54:11
Acquisition Date	2016-03-08	Scene Stop Time	2016 068 02:58:47
Site coordinates	20°19'24.84"N, 85°32'41.94"E	Target Path	140
NW Corner	21°00'17.13"N, 85°38'52.09"E	Target Row	46
NE Corner	20°59'24.48"N, 85°43'05.70"E	Sun Azimuth	109.534697
SW Corner	19°07'16.76"N, 85°12'44.88"E	Sun Elevation	32.224293
SE Corner	19°06'24.65"N, 85°16'55.60"E	Satellite Inclination	97.97
Cloud Cover	10% to 19%	Look Angle	8.4442

3.4.1.1.2 De-stripping

The radiometrically corrected Hyperion L1R contains vertical stripes in various individual bands of the data set. Such errors are caused by detector nonlinearities and temperature of push-broom imaging Hyperion (EO-1) sensor. The vertical stripes are found along the track direction and appear as a series of stripes either along the whole length of the image or intermittently at lower DN values of the image (Kar et al., 2016; Vyas et al., 2011). Occurrence of such stripes is known as striping noise. These vertical stripes and the corrupted pixels are referred to as abnormal pixels which should be removed before further processing. Such errors were eliminated by averaging neighbouring DN values to get the destriped image after thorough examination of each grey scale pixel.

3.4.1.1.3 Minimum Noise Fraction Transformation (MNFT)

Further, in order to reduce data dimensionality of the data set, Minimum Noise Fraction Transformation (MNFT) was adopted for the segregation of noise dominated bands from the bands containing important information. Lower signal-to-noise ratio bands were isolated from MNF bands. To resolve the cut off region between signal and noise, eigenvalues for MNF bands were calculated. It was found that the bands having eigen value less than or equal to unity were mostly noise dominated bands and eigen value greater than unity were the important bands contributing to the overall variance in the dataset. Consequently, the computational time for processing the data set was greatly reduced as there were very small number of noise-free components left after MNFT of the image.

3.4.1.1.4 Atmospheric and Geometric correction

Radiometrically calibrated hyperspectral imagery contains not only information related to the material properties of a surface target but also the noise due to the atmospheric layers between the surface target and the sensor. As the image is taken from a very high altitude, it attenuates with atmospheric interventions. Hence, there is a necessity of atmospheric correction to eliminate atmospheric influences on the Hyperion images. Fast Line-of-sight Atmospheric Analysis of Spectral Hypercubes (FLAASH) algorithm implemented in the FLAASH ENVI module was applied to filter out target reflectance from the mixed signal. To

convert the calibrated image to apparent reflectance image, input parameters such as sensor type, sensor altitude, ground elevation, pixel size, scene centre location and scaling factor for VNIR and SWIR were incorporated. The atmospherically corrected image has better and pronounced spectral properties.

Additionally, the Hyperion L1R product was not geometrically corrected, hence the processed output image was further examined to get geometrically corrected product using L1Gst Hyperion data of the same area. Here, nearest neighbourhood resampling method was applied in order to avoid spectral interpolation. At last, a spatial subset was selected from the whole scene from each of the study sites for analysis.

3.4.2 Multispectral Satellite Data

At present, India is one of the leading countries in the world known for the operational use of satellite remote sensing for developmental purposes. The Indian earth observation system is extensively acclaimed all over the world for its application driven approach**.** Crop studies is generally not possible using satellite data during monsoon season (July-November) due to cloud cover in the sky. So, completely cloud free images from IRS-P6 (Resourcesat-1) are not available during this period. IRS-P6, LISS IV sensor data covering the Study site 2 in Odisha, acquired on 22nd March, 2016, was procured for this study from National Remote Sensing Centre, India (https://www.nrsc.gov.in). IRS-P6 (Resourcesat-1) is regarded as a continuation of Indian Remote sensing (IRS-1C/1D) programme with significant improvements. Resourcesat-1 (IRS-P6) was launched on 17th October, 2003. The objective of Resourcesat-1 is to provide both multi-spectral and panchromatic imagery of the earth features. It is assimilated with three sensors on-board: a Linear Imaging and Self Scanning sensor (LISS-III), an Advanced Wide Field Sensor (AWiFS) and a high resolution multi-spectral camera LISS-IV along with an On-Board Solid State Recorder (OBSSR). The most interesting feature of this satellite is that the LISS-IV camera is a multi-spectral high resolution camera with a high spatial resolution of 5.8 m at nadir. This camera can be operated in two modes, i.e. in Mono and Multi-spectral modes. Another interesting feature of this camera is the potential of off-nadir viewing by tilting the camera up to ± 26° across the track direction. This way, it can deliver the data with a revisit of 5 days for a particular land surface.

The LISS-IV sensor has three bands in different regions of electromagnetic radiation (EMR) (b2: Green, b3: Red, b4: IR). The details of LISS-IV data is shown in the Table 3.4. Satellite based multispectral imagery contains various quantitative information related to the surface and the atmosphere. So, atmospheric correction is necessary to retrieve surface reflectance and eliminate the contamination due to influence of high altitude. In this study, atmospheric correction is done by the FLAASH module coupled with ENVI 4.5. Necessary parameters for the FLAASH were determined by the metadata of the image files. The multispectral remote sensing data has the capability of providing crop field variation at the plot scale during the crop developmental age, only when this high spatial resolution data is merged with the hyperspectral data.

Table 3.4 : LISS IV sensor data specification

Spectral Band (nm)	Swath Width	Spatial Resolution	Radiometric resolution
b2 : 520 – 590 b3 : 620 – 680 b4 : 770 –860	70/23 Km	5.8 m	10 bit

3.5 Plant Sampling

The plant leaf samples were collected from the experimental study site in Assam, India (Study site 1). The most important paddy crop growth parameters like chlorophyll, nitrogen and leaf relative water content were measured for each of the 24 rice genotypes from their respective experimental plots during their crop developmental phase. Just after each canopy spectral reflectance measurement, plant samples (7-15 plants/plot) were randomly selected and carried over to the laboratory facility of IIT Guwahati for the chemical analysis to retrieve the chlorophyll and leaf relative water content whereas nitrogen content was estimated by using laboratory facility under RRLRRS, Assam (Figure 3.9).

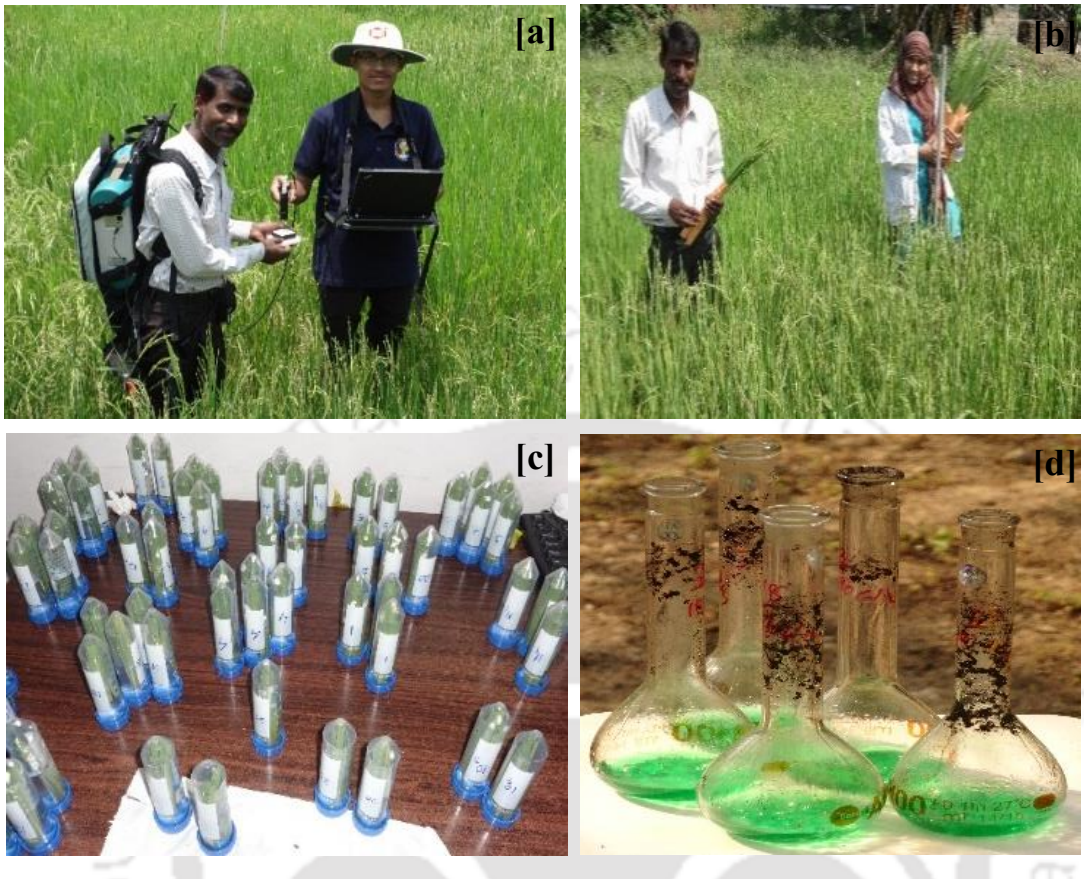

Figure 3.9 : (a) Spectral measurement (b) Plant samples collection just after spectral measurement (c) Preparation of plant sampling for laboratory measurements (d) Conducting chemical analysis experiments using plant samples

3.6 Conclusions

To study the field scale variability of paddy crop parameters and its mapping over a rice agriculture system, all the necessary data were collected from different sources to address such a challenging task. The *in-situ* data were required to capture the paddy crop behaviour as well as to validate the research findings. Hence, *in-situ* data were collected in-time covering the paddy crop developmental period in two different seasons. The satellite data has the capability to map the spatial distribution of paddy crop parameters from space platform and their variability at plot level within the paddy crop field to build a precision rice agriculture system. The important crop parameters like chlorophyll, nitrogen and leaf water content were also

measured for the rice leaves during the entire crop growth period. Field campaigns have also provided a great vision into this demarcated complex problem. Therefore, plant sampling and ground based measurements have offered much evidence to strengthen this research work.

4 Plant Growth Monitoring via Proposed Improved Vegetation Indices

4.1 Introduction

In this chapter, assessment of rice plant growth was demonstrated using *in-situ* hyperspectral data. Information on the spatial distribution of paddy rice fields is crucial for rice crop and water resource management. To achieve improvement in rice productivity, basic information on rice crop area and its distribution is indispensable. Remote sensing techniques provide effective means for producing data regarding agricultural cropping system over a large area quantitatively as well as qualitatively. For extracting crop area, crop growth profile and crop yield, cropping systems are being monitored using both optical and microwave remote sensing techniques. Extensive research work has been carried out globally with moderate resolution images from NOAA AVHRR and MODIS, to monitor large area rice fields **(**Fang et al., 1998; Xiao et al., 2006). However, in small rice areas the use of global satellite images with moderate spatial resolution is limited as it reduces the accuracy of the assessment**.** In this context, hyperspectral remote sensing plays a crucial role. The advantage of hyperspectral remote sensing data over other remotely sensed data is that it acquires information of an earth feature in the form of hundreds of narrow bands, which others cannot.

It is helpful for extracting additional detailed information with significant improvement over broad bands in the analysis of different physical variables of agricultural crops **(**Tang et al., 2007). Over the past few decades, extensive studies have been carried out on the spectral characteristics of vegetation cover, especially crop species. The MODIS data have been used

to establish relationship between spectral variation of paddy crop and the yield of rice, and also the relationship between rice age and NDVI have been evaluated (Nuarsa et al., 2011). Spectral signatures of crops at various wavelengths, which are governed by leaf inter cellular structure, chlorophyll content, carotenoid content, nitrogen content, water content (Asner 1998; Stimson et al., 2005) and rice plant growth (Yang and Chen, 2004) can be achieved through remotely sensed high spectral resolution data. Each of these features is significant at a specific wavelength (Lee et al., 2008; Zhu et al., 2008). However, field spectroradiometry enables us to directly assess spectral reflectance of land covers (Hill et al., 2012; Prasad et al., 2015). Spectral reflectance obtained from plants provides information on plant characteristics (Ray et al., 2006) and on the other hand, the spectral signatures of features obtained can used as end members in hyperspectral classifications (Kneubuehler et al., 1998).

Currently, with regards to high spatial and spectral resolutions, satellite hyperspectral remote sensing have been used as an effective method in estimation of nutrient concentration of vegetation over a large cultivated area (Darvishzadeh et al., 2008). However, very few research works have been carried out in India to understand the varietal rice management practices using hyperspectral remote sensing (Choudhury and Chakraborty, 2006;Kumar et al., 2013; Prasannakumar et al., 2014; Tripathi et al., 2013). Field based hyperspectral data utilization for different rice varieties may recognize the effect of application of nitrogen levels at different crop stages. In addition to this, hyperspectral remote sensing of biophysical and biochemical parameters has been achieved through the development of new hyperspectral indices (Galvao et al., 2009; Thenkabail et al., 2000). Spectral index is the mathematical transformation of spectral reflectance to augment signals coming from vegetation (Cho et al., 2008; Das and Seshasai, 2015; Nagendra, 2001). Therefore, an attempt has been made to evaluate the potential of hyperspectral narrow band indices in retrieving plant characteristics that differ in canopy structure and biochemical compositions. This study has been carried out to demonstrate the usability of hyperspectral data in obtaining the temporal spectral signatures of rice varieties with an emphasis on critical wavelengths and to derive advanced vegetation indices for monitoring rice growth in Indian rice agricultural system incorporating different levels of nitrogen applications.

4.2 Material and Methods

4.2.1 Study area

The agricultural paddy fields at experimental station of RRLRRS, Assam, India (Study site 1) centred at latitude 26°15'15.08"N and longitude 91°33'50.88"E was selected as the study site for taking measurements. The study area is described in detail in Chapter 3.

4.2.2 Data used

For the present study, a portable handheld spectroradiometer (FieldSpec-FR, ASD, India) with a spectral range 350-1050 nm has been used. This radiometer measures the radiance in narrow spectral bands within the spectral range of 350 nm to 1050 nm with an interval of 2 nm. Measurements were made in an irrigated experimental paddy field in 2009 (Study site 1). The field was under paddy cultivation already for several years prior to the studies. The paddy field was divided into 72 subplots of size 3.3 m × 3.4 m, each plot having similar soil type, temperature and field conditions. These studied plots include eight rice varieties namely *Gautam, IR-64, IET-18558, IET-19601, K.Hansa, Chandrama, IET-19600 and IET-20166.* The field layout is shown in Figure 4.1. Measurements were taken randomly from all the plots with same irrigation, soil properties and phenological stages but with different levels of nitrogen fertilizer applications (50, 100, 150 kg/ha). Measurements of the hyperspectral reflectance were made during January, 2009 to May, 2009 covering its transplanting to harvesting stage at weekly intervals for the eight rice varieties with different nitrogen fertilizer applications. The details of these field setup and measurements are described in Chapter 3.

Hyperspectral measurements obtained from the spectroradiometer were pre-processed and temporal profiles of spectral reflectance were generated for all the combinations of nitrogen applications and crop varieties. Temporal profile of one of the samples obtained from our study is displayed in Figure 4.2. The overall spectral signature for different varieties followed a similar trend but the changes were observed at different wavelengths for different varieties. During early crop days, the reflectance was found very less in blue wavelength range and on the other hand, in green band, reflectance value was quite noticeable.

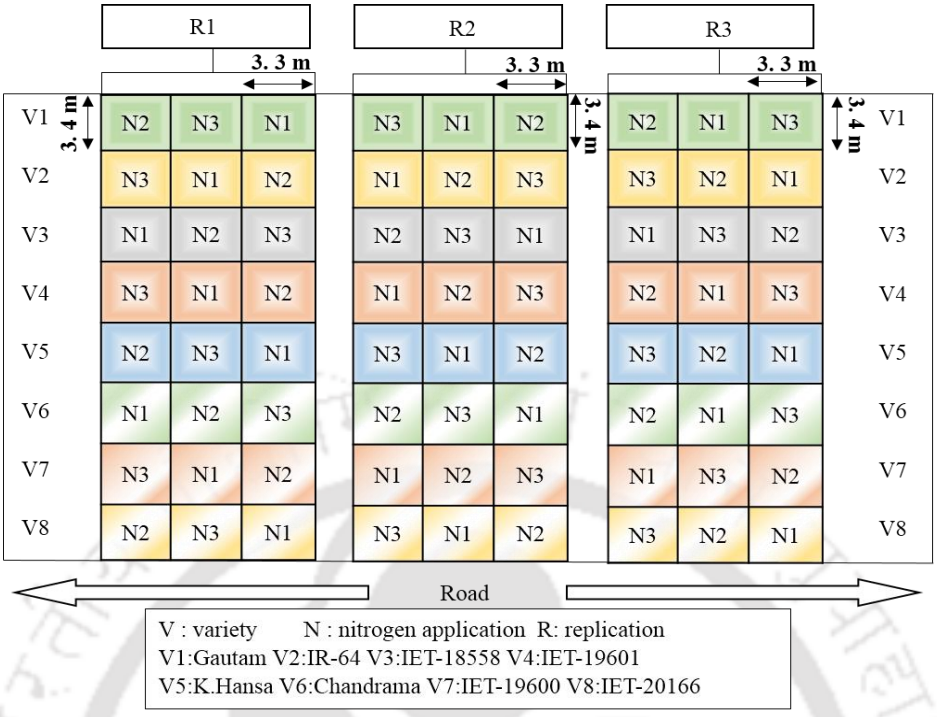

Figure 4.1 : The field layout of experimental plots

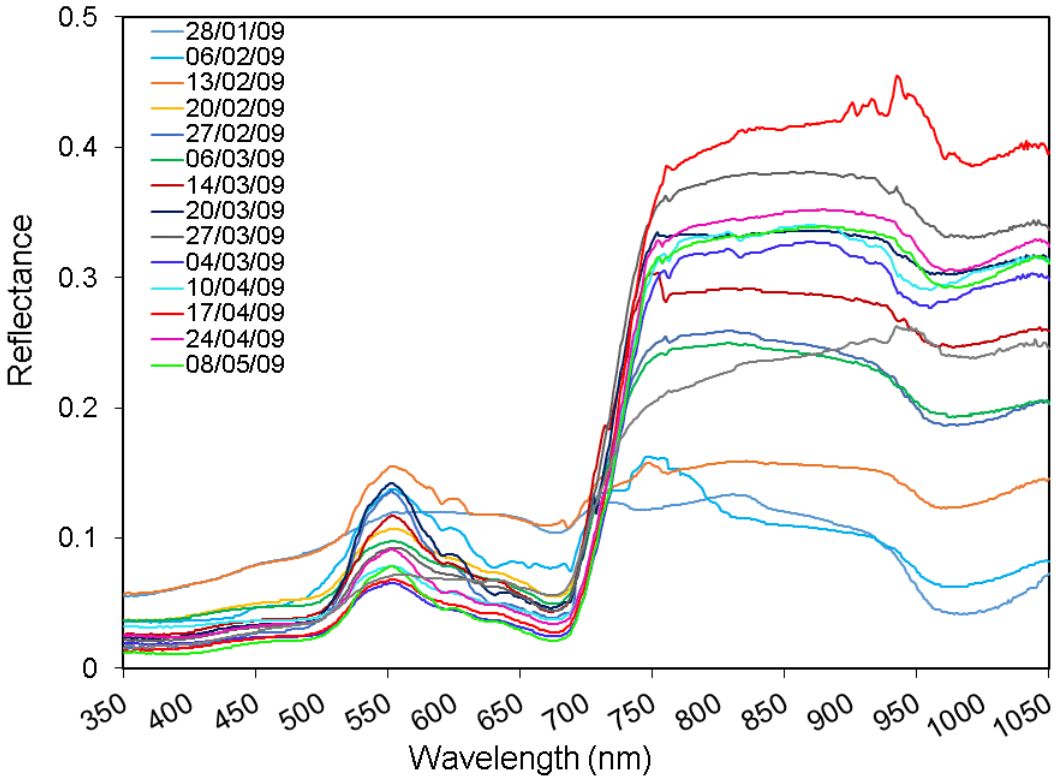

Figure 4.2 : Temporal signature of rice variety IET-19600

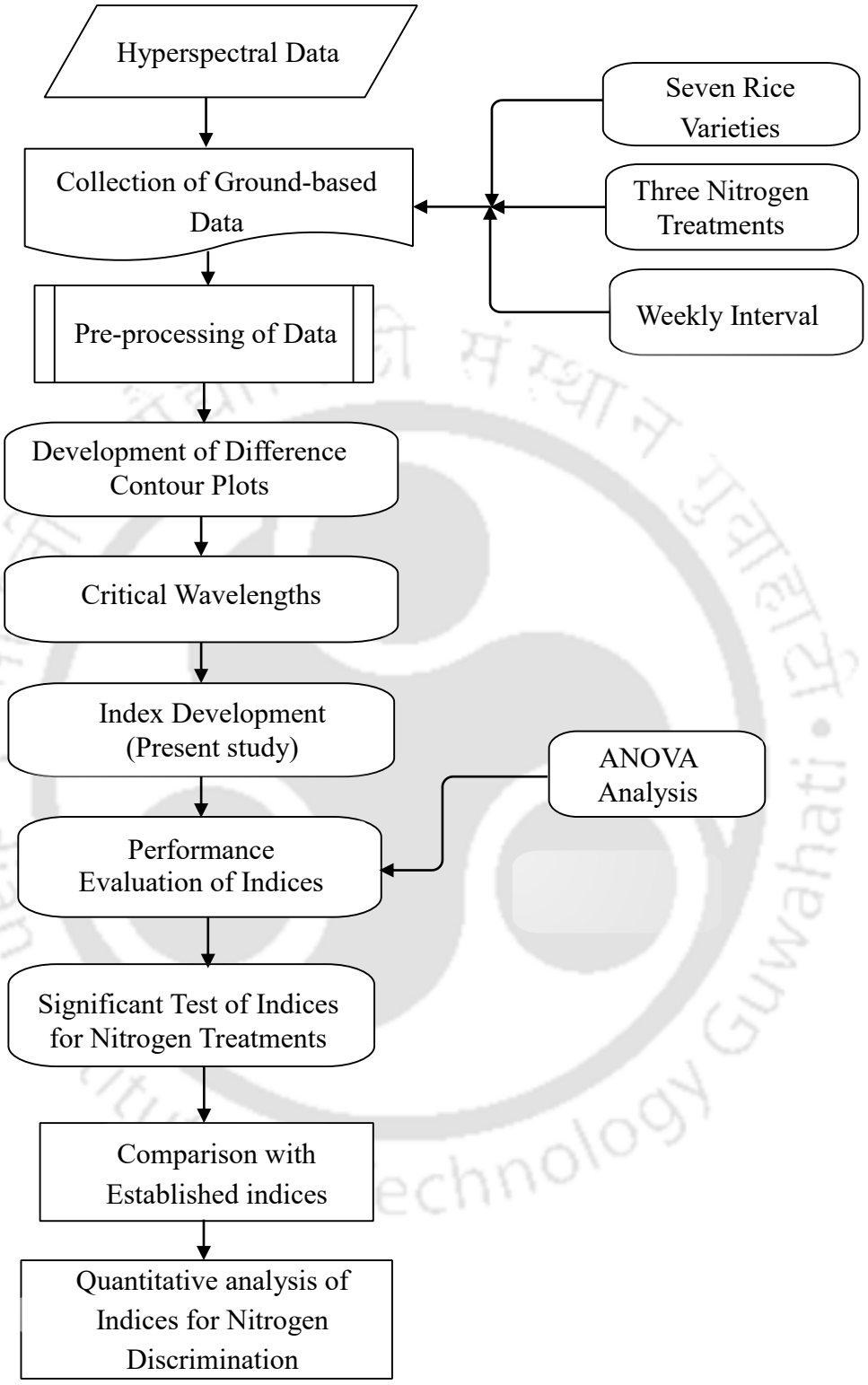

Figure 4.3 : Flow-chart showing methodology adopted for the discrimination of nitrogen treatments in paddy crop

4.2.1 Differential plot analysis

It is very much essential to know at which wavelengths, reflectance of rice canopy behaves significantly for the different nitrogen treatments. By knowing these critical wavelengths one will be able to analyse the effect of nitrogen on different rice genotypes easily. To find the critical wavelengths, difference analysis was employed for the present study. It includes three nitrogen levels (N_1, N_2 and N_3) along with eight rice varieties. Here nitrogen level 'N_1' was considered to be the base level of measurement.

Three criteria for selection of critical wavelengths are

(i) Differences $\Delta\rho_{N_{3-1},\lambda}$ and $\Delta\rho_{N_{2-1},\lambda}$ should be greater than 10% ρ_{N_1} at that wavelength

(ii) At the wavelength, there should be local maxima in the difference plot.

(iii) The difference should be consistently significant**,** at least two months**,** during crop growth period.

where, for a particular rice variety

$$\Delta\rho_{N_{3-1},\lambda} = \rho_{N_3,\lambda} - \rho_{N_1,\lambda} \tag{4.1}$$

$$\Delta\rho_{N_{2-1},\lambda} = \rho_{N_2,\lambda} - \rho_{N_1,\lambda} \tag{4.2}$$

where,

$\Delta\rho$ = spectral reflectance difference

λ = wavelength

Difference contour plots were developed for all the studied rice varieties. By following above criteria, some of the wavelengths were marked as critical wavelengths from these contour plots for different varieties and nitrogen applications. Taking these critical wavelengths into consideration, vegetation indices were developed. One-way ANOVA (Analysis of variance) was used to quantify the performance of indices and differentiate nitrogen variabilities among the rice genotypes. The values of different indices were compared to find significant differences between nitrogen levels of eight rice genotypes at wavelengths related to nitrogen

and the difference between pairs was found out by using paired Tukey's test at assumed level of significance, $p < 0.01$. According to the test result, if F-value > F-critical at $p = 0.01$ (chosen level of significance) then it implies that the vegetation indices have significant difference between their nitrogen levels. Chen and Wang (2014) applied ANOVA to study diagnosis of rice nitrogen stress. Step-wise procedure has been described in the flow chart (Figure 4.3) to discriminate different nitrogen treatments by employing improved vegetation indices.

4.3 Results and Discussion

4.3.1 Vegetation Indices

The experimental site was under paddy crop cultivation already for several years prior to our study. For our present study, same field conditions like soil type, climate, irrigation and cultivation practices were maintained. Therefore, the spectral reflectance at each wavelength of rice species was affected mainly by application of nitrogen neglecting any other controlling variables. Therefore, employment of vegetation indices derived from wavelengths sensitive to fertilizer nutrient can help to enhance probable differences between species. The spectral signature is a true indicator of this phenological change in rice crop. The spectral signature of different rice varieties with different levels of fertilizer are presented in Figure 4.4. From Figure 4.4, it is inferred that the spectral reflectance of rice genotype is higher at 82 days after transplanting (DAP) as compared to 67 DAP. The spectral reflectance of rice genotype is found to be lower for N_1 than N_2 application at 67 DAP. Moreover, it is noticed that spectral reflectance for N_3 is significantly higher than N_1 and N_2 at 67 DAP. While on the other hand, at 82 DAP, the spectral signatures of rice genotype are found to be significantly different for each treatment. This happened because the nitrogen treatments have no significant effect on rice growth at an early stage; however, they have substantial effect during its later stage of growth.

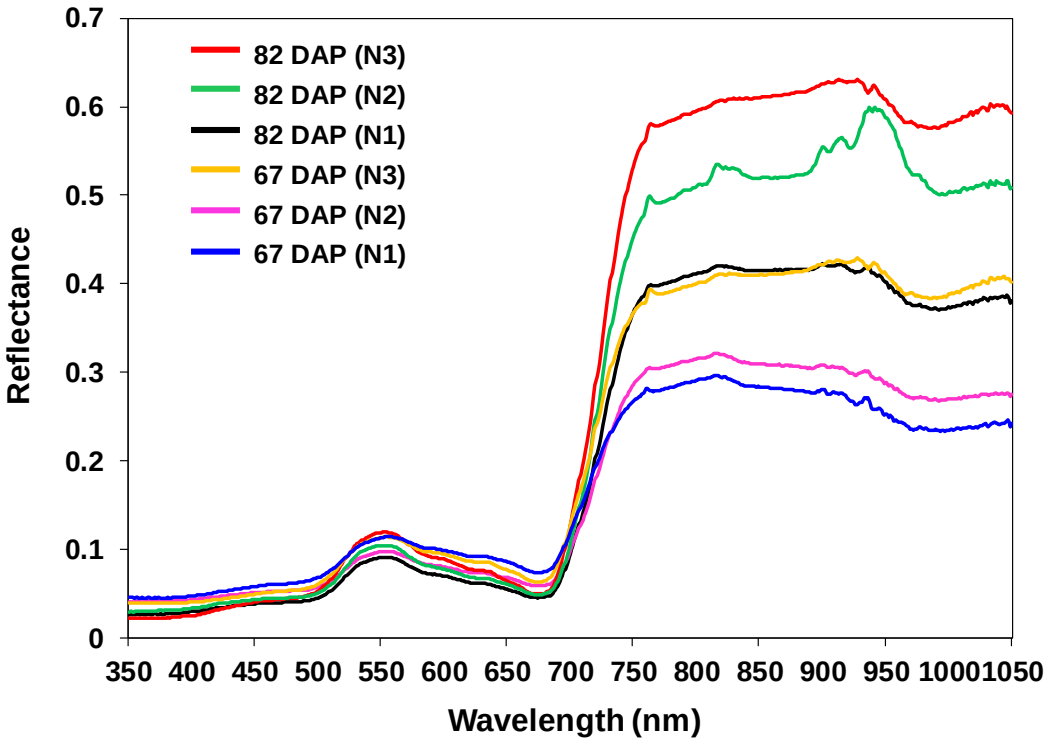

Figure 4.4 : Variation of nitrogen treatments at 67 DAP and 82 DAP

The observed spectral reflectance data were analysed to obtain the critical wavelengths at which the effect of nitrogen applications or crop varietal on spectral reflectance response is found significant. In order to find out these critical wavelengths, difference plots were developed for all the studied rice varieties (Figures 4.5-4.12). The contour maps were generated using the difference of nitrogen treatments and plotted in Grapher 8 platform.

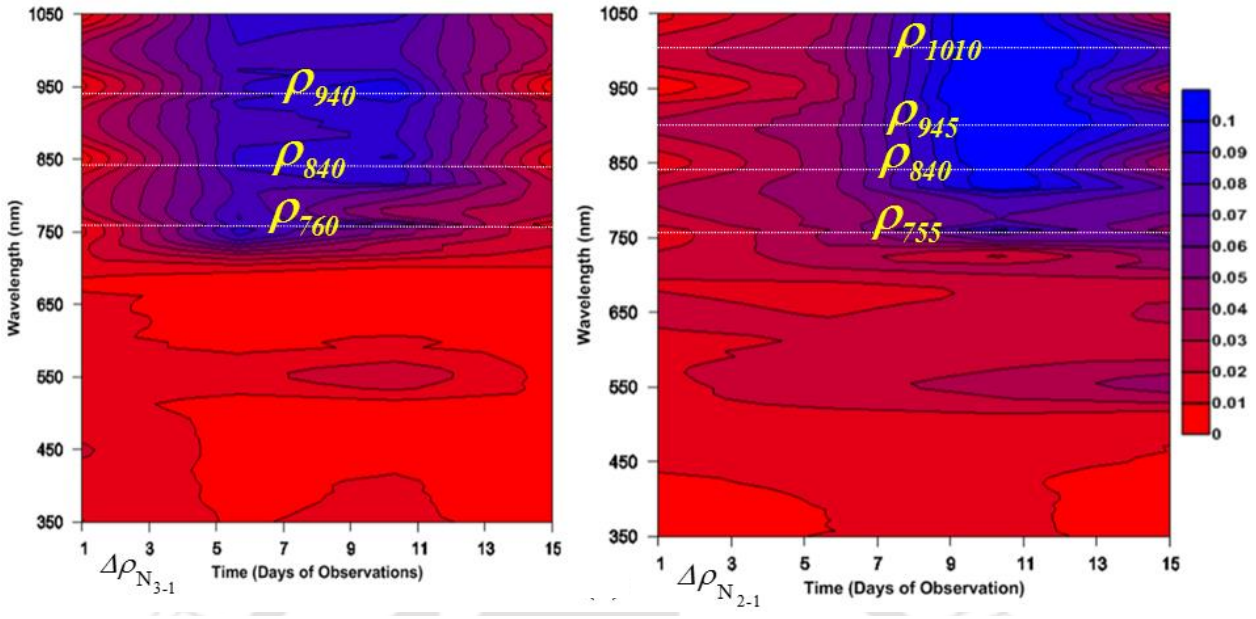

Figure 4.5 : Reflectance difference plots of rice genotype 'IR-64' with nitrogen applications showing critical wavelengths

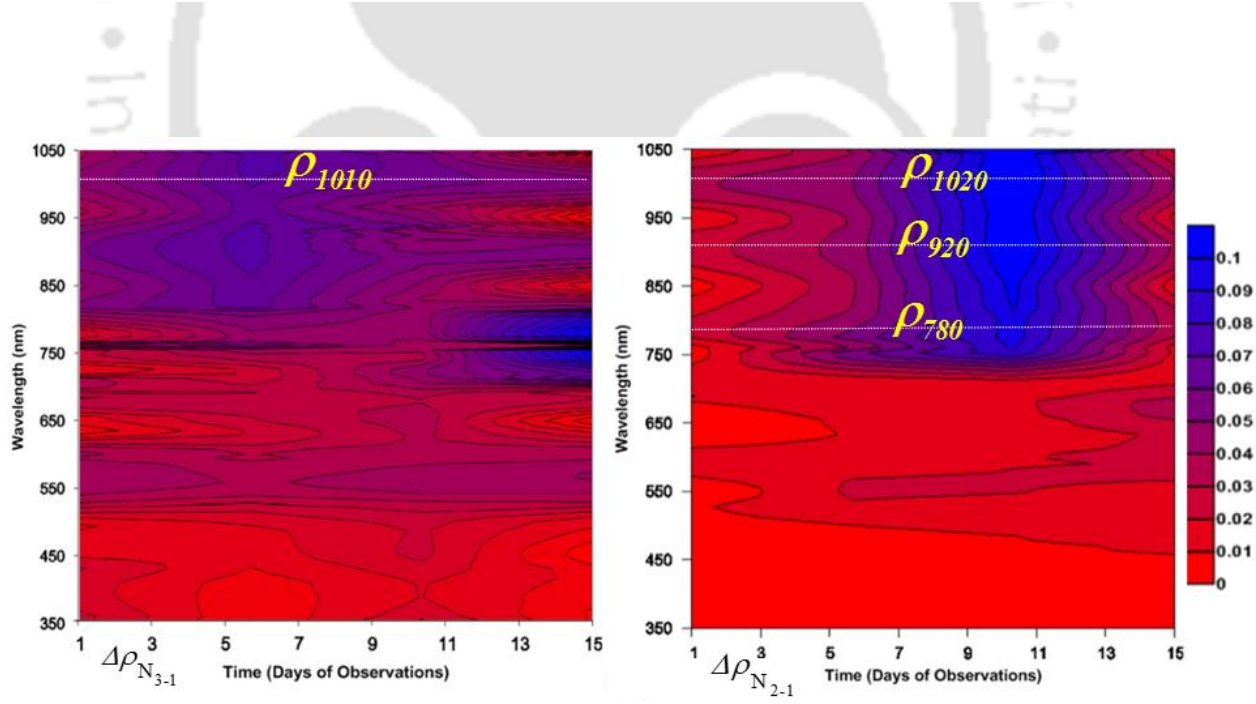

Figure 4.6 : Reflectance difference plots of rice genotype 'Chandrama' with nitrogen applications showing critical wavelengths

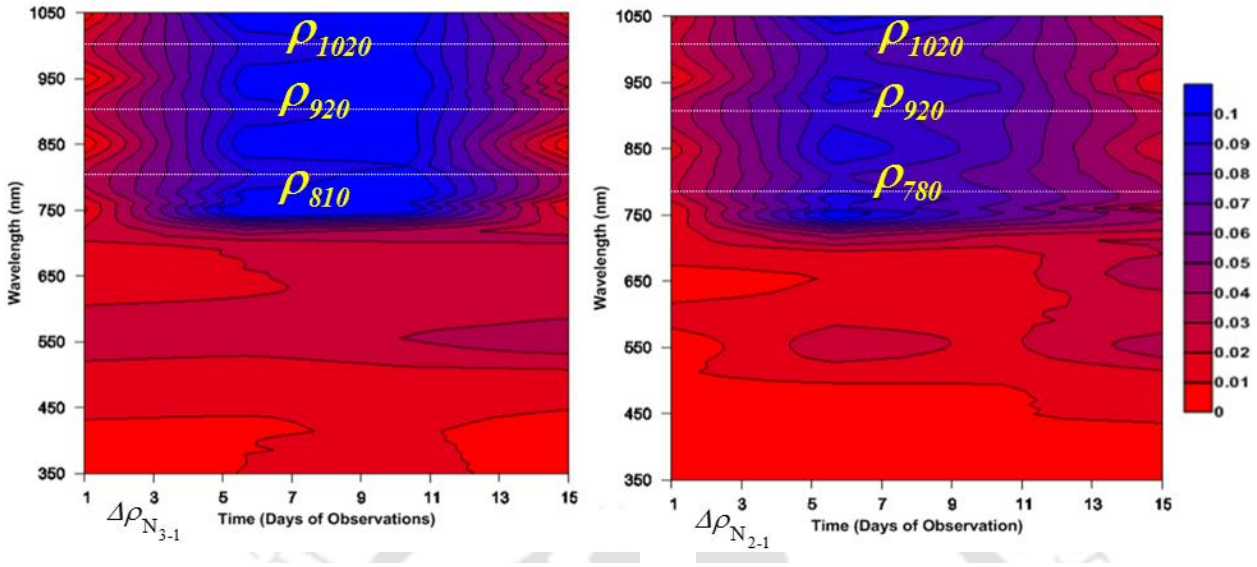

Figure 4.7 : Reflectance difference plots of rice genotype 'IET-19600' with nitrogen applications showing critical wavelengths

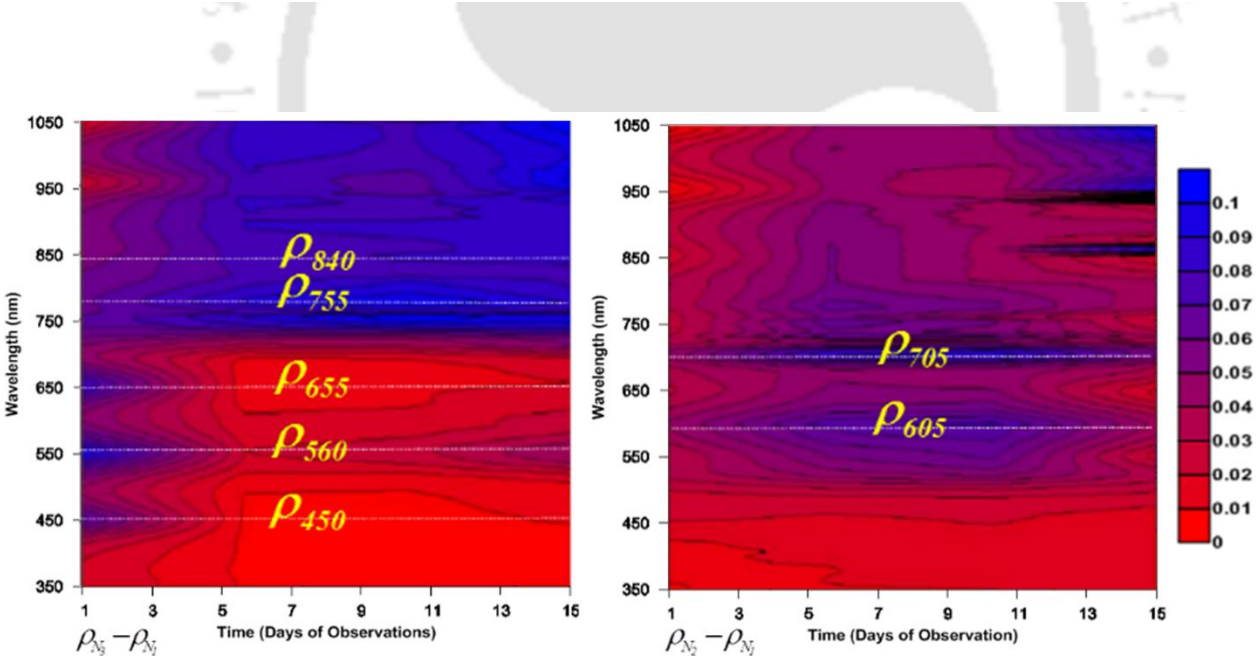

Figure 4.8 : Reflectance difference plots of rice genotype 'IET-19601' with nitrogen applications showing critical wavelengths

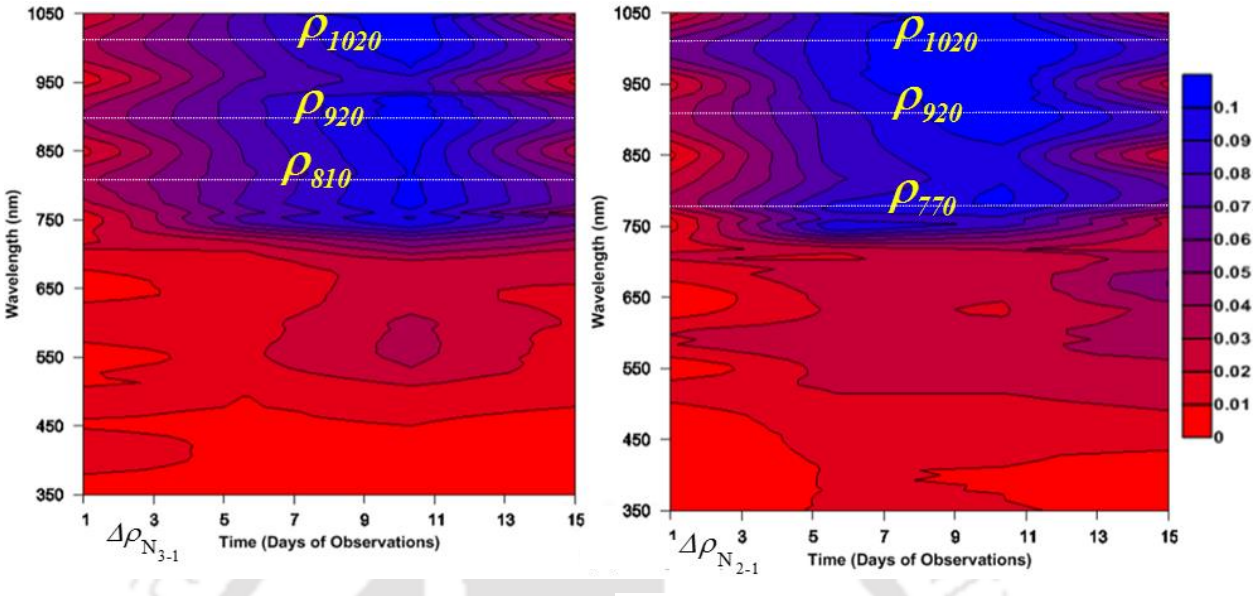

Figure 4.9 : Reflectance difference plots of rice genotype 'K.Hansa' with nitrogen applications showing critical wavelengths

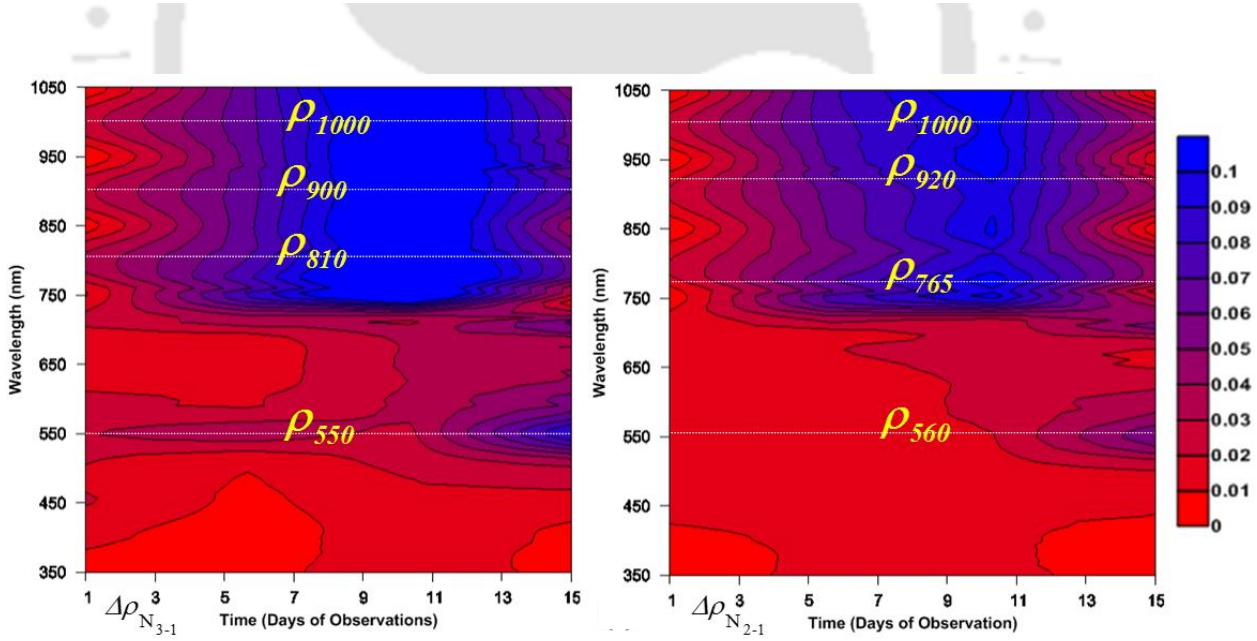

Figure 4.10 : Reflectance difference plots of rice genotype 'IET-20166' with nitrogen applications showing critical wavelengths

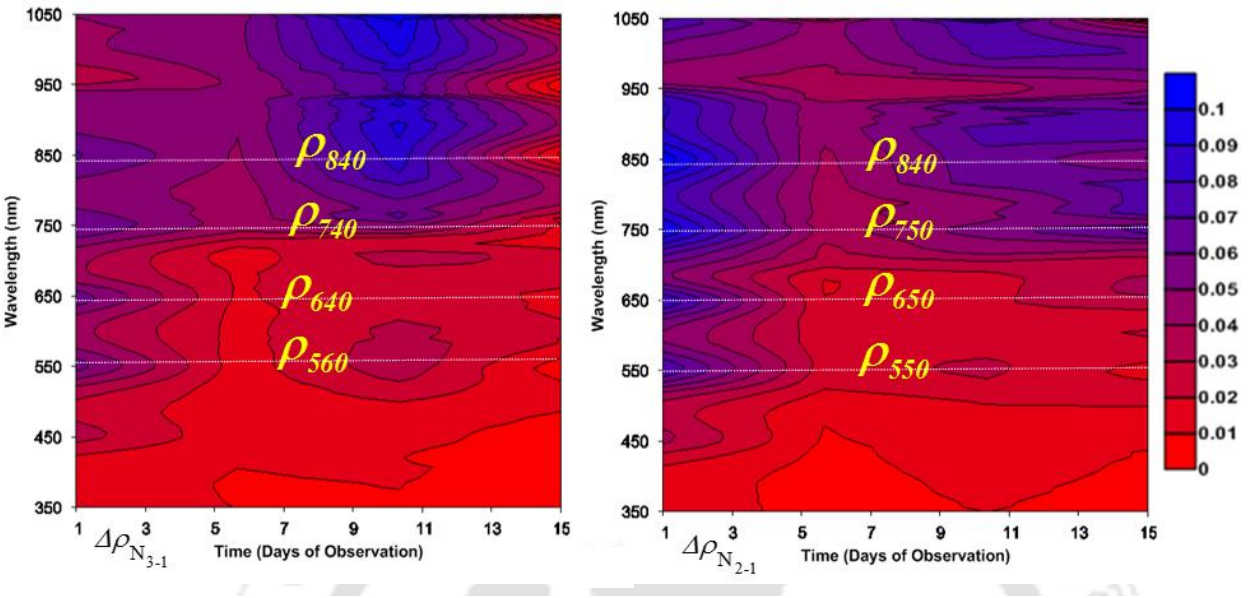

Figure 4.11 : Reflectance difference plots of rice genotype 'Gautam' with nitrogen applications showing critical wavelengths

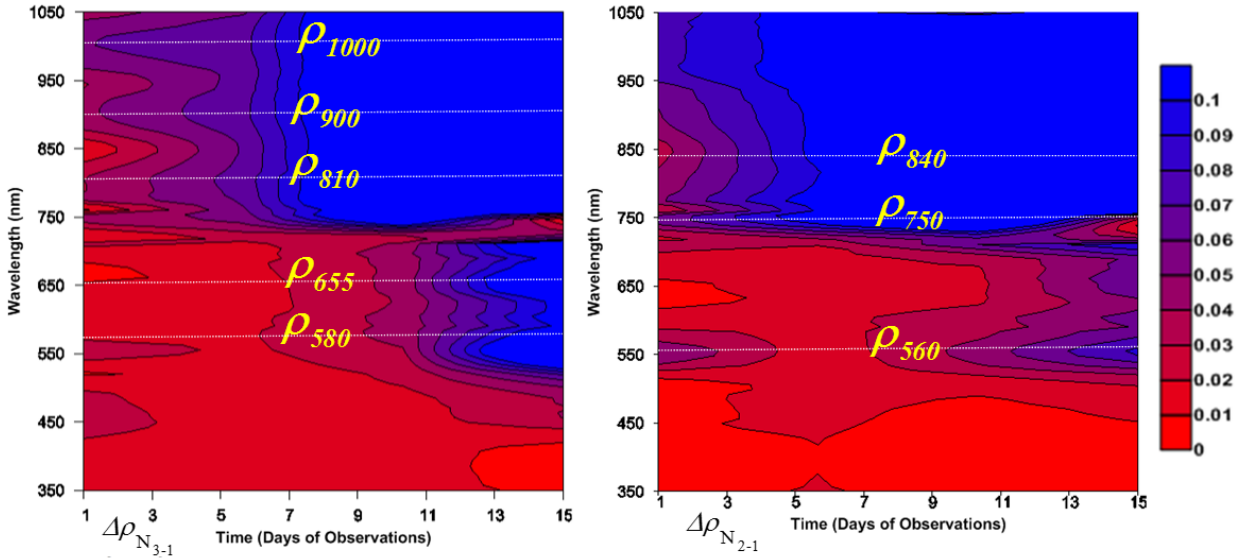

Figure 4.12 : Reflectance difference plots of rice genotype 'IET-18558' with nitrogen applications showing critical wavelengths

By analysing the difference contour plots of N_3-N_1 for eight different rice varieties, we observed that out of eight varieties, four varieties (*IR64, IET-19600, K.Hansa and IET-20166*) followed an identical trend i.e. growth appeared in the middle of the crop period and it diminished towards the end of the crop period. The critical wavelengths found were $\rho_{940}, \rho_{840}, \rho_{760}, \rho_{1020}, \rho_{920}, \rho_{810}, \rho_{1020}, \rho_{920}, \rho_{810}, \rho_{1000}, \rho_{900}, \rho_{810}, \rho_{550}$ (Figures 4.5, 4.7, 4.9 and 4.10). Another two species (*Chandrama, Gautam*) also followed similar trend like the above four varieties however with a less intensity of growth (Figures 4.6 and 4.11). For these two rice genotypes the critical wavelengths were found significant in near infrared region and visible region of the spectrum. Amongst the eight rice genotypes some peculiar characteristics were observed in two rice species, *IET-19601*(Figure 4.8) started growing at the same time similar to the aforementioned varieties but continued for a longer time than these varieties whereas in case of *IET-18558* (Figure 4.12) growth continued throughout the crop period. For these two rice species, the critical wavelengths were also found significant in near infrared region and visible region of the spectrum. Likewise, difference contour plots for N_2-N_1 were plotted for the same eight rice genotypes (Figures 4.5-4.12). From these contour plots, it was observed that the crop started growing in middle and then it decreased towards the end of crop developmental age. Such type of crop growth appeared almost in all rice varieties however, lesser intensity of growth was achieved in case of one or two varieties. An anomalous behaviour was marked in one amongst the eight rice species (*IET-18558*), where growth appeared late and continued for a longer time than other eight rice varieties (Figure 4.12). From all the differential contour plots, the wavebands that were demarcated as critical for different varieties are demonstrated in Figures 4.5-4.12.

From the above findings, it was manifestly displayed that specific wavelengths in the spectrum such as, $\rho_{550}, \rho_{560}, \rho_{655}, \rho_{750}, \rho_{755}, \rho_{780}, \rho_{810}, \rho_{840}, \rho_{900}, \rho_{920}, \rho_{1000}, \rho_{1010}, \rho_{1020}$ were highly assembled with a higher frequency of occurrence. To select the significant wavelengths from difference analysis, frequency of occurrence of wavelengths were evaluated (Figure 4.13) and a threshold frequency ≥ 2 was employed. The significant spectral wavebands were found in between Green, Red, and NIR spectral ranges (Table 4.1). With the selected significant wavelengths, we defined the most suitable vegetation indices that contain rich information on rice nitrogen content and the water content. These aforementioned critical

wavebands are sensitive to biophysical parameters of paddy crop and hence vegetation indices were selected according to Inoue et al. (2008) in which the ratio based vegetation indices are specifically aimed for one of the biophysical parameters i.e. nitrogen. Here, we examined advanced vegetation indices by taking critical wavebands sensitive to paddy growth into consideration which was different from earlier published indices (Inoue et al., 2008). Similarly, water index for this study was employed according to Penuelas et al. (1996) but with different narrow critical wavebands particularly designed for rice. Additionally, few indices having good statistical relationship with nitrogen content were found from extensive literature survey (Bolton and Friedl, 2013; Cammarano et al., 2014; Elvidge and Chen, 1995). Using the mentioned indices, one can evaluate spectral differences between various nitrogen levels with a better accuracy (Table 4.2).

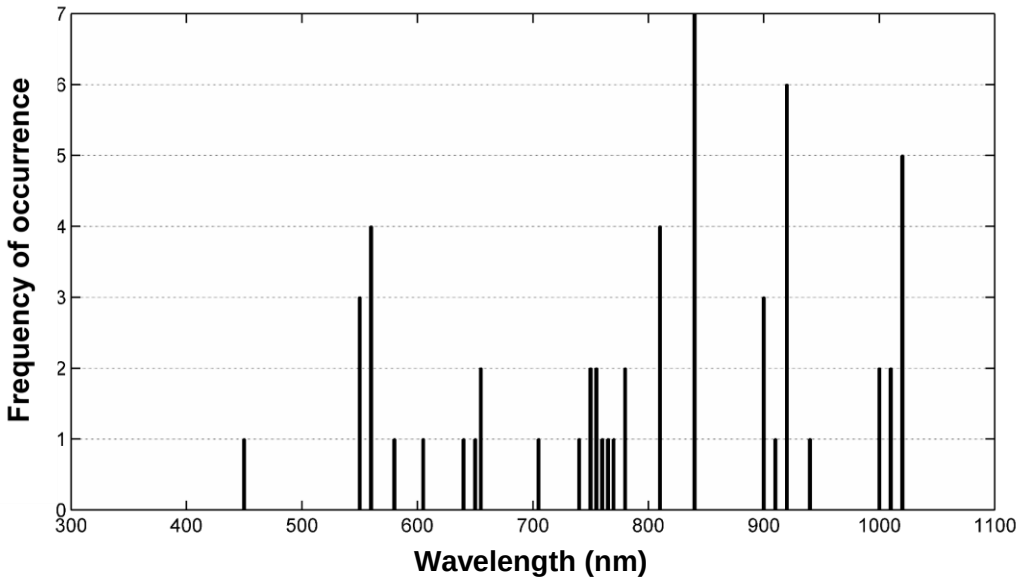

Figure 4.13 : Frequency of occurrence of wavebands selected from difference analysis

The temporal behaviour of the three vegetation indices are presented in Figure 4.14. From the Figure 4.14, it can be observed that by using three nitrogen based vegetation indices, growth occurred in an increasing trend, attained peak and then it decreased towards the end of the crop developmental age indicating its senescence period. Supply of water to the paddy crop is much important for its growth. Deficiency of water affects plant growth, development and also considerably affects the grain yield or crop failure (Sikuku et al., 2010). Therefore, the

temporal variation of proposed water index for different varieties was analysed and for instance, temporal variation for two varieties are shown in Figures 4.15 and 4.16.

Table 4.1 : Significant waveband selected for paddy crop prior to N application

Spectral range	Wavelengths (nm)
Green	550, 560, 569
Red	655
NIR	750,755,780,840,810,900, 920,1000,1010,1020

Table 4.2 : Vegetation indices derived for the present study

Vegetation Indices	Formulation	Reference
VI_1	ρ_{840}/ρ_{560}	Present Work
VI_2	ρ_{920}/ρ_{560}	Present Work
VI_3	ρ_{1020}/ρ_{560}	Present Work
WI	ρ_{1000}/ρ_{900}	Present Work
VI	ρ_{810}/ρ_{560}	Inoue et al. (2008)
GRI	ρ_{830}/ρ_{550}	Inoue et al. (2008)

* ρ : Reflectance

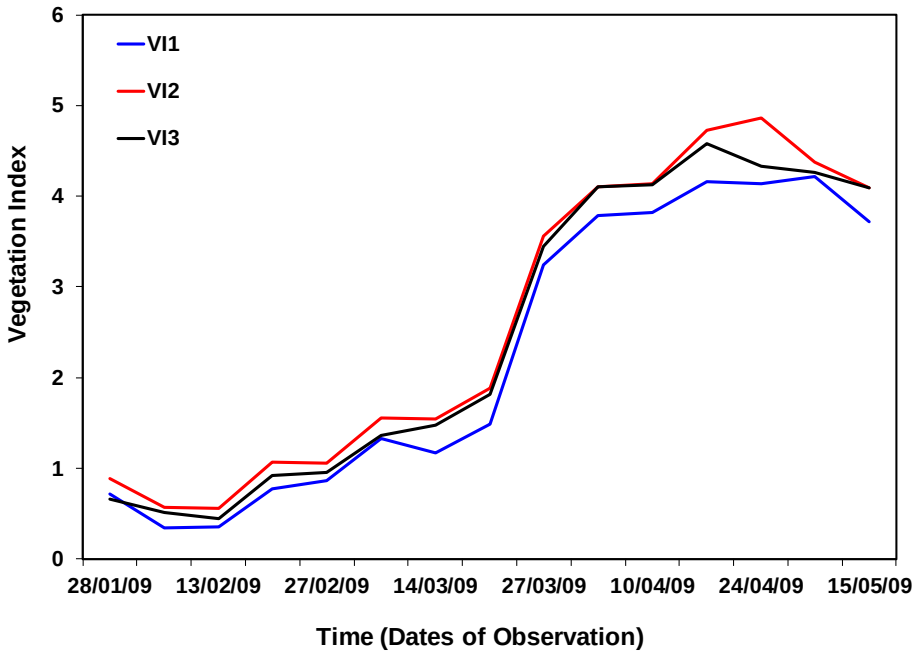

Figure 4.14 : Temporal variation of vegetation indices (VIs) of rice variety (IET-20166)

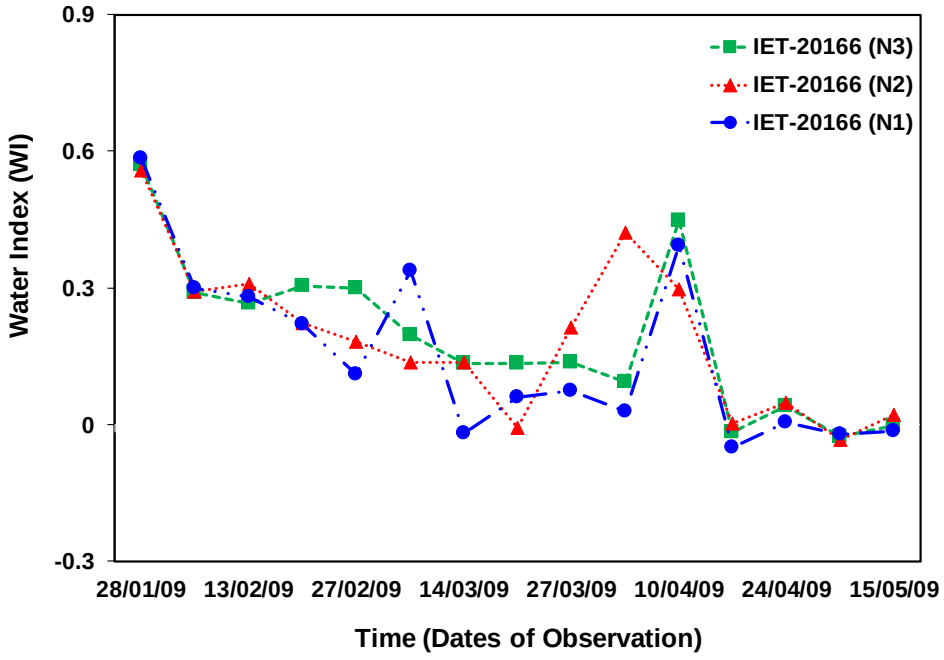

Figure 4.15 : Temporal variation of WI index of rice variety (IET-20166)

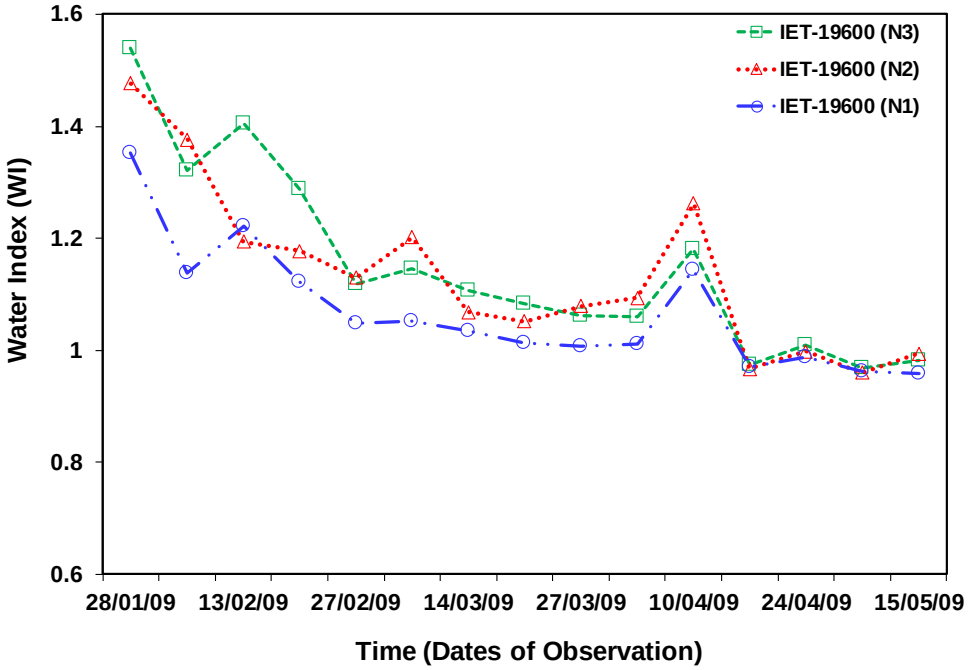

Figure 4.16 : Temporal variation of WI index of rice variety (IET-19600)

From Figure 4.15, it can be observed that the water stress index is linearly decreasing with crop developmental age and concluded that the crop was under water stress at earlier stage of its growth. Then the irrigation water was supplied to crop at the middle of the crop developmental stage. This index points out the water stress of the paddy throughout its crop period. The index mainly focuses on supply irrigation water not the application of fertilizer levels. It is also further clarified from another rice variety (Figure 4.16). From Figure 4.16, it is clearly reflected that the crop is under dry zone at its early crop stage. Later, it attained peak to recover from dry condition and reached in wet zone. It caught the peak after getting the supply of irrigation water. In addition, the water index pointed out that the application of water is needed during the crop growth stages. From this, it is confirmed that this water index has the potential to evaluate the water stress condition of paddy crop at a regional scale.

4.3.2 Statistical Analysis

The aforementioned indices for nitrogen applications were calculated based on spectral reflectance of each species. The difference between different nitrogen application levels was

evaluated using statistical methods like one-way ANOVA and paired Tukey's test with an assumed level of significance, $p < 0.01$. Statistical analysis using both the derived and existing indices were employed for the confirmation of significant difference between different nitrogen levels at wavelengths sensitive to nitrogen. The result of this test is shown in Table 4.3. Analysis of variance of the spectral reflectance of rice varieties using water index is presented in Table 4.4, and it exhibited satisfactory results for the studied rice genotypes. By applying the vegetation index $\mathbf{VI}_1(\rho_{840}/\rho_{560})$, we observed that there was a significant difference between N_1 and N_3 treatments in six out of eight rice varieties. Such difference was also noticed in between N_1 and N_2, and N_2 and N_3 treatments for three and five rice genotypes respectively. Similar analysis was carried out for other two derived indices $\mathbf{VI}_2(\rho_{920}/\rho_{560})$, $\mathbf{VI}_3(\rho_{1020}/\rho_{560})$ and the established indices $\mathbf{VI}(\rho_{810}/\rho_{560}), \mathbf{GRI}(\rho_{830}/\rho_{550})$ proposed by Inoue et al. (2008). The results of the same are shown in Table 4.5.

The proposed vegetation indices are specifically aimed for nitrogen status of paddy crop growth. These three indices were compared with published indices, VI and Green Ratio Index (GRI), sensitive to one of the biophysical parameters i.e. nitrogen. By using the VI_1, the difference between higher and lower nitrogen treatments were confirmed among most of the rice genotypes namely IR64, Chandrama, K.Hansa, IET-19600, IET-19601, IET-18558 whereas the published nitrogen index (VI) was not able to demarcate this variation except only for one rice genotype (IET-20166). In addition to this, GRI did not perform well as compared to VI_2 and VI_3 indices. It was revealed that, by employing GRI, the difference between nitrogen treatments such as N_1-N_2, and N_2-N_3 were substantially discriminated in only two and three rice genotypes respectively, whereas other varieties were not responding to such variation. The difference between N_1-N_3 treatments was found in only one rice variety (IET-20166). On the other hand, the proposed index VI_2 performed efficiently and achieved satisfactory results in all the rice varieties. The nitrogen treatments such as N_1-N_2, N_2-N_3, and N_1-N_3 were found extensively discriminated in a number of rice varieties i.e. seven, four and five varieties respectively. Furthermore, VI_3 performed well in studied rice varieties as compared to the published VI and GRI indices.

Table 4.3 : Analysis of variance of the spectral reflectance of rice varieties using the studied indices

	VI_1			**VI_2**			**VI_3**			**VI Inoue et al. (2008)**			**GRI Inoue et al. (2008)**		
IR-64		N_1	N_2		N_1	N_2		N_1	N_2		N_1	N_2		N_1	N_2
	N_1		ns	N_1		ns	N_1		ns	N_1		ns	N_1		ns
	N_2	ns		N_2	ns		N_2	ns		N_2	ns		N_2	ns	
Chandrama		N_1	N_2		N_1	N_2		N_1	N_2		N_1	N_2		N_1	N_2
	N_1		ns	N_1		ns	N_1		ns	N_1		**	N_1		ns
	N_2	ns		N_2	ns		N_2	ns		N_2	**		N_2	ns	
K.Hansa		N_1	N_2		N_1	N_2		N_1	N_2		N_1	N_2		N_1	N_2
	N_1		**	N_1		**	N_1		**	N_1		ns	N_1		ns
	N_2	**		N_2	**		N_2	**		N_2	ns		N_2	ns	
IET-19600		N_1	N_2		N_1	N_2		N_1	N_2		N_1	N_2		N_1	N_2
	N_1		**	N_1		**	N_1		ns	N_1		ns	N_1		ns
	N_2	**		N_2	**		N_2	ns		N_2	ns		N_2	ns	
IET-19601		N_1	N_2		N_1	N_2		N_1	N_2		N_1	N_2		N_1	N_2
	N_1		ns	N_1		ns	N_1		ns	N_1		ns	N_1		**
	N_2	ns		N_2	ns		N_2	ns		N_2	ns		N_2	**	
IET-20166		N_1	N_2		N_1	N_2		N_1	N_2		N_1	N_2		N_1	N_2
	N_1		**	N_1		ns	N_1		**	N_1		ns	N_1		ns
	N_2	**		N_2	ns		N_2	**		N_2	ns		N_2	ns	
Gautam		N_1	N_2		N_1	N_2		N_1	N_2		N_1	N_2		N_1	N_2
	N_1		ns	N_1		**	N_1		ns	N_1		**	N_1		**
	N_2	ns		N_2	**		N_2	ns		N_2	**		N_2	**	
IET-18558		N_1	N_2		N_1	N_2		N_1	N_2		N_1	N_2		N_1	N_2
	N_1		ns	N_1		**	N_1		ns	N_1		ns	N_1		ns
	N_2	ns		N_2	**		N_2	ns		N_2	ns		N_2	ns	

** Significant difference (α= 0.01),

ns = not significant

Table 4.4 : Analysis of variance of the spectral reflectance of rice varieties using water index

Water Index	Rice Genotypes															
	IR-64				Chandrama				K.Hansa				IET-19600			
WI		N_1	N_2	N_3		N_1	N_2	N_3		N_1	N_2	N_3		N_1	N_2	N_3
	N_1		**	**	N_1		ns	**	N_1		**	**	N_1		ns	**
	N_2	**		ns	N_2	ns		**	N_2	**		ns	N_2	ns		**
	IET-19601				IET-20166				Gautam				IET-18558			
WI		N_1	N_2	N_3		N_1	N_2	N_3		N_1	N_2	N_3		N_1	N_2	N_3
	N_1		**	**	N_1		**	**	N_1		**	ns	N_1		ns	**
	N_2	**		**	N_2	**		ns	N_2	**		ns	N_2	ns		ns

** Significant difference (α= 0.01),

ns = not significant

Table 4.5 : Quantitative details of rice genotypes showing significant difference between nitrogen levels

Vegetation Indices	No of rice genotypes showing significant difference between fertilizer application levels		
	N_3 - N_1	N_2 - N_1	N_3 - N_2
$VI_1(\rho_{840}/\rho_{560})$	6	3	5
$VI_2(\rho_{920}/\rho_{560})$	7	4	5
$VI_3(\rho_{1020}/\rho_{560})$	4	1	1
$VI(\rho_{810}/\rho_{560})$	1	3	1
$GRI(\rho_{830}/\rho_{550})$	3	2	1

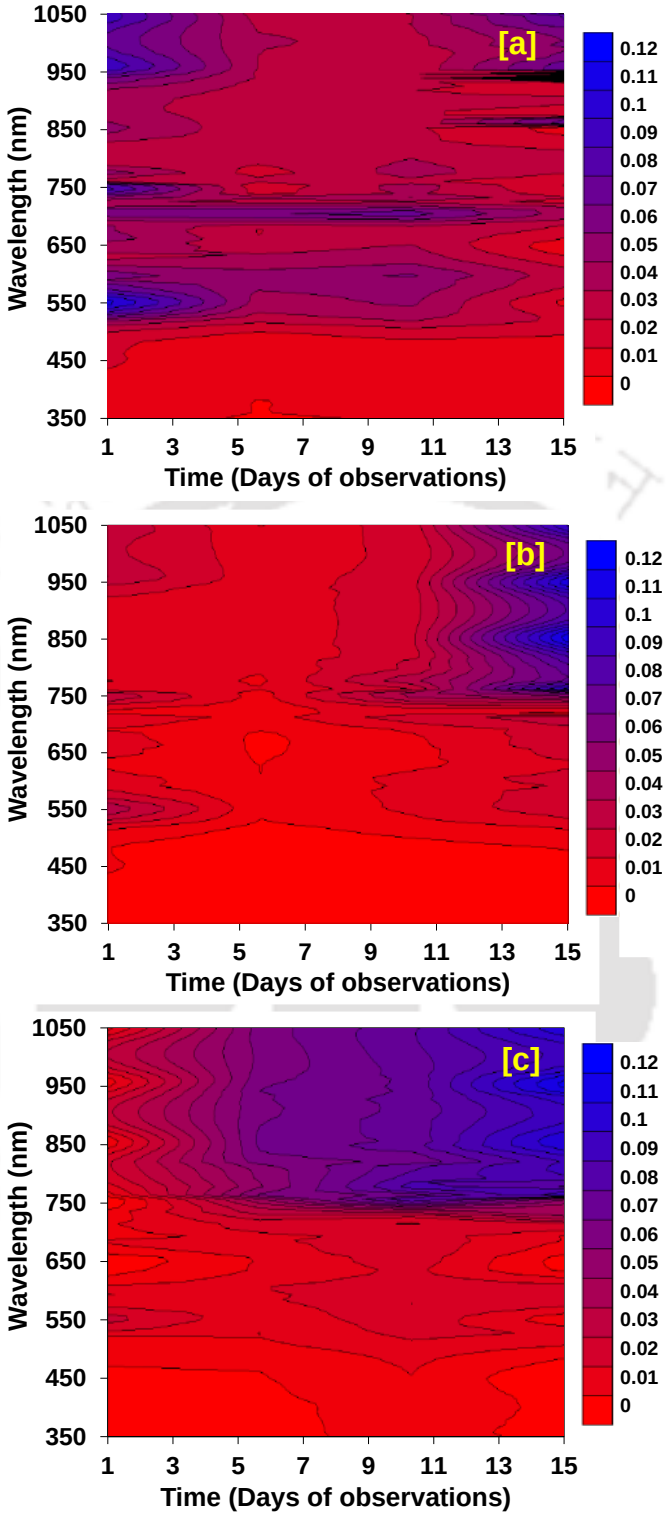

Figure 4.17 : Reflectance difference plots showing varietal difference for some of the typical rice genotypes – (a) Chandrama (b) IET-19600 (c) K.Hansa

4.3.3 Varietal effects

An attempt has been made to examine the difference between different varieties of rice. For this, spectrum was analysed for all the eight rice species and found that the reflectance of paddy crop with open canopies is not greatly influenced by variety. It is further confirmed from the difference plots of spectral reflectance of rice genotypes, which is demonstrated for some of the typical rice genotypes in Figure 4.17. From Figures 4.17(a) and (b), significant difference is not found in growth level for the two rice varieties (*Chandrama, IET-19600*). From these difference plots of spectral reflectance, it was found that there is no broad difference in growth level for most of the varieties. However, one of the rice genotypes (*K.Hansa)* showed different behaviour where the difference in growth was found to be considerably significant (Figure 4.17(c)). It is confirmed that the difference in growth levels among different rice genotypes is not much significant except for a very few rice varieties. From difference plot analysis, it can be concluded that there is no substantial variation in the growth levels of rice varieties.

4.4 Conclusions

The observed spectral reflectance data were analysed to obtain the critical wavelengths at which the effect of nitrogen applications or crop varietal on spectral reflectance response is found significant. The critical wavebands derived from contour plots are $\rho_{550}, \rho_{560}, \rho_{655}, \rho_{750}, \rho_{755}, \rho_{780}, \rho_{810}, \rho_{840}, \rho_{900}, \rho_{920}, \rho_{1000}, \rho_{1010}, \rho_{1020}$, close to near infrared, red and green regions of the spectrum. The proposed advanced indices includes $\rho_{560}, \rho_{840}, \rho_{920}, \rho_{1020}$ that efficiently differentiated between nitrogen levels in all rice varieties but the existing indices sensitive to nitrogen including $\rho_{550}, \rho_{560}, \rho_{810}, \rho_{830}$ were not able to differentiate properly between nitrogen treatments. From the difference plots of nitrogen applications, it is revealed that the crop growth has started earlier with N_3 (150 kg/ha) application than N_2 (100 kg/ha) application in most of the rice varieties. Also difference plots of different rice varieties were derived and found there is no broad difference in growth level for different varieties. The derived indices were compared with published indices specifically

meant for nitrogen i.e. VI and GRI (Inoue et al., 2008). From the results, it is confirmed that the proposed indices VI_1 and VI_2 were effectively able to differentiate the level of nitrogen treatments for most of the varieties except for one or two rice varieties. Whereas, the existing indices were not able obtain the difference between the rice varieties except for two or three varieties. It can be concluded from quantitative analysis of rice genotypes, VI_2 can be applied functionally for the assessment of nitrogen stress in rice agriculture system. Each level of nitrogen applications was found effective and different for different varieties in an Indian rice agriculture system by using the advanced vegetation indices rather than the existing indices. Thus, in future study, the potential of presently developed vegetation indices will be helpful for mapping of nitrogen treatments in rice crop by employing hyperspectral imagery obtained from space platform.

5 Discrimination of Paddy Crop Species using Advanced Clustering Technique

5.1 Introduction

Population of the world is growing rapidly day-by-day, so is the food demand. As a major portion of world population relies on rice, its consumption is also increasing very fast. In that respect, achieving greater productivity is of vital importance for which rice species information is progressively receiving keen attention towards real-time assessment of paddy crop yield. To improve rice productivity over large area of cultivation, enhanced soil-water-fertilizer-crop management practices at species level within the field is very crucial. Nitrogen is an essential element for plant growth. Plant intakes nitrogen fertilizer as per its requirement not in excess. Therefore, application of excessive nitrogen fertilizer will lead to ground water contamination (Jain et al., 2007; Jaynes et al., 2001). In this context, optimizing the application of fertilizer is very much essential in paddy cultivation so that fertilizer is not wasted resulting in reduced environmental pollution and water quality degradation. It can be possible only when one has a primary knowledge on crop species' fertilizer requirement. Traditionally, the most common methodology of agricultural crop species detection is visual investigation, which has several limitations like it is time-consuming, inaccurate, site specific and labour-intensive. Remote sensing techniques have proven to be very cost-effective, non-destructive and efficient in the management and classification of different agricultural crops, weed species and other plants within a field. In recent years, several research studies (de Castro et al., 2012; Jorgensen et al., 2006; Pena-Barragan et al., 2011) have implied that remote sensing, particularly hyperspectral remote sensing, is more suitable for agricultural research studies as

it has the flexibility to identify minor changes in crop characteristics. Moreover, this technique is capable of guiding the farmers to apply agricultural inputs to the rice plants with a prior knowledge on the paddy crop species, which is the central idea behind precision rice agriculture.

In past few decades, a number of studies carried out by some researchers have focused on the relation between spectral reflectance and different crop species (Liu and Bo, 2015), classification of crops (Boitt et al., 2014; Wardlow et al., 2007), discrimination of weed species (Borregaard et al., 2000; Rumpf et al., 2012), separation of cultivars levels of rice, wheat and cotton (Blackmer and Schepers, 1995; Feng et al., 2008; Filella et al., 1995; Kong et al., 2013; Nguyen and Lee; 2006), irrigation levels of potato crop (Kashyap and Panda, 2003; Onder et al., 2005), identification of different vegetated species together (Bunting and Lucas, 2006; Cochrane, 2000) and also discrimination of rice panicle (Liu et al., 2010). In these studies, various methodologies have been adopted such as support vector machine analysis, principal components analysis, discriminant analysis, multiple least square regression method, neural network techniques. It is reported that visible, red-edge, NIR regions of the spectrum are responsible for crop discrimination, but they vary-significantly with location and crop type. On the other hand, all these studies emphasized only on a specific field condition and growth stage. However, it is observed from the paddy crop field that with fertilizer application the phenology of crop species changed significantly throughout the growth stage.

Therefore, this study has increased attention in defining the most suitable narrow bands to discriminate rice genotypes subjected to different nitrogen treatments and no nitrogen treatment at two different stages during the growing season using field hyperspectral remote sensing. It is very difficult to distinguish the paddy crop species with naked eye in their early stages, as they look very similar. Here the differences are very small to be discerned with ordinary aerial or multispectral satellite imagery. They cannot be captured through high spatial multispectral aerial images because of their wider spectral widths. So, hyperspectral *in-situ* data is used to accurately discriminate between visually similar rice varieties using waveform classification technique. Identification of narrow spectral bands is the key feature in rice species discrimination. The aim of the study is to acquire the spectral response of paddy crop

species at canopy scale, which is unique. This signature can be used to measure the differences in reflectivity for different rice varieties either for real-time monitoring or for rice map creation. Moreover, *in-situ* signatures should be free from noise so as to build pure spectral libraries for remote sensing. Here, an attempt has been made to get pure spectral library along with powerful discrimination through waveform classification technique. Besides these, the present study attempted to identify the most suitable narrow bands in the electromagnetic spectrum sensitive for rice species discrimination.

5.2 Data description

For this study, ground based hyperspectral measurements were taken from the experimental station of the Regional Rainfed Lowland Rice Research Station, Assam (Study site 1) with the utilization of an ASD hand held portable spectroradiometer having a spectral range of 350-1050 nm. Two sets of *in-situ* hyperspectral measurements were taken from the same study site in two different years. One set was taken from 72 plots covering eight rice varieties prior to different nitrogen applications in 2009. The other set was taken from 24 plots comprising 24 rice varieties, which are most commonly cultivated Indian rice varieties with different crop developmental age, with no nitrogen treatment in 2014. The study area and data collection have been described in detail in Chapter 3. The details of presently used hyperspectral ground based data are given in Table 5.1.

Table 5.1 : Details of ground based hyperspectral measurements

Dates of Observation	Crop Stage	Rice Genotypes	Plots
03/04/2009 10/04/2009 17/04/2009 24/04/2009	Fully vegetative stage	8	72
21/05/2014 31/05/2014	Pre-vegetative stage*	24	24

**Pre-vegetative stage covers tillering and panicle initiation phase.*

5.3 Methodology

Experimental measurements have been assessed to characterize the canopy reflectance properties in a rice agriculture system accompanied with various rice species and nitrogen treatments. Rice species discrimination with different nitrogen treatments and extraction of pure rice spectra for the development of paddy crop spectral library are presented.

5.3.1 Waveform classification approach

The rice genotypes were tried to be discriminated based on their reflectance characteristics. Here an attempt has been made to discriminate the rice varieties on the basis of waveform classification approach. The aim of waveform classification procedure is to automatically split or classify each data set into different consistent groups. This basically can be done by supervised classification, corresponding to situations when different groups of waveforms are identified before the beginning of the classification. However, as waveforms show different patterns over different rice varieties, identifying the groups of waveforms might lead to neglecting a group of unexpected waveforms. In fact, good classification should extract any of the existing consistent waveforms as a separate group. Waveform classification was carried out on the data from each of the 72 plots comprising eight rice varieties namely Gautam, IR-64, IET-18558, IET-19601, K.Hansa, Chandrama, IET-19600 and IET-20166 with three different rates of nitrogen applications. Similarly, waveform classification was done for 24 rice varieties with no nitrogen treatment at all. The waveform is a function of wavelength and reflectance in the present study. The number of waveforms are 701 comprising full range of the spectral band (350-1050 nm). Then, hierarchical clustering technique was employed to classify waveforms into different groups.

5.3.2 Cluster analysis of rice varieties

The unique feature of cluster analysis among other techniques is reducing the number of observations by classifying them into homogeneous clusters, identifying groups without previously knowing group membership or the number of possible groups. It mainly includes factor analysis and discriminant analysis to reduce the data dimensionality (Yim and Ramdeen, 2015). Hierarchical algorithms create a hierarchical decomposition of data set. The main goal is to increase within-group homogeneity and between-groups heterogeneity. In this

study, agglomerative hierarchical clustering was preferred as it allows to compare the clustering result with a number of clusters where there is no need of a number of final clusters to be decided a priori. The agglomerative algorithms created a hierarchical decomposition of data set. It is represented by a tree structure which splits a data set into small subsets. The leaves of the tree comprise single objects. The clustering method basically follows distance measure for finding similarity or dissimilarity between the pairs of entities. The distance between the two entities can be measured using the Minkowski metric (Han and Kamber, 2011) and is given by

$$d(x_i, x_j) = (|x_{i1} - x_{j1}|^g + |x_{i2} - x_{j2}|^g + ... + |x_{ip} - x_{jp}|^g)^{1/g} \quad (5.1)$$

where

$$x_i = (x_{i1}, x_{i2}, ...x_{ip})$$

$$x_j = (x_{j1}, x_{j2}, ...x_{jp})$$

where x_i, x_j = groups of entities

when g = 2, distance between two objects is the Euclidean distance.

To avoid the effect of measurement unit in clustering, the data should be standardized. Standardizing measurements attempt to give all variables an equal weight. However, if each variable is assigned with a weight according to its importance, then the weighted distance can be computed by the metric (Rokach and Maimon, 2005) as given below

$$d(x_i, x_j) = (w_1 |x_{i1} - x_{j1}|^g + w_2 |x_{i2} - x_{j2}|^g + ... + w_p |x_{ip} - x_{jp}|^g)^{1/g} \quad (5.2)$$

where

$w_i \in [0, \infty]$

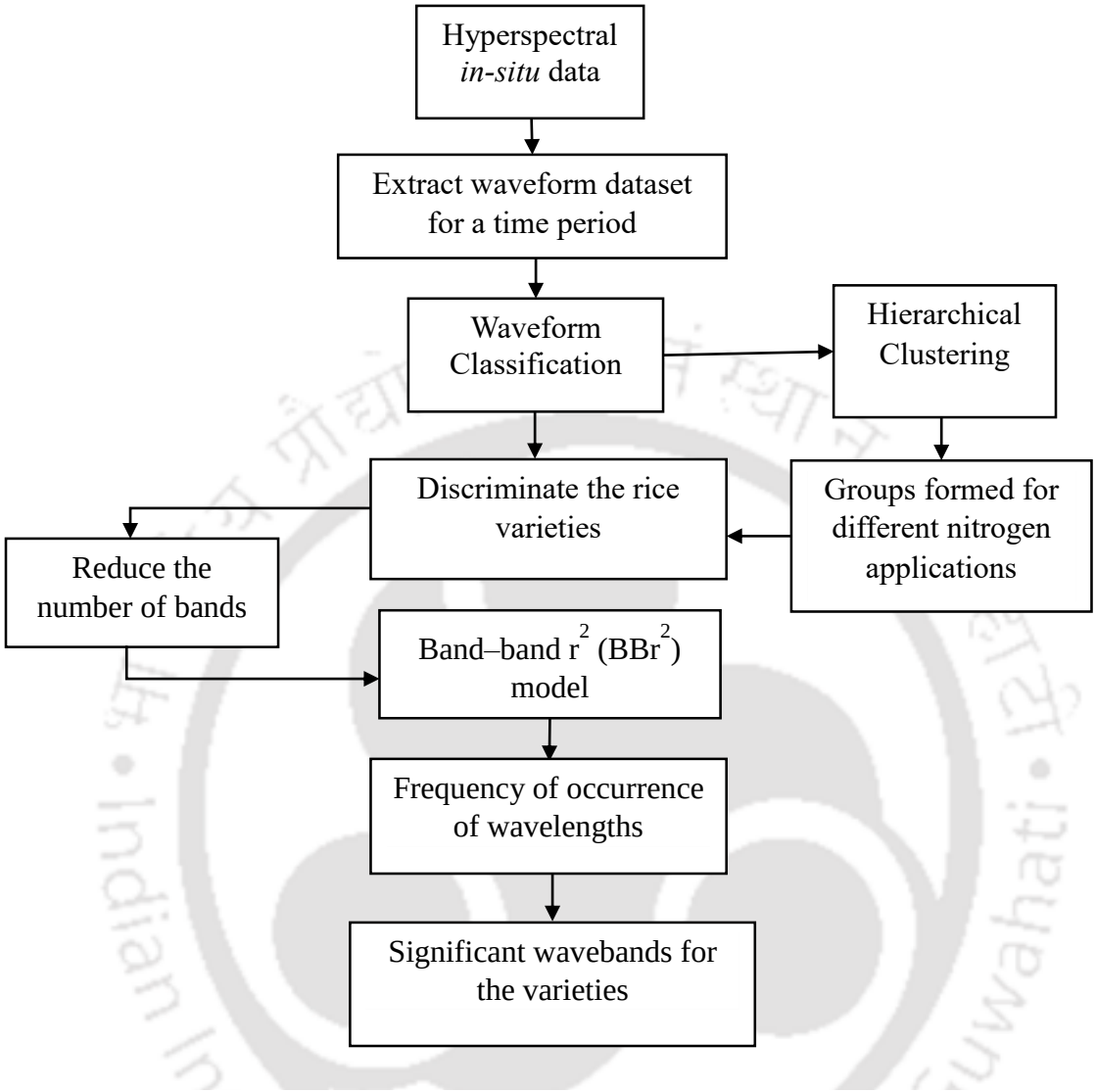

Figure 5.1 : Flowchart representing the methodology adopted to find the critical bands for rice species discrimination

5.3.3 Significant Wavebands

The significant wavebands were those that possessed least correlation among themselves, contained high information content and fairly differentiated the treatments (Jain et al., 2007). This can be quantified by band–band r^2 (BBR^2) analysis (Thenkabail et al., 2004), which provides more supplementary information of vegetation characteristics by excluding the redundant bands. The correlation between one spectral band with another spectral band was

expressed in terms of r^2. If a high correlation coefficient existed between any two spectral bands then it signified they have similar characteristics. In other words, lower correlation between any two bands showed redundant information between the species that indicate presence of distinctive features (Jain et al., 2007; Thenkabail et al., 2004). To evaluate spectral band performance, the reflectance data recorded for eight rice varieties from the 72 rice plots with different rates of nitrogen application were combined and analyzed. The overall methodology is depicted in Figure 5.1.

5.4 Results and Discussion

The spectral characteristics of rice genotypes were analyzed by using ground-based hyperspectral measurements. The methodology proposed in this study performed well in discriminating the rice varieties with different nitrogen treatments. The waveform classification approach was adopted in this study to build spectral library by eliminating noisy waveforms present in the spectral acquisition. Further, band-band correlation was carried out to define the optimal spectral narrow bands for species discrimination. With the help of improved methodology, development of spectral library along with classification of rice species could be done with more accuracy.

5.4.1 Spectral reflectance characteristics

The hyperspectral measurements in the range of 350 to 1050 nm were collected from the experimental site for the eight rice varieties with three different nitrogen applications (N_1 = 50, N_2 = 100 and N_3 = 150 kg/ha) and twenty four rice varieties without nitrogen application. The temporal effect of nitrogen treatments on crop species was found significant at two different growth stages. This is represented in Figure 5.2. Here, it clearly observed that the nitrogen application N_3 has more impact on crop growth than the other two applications both at 67 and 82 days after planting (DAP), whereas the behaviour of N_1 is found quite opposite. Growth is less in case of N_1 application as compared to N_2 and N_3 applications. At 82 DAP, crop growth is found to be significant than at 67 DAP. Furthermore, the detailed explanation of variation of nitrogen treatments is presented in Chapter 4 (Figure 4.4). The spectral profiles

for twenty four different rice varieties with no variation in nitrogen application are represented in Figure 5.3. Here, it is observed that the spectral response for all the varieties are similar in nature at 67 DAP. From Figure 5.4, the spectral signatures found are quite different for some of the varieties at 82 DAP. From the above spectral characteristics, it is observed that the reflectance is high in green region. The transition phase where the reflectance changes from red to NIR is called red edge, which slightly varies between 680-710 nm from variety to variety. There is a higher reflectance behaviour exhibited near NIR region mostly greater than the 720 nm spectral band. The water absorption band appeared approximately in the region of 940-960 nm. By observing the paddy crop signature behaviour, clustering technique was attempted to discriminate the rice varieties in an easy way.

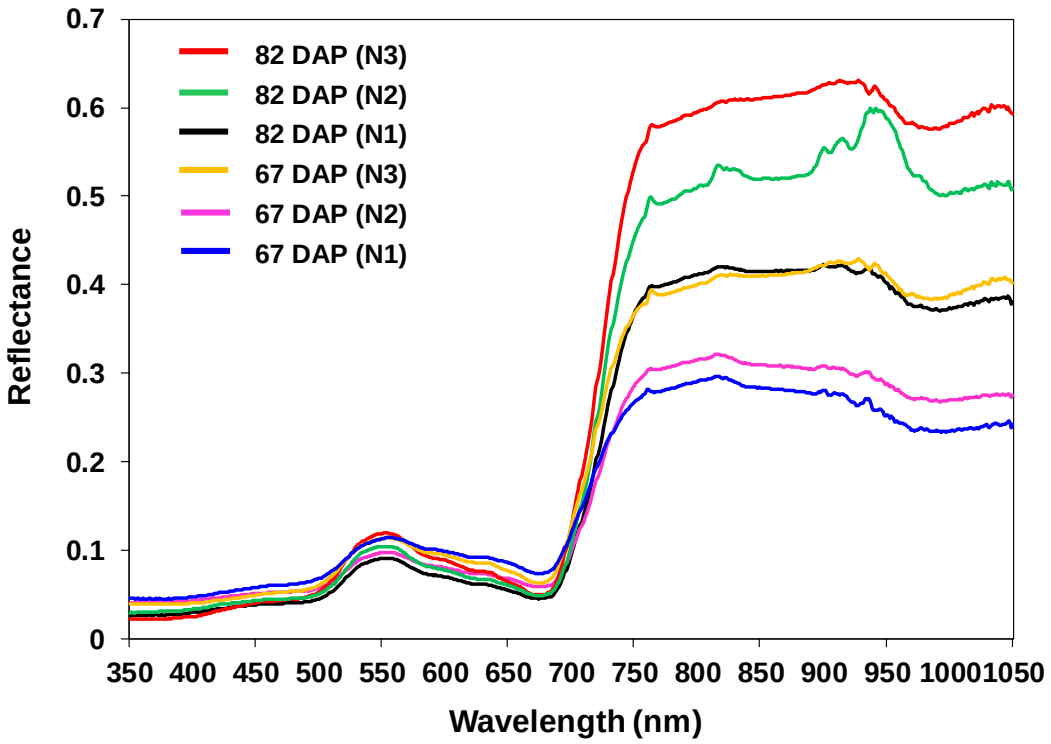

Figure 5.2 : Variation of nitrogen treatments at 67 DAP and 82 DAP

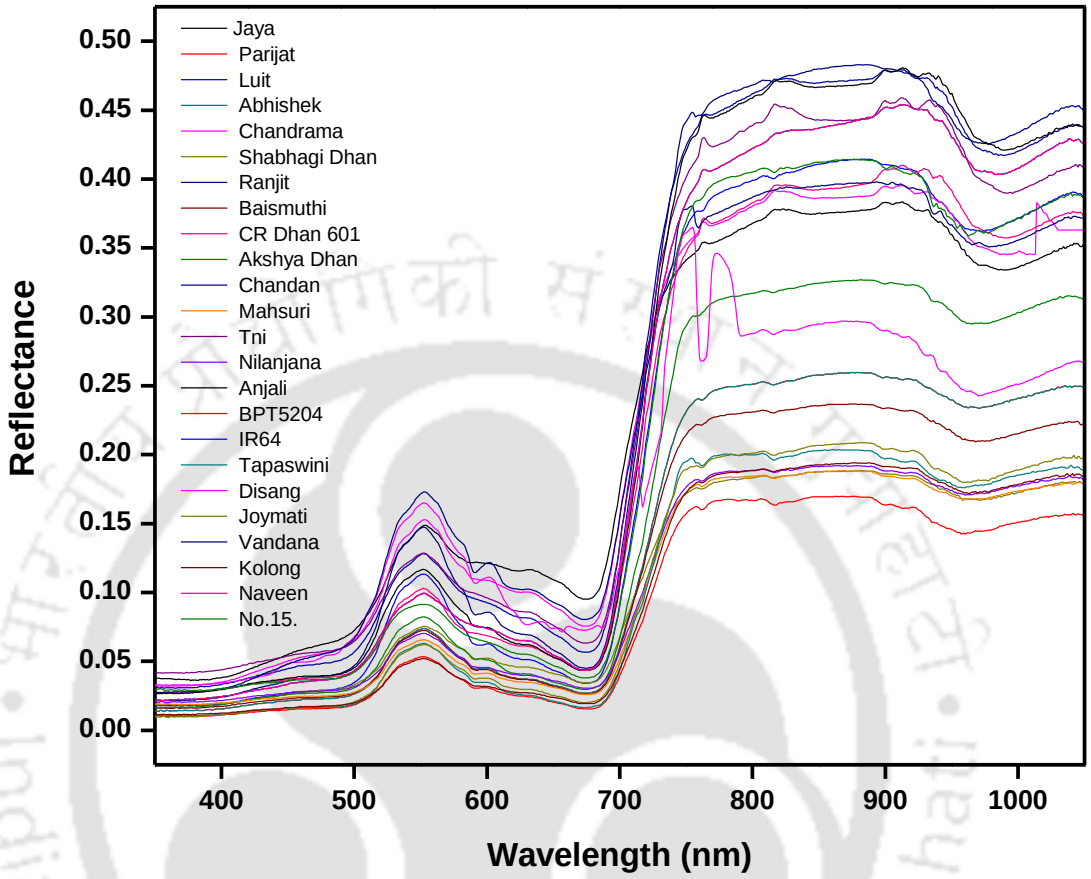

Figure 5.3 : Spectral signature of rice genotypes at 67 DAP

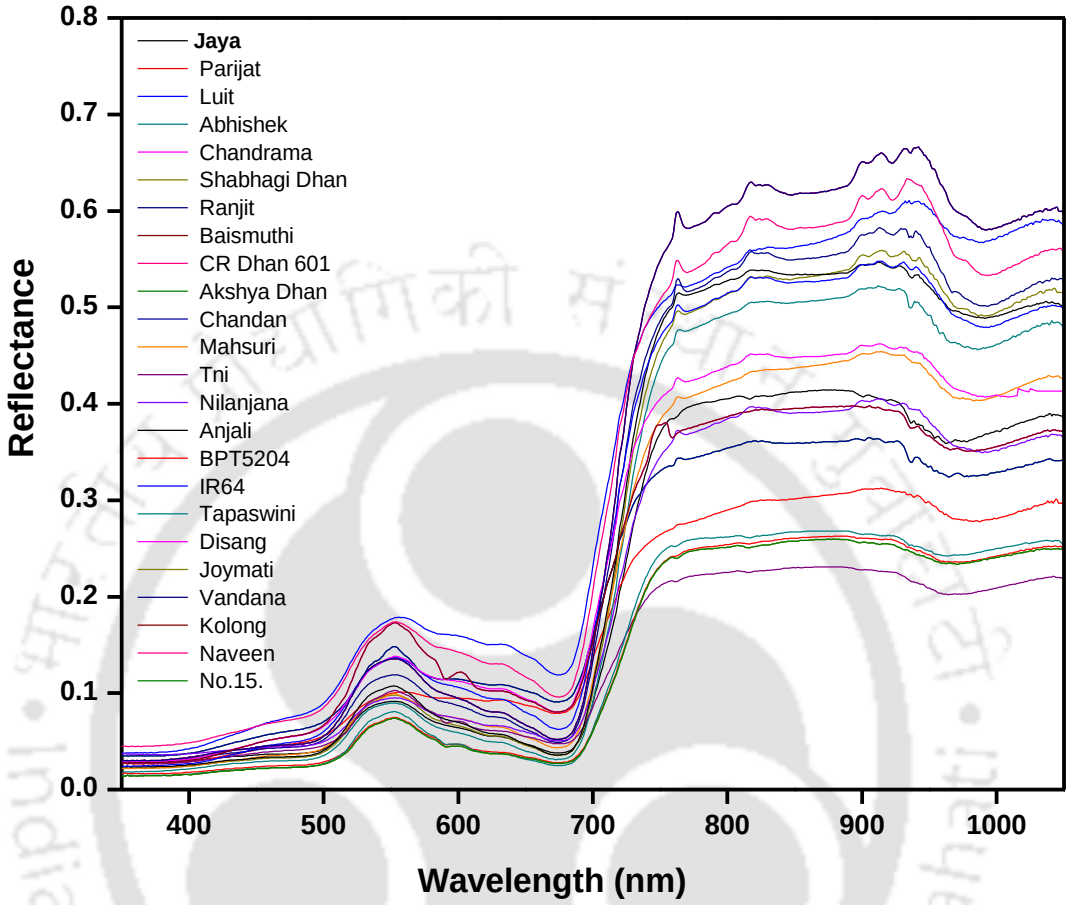

Figure 5.4 : Spectral signature of rice genotypes at 82 DAP

5.4.2 Discrimination of rice varieties

By employing hierarchical agglomerative clustering technique, rice varieties were separated into different groups based on three nitrogen applications: N_1 = 50kg/ha (Figure 5.5), N_2 = 100kg/ha (Figure 5.6), N_3 = 150 kg/ha (Figure 5.7). Figures 5.5-5.7 show that the noise attained during hyperspectral data acquisition was captured in the clustering of waveforms. The heterogeneity present within the spectral measurements reflect the signature response of plant species at canopy or single leaf scale, which was recorded by the waveform classification. Hence, non-uniformity is observed in the peak of the spectral signature for some of the rice varieties (Figures 5.5-5.7). By neglecting the noisy waveforms, accurate spectral signatures for the rice genotypes were achieved. Furthermore, spectral library could be developed by considering single peak waveforms, which represent the signatures of paddy crop genotypes dominant within the crop field. The clustering of waveforms has also increased the accuracy of spectroradiometric measurements to precisely distinguish the rice species under different nitrogen treatments. Hence by comparing the clusters of spectral signatures of any two N applications, plant species were classified (Table 5.2).

Table 5.2 : Clusters showing discriminated rice varieties with three nitrogen applications

Clusters	**Discriminated Rice species (N_3-N_1)**	**Clusters**	**Discriminated Rice species (N_2-N_1)**
C3, C6, C10, C5, C7	IR-64, Gautam, IET-18558, IET-19601, Chandrama	C3,C10,C1,C3	IR-64, IET-18558, K.Hansa, IET-19600
Clusters	**Mixed Rice species (N_3-N_1)**	**Clusters**	**Mixed Rice species (N_2-N_1)**
C6,C1,C4	Gautam, IET-19600	C9	IET-20166, IET-19601, K.Hansa

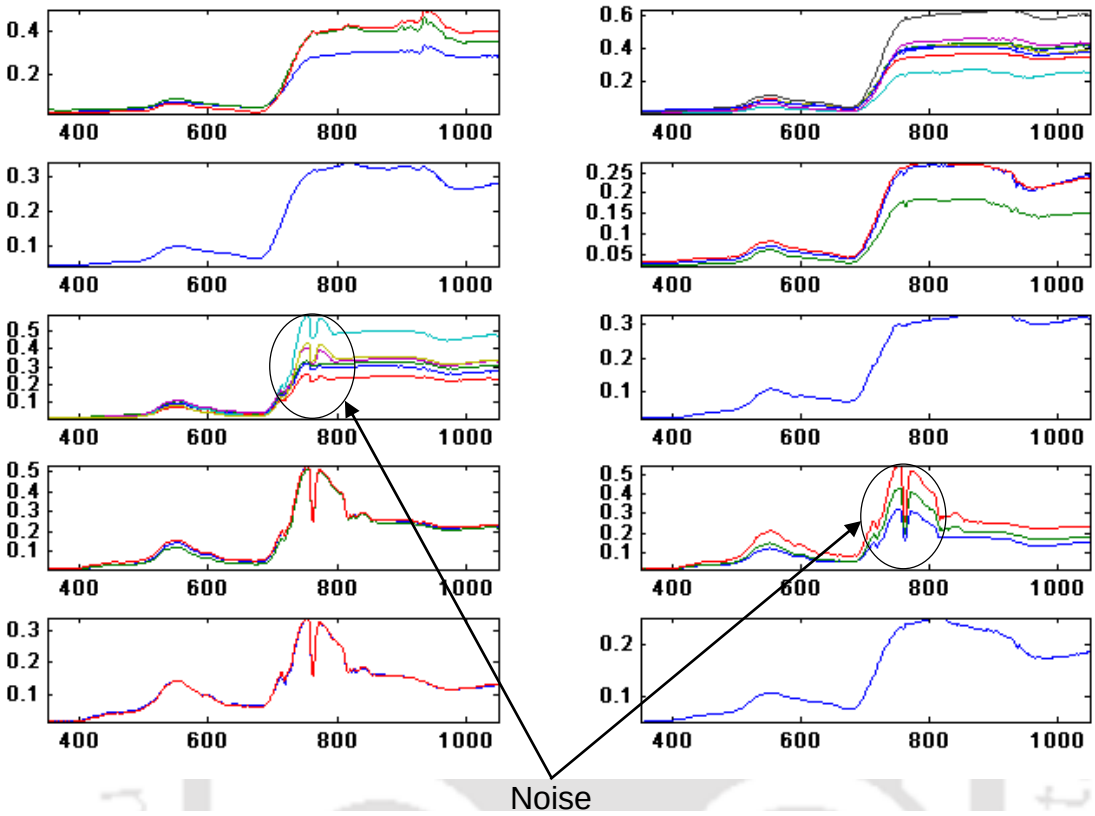

Figure 5.5 : Hierarchical clustering of waveforms for rice varieties (N_1 (50kg/ha))

Table 5.2 reveals that some of the rice varieties got separated from each other, whereas some of the varieties were not distinguished. Three clusters represented two varieties and one cluster represented three varieties with N_3 and N_2 applications respectively in comparison to N_1. This may have happened because of the variation in growth levels due to different nitrogen treatments. Here, the implementation of this method was found to be instrumental in extracting pure rice spectra to bring the intra-species variability and unique discrimination among vegetation species.

By following this hierarchical agglomerative clustering technique, twenty four rice varieties were clustered and formed into different groups (Figure 5.7). Figure 5.7 shows that the noise is nullified, thus, resulting in a very good spectral library for different rice genotypes. Clustering algorithm has performed well in capturing the spectral differences, which are very fine among rice genotypes owing to their spectral similarity. Hence, it is very useful to build

pure spectral library for paddy crop species so that it can further label the presence of any unknown crop spectra by the method of spectral matching of pure spectral signatures of rice crop.

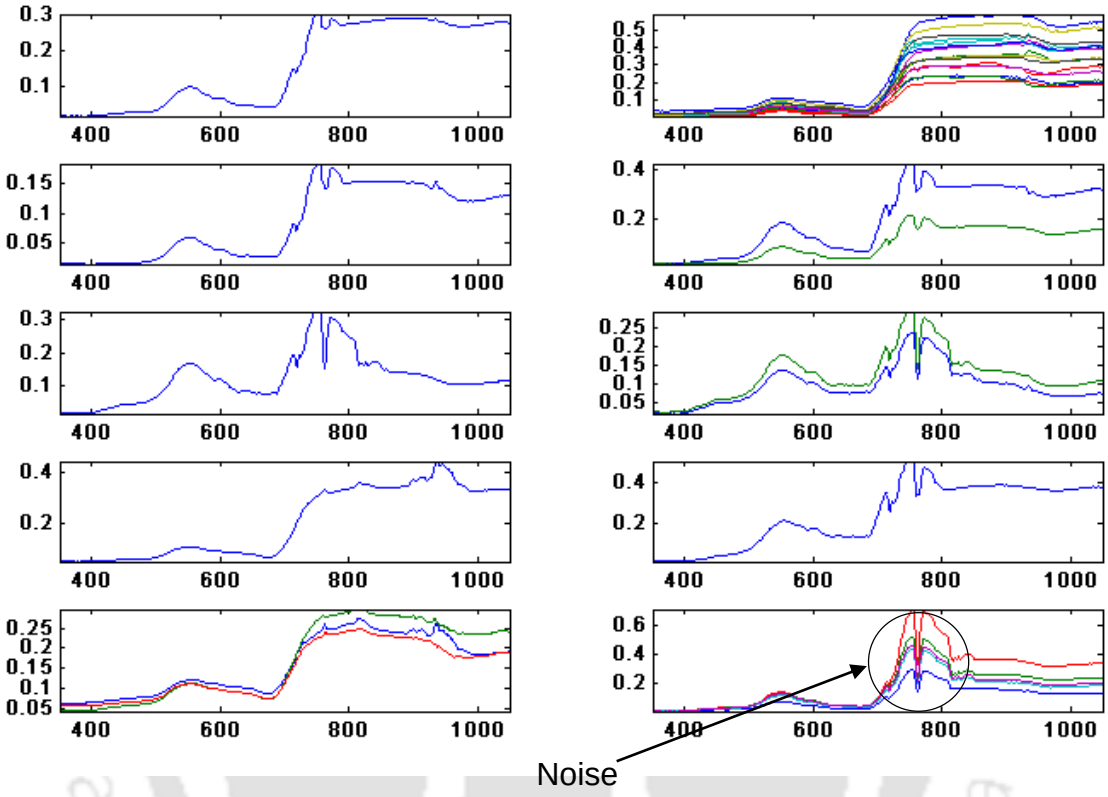

Figure 5.6 : Hierarchical clustering of waveforms for rice varieties (N_2 (100kg/ha))

Figure 5.8 shows the rice species, which prominently got separated from other varieties based on their spectral characteristics. Still there are some varieties, which could not be discriminated, are rather grouped representing a single variety. During the crop developmental age, the spectral reflectance characteristics of rice species have less variation because of the agricultural practices that were carried out under controlled environmental conditions. Hence, it is a very challenging task to detect the dissimilarities using hyperspectral data. Additionally, some of the studied varieties were grouped resulting in a single variety or mixed rice varieties. Therefore, we did not get all the twenty four varieties separated. Some genotypes were discriminated as single varieties, whereas others were mixed together thereby forming single groups of mixed varieties. This may have happened because the measurements were taken in

the narrow range from 350-1050 nm rather than the full visible-NIR-SWIR spectra. The details are provided in Table 5.3.

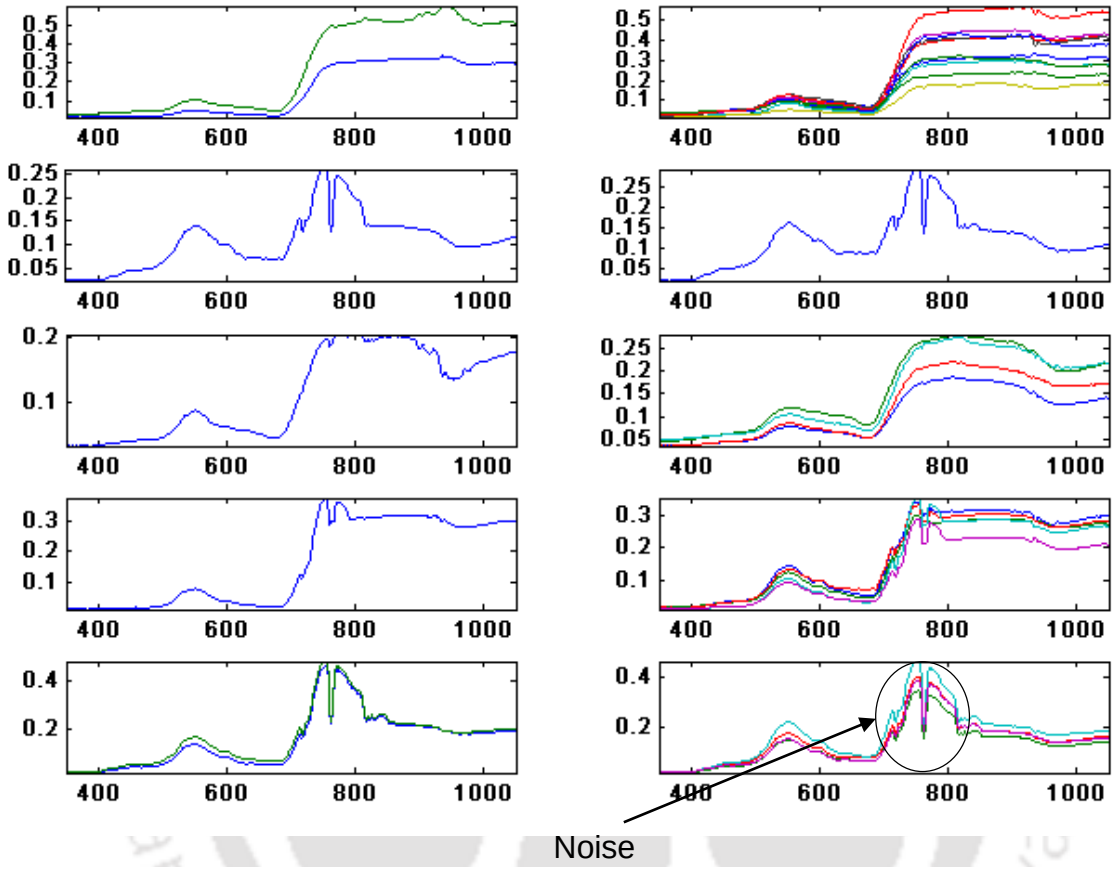

Figure 5.7 : Hierarchical clustering of waveforms for rice varieties (N_3 (150kg/ha))

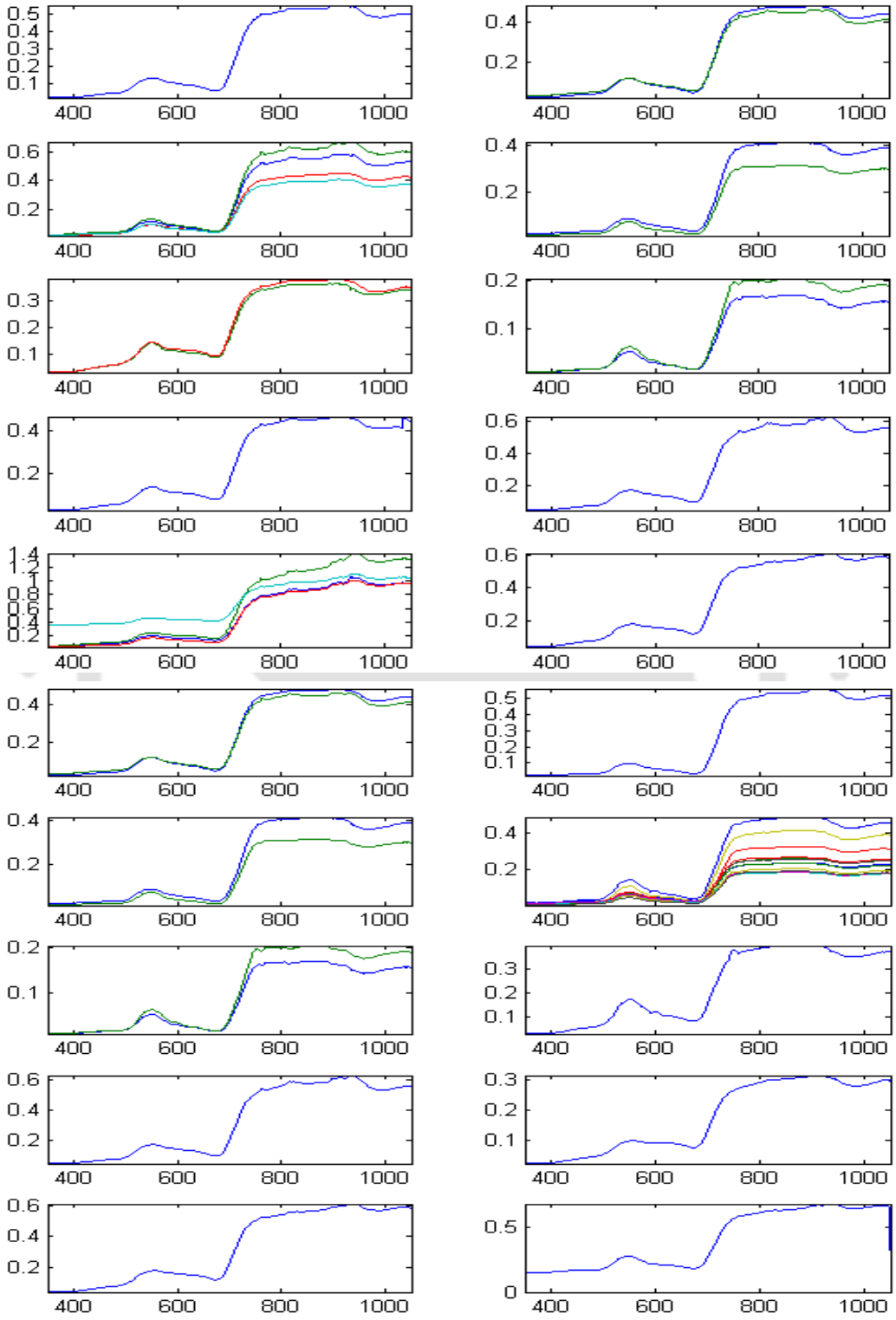

Figure 5.8 : Clustering of different rice varieties with no nitrogen application

Table 5.3 : Discriminated and mixed rice genotypes from clustering

Clusters	Discriminated Varieties	Clusters	Mixed Varieties
C1	Mahsuri	C2	Joymati, Vandana
C7	Chandan	C3	Chandrama, CR Dhan, Vandana
C8	BPT5204	C4	Ranjit, IR64, Shabhagi
C10	no.15	C5	Akshya Dhan, Mahsuri, Chandan
C12	Tni	C6	CR Dhan601, Akshya Dhan, Chandan
C16	Naveen	C9	Ranjit, Baismuthi, Tni
C17	Parijat	C11	Tapaswini, Disang, Joymati
C18	Shabhagi	C13	Vandana, Kolong
C19	Luit	C14	Akshya Dhan, Chandan, Mahsuri, Tni, Nilanjana, Anjali, Naveen and no.15
C20	Baismuthi	C15	CR Dhan601, BPT5204

5.4.3 Critical wavebands

By employing band-band correlation, significant wavebands were selected for the above discriminated rice varieties. For this analysis, the wavelengths were reduced to 70 spectral wavelengths. As the neighbouring wavelengths contain similar information, the reflectance of spectra was averaged over 10nm band (Jain et al., 2007; Thenkabail et al., 2004), which resulted in a total of 70 bands ranging from 359-1049 nm. Here, significant waveband combinations were selected by considering the hyperspectral measurements of eight rice varieties and three nitrogen applications. It comprised of 70 × 69 band-band combinations to fulfil the objective criteria. It was found that the band combinations having least correlation were distinctly different for N_3-N_1 and N_2-N_1 applications for the resulting discriminated rice varieties found in the study. It was observed that some hyperspectral data cubes have very weak correlation values. Table 5.4 illustrates the details of each data samples that reflect the correlation coefficient values between the narrow bands derived from N_3-N_1 analysis. Furthermore, the discriminated rice genotypes subjected to N_2-N_1 variation exhibited least correlation values between the hyperspectral bands and is presented in Table 5.5. The band

combinations having least correlation indicate least redundancy of information.

Table 5.4 : Waveband combinations having least correlation between narrow bands (N_3-N_1)

Name of the variety (N_3-N_1)	Spectral band 1 (nm)	Spectral band 2 (nm)	r^2
Gautam	559	729	0.000488
	489	740	0.000260
	510	789	0.000674
	609	799	0.000581
IR-64	559	769	0.000456
	519	789	0.000512
	559	809	0.000451
	559	799	0.000581
	689	729	0.000456
IET-18558	459	809	0.005889
	519	779	0.00788
	499	729	0.001128
	629	799	0.002433
IET-19601	489	819	0.000636
	649	839	0.000104
	649	849	0.000135
	659	959	0.000636
Chandrama	519	769	0.000512
	659	849	0.000456
	489	749	0.000512
	649	969	0.000451

To select the significant wavelengths from band-band analysis, frequency of occurrence of wavelengths were evaluated (Figure 5.9) and a threshold frequency >3 was employed to discriminate the rice genotypes. The significant spectral wavebands were found in between Green, Red, and NIR regions of the spectrum in discriminating the rice genotypes with nitrogen applications (Table 5.6). Our findings show that wavelengths in green region (519, 549, 559 nm) showed high reflectance due to heavy chlorophyll absorption in the green region. These findings were also similar to green band peak (550nm) noticed by Thenkabail et al. (2004). The pre-maxima absorption band (650 nm) cited by Jain et al. (2007) and the red edge

centred in the range of 700–720 nm (Daughtry et al., 2000) were found similar to the results (649,729 nm) obtained in the present study. The proposed methodology identified the narrow band reflectance characteristics at wavelengths (789,799,809,819 nm) that have the potential to discriminate the rice species in an effective way. This significant wavelengths matched with the findings (810,830 nm) obtained by Inoue et al. (2008) that are sensitive to nitrogen. Hence, these wavelengths have an advantage to identify pure rice spectra and to classify the rice genotypes prior to nitrogen applications accurately. Furthermore, these wavelengths may be used for developing three or four band indices which will help to distinguish the rice varieties prior to nitrogen applications.

Table 5.5 : Waveband combinations having least correlation between narrow bands (N_2-N_1)

Name of the variety (N_2-N_1)	**Spectral band 1 (nm)**	**Spectral band 2 (nm)**	**r^2**
IR-64	499	789	0.002243
	539	799	0.003165
	639	749	0.00488
	539	799	0.007225
IET-18558	549	799	0.007449
	549	809	0.008279
	519	809	0.002298
	579	789	0.009315
	649	819	0.003345
K.Hansa	510	819	0.002720
	549	839	0.006801
	549	849	0.000998
Chandrama	659	729	0.000456
	549	769	0.000512
	549	809	0.000451
	649	819	0.000581

Table 5.6 : Significant waveband in discriminating rice species prior to nitrogen application

Spectral range	Wavelengths (nm)
Green	519, 549, 559
Red	649
Red edge	729
NIR	789,799,809,819

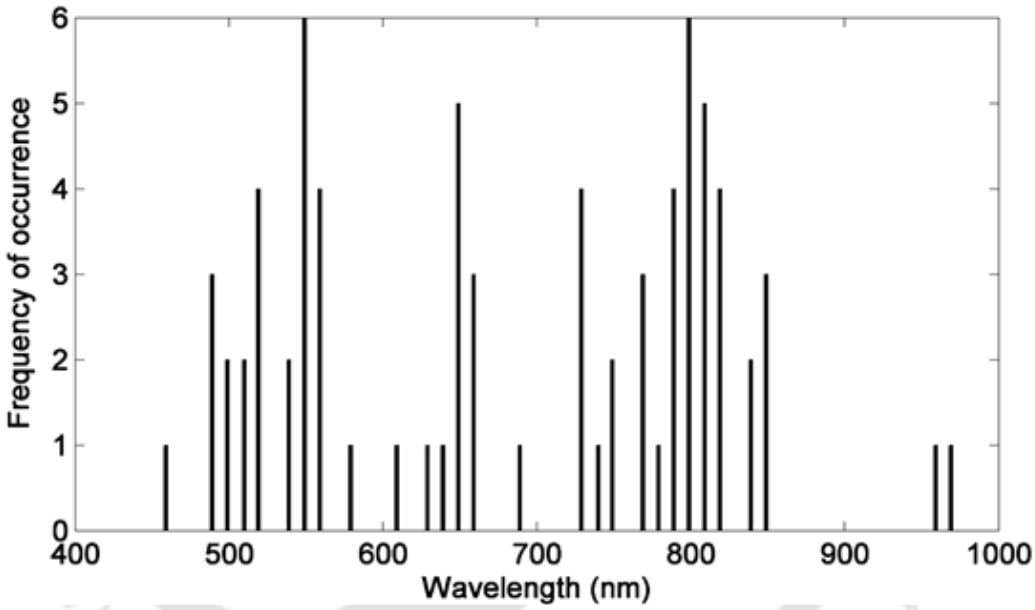

Figure 5.9 : Frequency of occurrence of wavebands selected from band–band analysis

5.5 Conclusions

The hyperspectral measurements were taken from eight rice species that were subjected to three nitrogen treatments and 24 rice species with no nitrogen application. It was attempted to discriminate the rice genotypes along with their treatments through clustering technique and it was revealed that rice varieties were significantly distinguished from each other. Thus, utilization of waveform classification followed by clustering technique performed successfully for the present study. Noise in the hyperspectral data was eliminated resulting in

accurate spectral signatures of rice genotypes. Thus, a better spectral library for the rice genotypes with application of varying nitrogen treatments and with no nitrogen treatment at all were achieved. Furthermore, a few varieties were mixed representing one cluster in which the fine difference among the rice varieties could not be determined. The significant wavelengths for this discrimination were found in green (519, 549, 559 nm), red (649 nm), red edge (729 nm) and NIR (789, 799, 809, 819 nm) regions of the spectrum. These optimal narrow bands can be useful to develop three band or four band indices specially designed for paddy crop that will provide the most essential information in regards to precision rice farming. However, it requires to be validated with more number of field hyperspectral data sets for practical applicability.

6 Estimation and Variability Study of Crop Parameters of Rice from Hyperspectral Imagery

6.1 Introduction

Nitrogen (N) is one of the most important crop elements closely related to its growth. It influences the crop chlorophyll content (Chl) and regulates its photosynthesis rate, thereby impacting the grain yield of rice crop. Photosynthetic pigments like chlorophyll-a, chlorophyll-b and carotenoids are strongly related to crop biophysical conditions, which influence crop productivity. Moreover, leaf nitrogen content is a strong factor influencing (Kergoat et al., 2008) both optimum canopy light use efficiency and canopy photosynthesis rate. Besides enhancing the crop productivity, nitrogen is also responsible for surface and groundwater contamination and atmospheric pollution (Chhabra et al., 2010; Manjunath et al., 2006). Therefore, it is very important to increase rice productivity for augmenting growth, while at the same time taking care of its adverse environmental impacts through precision nitrogen fertilizer management practices and recent advances in hyperspectral remote sensing techniques (Crutzen et al., 1986; Neue, 1993).

Previous studies have demonstrated the potential use of hyperspectral remote sensing for the assessment of biophysical variables (Goel et al., 2003) and biochemical components (Inoue et al., 2012; Main et al., 2011) of plant, indicating the plant's nutrient status. Chlorophyll content (Daughtry et al., 2000; Main et al., 2011; Schlemmer et al., 2013) and nitrogen content

(Lee et al., 2007; Tian et al., 2011; Zhu et al., 2007) at both leaf and canopy level can be extracted non-destructively by employing vegetation indices (VIs) from hyperspectral data. Importantly, the narrow band indices were developed and tested for leaf and canopy level estimation of Chl and N content, rather than mapping these essential parameters from space platform for a regional or global scale. Literatures discussed in Chapter 2 have confirmed that, they have the potential for a wide varieties of leaf species, plants, cash crops and agricultural crops, however there are no such indices specifically aimed for Chl and N content estimation of paddy crop. Moreover, very few literatures have supported the testing of indices for paddy crop and have also proposed one or two indices for estimation of these parameters from *in-situ* data (Tian et al., 2011). However, these are not robust indices as paddy cultivation varies with topography and climatic conditions. On the other hand, agricultural applications for precision farming, particularly for rice, are time specific, require accurate supply of nutrients and demand practical feasibility (Haboudane et al., 2002; Miao et al., 2009; Peng et al., 2010). Thus, they are more critical than other remote sensing applications. Treating a large crop region as a uniform area and applying farming inputs uniformly all over the field without considering within the field variation will result in inefficient use of inputs and loss of productivity. Thus, information on spatial variability of the field is an essential requisite to make efficient utilization of inputs for increasing farm profitability. Thus, advanced algorithms need to be developed to fully make use of hyperspectral image to get the field variability requisites for precision farming.

This study evaluated the potential of published Chl and N related VIs to map spatial variation of Chl and N, especially for rice agriculture system in India. Firstly, the performance of chlorophyll related indices to retrieve chlorophyll content in paddy leaf was examined. Furthermore, published indices related to nitrogen specifically tested for rice were considered to estimate nitrogen content in rice leaf. Secondly, relationships between the indices and rice plant parameters from ground based hyperspectral measurements were established. Different vegetation index models were developed to generate classified Chl and N map showing their spatial variation in a rice agriculture area from a high dimensional hyperspectral Hyperion data. Finally, crop field variation showing heterogeneity in the field was established from space platform. This study can be used as source for extracting different types of information for precision rice agriculture.

6.2 Study Site and Field Survey

For this research work, the experimental station of RRLRRS, Assam, India (Study site 1) centred at latitude 26°15'15.08"N and longitude 91°33'50.88"E was selected as the study site. Field campaign was carried out to get detail information on winter rice cultivation practice from farmers of the area. The information regarding rice varieties, fertilizer application and dozes, crop growth status, crop yield and topography variation were collected. The detailed description of study area is reported in Chapter 3.

6.3 Data Required: Hyperspectral Reflectance Measurements

6.3.1 Ground-based hyperspectral measurements

Paddy crop physiological data and reflectance from rice canopy cover were retrieved from different rice plots comprising different rice varieties, and these selected paddy fields were made homogeneous for rice breeding and field management. Different aged cropping rice species providing different yields for the estimation of Chl and N content in Indian climatic condition were considered for the present work. Paddy crop canopy spectra covering the crop developmental period were acquired under cloud free sky conditions using portable spectroradiometers (FieldSpec-FR, ASD, India). The spectral ranges of the sensors were 350-1050 nm with a field of view of 25°. Spectral resolution was 2 nm for the region 350-1050 nm for the Field Spec-FR. There were 24 rice genotypes namely Jaya, Parijat, Luit, Abhishek, Chandrama, Shabhagi Dhan, Ranjit, Baismuthi, CR Dhan 601, Akshya Dhan, Chandan, Mahsuri, Tni, Nilanjana, Anjali, BPT5204, IR64, Tapaswini, Disang, Joymati, Vandana, Kolong, Naveen and No.15. The details of experimental field setup and data collection is discussed in Chapter 3. After the spectroradiometric measurements, the plant samples were collected and immediately stored in a liquid nitrogen container to transport it from fields to the laboratory to perform chemical analysis to measure leaf Chl and N content.

6.3.2 Hyperspectral measurement from EO-1 satellite

The data used for current analysis was radiometrically corrected Hyperion L1R dataset. Its

temporal resolution was very low, hence getting temporal data for a certain area was very difficult. An image providing critical growth information of paddy was acquired i.e. during its reproductive phase. The Hyperion image covering the farm area in Assam (Study site 1) was acquired on 3rd October, 2014 at 3.30 GST. The scene characteristics of the acquired Hyperion image is enumerated in Chapter 3. The acquired Hyperion image was radiometrically corrected but it required careful processing to nullify the sensor noise. It was processed by using remote sensing (RS) image processing software ENVI 4.5. Pre-processing was necessary not only for elimination of sensor noise during acquisition but also for the reduction of data dimensionality in order to reduce computational complexity. Pre-processing steps like rescaling, abnormal pixels stripping, cross-track illumination correction, and elimination of bad columns prior to atmospheric correction were applied to the dataset. The details of pre-processing is discussed in Chapter 3.

Finally, spatial subset was selected from the whole scene for the experimental study site.

6.4 Plant measurements

Plant biophysical parameters were measured for 24 rice varieties during their booting stage from each experimental plot. Just after each canopy spectral measurement, plant samples (7-15 plants/plot) were selected randomly to determine the Chl and N content. Plant leaves were removed from its stem for the measurement by standard procedures. Leaf chlorophyll content was estimated by 80% acetone extraction method. After recording the fresh weight of each leaf sample, the leaf pigments were extracted in 80% acetone and leaf was pulverized completely. The sample was centrifuged at 3000 rpm for 15 mins to precipitate the cell debris. Then the supernatant was separated and extract of the sample was collected in a test tube. The absorbance (A) of the same was measured using spectrophotometer at 645 nm and 663 nm. Chlorophyll a, chlorophyll b and total chlorophyll contents of each sample were computed from the equations described below.

Using Arnon's following equations:

$$\text{Chl a } (\text{mg g}^{-1}) = [(12.7 \times A_{663}) - (2.6 \times A_{645})] \times (v/1000 \times w) \quad (6.1)$$

$$\text{Chl b } (\text{mg g}^{-1}) = [(22.9 \times A_{645}) - (4.68 \times A_{663})] \times (v/1000 \times w) \quad (6.2)$$

$$\text{Total Chlorophyll} = [(20.3 \times A_{645}) + (8.02 \times A_{663})] \times (v/1000 \times w) \quad (6.3)$$

or

$$\text{Total Chl} = \text{Chl a} + \text{Chl b} \quad (6.4)$$

where,

$w = \text{weight of the sample}$

$v = \text{total volume of the sample}$

The micro-Kjeldahl method was used for quantitative determination of nitrogen concentration in paddy leaf. Initially plant leaves were separated from their stem and kept in oven to dry at 70°C for 72 hrs to derive a constant weight of each sample and then leaves in each sample were properly crushed. 0.5 g of the each dried sample was taken for chemical analysis. The leaf nitrogen content of sample was calculated from the amount of ammonia present in it. The amount of ammonia present was determined by titration with sulphuric acid solution with a methyl orange pH indicator. Percentage of nitrogen was calculated using the following formula,

$$\text{Nitrogen}(\%) = \frac{(0.014 \times \text{Volume of } H_2SO_4 \text{ required} \times \text{Normality of } H_2SO_4}{\text{Sample weight of the collected leaves}} \quad (6.5)$$

6.5 Spectral Index approach-estimating Biophysical variables from Space platform

Spectral indices are the true indicators of the biophysical parameters of agricultural crop (Chen et al., 2010; Heiskanen et al., 2013). Specifically ratio based index and normalized difference spectral index produce effective results in different plant variables by using ground based and airborne reflectance spectra (Eitel et al., 2007; Hansen and Schjoerring, 2003; Zhao et al., 2007). Inoue et al. (2012) has reported that both reflectance and derivative spectra index have worked well in evaluating plant physiological variables. For the present study, indices

specifically aimed at leaf Chl and N content estimation of different crops were applied to paddy crop to quantify the Chl and N concentrations.

Mathematically, expression for Normalized Difference Spectral Index (NDSI) and Ratio Spectral Index (RSI) can be written as

$$NDSI(x,y) = (y - x)/(x + y) \quad (6.6)$$

$$RSI(x,y) = (x/y) \quad (6.7)$$

Here, x and y are the reflectances (R_i and R_j) or first derivative (D_i and D_j) values at i and j nm over the whole hyperspectra (Inoue et al., 2008).

Spectral indices were established using combinations of whole hyperspectral bands or some specific wavelengths helpful for the estimation of plant variables (Maccioni et al., 2001; Tian et al., 2011; Xu et al., 2010). There are indices available for estimation of biophysical parameters of different crops (Main et al., 2011; Marshall and Thenkabail, 2015), trees and forests, but there are no spectral indices specifically developed for paddy crop, as it is a very dynamic crop that varies with different topographical positions and climatic zones. Instead, paddy crop was tested with field hyperspectral data using previously published indices those were not meant for it. Therefore, an attempt has been made to estimate Chl and N content from hyperspectral imagery using the indices tested for rice and other well performed Chl and N aimed indices. For the present study, ten selected spectral indices that were found effective for the assessment of Chl and N content at leaf or canopy level for different species, were considered for Chl and N estimation in rice. These indices are given in Table 6.1 and Table 6.2.

Table 6.1 : Vegetation indices examined for nitrogen content estimation

Index	Equation	Related to	Reference	Tested species
Simple Ratio Index	R_{533}/R_{565}	N	Tian et al. (2011)	Rice (*Oryza sativa* L.)
LNC Index	$R_{705}/(R_{717} + R_{491})$	N	Tian et al. (2011)	Rice (*Oryza sativa* L.)

Table 6.2 : Vegetation indices examined for chlorophyll content estimation

Index	Equation	Related to	Reference	Tested species
Simple ratio Index	R_{533}/R_{565}	N	Tian et al. (2011)	Rice (*Oryza sativa L.*)
mND_{705}	$(R_{750}-R_{705})/(R_{750}+R_{705}-2R_{445})$	Chl	Sims and Gamon (2002)	Thin leaves (herbaceous), High dry mass leaves (sclerophyllous), Succulent leaves, Pubescent leaves, Waxy leaves, Grasses
Maccioni	$(R_{780}-R_{710})/(R_{780}-R_{680})$	Chl	Maccioni et al. (2001)	Four different plants (i)croton, Codiaeum variegatum (ii) spotted eleagnus, Eleagnus pungens Maculata (iii) Japanese pittosporum, Pittosporum tobira (iv) Benjamin fig, Ficus benjamina Starlight
PRIc	$(R_{570}-R_{539})/(R_{528}+R_{539})$	N	Gamon et al.(1992)	Sunflower
MTCI (MERIS Terrestrial chlorophyll Index)	$(R_{574}-R_{709})/(R_{709}-R_{681})$	Chl	Dash and Curran (2004)	Douglas fir (Pseudotsuga enziesii) and bigleaf maple (Acer macrophyllum)
LNC	$R_{705}/(R_{717}+R_{491})$	N	Tian et al. (2011)	Rice (*Oryza sativa L.*)
Datt	$(R_{850}-R_{710})/(R_{850}-R_{680})$	Chl	Datt (1999)	Eucalyptus leaves
OSAVI (Optimised Soil-Adjusted Vegetation Index)	$(1+0.16)(R_{750}-R_{705})/(R_{750}-R_{705}+0.16)$	Chl	Wu et al. (2008)	Wheat and Corn Triticum aestivum L.; Zea mays L.
Gitelson	$(R_{750}-R_{800}/R_{695}-R_{740})-1$	Chl	Gitelson et al. (2003)	Higher plant leaves Norway maple (Acer platanoides L.); horse chestnut (Aesculus hippocastanum L.); flush beech leaves (Fagus sylvatica L.); wild vine shrub (Parthenocissus tricuspidata L.)
mSR	$(R_{750}/R_{705})-1/\mathrm{sqrt}((R_{750}/R_{705})+1)$	Chl+LAI	Chen (1996)	Boreal forests plants (e.g Pine (Pinus banksiana) and Black Spruce (Picea mariana))

6.6 Results and Discussions

6.6.1 Estimation of Chlorophyll content

The relationship between the chlorophyll content retrieved using laboratory chemical analysis and the indices calculated from field reflectance spectra data are presented and discussed in two different parts. At first, relation between calculated chlorophyll indices and total chlorophyll content are demonstrated. The total chlorophyll content of the studied rice genotypes ranged from 1.13 mg/g to 7.26 mg/g at the reproductive stage of paddy crop. Secondly, the best performing chlorophyll indices are selected based on performance of statistics. Finally, the selected chlorophyll indices are considered for chlorophyll mapping of rice agriculture area from Hyperion data in Assam, India.

To establish the relationship between the indices and chlorophyll content, the selected indices are calculated for a controlled and well managed rice agriculture practice field from canopy hyperspectral spectral reflectance data rather than Hyperion image. The results of the tested indices are summarized in Table 6.3. The result showed, SR, mND_{705}, Maccioni, PRIc and Datt indices provided unsatisfactory results. It was interesting to note that the best predicting chlorophyll Datt index was unable to produce satisfactory results for assessment of rice chlorophyll content, though it exhibited higher performance with eucalyptus leaves, wheat crop (Datt, 1999; Haboudane et al., 2002). Besides these, it was quite interesting to point out that, the indices proposed by other researchers such as SR (R_{533}, R_{565}), mND_{705} (R_{750}, R_{705}), and PRIc (R_{528}, R_{539}), which performed well for rice nitrogen content, provided unsatisfactory results for chlorophyll content. Even if three band indices like mND_{705} and PRIc have shown a good prediction for rice nitrogen content (Tian et al., 2011), they exhibited unsatisfactory results in rice chlorophyll estimation. Moreover, the index mND_{705} (Sims and Gamon, 2002) has been proved by Main et al. (2011) to be one of the best indices for leaf chlorophyll estimation. This is in clear contrast to what our result showed for paddy crop. This may have happened due to the phenological stages of crop species and variability in vegetation types as well as moisture content, because the index was tested for crops other than rice species. Based on the performance of statistics, five indices exhibited improved results in estimation of rice chlorophyll pigment. The result is summarized in Table 6.4.

Table 6.3 : Relationship between the chlorophyll indices calculated from ground based hyperspectral spectra and chlorophyll content (and R^2 is significant at $p < 0.01$or $p < 0.05$)

Index	Fit-equation (Linear)	RMSE	R^2	p-value	Fit-equation (Nonlinear)	RMSE	R^2	p-value
SR	$y = 27.319x - 22.461$	1.341	0.155^{*}	0.058	$y = -1192.5x^2 + 2285.1x - 1090.6$	1.155	0.326^{**}	0.001
mND_{705}	$y = 11.353x - 2.5683$	0.8261	0.286^{*}	0.09	$y = 41.541x^2 - 30.986x + 8.0046$	1.123	0.312^{**}	0.006
MTCI	$y = 3.9064x - 3.545$	0.731	0.748^{**}	0.0002	$y = 3.5322x^2 - 8.2012x + 6.4558$	0.6197	0.829^{**}	0.008
Maccioni	$y = 14.461x - 6.089$	1.319	0.184^{*}	0.07	$y = 140.18x^2 - 164.59x + 50.738$	1.19	0.241^{**}	0.001
Gitelson	$y = 28.41x + 28.302$	0.673	0.771^{**}	0.000	$y = -18.703x^2 - 4.1183x + 14.187$	0.6228	0.771^{**}	0.000
PRIc	$y = 48.37x + 5.3982$	0.6575	0.396^{**}	0.0009	$y = -123.22x^2 + 40.908x + 5.375$	0.9872	0.426^{**}	0.009
LNC	$y = 59.632x - 28.985$	0.7096	0.763^{**}	0.003	$y = -226.05x^2 + 313.56x - 100.14$	0.7197	0.776^{**}	0.007
Datt	$y = 11.44x - 4.156$	0.8847	0.088^{**}	0.007	$y = 138.55x^2 - 170.91x + 55.449$	1.265	0.106^{**}	0.000
OSAVI	$y = 20.003x - 3.4824$	0.7514	0.734^{**}	0.000	$y = 29.038x^{2.0553}$	0.6213	0.822^{**}	0.000
mSR	$y = 5.2401x - 0.8858$	0.1407	0.69^{**}	0.000	$y = 7.9098x^2 - 6.9576x + 3.384$	0.6602	0.819^{**}	0.002

**denotes significant at 0.01 level, *denotes significant at 0.05 level

where y = Chlorophyll content

x = Chlorophyll based Indices

Table 6.4 : Best correlated chlorophyll indices for the estimation of paddy crop chlorophyll content

Index	Fit-equation (Linear)	RMSE	R^2	RE(%)	SSE(%)
MTCI	$y = 3.9064x - 3.545$	0.7319	0.748	22.81	11.78
Gitelson	$y = 28.41x + 28.302$	0.673	0.771	20.69	9.96
LNC	$y = 59.632x - 28.985$	0.7096	0.763	24.53	11.08
OSAVI	$y = 20.003x - 3.4824$	0.7514	0.734	26.62	12.42
mSR	$y = 5.2401x - 0.8858$	0.1407	0.69	21.03	14.5

Index	Fit-equation (Nonlinear)	RMSE	R^2	RE(%)	SSE(%)
MTCI	$y = 3.5322x^2 - 8.2012x + 6.4558$	0.6164	0.829	14.05	7.97
Gitelson	$y = -18.703x^2 - 4.1183x + 14.187$	0.6795	0.773	19.11	9.64
LNC	$y = -226.05x^2 + 313.56x - 100.14$	0.7197	0.776	16.85	10.47
OSAVI	$y = 29.038x^{2.0553}$	0.7499	0.813	10.62	11.81
mSR	$y = 7.9098x^2 - 6.9576x + 3.384$	0.6602	0.757	9.62	11.39

where y = Chlorophyll content
x = Chlorophyll based Indices

The goodness of fit of these five spectral index-based models were tested based on the root mean square error (RMSE), mean relative error (RE) and sum of squared error (SSE) values, which can be defined as:

$$RMSE = \sqrt{\frac{1}{n} \times \sum_{i=1}^{n} (P_i - O_i)^2} \tag{6.8}$$

$$RE = \sqrt{\frac{1}{n} \times \sum_{i=1}^{n} \left(\frac{P_i - O_i}{O_i} \right)^2} \times 100 \tag{6.9}$$

$$SSE = \sum_{i=1}^{n} (P_i - O_i) \tag{6.10}$$

where P_i and O_i are predicted and observed values of i^{th} data point of a biophysical parameter respectively and n is the number of data points.

Although the indices, OSAVI and MTCI, provided significant results for rice chlorophyll content, they had negligible results in estimation of wheat chlorophyll content (Bannari et al., 2008). Additionally, the performance of the modified indices (mSR and OSAVI) were found noticeable for assessing rice chlorophyll content. These findings were found to be similar to the findings of Xu et al. (2010) where the VIs, mSR and OSAVI showed better performance in estimating rice chlorophyll content than other VIs. Also another index i.e. LNC index (Tian et al., 2011), which is regarded as the best performer for nitrogen content of rice, exhibited outstanding potential for retrieval of chlorophyll content in rice. This happened because the Chl and N were highly correlated ($R^2 = 0.94$) in maize crop (Schlemmer et al., 2013). Besides these, index proposed by Gitelson et al. (2003) has also performed well in rice chlorophyll estimation. Similar result has been found to be optimal for chlorophyll estimation in maize crop and soybean (Peng and Gitelson, 2012; Schlemmeer et al., 2013).

6.6.2 Estimation of Nitrogen content

There are a very few literatures showing the assessment of nitrogen in rice (Inoue et al., 2008; Inoue et al., 2012; Tian et al., 2011). Indices proposed by Tian et al. (2011) for non-destructive and quick assessment of rice nitrogen content using hyperspectral measurements were implemented in our research work. To investigate the robustness of the proposed indices, relationship between each index and nitrogen content were established for the studied region. The indices were derived from canopy hyperspectral measurement and leaf nitrogen content

was estimated from laboratory chemical analysis. The nitrogen content of the studied rice genotypes ranged widely from 1.12% to 3.92% at their reproductive stage. The relationships between the indices for present and established work are presented (Table 6.5).

Table 6.5 : Relationship between the nitrogen indices calculated from ground based hyperspectral spectra and nitrogen content

Index	Fit-equation	RMSE	R^2	Reference
SR	$y = 29.178x - 25.294$	0.5828	0.710^{**}	Present work
LNC	$y = -306.34x^2 + 372.74x - 109.56$	0.6428	0.801^{**}	Present work
SR	$y = 12.07x - 8.829$		0.76	Tian et al. (2011)
LNC	$y = -9.448x + 7.556$		0.81	Tian et al. (2011)

**denotes significant at 0.01 level

where y = Nitrogen content

x = Nitrogen based Indices

From Table 6.5, it is clearly noticed that there is no significant difference between R^2 value calculated from SR index, which is 0.71 and 0.76 with a significant level ($p < 0.01$) for present and previous study respectively but they followed different linear relationships. Additionally, it is interesting to note that, the LNC index followed a nonlinear relationship for the present hyperspectral data while Tian et al. (2011) LNC index demonstrated linear relationship in estimating rice nitrogen content, however both show almost same correlation coefficient value of 0.801 and 0.81 respectively with a significant level ($p < 0.01$). The present regression models are compared with the established models to examine the performance of models in predicting rice nitrogen content in an agriculture area from ground based hyperspectral data (Figures 6.1 and 6.2).

From Figure 6.1, it is observed that both the present and established SR models followed linear trends with different relationships as a result of which Tian et al. (2011) model slightly overpredicted where the percentage of nitrogen content was less as compared to the present model. It is due to the cultivated rice varieties and irrigation practices that are followed in

India are completely different from China. Besides this, two outliers are found to be containing very low nitrogen value in present modified SR model. It is mainly because of the variation in rice genotypes in a crop calendar. The standard error associated with the predicted values of leaf nitrogen content with less than 3% is evaluated for both Tian et al. (2011) and present modified SR models from statistical formula and is found to be 46% and 33% respectively. Whereas, standard error for the predicted values of leaf nitrogen content with more than 3% is found to be to be 28.2% and 17.7% for both Tian et al. (2011) and present modified SR models respectively.

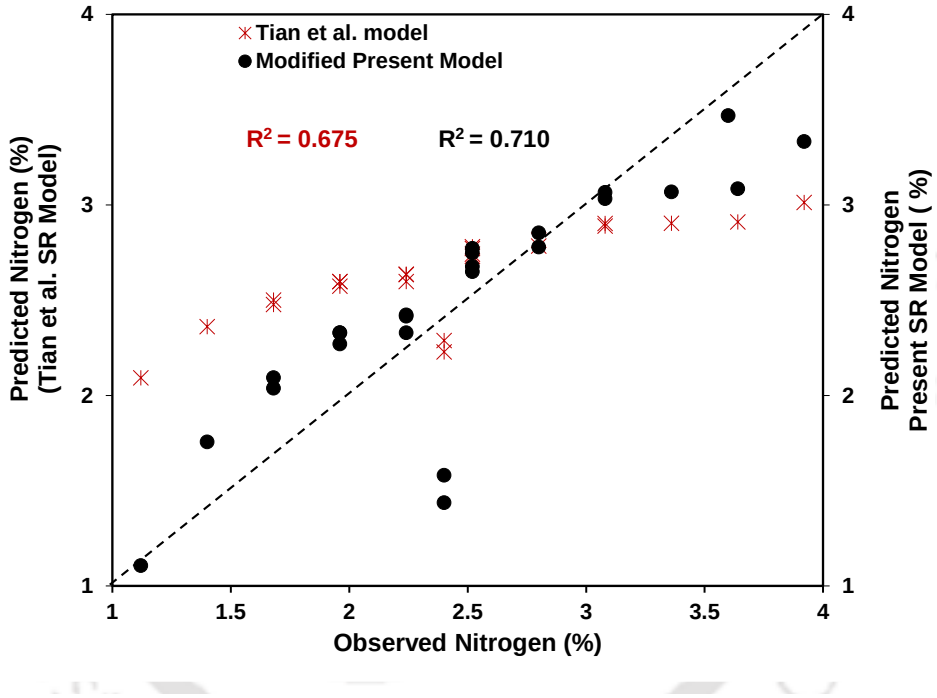

Figure 6.1 : Comparison of SR indices for the assessment of N content from hyperspectral data

From Figure 6.2, it is observed that the present and Tian et al. (2011) LNC model perform opposite to each other in predicting rice nitrogen content. While the established model exhibited a decreased value of nitrogen with linear trend (R^2 = 0.81), at the same point the present model exhibited an increased value of nitrogen with nonlinear trend (R^2 = 0.801). The standard error associated with the predicted values of leaf nitrogen content with less than 3% is evaluated for both Tian et al. (2011) and present modified LNC models from statistical formula and is found to be 52.5% and 28.7% respectively, whereas standard error for the

predicted values of leaf nitrogen content with more than 3% is found to be 69.4% and 11.8% for Tian et al. (2011) and present modified LNC models respectively.

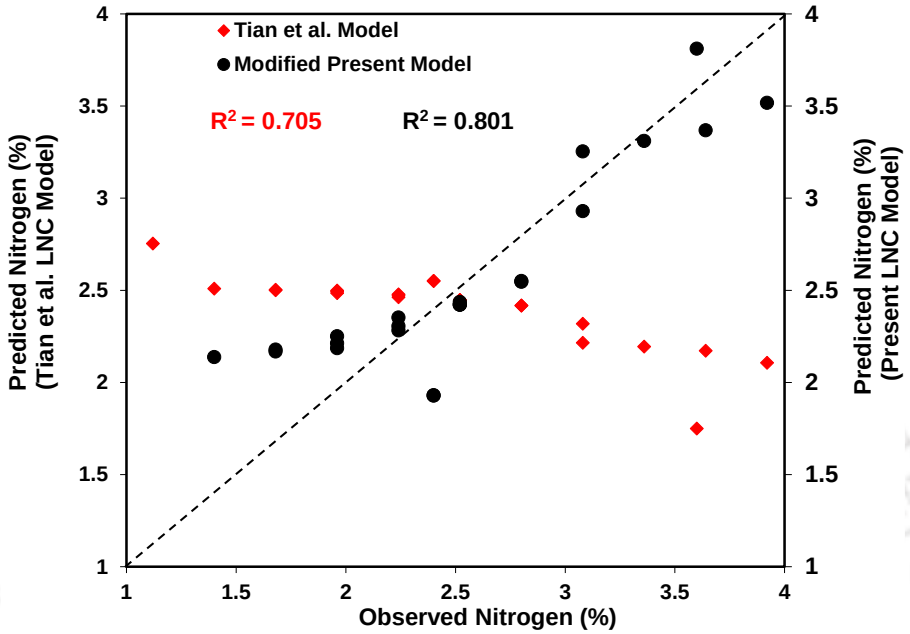

Figure 6.2 : Comparison of LNC indices for the assessment of N content from hyperspectral data

Our findings show that the index proposed by Tian et al. (2011) performed well in predicting nitrogen content with a different relation for Indian regional scale. The performance of an index varies from region to region in monitoring rice nitrogen content (Inoue et al., 2012 and Lee et al., 2008), and similar findings are demonstrated with the results obtained in our study. The established and present index models are further used for mapping of nitrogen in rice agriculture area in Assam, India.

6.6.3 Agricultural pigment and nutrient mapping from hyperspectral imagery

6.6.3.1 Application of published indices to map nitrogen content of rice

Mapping of nitrogen is an important aspect of paddy crop in India as well as globally. It is a challenging task because hyperspectral data is not available globally and it comprises of more than hundreds of bands that requires field *in-situ* measurements. At present, an effort has been

made to map the spatial distribution of nitrogen content in a rice agricultural area in Assam, India (Study site 1) from Hyperion imagery by using both published (Tian et al., 2011) and present modified regression index models. The model development was carried out in ERDAS 9.2 environment using Hyperion L1R product. The Hyperion image acquisition was carried out during the reproductive stage of paddy crop from the study site. To accompany this, field measurements were taken from the experimental field having different rice species at their growth period. The nitrogen mapping using present and published index models are shown in Figure 6.3.

Table 6.6 : Nitrogen content statistics derived from N classified map

Index Map	Mean	Std. Dev.
SR (Published)	3.821	0.726
SR (Present)	5.286	0.300
LNC (Published)	2.575	0.194
LNC (Present)	1.689	1.058

Both the present and established nitrogen maps were classified and the statistics of the nitrogen maps are summarized in Table 6.6. Nitrogen mapping by using published and modified SR index models are shown in Figure 6.3 (a, b). The SR index which has given the best performance in ground based hyperspectral data did not give satisfactory result in Hyperion imagery. While, the spatial variation in case of observed rice nitrogen is from 1.12 - 3.92% at its reproductive phase, for Hyperion imagery it varied from 5 - 8%. Our findings matched well with Tian et al., (2011), who has also reported that SR index did not give desired output from Hyperion based spectral data. Nitrogen mapping by using published and present LNC models are shown in Figure 6.3 (c, d). The nitrogen content which varied from 2.36 - 2.51% for the published linear model, varied from 2.35 - 3.82% by using presently developed nonlinear model. It is interesting to note that both the observed and predicted nitrogen content from Hyperion imagery are in the same range. On the other hand, the results obtained from Tian et al. (2011) model did not produce significant spatial variability of rice nitrogen content

in an agricultural system from Hyperion imagery. The nitrogen map captured well the spatial heterogeneity in the paddy fields which is the most valuable information for precision farming. Paddy agriculture area is clearly identified with a wide variation of nitrogen content through the presently developed relationships.

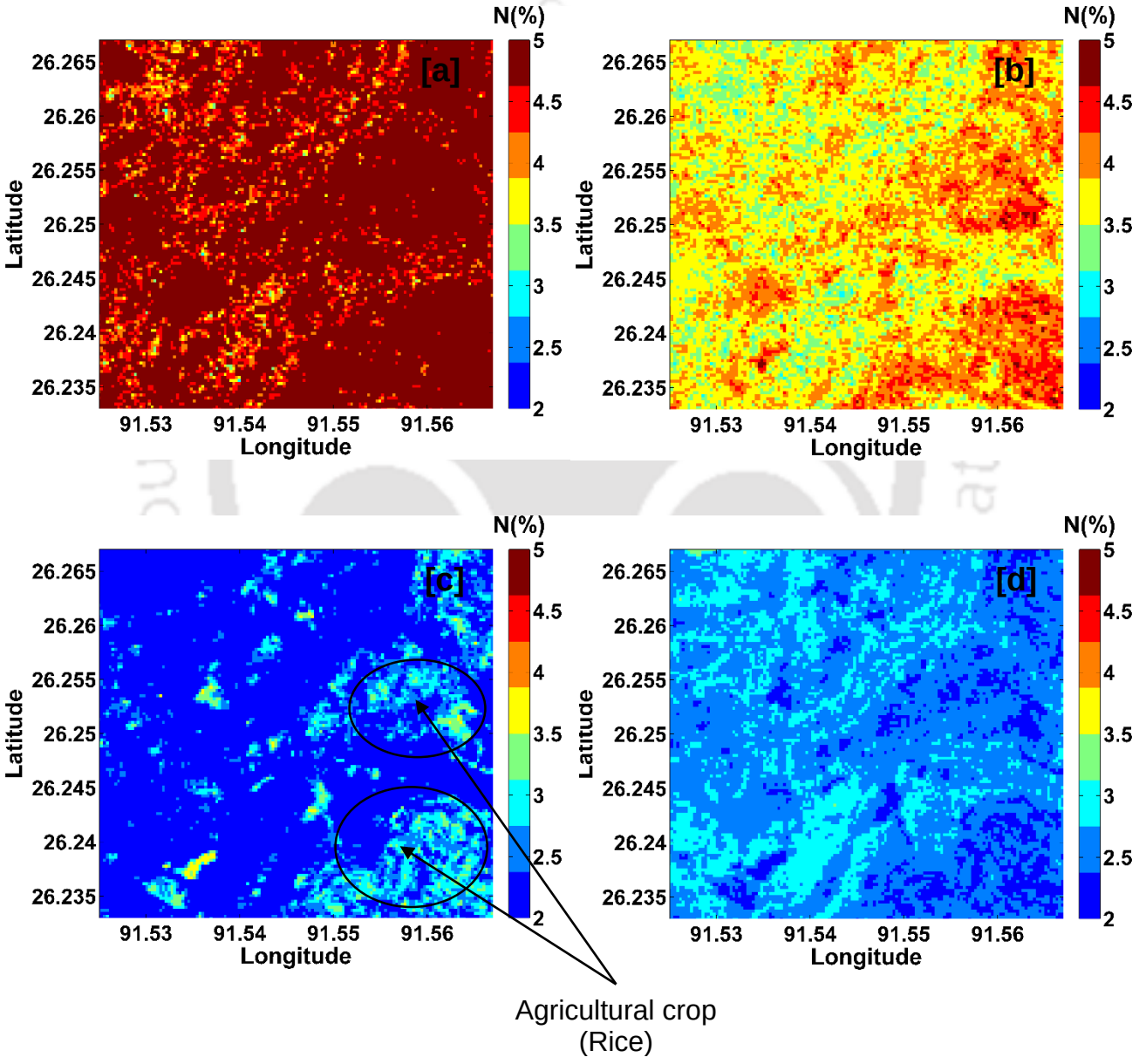

Figure 6.3 : Nitrogen mapping using (a) published SR index model (b) modified present SR index model (c) published LNC index model (d) modified present LNC index model

6.6.3.2 Application of published indices to map chlorophyll content of rice

Researchers focused on non-destructive estimation of chlorophyll content for a wide variety of leaves species containing high and low chlorophyll content, but very few agricultural crops like wheat, maize, soybean were considered. There was no focus towards mapping of rice chlorophyll content for an agriculture system from hyperspectral imagery. Present study deals with mapping of spatial variability of chlorophyll from Hyperion imagery using both linear and nonlinear regression index models in ERDAS 9.2 environment (Figures 6.4 - 6.8). This work will help in developing an informative system for paddy crop by monitoring its growth status from the imagery which will not only reduce laborious and tedious jobs like field visit, but also be less time consuming.

From Figure 6.4 (a, b), it is inferred that chlorophyll is well distributed spatially by using nonlinear LNC model than linear LNC model. The chlorophyll content which resulted from Hyperion imagery ranged from 1.77 mg/g to 5.77 mg/g (Figure 6.4 (b)) and has a good agreement with the observed chlorophyll content of the studied rice genotypes that ranged from 1.13 mg/g to 7.26 mg/g. Moreover, linear LNC model overestimates the chlorophyll content within the same rice agricultural field (Figure 6.4 (a)). Similarly from Figure 6.5 (a, b), the result demonstrates that the OSAVI nonlinear model overpredicted chlorophyll content of rice up to 9 mg/g while the linear model estimated it as 3.5 mg/g. This is because of different narrow bands associated with the proposed indices which are responsible for developing different relationships between the index and chlorophyll content. It is revealed from Figure 6.6 (a, b), both linear and nonlinear Gitelson index models were not able to quantify the chlorophyll content for paddy agriculture from Hyperion imagery which accomplished satisfactory results from *in-situ* chlorophyll content measurement with R^2 value 0.77 (Table 6.3). It may have happened because the tested index is designed for higher plant leaves like maple, hence the Hyperion sensor taking image at a higher altitude is not able to predict the same for a lower chlorophyll containing paddy crop. On the other hand, by analyzing mSR index models (Figure 6.7 (a, b)), it is found that nonlinear mSR model exhibited well acceptable performance providing wide spatial variation of chlorophyll content from 2.44 mg/g to 4.09 mg/g in some of the rice genotypes, whereas the linear mSR model exhibited higher chlorophyll value that ranged from 4.09 mg/g -10.6 mg/g in other genotypes leading to

spatial heterogeneity of rice fields in an agricultural system.

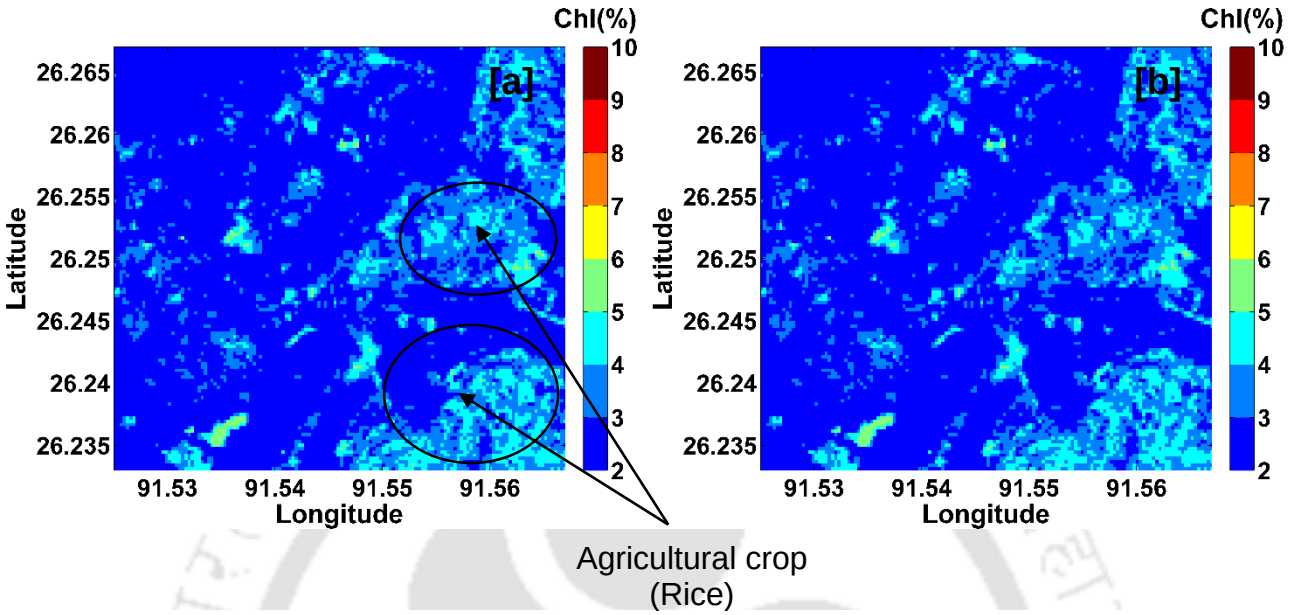

Figure 6.4 : Chl mapping using (a) Linear LNC model (b) Nonlinear LNC model

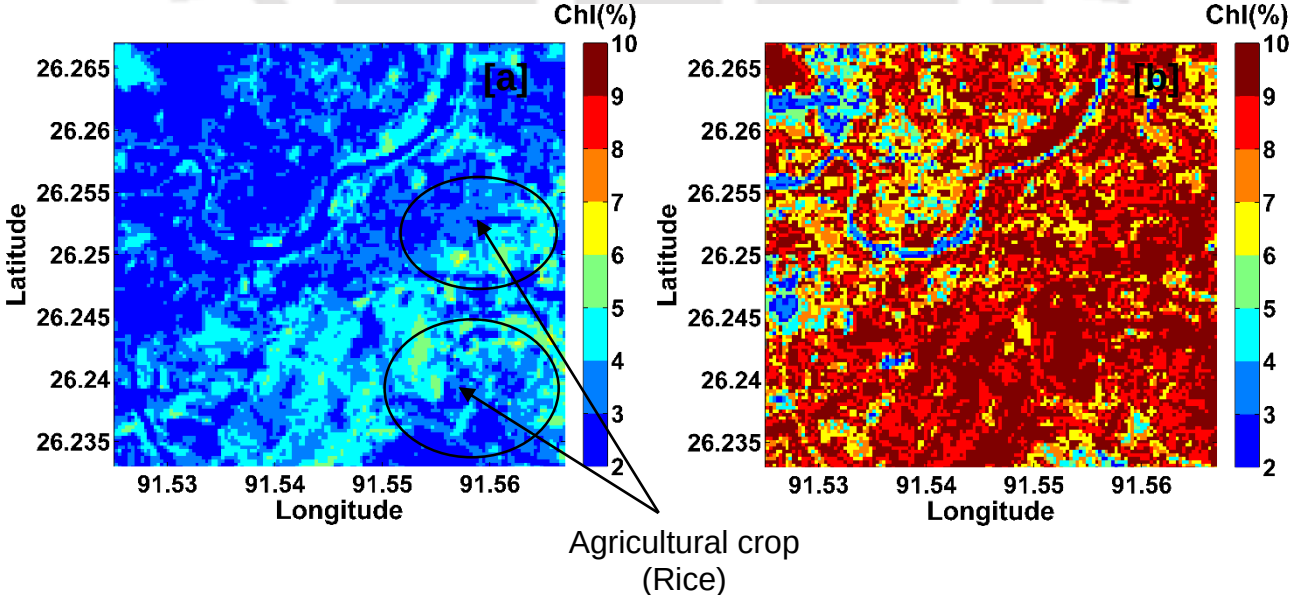

Figure 6.5 : Chl mapping using (a) Linear OSAVI model (b) Nonlinear OSAVI model

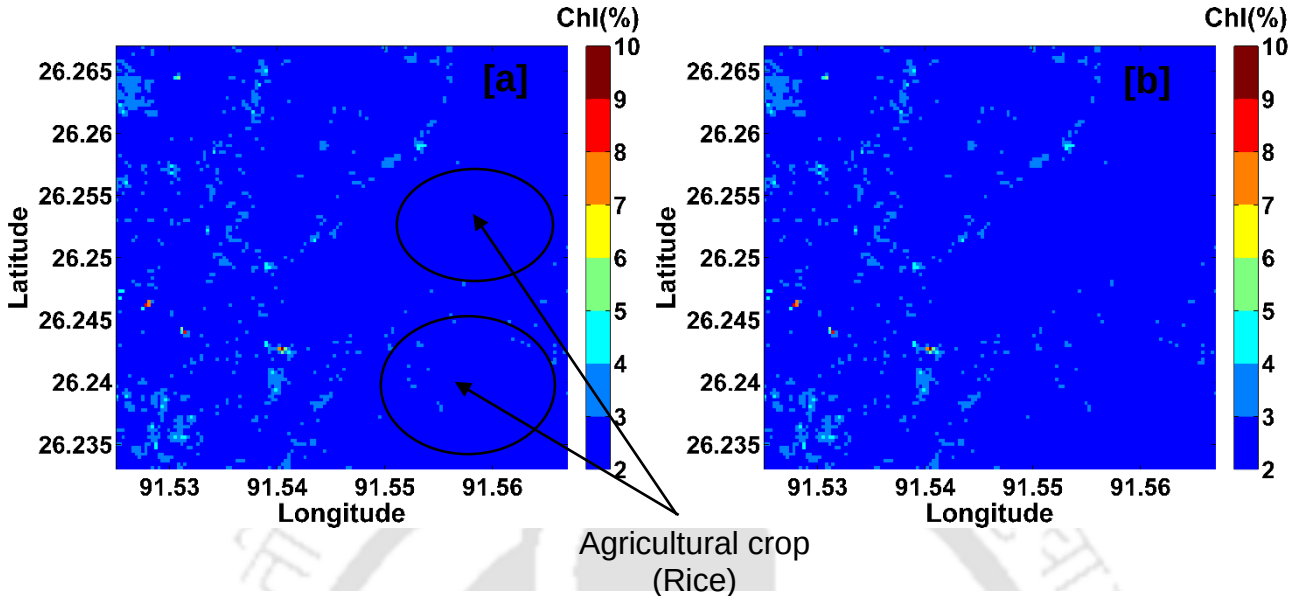

Figure 6.6 : Chl mapping using (a) Linear Gitelson model (b) Nonlinear Gitelson model

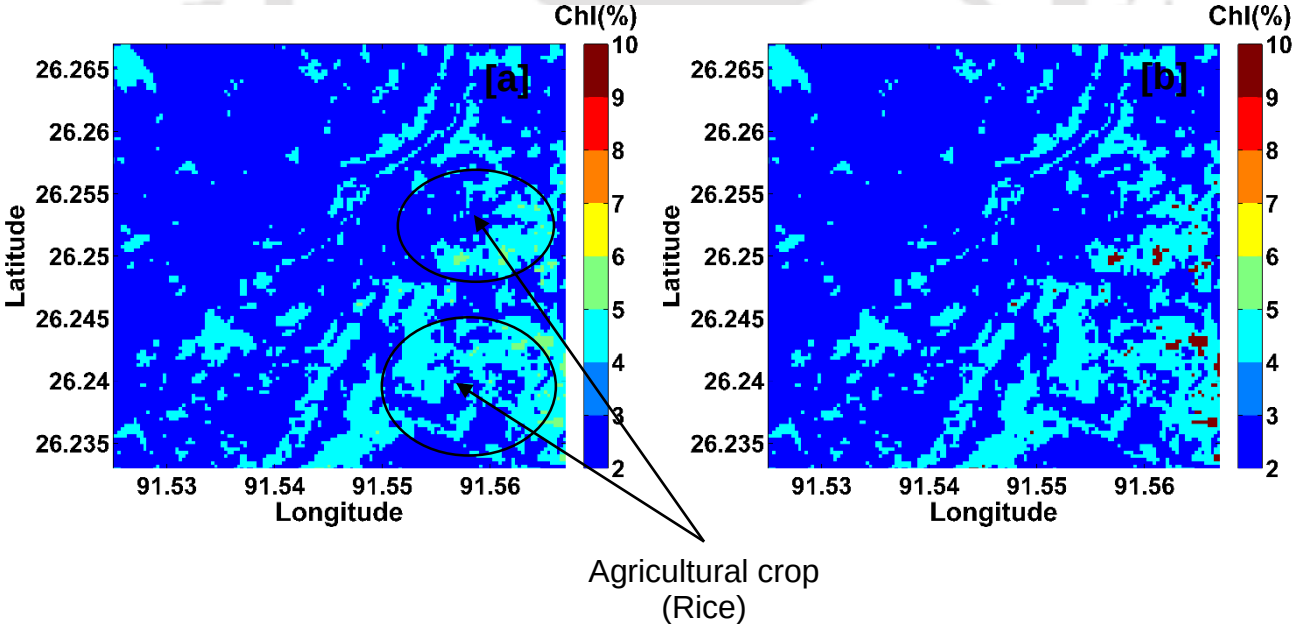

Figure 6.7 : Chl mapping using (a) Linear mSR model (b) Nonlinear mSR model

It is reported that, MTCI nonlinear model has extremely over predicted the same, additionally linear model has failed to provide satisfactory result. Therefore, the spatial variation of chlorophyll content of rice generated from MTCI linear model is demonstrated here (Figure 6.8). It is interesting to note that total chlorophyll content mapped from Hyperion image has a good agreement with the observed chlorophyll content. The observed mean chlorophyll content obtained from the rice varieties grown in the rice agriculture system of our study site varied from 1.84 to 2.19 mg/g and their standard deviation ranged from 0.638 to 1.095. The statistics of the above chlorophyll mapping of paddy crop obtained from different models are reported in Table 6.7. It is inferred from Table 6.7, within the observed chlorophyll range, these index models well predicted the chlorophyll content from Hyperion imagery, except OSAVI non-linear model which over predicted the chlorophyll content. However, it was not possible to synchronize Hyperion findings with ground measurements of the rice agriculture system. Considering the observed chlorophyll content of rice varieties in study area grown in the rice agriculture system, these index models (MTCI, OSAVI, Gitelson, mSR, LNC) performed approximately in the same range of the spatial distribution of chlorophyll for the agriculture system from Hyperion imagery. On the contrary, the findings from the present study of spatial variation of chlorophyll mapping revealed, the index models that have the potential to retrieve rice chlorophyll content from Hyperion imagery is in an acceptable range for a rice agriculture system.

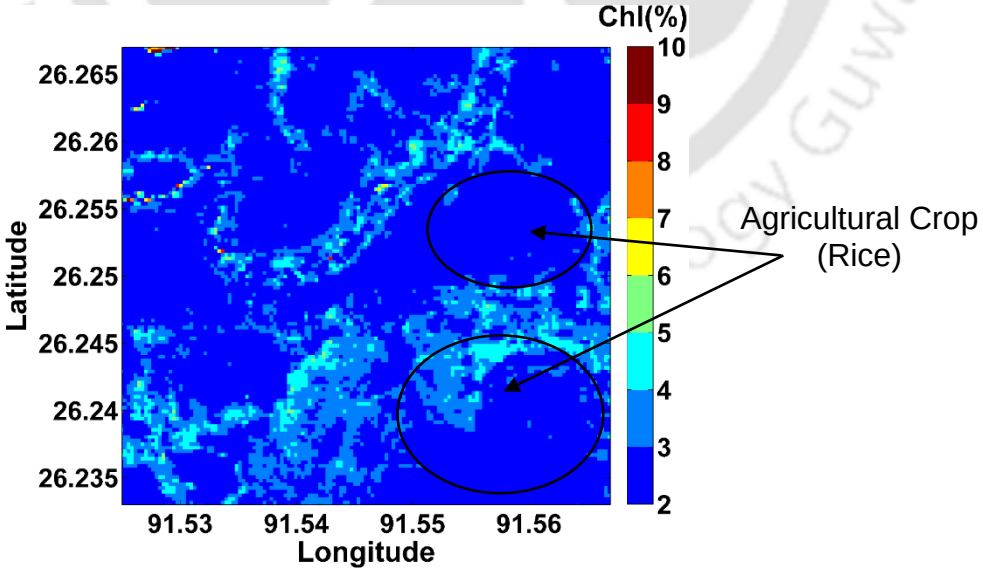

Figure 6.8 : Chl mapping using Linear MTCI model

Table 6.7 : Chlorophyll content statistics derived from Chl classified map

Index Model	Linear Model		Nonlinear Model	
	Mean	Std Dev.	Mean	Std Dev.
LNC	2.237	1.427	2.138	1.785
OSAVI	2.874	1.492	7.919	2.281
Gitelson	1.104	1.535	0.9573	1.781
mSR	2.252	1.54	1.537	3.506
MTCI	3.967	2.176		

6.7 Field Variability

Remote sensing has been used as an effective means to characterize rice spatial coverage over a large geographical area. However, field variability of a single vegetation cover does not give satisfactory results mainly due to non-availability of high spectral resolution remote sensing data. Hyperspectral data, which comprises of fine spectral resolution, has the potential to identify the crop parameters variability at plot scale within the crop field. Therefore, an advanced algorithm needs to be developed to investigate the variation between the spectral characteristics of a vegetative crop and its genotypes discrimination to obtain the field variation. Cluster algorithm is an effective approach for identifying different field management zones by using different layers of information. Cluster analysis based multivariate classification enables the identification of sub-regions in the fields that internally have similar characteristics. Aaron et al. (2004) used yield data, whereas fuzzy clustering of combined soil properties was used by Fleming et al. (2000) to divide a field into potential management zones. It is questionable whether spectral information acquired from spaceborne platform can be linearly scaled to map the field variation. Thus, spectral information acquired from Hyperion image has been investigated to map the spatial variation at plot scale within the crop field for a small agriculture field in an Indian rice agriculture system.

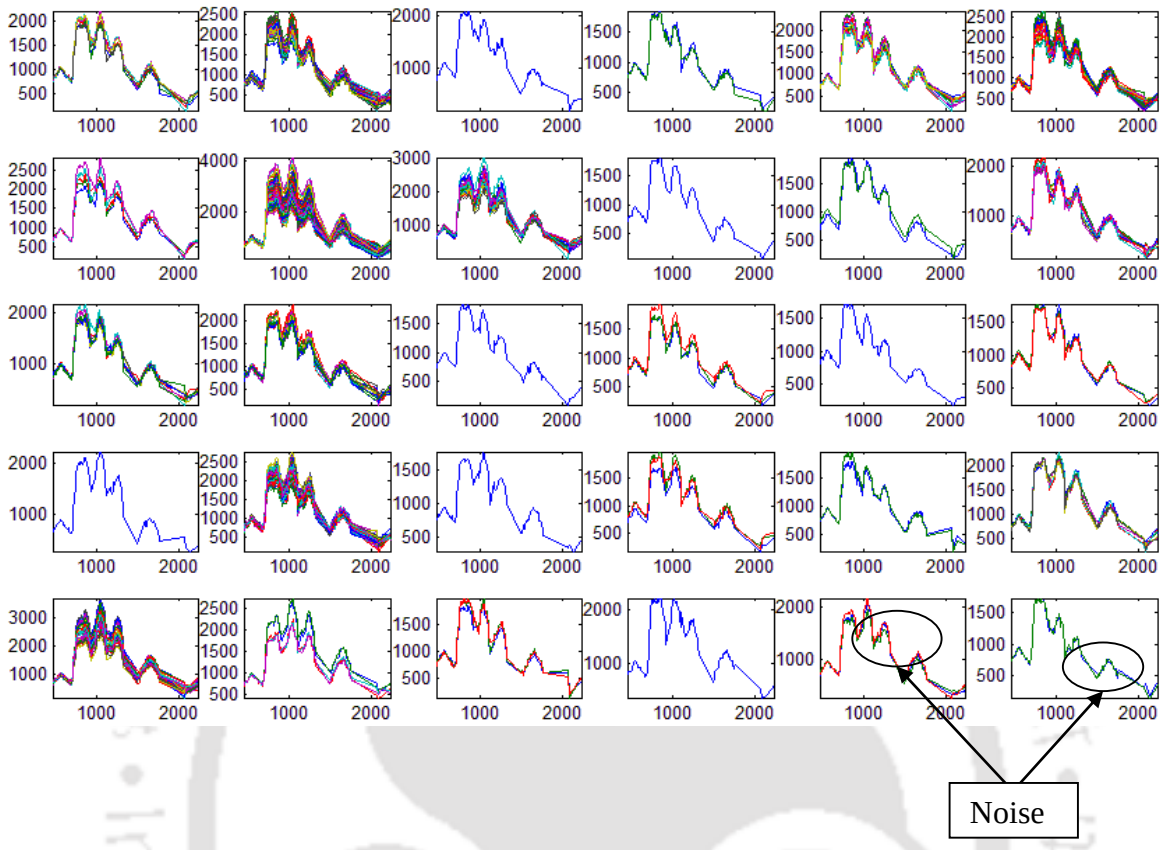

Figure 6.9 : Clustering of spectral waveforms from Hyperion image, 3rd October, 2014 (Rice agriculture site-I)

6.7.1 Clustering Analysis of paddy crop

For the present study, twelve rice agriculture sites were considered for the investigation in Kamrup district of Assam. Waveforms were extracted from Hyperion imagery for each of these sites and waveform classification followed by hierarchical clustering analysis were carried out. Figures 6.9 and 6.10 demonstrate two sample sites. From Figure 6.9 it is clearly observed that by employing hierarchical clustering technique, different groups of rice genotypes are being reformed and embedded noise are also being captured. This is an advantage of adopting clustering technique. Among the thirty classified groups that were well captured, some groups represented single rice species whereas some groups represented a mixture of different rice species. From Figure 6.10, similar findings are observed for another

rice agriculture site. Rice genotypes varied from one site to another, mainly on the basis of water availability in the rice field. As a result of which paddy crop cultivation with different varietal information can be mapped from space platform using Hyperion imagery through their spectral characteristics behaviour.

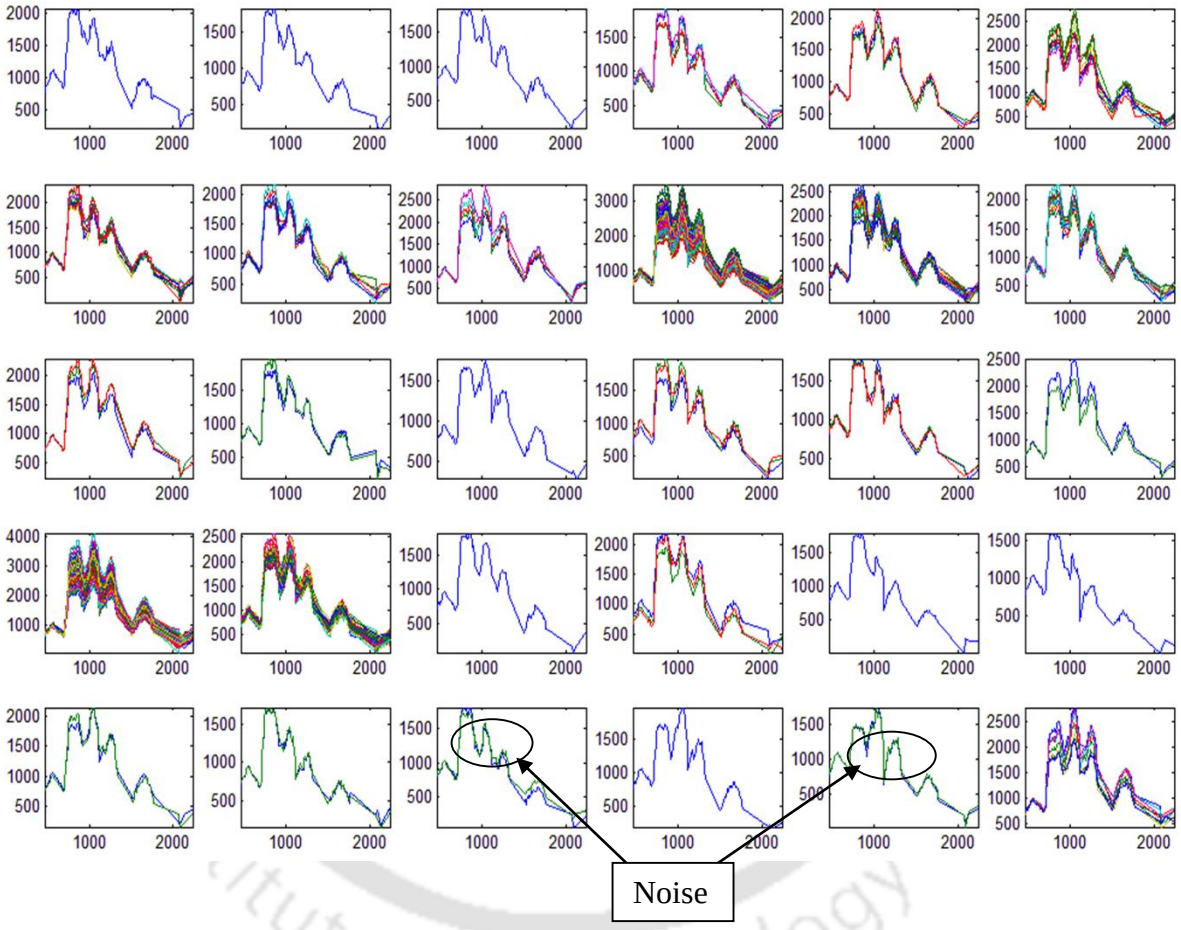

Figure 6.10 : Clustering of spectral waveforms from Hyperion image, 3rd October, 2014 (Rice agriculture site-II)

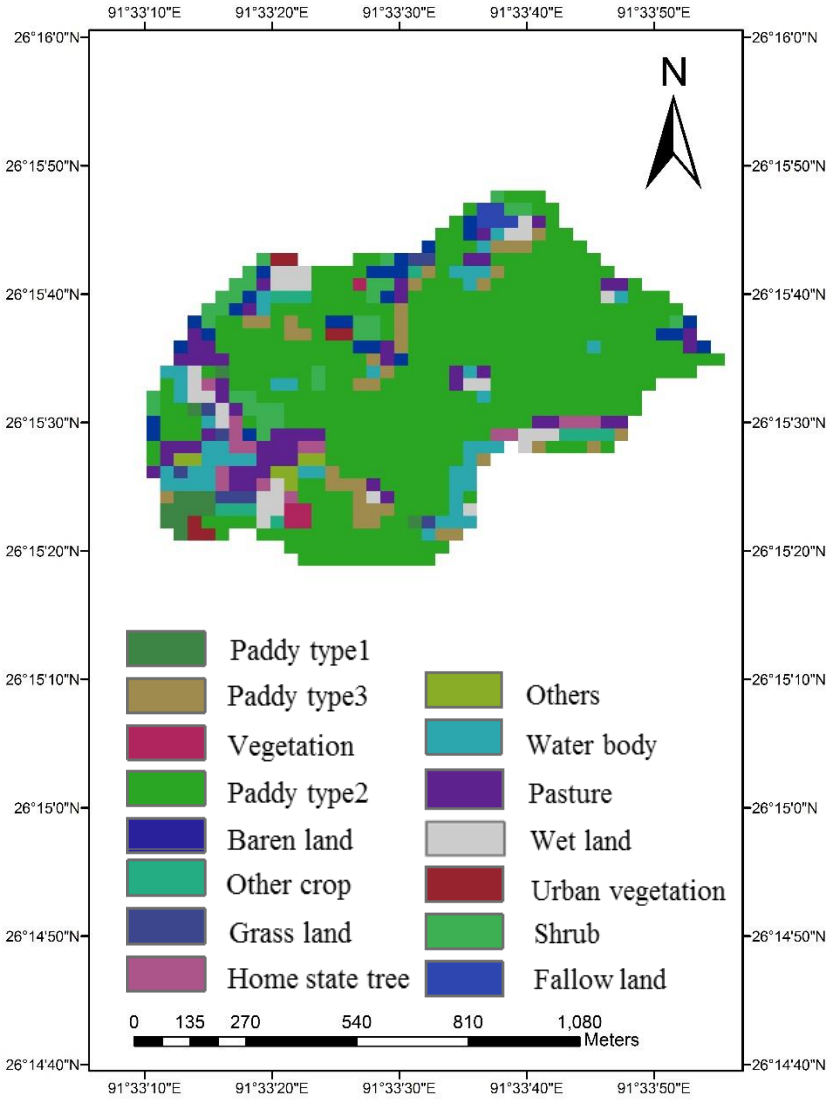

Figure 6.11 : Spatial distribution of rice agriculture site - I

6.7.2 Spatial Distribution of rice agriculture system

The obtained clustered groups were mapped spatially into classified maps of twelve rice agriculture sites. The spatial variation for the same two sample sites are presented in Figures 6.11 and 6.12. The results demonstrate a lack of homogeneity throughout the studied sites showing a high spatial heterogeneousness of the fields selected for a long-term rice cultivation practice. Such type of responses were observed mainly due to the variation of water levels

associated with the paddy crop fields. To reconfirm this, variability slope maps were generated from 30 m SRTM Digital Elevation Model (DEM) for the studied agricultural sites (Figures 6.13 and 6.14). It was found that the slope of the crop field is a measure of water availability in the paddy crop field. It was observed that the variability in rice agriculture system in India is purely a function of field topography. The rice field heterogeneity is mainly a result of large scale variations in soil moisture and water availability due to rapid change in topography within a very small field scale in an Indian rice agriculture system. Therefore, it is necessary to investigate spatial heterogeneity of the field. The variability of rice agriculture system for the twelve agricultural sites are shown in Figure 6.15.

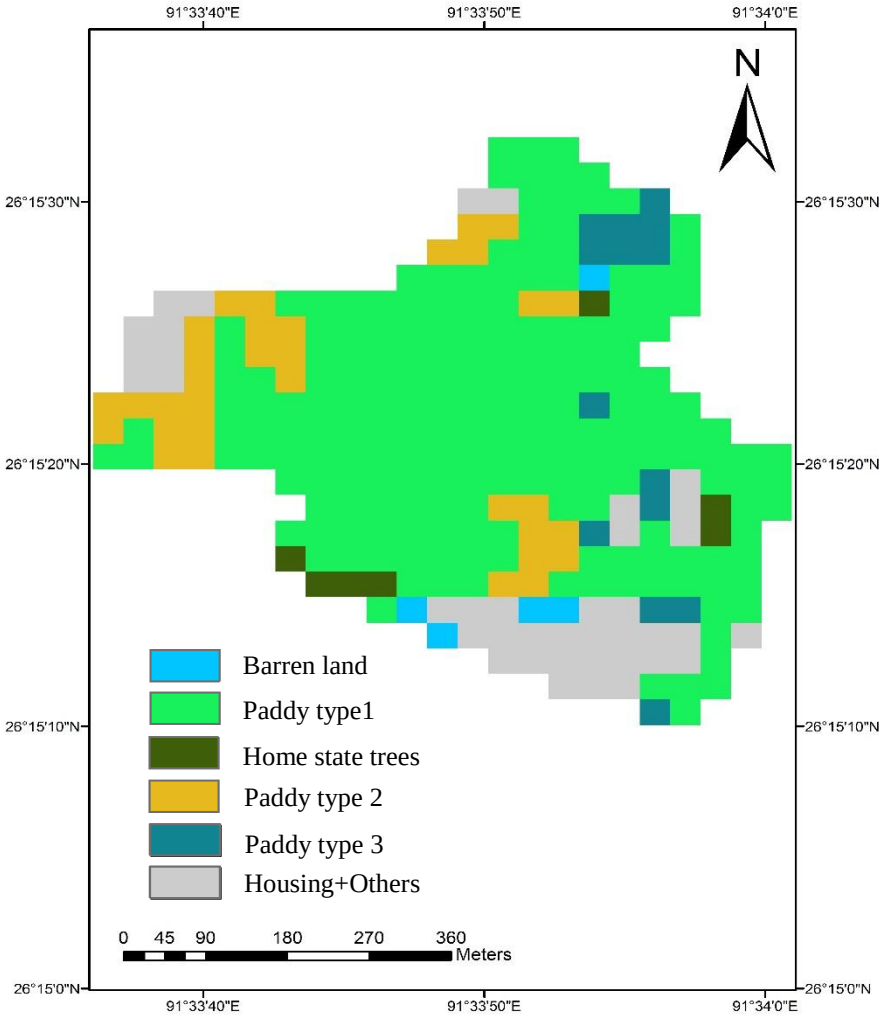

Figure 6.12 : Spatial distribution of rice agriculture site - II

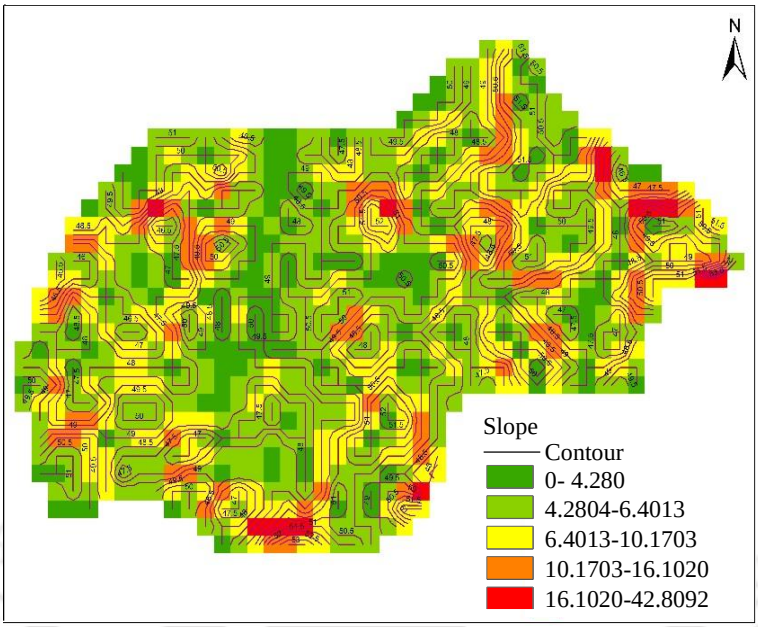

Figure 6.13 : Slope map generated from 30 m SRTM DEM for agriculture site I

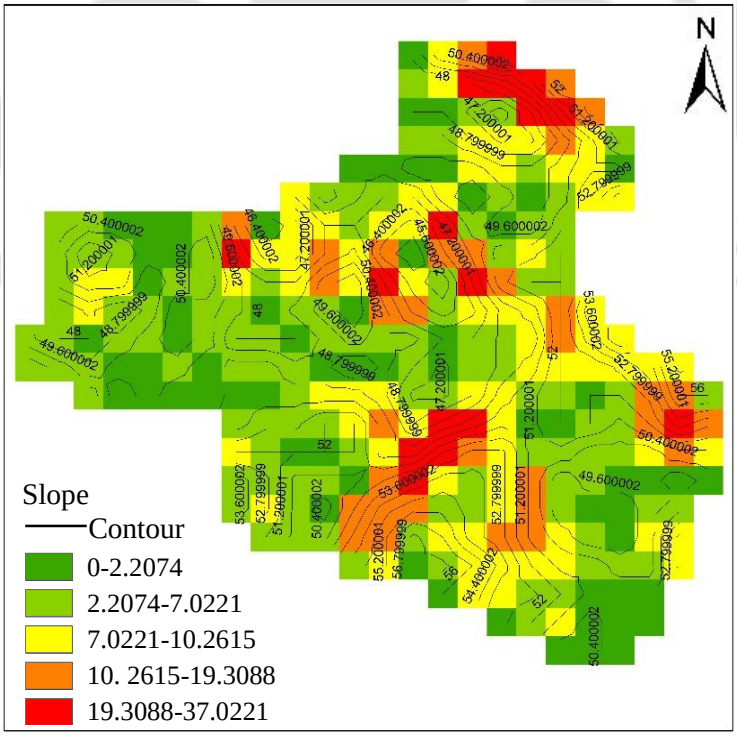

Figure 6.14 : Slope map generated from 30 m SRTM DEM for agriculture site II

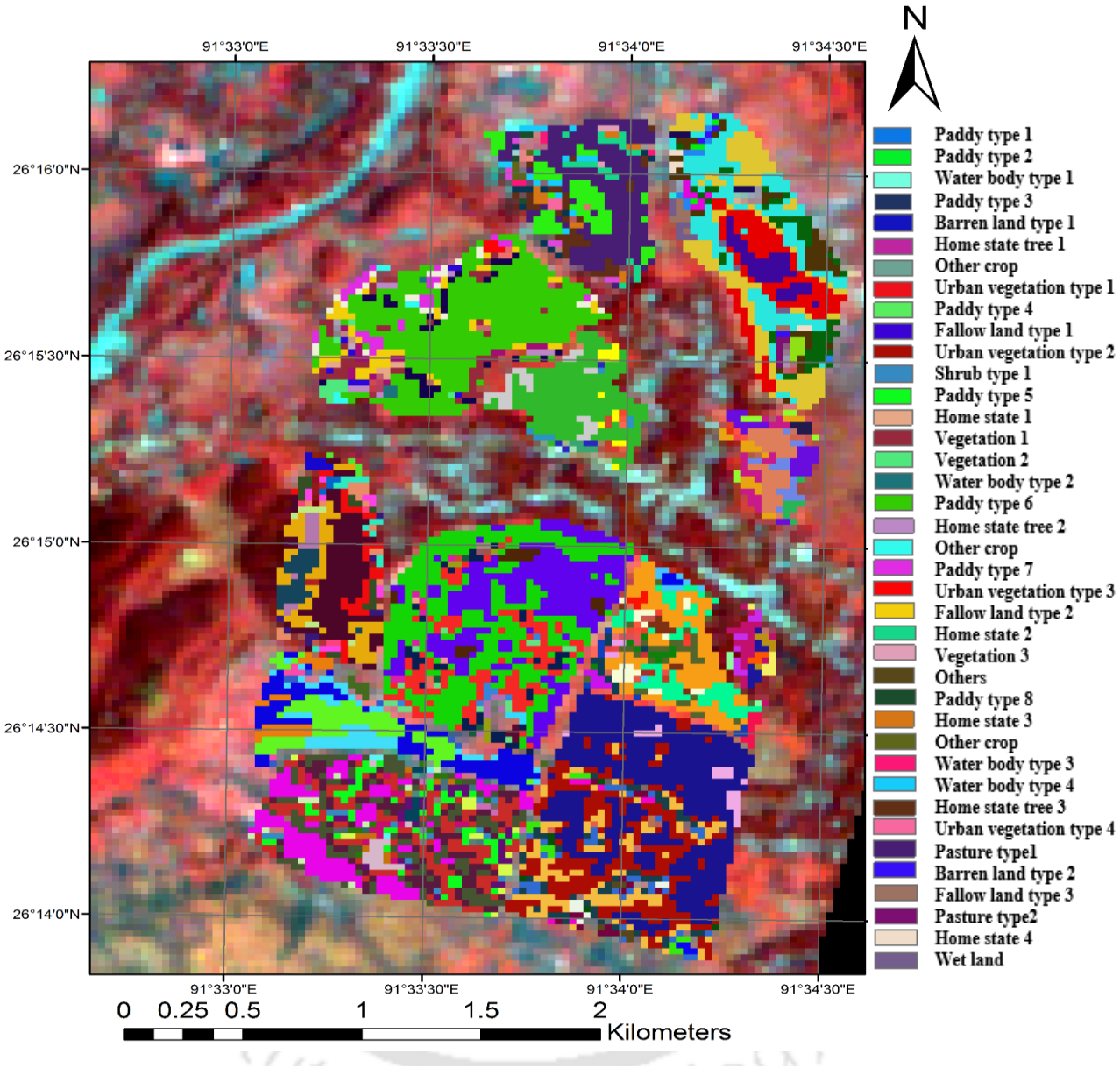

Figure 6.15 : Spatial distribution of paddy agriculture system, Assam, India

6.8 Conclusions

The SR index model, which gave best performance in destructive estimation of nitrogen content for *in-situ* hyperspectral data, did not quite produce satisfactory result from Hyperion imagery. The modified LNC index model, which followed a nonlinear relationship performed better than that of the established Tian et al. (2011) model as far as estimated nitrogen content

from Hyperion imagery was concerned. By employing modified nonlinear LNC model, rice nitrogen content resulting from Hyperion imagery varied spatially from 2.35 - 3.82% in a rice agriculture system and it matched well with the observed nitrogen content, while it was only 2.36 - 2.51% in case of Tian et al. (2011). Therefore, it can be inferred that this index model is more adaptive for the spatial nitrogen variation mapping of rice from Hyperion imagery in an agriculture system.

Exploiting *in-situ* hyperspectral measurements, MTCI, OSAVI, Gitelson, mSR, LNC indices were considered for the assessment of chlorophyll from L1R Hyperion data. Within the observed chlorophyll range obtained from the studied rice varieties grown in the rice agriculture system, these were the index models which well predicted the chlorophyll content of paddy crop from Hyperion imagery. Total chlorophyll content had a wide spatial coverage ranging from 1.77-5.81 mg/g (LNC index), 3.0-13 mg/g (OSAVI Index), 0.5-10.43 mg/g (Gitelson index), 2.18-10.61 mg/g (mSR index) and 2.90-5.40 mg/g (MTCI index). The investigated models well predicted chlorophyll content from satellite hyperspectral data whereas OSAVI non-linear model overpredicted the chlorophyll content. The proposed index models were more convincing for estimation of rice chlorophyll content spatially over an agricultural system from Hyperion imagery. Moreover, satellite data (Hyperion L1R) incorporated with index models were applied to retrieve the distribution of chlorophyll of paddy crop from space platform, but for operating in an agriculture system, the models still need to be improved with *in-situ* measurements in future studies.

Field heterogeneity of the crop can easily be quantified from hyperspectral satellite imagery and consequently, spatial variation of Chl and N mapping of paddy crop from Hyperion imagery can be used to develop an informative system for precision rice agriculture system. It is concluded that variability attributed to small scale farming system in India is controlled by slope of the field. The rice field heterogeneity is observed as a result of large scale variations in soil moisture and water availability due to rapid change in topography within a very small field scale in an Indian rice agriculture system. Additionally, with an aim to make the discussed index models operational in spatial variation mapping of Chl and N, they require further improvement along with ground measurements of an agriculture system in future studies.

7 Water Stress Variability Mapping in Rice Agriculture System

7.1 Introduction

Water is one of the most dominant components in agricultural crops. Plant–water relations control several elementary plant processes like stomatal regulation, creating close linkages between carbon, water, energy, and nitrogen cycles (Chavarria and Santos, 2012; Ustin et al., 2012). Therefore, determination of crop water status is an important task in order to monitor crop health. It aids in drought assessment thus facilitating timely application of irrigation to crops, thereby improving the crop yield. During water stress, the pathway meant for exchange of oxygen, water and carbon dioxide closes due to lack of stomata production resulting in decreased photosynthesis rate (Law et al., 2002; Long et al., 1996; Porporato et al., 2001), hence growth and development of rice leaves are affected by water stress that ultimately leads to reduction in rice production.

Water stress can be remotely sensed using visible, near infrared (NIR), shortwave infrared (SWIR) bands of the spectrum. This is achieved through hyperspectral air-borne sensor, hand held spectroradiometer and other earth observation multispectral sensors (Cheng et al., 2014; Clevers et al., 2010; de Jong et al., 2014; Wang et al., 2017). Zarco-Tejada et al. (2012) conducted an experiment in order to detect water stress in a citrus orchard by taking images acquired from a thermal camera and a micro-hyperspectral imager mounted on an unmanned aerial vehicle. He reported that temperature, narrow-band VIS–NIR formulations, and chlorophyll fluorescence are best related to water stress at 747, 760, 762 and 780 nm wavebands. Therefore, in the present study the reflectance characteristics of paddy crop

canopies at near NIR and SWIR regions have been investigated further for estimating leaf water contents in a rice agriculture system.

Although previous studies have accounted for estimating the leaf water content of crops like wheat, maize and cotton by considering appropriate narrow wave bands, still there is lack of research with regards to whether the proposed studies can suitably work in estimating the LRWC of a really dynamic crop like paddy. Now the question is whether the findings in previous literatures are validated for other crops and can be used by farmers for precision farming of paddy crop in Indian climatic condition. The present study envisages the detection of paddy crop water stress from space platform by employing different water indices. Primarily, the performance of water indices to retrieve water content in rice leaf is examined and a relationship between the index and leaf water content of rice from ground based hyperspectral measurements is established. Secondly, SWIR narrow band water index regression models are derived for the paddy crop. Finally, by using advanced remote sensing techniques, different water stresses index models are examined to generate water stress maps showing their spatial variation for winter/kharif rice (June/July to November/December) and summer/rabi rice (November/February to March/June) during monsoon and pre-monsoon periods respectively in a rice agriculture system from high spectral resolution Hyperion (EO-1) imagery.

7.2 Study Sites

For this objective, two study sites were considered, one for winter/kharif rice cultivation and another for summer/rabi rice cultivation. The experimental station of RRLRRS, Assam, India (26°15'18.84"N, 91°33'50.68"E) (Study site 1) was chosen as site for winter rice cultivation during monsoon period. Agricultural farmers' fields in the district of Cuttack, Odisha, India (20°19'24.84"N, 85°32'41.94"E) (Study site 2) was considered as site for summer rice cultivation during pre-monsoon period. Study sites are discussed in detail in Chapter 3.

7.3 Field Campaign

A field campaign was conducted in the district of Cuttack, Odisha, India (Study site 2) during

pre-monsoon period in the year 2016 to collect detailed information regarding paddy crop varieties, application of fertilizers and mode of irrigation used in the agricultural farmland. Rice genotypes such as Khandagiri, Konark, Lalata, Laxmisagar, Naveen, No 303, Purusotum, Pratikhya and Surendra are grown with assured irrigation. Mostly, urea was applied as fertilizer in three splits in addition to organic farmyard manure and irrigation was provided by pumping water from the river bed or bore well for adequate water supply to paddy crop during pre-monsoon period. Another field campaign was also conducted in the Kamrup district, Assam, India (Study site 1). The rice varieties such as Jaya, Abhishek, Chandrama, Shabhagi Dhan, Ranjit, Baismuthi, Nilanjana, IR64, Joymati, Vandana, Kolong, and Naveen were cultivated. Urea and organic manure were applied as fertilizer. There was provision of assured irrigation for crop water requirement, to provide adequate water to the rice plants throughout the crop growing period. Here weed was totally controlled in each of the rice plots. Details of field campaign is discussed in Chapter 3.

7.4 Data used

7.4.1 *In-situ* hyperspectral data

Paddy crop physiological data and reflectance from rice canopy cover were retrieved from different rice plots comprising different rice varieties, and these selected paddy fields were made homogeneous for rice breeding and field management. It was our intention to use differently aged cropping rice species providing different yields for the estimation of leaf water content of winter and summer rice in Indian climatic condition. The spectroradiometric spectral reflectance was measured at a weekly interval starting from vegetative phase to ripening phase of the rice species. All the spectral measurements were acquired from the experimental fields of RRLRRS, Assam in 2014 under controlled environmental conditions i.e. at the rice research station which was managed based on standard agriculture management practices of the region. Details already discussed in Chapter 3.

7.4.2 Space-borne hyperspectral data

The temporal resolution of Hyperion sensor is very poor, hence getting high temporal data

sets for a specified study site in a particular time period is very difficult. We have collected the images during its reproductive phase that provide critical growth information of paddy crop. While the Hyperion image covering winter rice crop area during monsoon period was acquired in Assam on 3rd October, 2014 at 3.30 GST, the Hyperion image covering the summer paddy crop area during pre-monsoon period area in Odisha (Study site 2) was acquired on 8th March, 2016 at 3.53 GST. Details are described in Chapter 3.

7.5 Leaf Relative Water Content (LRWC) measurements

The plant leaf samples were collected from the experimental study site in Assam, India. Leaf water content was measured for 24 rice genotypes during their vegetative, reproductive and ripening phases from each experimental plot. Just after each canopy spectral reflectance measurement, plant samples (7-15 plants/plot) were randomly selected. Plant leaves were removed from its stem for measurement by standard procedures. LRWC was calculated based on oven dry method (Pask et al., 2012). Individual leaves were first removed from stem with tweezers and a sharp razor blade was used to recut them. Leaves were then immediately weighed to obtain fresh mass (FM). In order to determine the turgid mass (TM), leaves were soaked in distilled water for 6 hours inside a closed petri dish and weighed again to record the turgid weight (TW) after gently wiping the water from the leaf surface with tissue paper. At the end of the imbibition period, leaf samples were placed in a pre-heated oven at 80°C for 48 hours in order to obtain dry mass (DM). Values of FM, TM and DM were used to calculate leaf relative water content LRWC using the following formula.

$$\mathrm{LRWC}(\%) = \left[\frac{(\mathrm{FM} - \mathrm{DM})}{(\mathrm{TM} - \mathrm{DM})}\right] \times 100 \qquad (7.1)$$

7.6 Narrow Band Index approach to evaluate Water Stress from Space platform

The functional relationship between relative water content in leaves and spectrum reflectance in visible and NIR regions provided a non-destructive technique employing visible spectral reflectance for accurate assessment of LRWC (Zygielbaum et al., 2009). Additionally, water

absorption bands are strongly correlated with narrow-band reflectance and derivative spectra in the visible-near infrared (VNIR) and shortwave infrared (SWIR) (Ullah et al., 2012). It was proved to be insufficient to find out LRWC using single band reflectance information. Thus, in order to estimate LRWC more accurately, narrow band indices with reflectance at two or more bands are being used (Mariotto et al., 2013; Mutanga et al., 2004; Zhang et al., 2012). This study aims to employ the narrow band indices specifically designed for water stress of different agricultural crops to quantify the rice leaf water content accurately from space-borne hyperspectral imagery. The mathematical formulae for computing narrow band simple ratio and normalized difference indices were derived from combinations of the reflectance spectra.

Narrow band index for the estimation of leaf water content can be expressed as Normalized Difference Water Index (NDWI) and Simple Ratio Water Index (SRWI).

Mathematically it can be defined as,

$$NDWI(x, y) = (y - x)/(x + y) \quad (7.2)$$

$$SRWI(x, y) = (x/y) \quad (7.3)$$

where, x and y are the narrow band reflectances (R_i and R_j) or first derivative (D_i and D_j) values at i and j nm respectively over the whole spectrum obtained from hyperspectral sensor.

An investigation was carried out to assess the strength of the VNIR vegetation water indices in estimating leaf water content of paddy crop at three different growth phases, i.e. the vegetative phase, the reproductive phase and the ripening phase. Furthermore, the SWIR vegetation water indices were tested to map the leaf water content of paddy in a crop calendar during pre-monsoon and monsoon period. Based on published literatures, 17 vegetation water indices, those better elucidate the relationship between LRWC and index, were implemented in the present study and listed in Table 7.1. The overall methodology adopted in this study is schematically depicted in a flowchart (Figure 7.1).

Table 7.1 : Summary of selected vegetation water indices, equations, tested species, and references for the measurement of LRWC

Index	Equation	Tested species	References
Floating-position water band index (fWBI)	R_{900} / min(R_{930}-R_{980})	Corn (Zea mays), spinach (Spinacia oleracea), and snap beans (Phaseolus vulgaris)	Strachan et al. (2002)
Ratio Vegetation Index (RVI)	(R_{954} / R_{985})	Wheat (Triticum aestivum L.)	Major et al. (1990)
Normalized Difference Vegetation Index (NDVI)	(R_{900}–R_{680}) / (R_{900}+R_{680})	Two conifers (Pinus edulis and Juniperus monosperma, Wheat (Triticum aestivum L.), winter wheat	Stimson et al. (2005)
Water Band Index (WBI)	(R_{970} / R_{900})	Phaseolus vulgaris, Capsicum annuum, and Gerbera jamesonii	Penuelas et al. (1993)
Normalized Water Index-1 (NWI--1)	(R_{970}–R_{900} / (R_{970}+R_{900})	Wheat (Triticum aestivum L.),	Babar et al. (2006)
Normalized Water Index-2 (NWI-2)	(R_{970}–R_{850}) / (R_{970}+R_{850})	Wheat (Triticum aestivum L.)	Babar et al. (2006)
Normalized Water Index-3 (NWI-3)	(R_{970}–R_{880}) / (R_{970}+R_{880})	Winter wheat	Prasad et al. (2007)
Normalized Water Index-4 (NWI-4)	(R_{970}–R_{920}) / (R_{970}+R_{920})	Winter wheat	Prasad et al. (2007)
Simple Ratio Water Index (SRWI)	(R_{860} / R_{1240})	Douglas fir (Pseudotsuga menziesii) and bigleaf maple (Acer macrophyllum)	Zarco-Tejada et al. (2003)

Index	Equation	Tested species	References
Moisture Stress Index (MSI)	(R_{1600} / R_{820})	Quercus agrifolia (sclerophyllous leaves), Liquidambar styraciflua (hardwood deciduous tree leaves), Picea rubens and Picea pungens (conifer needles), and Glycine max (herbaceous dicot leaves)	Hunt and Rock (1989)
Normalized Difference Water Index-1240 (NDWI-1)	$(R_{860} -R_{1240}) / (R_{860} + R_{1240})$	Wheat (Triticum aestivum L.)	Gao (1996)
Normalized Difference Water Index-1640 (NDWI-2)	$(R_{860} -R_{1640}) / (R_{860} +R_{1640})$	Corn (Zea mays) and soybeans (Glycine max)	Chen et al. (2005)
Normalized Difference Infrared Index (NDII)	$(R_{819} -R_{1600}) / (R_{819}+R_{1600})$	Smooth cordgrass (Spartina alterniflora)	Hardisky et al. (1983)
Normalized Difference Water Index–Hyperion (WI-Hyperion)	$(R_{1070} – R_{1200}) / (R_{1070} + R_{1200})$	Green vegetation (green leaves)	Ustin et al. (2002)
Normalized Multi-band Drought Index (NMDI)	$R_{860}-(R_{1640}-R_{2130})/ R_{860}+(R_{1640}+R_{2130})$	Vegetation in savanna	Wang and Qu (2007)
Semi-arid Water Index-1 (SAWI-1)	R_{780} / R_{1750}	Spring wheat	Wang et al. (2015)
Semi-arid Water Index-2 (SAWI-2)	$(R_{780}-R_{1750}) / (R_{780}+R_{1750})$	Spring wheat	Wang et al. (2015)

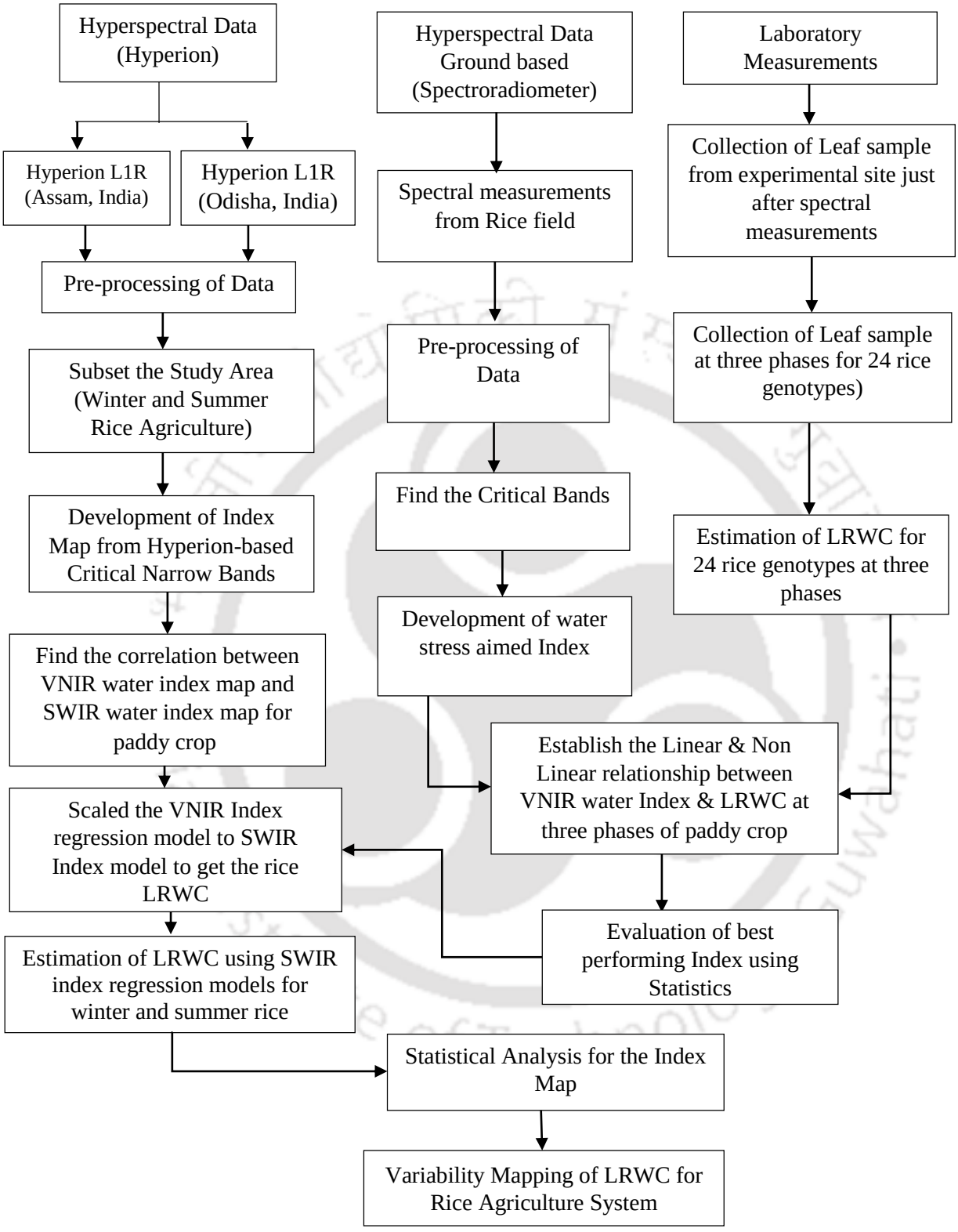

Figure 7.1 : Complete sequence to map LRWC variability from space platform

7.7 Results and Discussion

7.7.1 Estimation of Leaf Relative Water Content

The field reflectance spectra were collected for twenty-four rice genotypes at their three phases of growth - particularly the vegetative, the reproductive and the ripening phases. At the same time, leaf water content of the respective species was measured in the laboratory. In the first part, the relation between derived narrow band indices and LRWC at their three phases are demonstrated. The relationships are established between the estimated leaf water content and the VNIR narrow band vegetation water indices derived from the observed reflectance spectra of winter rice in its three phases during the monsoon period. In the second part, the best performing vegetation narrow band water indices in different crop developmental phases are selected based on performance of statistical analysis. At the end, the SWIR water indices are selected for the mapping of LRWC variation in winter and summer rice agriculture system from Hyperion imagery during monsoon period (in Assam) and pre-monsoon period (in Odisha) respectively in a crop calendar in Indian climatic condition.

To correlate the relationship between the vegetation water indices and rice LRWC at their crop developmental phases, the VNIR indices are calculated for a controlled and well managed rice agriculture practice field from canopy spectral reflectance data rather than Hyperion image. The results of the tested VNIR narrow band vegetation water indices for different growth phases are summarized in Table 7.2. Linear and nonlinear regression analyses were established with the nominated spectral water indices serving as independent variables. The result implied that all the eight VNIR narrow band vegetation water indices, i.e. water band index (WBI), ratio vegetation index (RVI), normalized difference vegetation index (NDVI), floating-position water band index (fWBI), normalized water index-1 (NWI-1), normalized water index-2 (NWI-2), normalized water index-3 (NWI-3) and normalized water index-4 (NWI-4) performed differently in all the three phases of winter rice during monsoon period.

Table 7.2 : Relationship between the water indices calculated from ground based hyperspectral spectra and LRWC

(* R^2 is significant at $p < 0.05$ and number of samples, n = 24)

Performance	WBI	RVI	NDVI	fWBI	NWI-1	NWI-2	NWI-3	NWI-4
Vegetative phase								
Fit-equation	$y = -93.328x^2 + 324.75x - 146.16$	$y = 44.062x + 12.06$	$y = 206.87x^2 - 450.9x + 301.09$	$y = -14.732x + 80.637$	$y = 429.82x + 69.284$	$y = -34.498x + 76.44$	$y = 44.22x + 72.535$	$y = 471.89x + 73.704$
RMSE	4.635	4.275	3.726	3.561	4.383	2.316	4.365	5.31
R^2	**0.739***	0.123	0.332	**0.350***	0.205	0.005	0.007	**0.361***
p-value	0.0425	0.086	0.0698	0.0498	0.098	0.1594	0.185	0.049
Reproductive phase								
Fit-equation	$y = -89.244x + 139.82$	$y = 82.246x - 23.779$	$y = 73.563x - 20.809$	$y = -25.443x + 77.734$	$y = -245.15x + 65.105$	$y = -152.73x + 68.713$	$y = -144.57x + 70.496$	$y = -343.3x + 60.155$

Performance	WBI	RVI	NDVI	fWBI	NWI-1	NWI-2	NWI-3	NWI-4
RMSE	2.544	4.061	3.461	5.5691	4.159	2.367	3.15	1.573
R^2	**0.819***	**0.556***	**0.394***	0.1533	0.375	**0.414***	**0.544***	**0.645***
p-value	0.0152	0.0493	0.0498	1.258	0.562	0.021	0.0505	0.039
Ripening phase								
Fit-equation	y = 261.5x - 165.34	y = -211.69x + 289.37	y = 113.3x - 47.404	y = 9.9986x + 52.888	y = -215.57x + 61.756	y = -423.05x + 39.104	y = -791.93x + 10.647	y = -285.86x + 58.518
RMSE	2.34	4.551	3.941	5.131	1.679	3.541	2.525	2.573
R^2	**0.601***	0.064	0.106	0.134*	0.106*	0.115	**0.521***	0.12*
p-value	0.0256	2.526	0.108	0.0223	0.026	0.261	0.044	0.016

* denotes significant at 0.05 level

7.7.2 Determination of critical stage for LRWC measurement

The index, WBI exhibited a satisfactory correlation with LRWC at the vegetative, reproductive and ripening phases of paddy crop indicating R^2 values 0.739, 0.819 and 0.601 respectively. The narrow band index WBI displayed significant correlation with LRWC at all the three phases, with nonlinear regression relation at vegetative phase having $R^2 = 0.739$ and linear regression relation at reproductive and ripening phase of paddy crop with R^2 values 0.819 and 0.601 respectively.

Moreover, the index WBI, one of the best indices for leaf water estimation, which has not exhibited satisfactory result for wheat crop (Ranjan et al., 2015), produced satisfactory results for rice crop leaf water content. The index NDVI, which worked well in predicting LRWC in winter wheat and other natural vegetation reported by Stimson et al. (2005) and Liu et al. (2015), did not perform well for paddy crop. Meanwhile, the narrow band indices, RVI and fWBI followed linear regression models for all the three phases. Here, it is interesting to note that satisfactory results for assessment of rice water content is observed only at reproductive and vegetative phases of paddy crop for RVI and fWBI respectively. Besides these, the two normalized water indices- NWI-1 and NWI-2, proposed by Babar et al. (2006), which predicted attainable grain yield in spring wheat genotypes under water irrigated, deficient and stressed conditions, in our present study produced unsatisfactory results in predicting leaf water content for the three phases of rice crop except the reproductive phase in case of NWI-2. The NWI-3 and NWI-4 indices exhibited satisfactory results for reproductive phase of paddy crop.

From the regression model analysis, it can be observed that reproductive phase is the most sensitive phase in estimating LRWC for paddy crop. Furthermore, WBI, NWI-3 and NWI-4 among the tested eight indices showed a very good correlation with LRWC at reproductive phase. Based on the performance of statistics, these three indices produced improved results in estimation of rice LRWC which are demonstrated in Figures 7.2-7.4. The goodness of fit of these narrow band vegetation water index models are verified on the basis of descriptive measures i.e Wilmot's index of agreement (IoA), root mean square error (RMSE), mean relative error (RE) values, which can be defined as:

$$IoA = 1 - \frac{\sum_{i=1}^{n}\left(P_i - O_i\right)^2}{\sum_{i=1}^{n}\left(\left|P_i'\right| - \left|O_i'\right|\right)^2} \qquad 0 \le IoA \le 1 \tag{7.4}$$

$$RMSE = \sqrt{\frac{1}{n} \times \sum_{i=1}^{n}\left(P_i - O_i\right)^2} \tag{7.5}$$

$$RE = \sqrt{\frac{1}{n} \times \sum_{i=1}^{n}\left(\frac{P_i - O_i}{O_i}\right)^2} \times 100 \tag{7.6}$$

where P_i and O_i are the predicted and observed values of i^{th} data point respectively of LRWC and n is the number of data points, and $P_i' = P_i - \overline{P}$, $O_i' = O_i - \overline{O}$

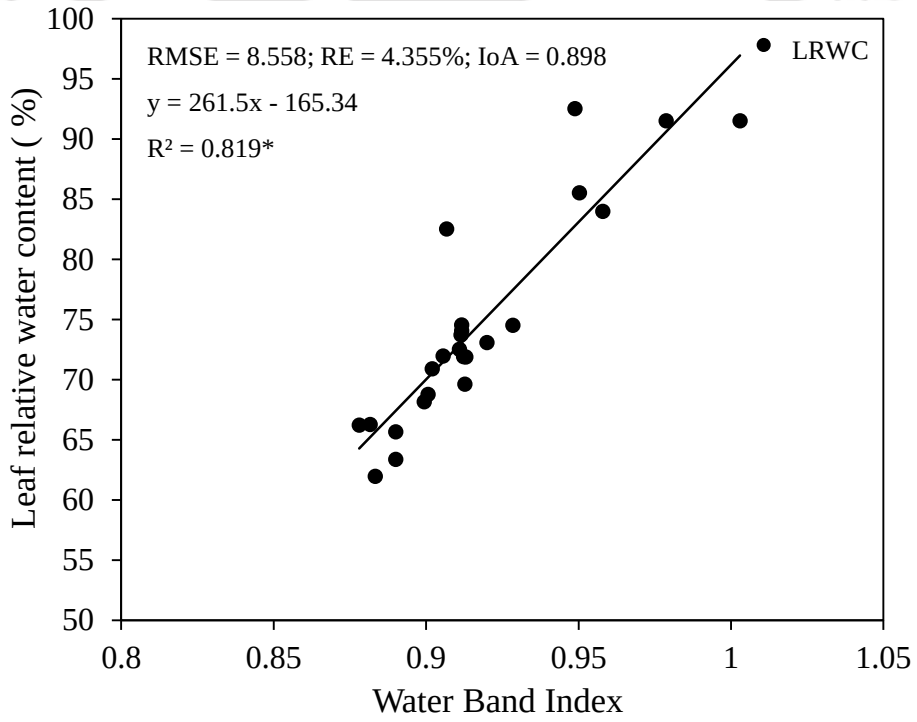

Figure 7.2 : Scatter plot between WBI and LRWC

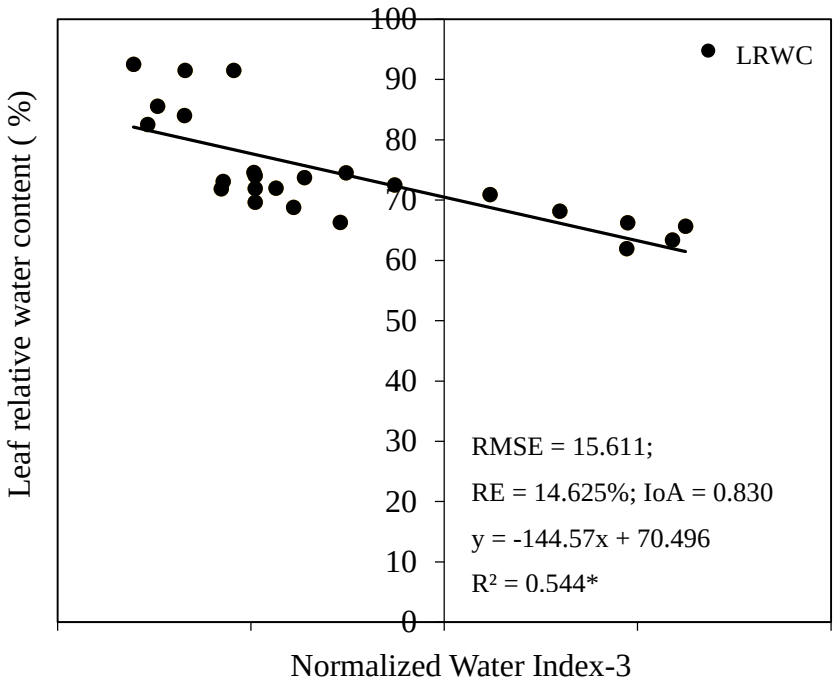

Figure 7.3 : Scatter plot between NWI-3 and LRWC

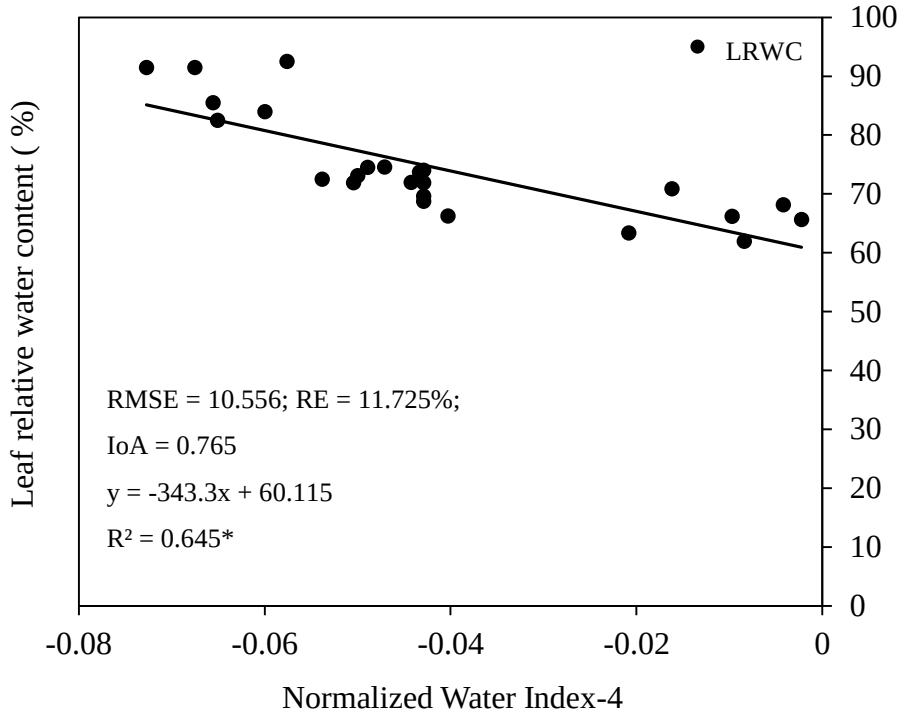

Figure 7.4 : Scatter plot between NWI-4 and LRWC

As mentioned earlier it is important to precisely predict the LRWC of rice genotypes, therefore it is further compared with narrow band indices regression models developed for wheat species published by some other researchers (Jin et al., 2013 and Ranjan et al., 2015). Comparison between the present and published WBI regression models is demonstrated in Figure 7.5. It is found that the present WBI regression model indicated a strong agreement between the observed and the predicted LRWC of paddy rice with RE = 4.355%, IoA = 0.898. Meanwhile, the published WBI regression models from literature that have exhibited satisfactory results for various wheat species predicted unacceptable results for paddy crop evident from the statistical analysis in Table 7.3. The observed LRWC varied from 61% to 92% for studied rice genotypes whereas Jin et al. (2013) and Ranjan et al. (2015) showed a limited variation in predicted LRWC for paddy crop. The LRWC showed higher value for drought tolerant rice genotypes specifically Shabhagi Dhan, CR Dhan 601, Anjali, Vandana and Naveen. It happened so, because the parameters of genetic variability on morphological traits like plant height, panicle length, number of panicles per meter, days to 50% flowering, number of grains per panicle, grain weight and grain yield have influences in expression of characters which is amenable for LRWC variation (Babu et al., 2003). Additionally, some researchers have concluded that quantitative trait locus (QTL) may limit LRWC and drought tolerance (Kumar et al., 2007; Lafitte et al., 2007; Wade et al., 1999). However, in comparison to medium or semi-dwarf rice plants, taller rice plants generally lodge under non stress conditions in highly fertile soils, thus limiting fertilizer application and therefore yield potential (Kumar et al., 2008). This strong linkage between QTL and drought-tolerance genes would have an influence on the crop LRWC and would help in development of drought tolerant species for different environmental conditions (Venuprasad et al., 2012). Moreover, it is inferred from Figure 7.5, that there should be a unique regression model for paddy crop to predict LRWC rather than using the regression models developed for crops other than paddy crop. The results suggested that WBI, NWI-3 and NWI-4 regression models could be used to estimate LRWC of paddy crop more efficiently.

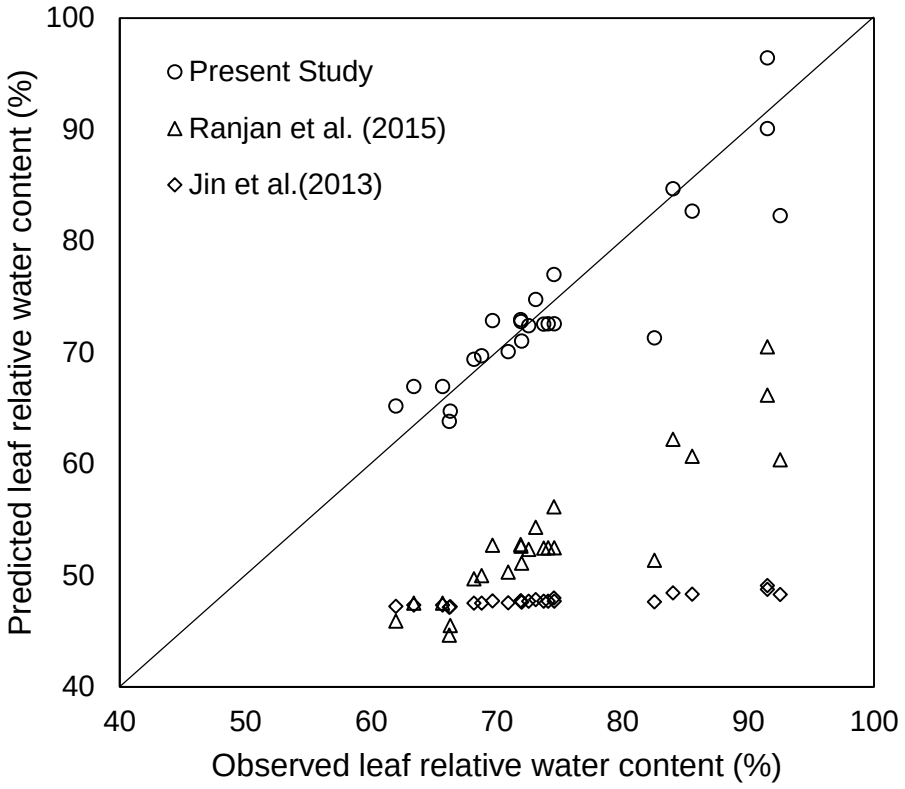

Figure 7.5 : Comparison between predicted and observed LRWC using different models

Table 7.3 : Statistics of different predictive models for LRWC at reproductive phase

Index Model	Regression Model	RE(%)	RMSE	IoA	Related to
Present Study (WBI Index)	$y = 261.5x - 165.34$	4.355	8.558	0.898	Leaf water content
Ranjan et al. (2015)	$y = -286x^2 + 746.3x - 389.6$	8.056	21.409	0.459	Leaf water content
Jin et al. (2013)	$y = 0.1466 \ln(x) + 0.4906$	12.725	27.926	0.358	Leaf water content

7.7.3 Development of SWIR water index models from VNIR water index models

Spectroradiometers with high wavelength ranges to measure the reflectance at these wavebands are too expensive. It is also difficult to measure water stress from air-borne satellite as the signal attenuates with high level of water absorption in the earth's atmosphere but NIR wavelengths at 900 nm to 970 nm penetrate deeper into the canopy and thus can be considered to estimate water content accurately (Babar et al., 2006; Gutierrez et al., 2010). Therefore, regression method is adopted here to compare how well the selected three best correlated narrow band water indices (WBI, NWI-3, and NWI-4) correlate with other water indices in the SWIR region like NDWI-1, NDWI-2, NDII, SRWI, MSI, semi-arid water index-1 (SAWI-1), semi-arid water index-2 (SAWI-2) and normalized difference water index–Hyperion (WI-Hyperion). The findings of the correlations between these indices are summarized in Table 7.4.

Table 7.4 : Correlation between the VNIR and SWIR water indices for a rice agriculture system

Narrow band water Index in SWIR regions	**Best correlated Index with LRWC**					
	Winter Rice Agriculture (Monsoon period in India) Correlation coefficient 'r'			Summer Rice Agriculture (Pre-monsoon period in India) Correlation coefficient 'r'		
	WBI	NWI 3	NWI-4	WBI	NWI 3	NWI-4
NDWI 1	**0.6404**	0.4763	0.4816	**0.6557**	0.6327	0.5412
NDWI 2	**0.4572**	0.3682	0.3491	**0.5710**	0.5367	0.5445
MSI	- 0.4153	0.3750	**0.4330**	0.5500	0.3750	**-0.5602**
NMDI	0.4541	**- 0.5811**	- 0.4173	- 0.4173	**-0.4651**	-0.4472
SRWI	**0.6361**	- 0.5841	- 0.6333	**0.6436**	-0.5467	- 0.5781
NDII	**-0.5726**	- 0.4191	- 0.4568	**-0.6456**	- 0.6148	- 0.5604
SAWI-1	**0.4460**	- 0.4122	- 0.4322	- 0.4284	- 0.3874	**0.5201**
SAWI-2	0.4201	- 0.3874	**- 0.4284**	0.5139	- 0.4436	**- 0.5284**
WI-Hyperion	**0.2309**	- 0.2151	- 0.2247	**0.3221**	- 0.2711	- 0.3127

There is a strong correlation between WBI and NDWI-1, NDWI-2, SRWI, NDII, SAWI-1 (only for winter rice agriculture), WI–Hyperion. Similarly, NWI-4 exhibited strong correlation with MSI, SAWI-1 (only for summer rice agriculture), SAWI-2, and NWI-3 exhibited correlation with NMDI. Therefore, the presently developed WBI, NWI-3 and NWI-4 regression index models are incorporated into narrow band water index models in SWIR regions to determine LRWC of a rice agriculture system in a crop calendar. Furthermore, mapping of the spatial distribution LRWC in an Indian rice agriculture system from Hyperion imagery by employing presently developed regression index models is achieved.

7.7.4 Mapping of LRWC from hyperspectral imagery

7.7.4.1 Mapping of LRWC for winter rice agriculture system

A detailed quantitative assessment of spatial variability of LRWC has been carried out for winter rice agriculture system in Assam, India (Study site 1) from Hyperion imagery by using SWIR band index models derived from the three well established index models - WBI, NWI-3 and NWI-4. To study the variation of leaf water content on winter rice, Hyperion image was acquired during the reproductive phase of paddy crop in Assam, India. The LRWC mapping using the presently developed index models are shown in Figures 7.6(a-i).

From Figure 7.6 (a), it is inferred that LRWC is well-distributed spatially using linear NDWI-1 model derived from WBI regression model. The LRWC determined from Hyperion imagery ranged from 68% to 90% which has a good agreement with the observed LRWC of the studied rice genotypes that ranged from 61% to 92% for winter rice agriculture system. Likewise, Figure 7.6 (b) represents the LRWC variation resulting from NDWI-2 model derived from linear WBI regression model. Here, the LRWC varied from 60% to 87% for winter rice agriculture system. Comparing with NDWI-1, NDWI-2 produced LRWC closer to the observed value. It can be clearly understood that narrow wavebands at 1640 nm is significantly correlated to water stress of paddy crop. Additionally, MSI is a good indicator of plant water stress condition which exhibited LRWC spatial variation from 65% to 97% (Figure 7.6 (c)). Here, LRWC is found to be over predicted in winter rice agriculture system, because different narrow bands accompanied with the proposed index are responsible for developing different regression relationships between the index and LRWC of paddy crop.

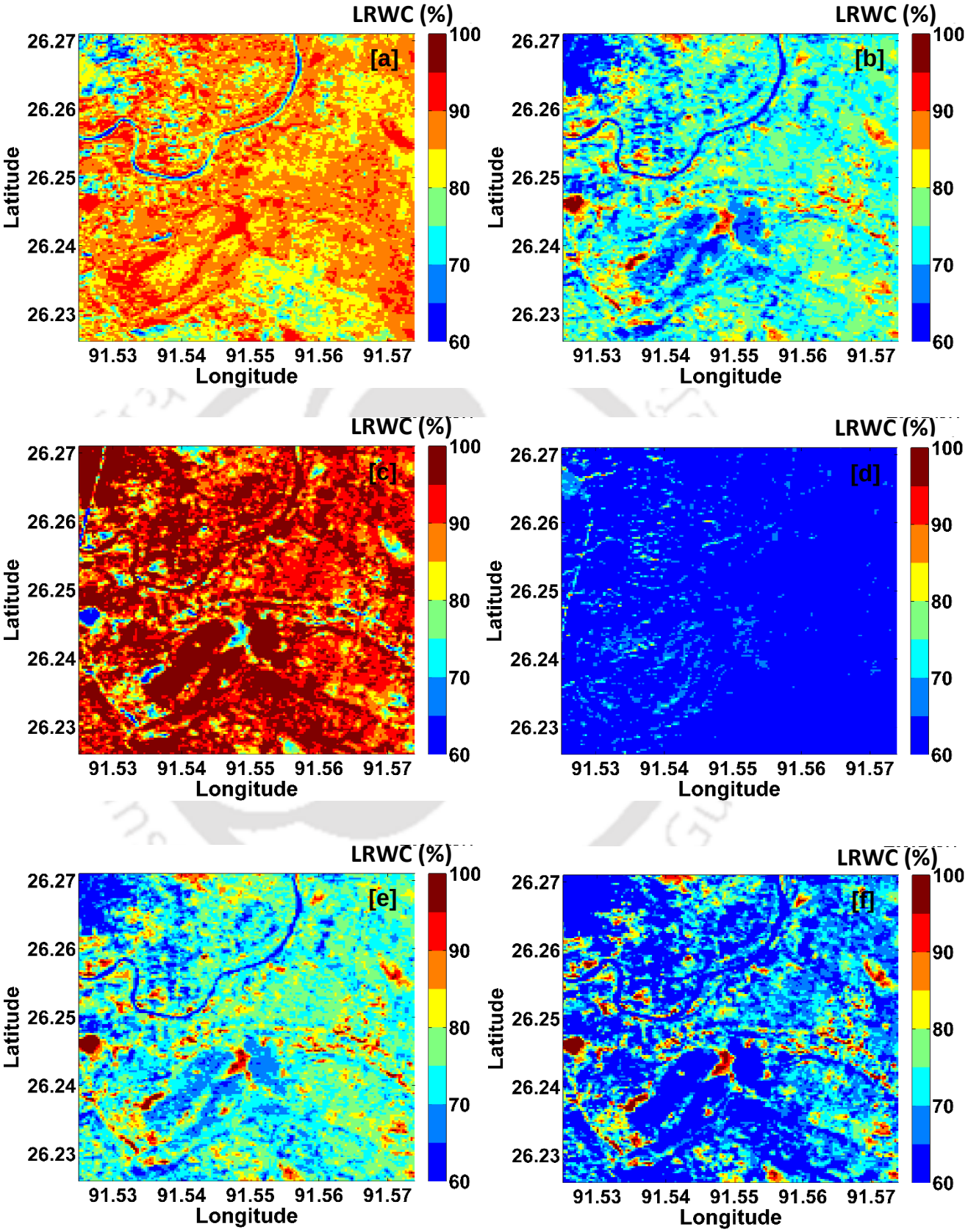
LRWC (%)
[a]
[b]
[c]
[d]
[e]
[f]
Latitude
Longitude
26.27
26.26
26.25
26.24
26.23
91.53
91.54
91.55
91.56
91.57
100
90
80
70
60

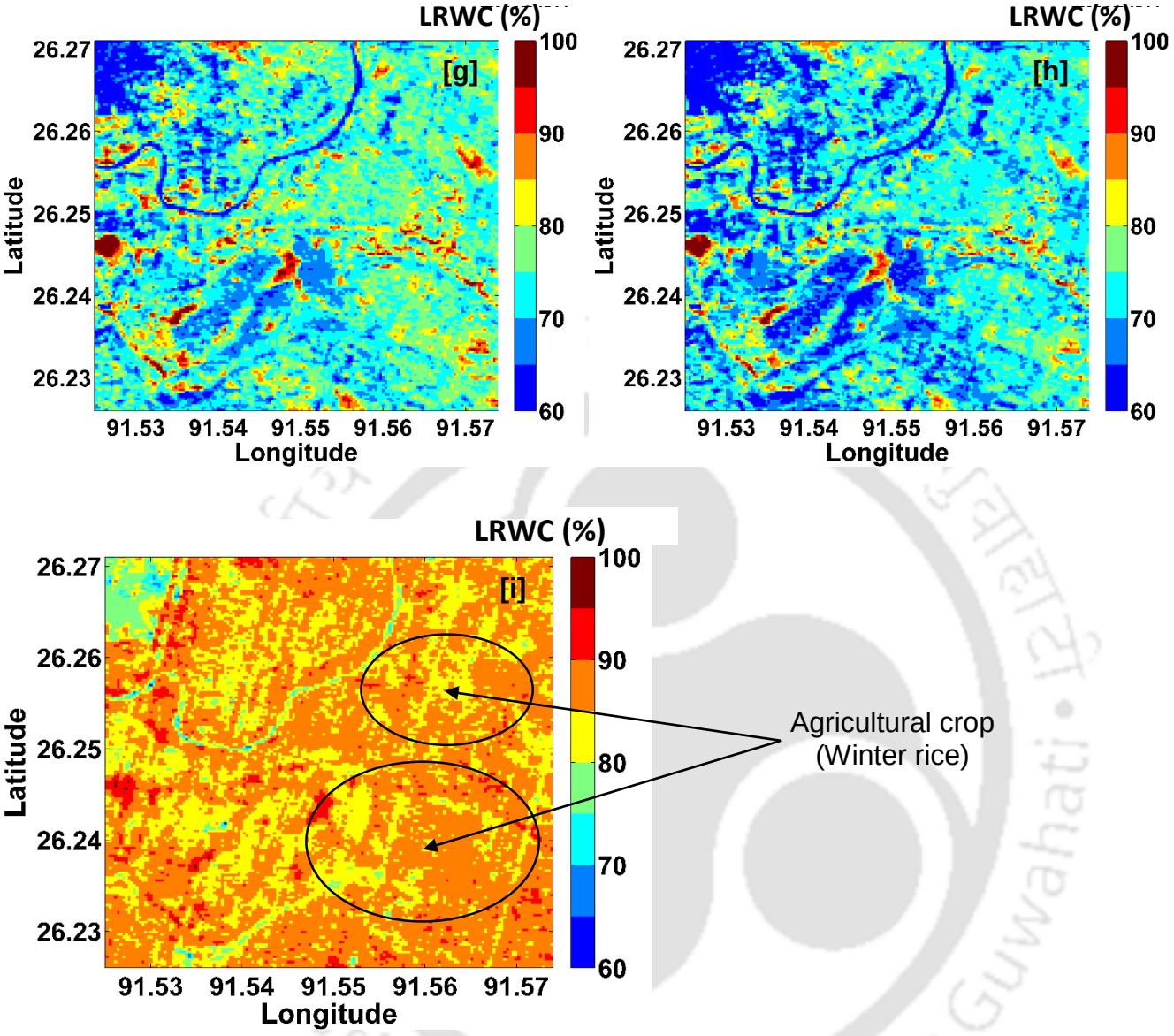

Figure 7.6 : Variability mapping of LRWC in a winter rice agriculture system derived from different narrow band index models during monsoon period ((a): NDWI-1, (b): NDWI-2, (c): MSI, (d): NMDI, (e): SRWI, (f): NDII, (g): SAWI-1, (h): SAWI-2, (i): WI-Hyperion)

It is revealed from Figure 7.6 (d) that NMDI model, which displayed satisfactory results from *in-situ* observations, underestimates the LRWC for winter rice agriculture from Hyperion imagery varying from 64% to 72%. The estimated LRWC is found to be less than the observed value. It may have happened because the tested index, which is developed for monitoring drought for an agricultural crop, may not hold good for the crop having high water requirement like paddy crop, and hence the Hyperion sensor taking image at a higher altitude is not able

to predict the same for a winter rice agriculture system. On the other hand, by analyzing SRWI model (Figure 7.6 (e)), a lower LRWC variation from 61 - 82% is achieved during monsoon period. From Figure 7.6 (f), the spatial distribution obtained from NDII linear regression model exhibited well acceptable performance where LRWC varied widely from 62 – 92%. It has a good agreement with rice leaf water content because the water absorption band 1600 nm is strongly related to water content of crop plant. The variability is clearly distinguished showing the field heterogeneity in the agriculture field. LRWC variation using SAWI-1 model which is derived from WBI for monsoon paddy crop from Hyperion image is found to be 65 – 93% (Figure 7.6 (g)), while the observed value varied from 61 – 92%. It is clearly confirmed from this index model that there is a strong relationship between SWIR narrow band index and WBI to determine LRWC accurately. The index SAWI-2 exhibited LRWC variation from 68% to 89% for the same agriculture area (Figure 7.6 (h)). The index WI-Hyperion with LRWC variation of 80 – 90% did not produce adequate findings for the rice agriculture area during monsoon period (Figure 7.6 (i)). This model could not provide significant variability in the field level for winter rice agriculture system.

7.7.4.2 Mapping of LRWC for summer rice agriculture system

To investigate the variability of LRWC for summer rice, field survey was carried out in farmers' agricultural fields in Cuttack, Odisha, India (Study site 2) where different summer rice species were grown during the pre-monsoon period in 2016. A detailed quantitative assessment of spatial variability of LRWC has been carried out for a summer rice agriculture system Hyperion imagery by using SWIR band index models derived from the three well established index models - WBI, NWI-3 and NWI-4. The LRWC mapping using the presently developed index models are shown in Figures 7.7(a-i).

From Figure 7.7 (a), it is observed that the LRWC variation ranged from 48 - 77% in a summer rice agriculture system obtained from NDWI-1 regression model while the same model exhibited 61- 92% spatial variation for winter rice. It happened so because of the seasonal variation of rice agriculture system.

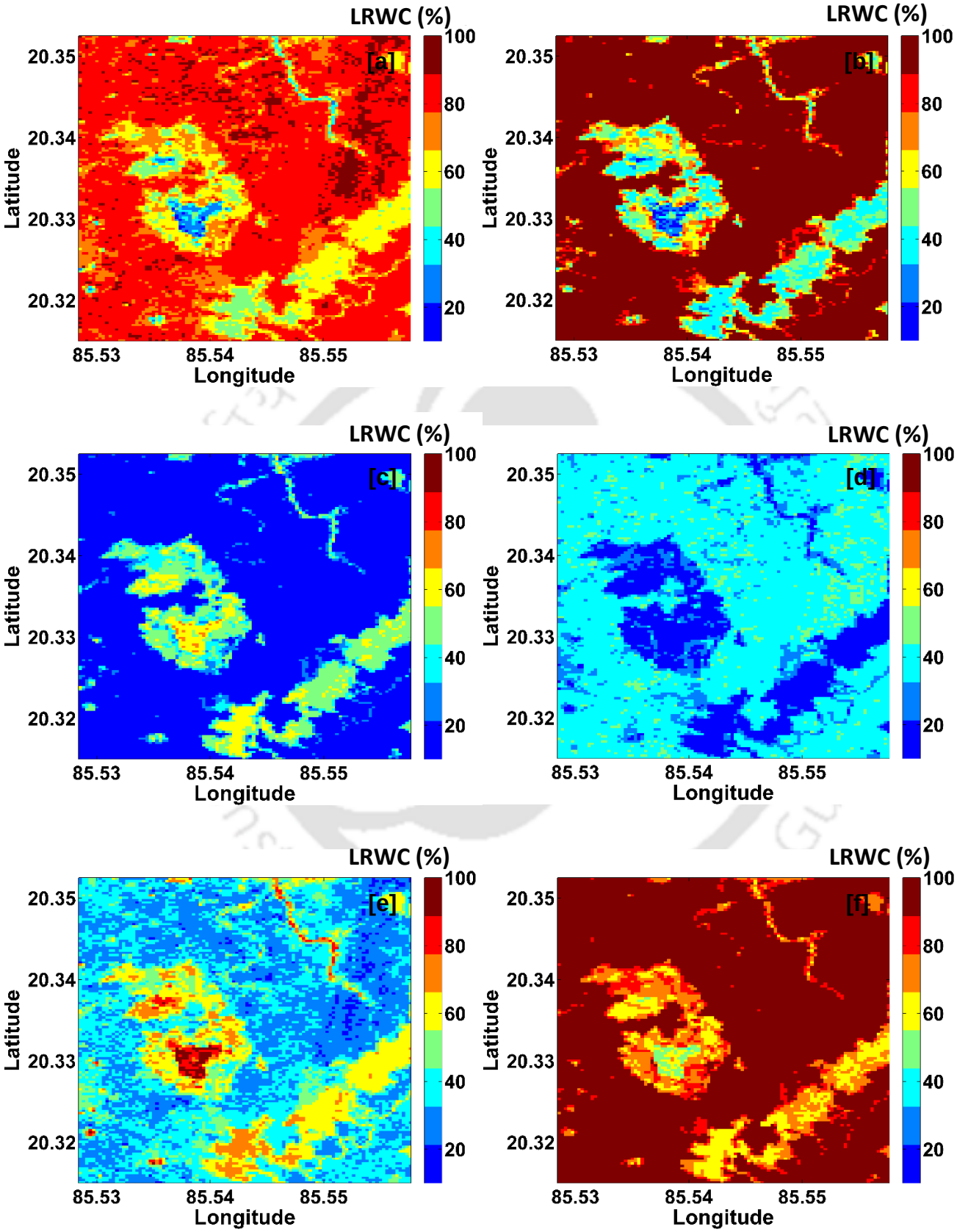
LRWC (%)
[a]
[b]
[c]
[d]
[e]
[f]
Latitude
Longitude
20.35
20.34
20.33
20.32
85.53
85.54
85.55
100
80
60
40
20

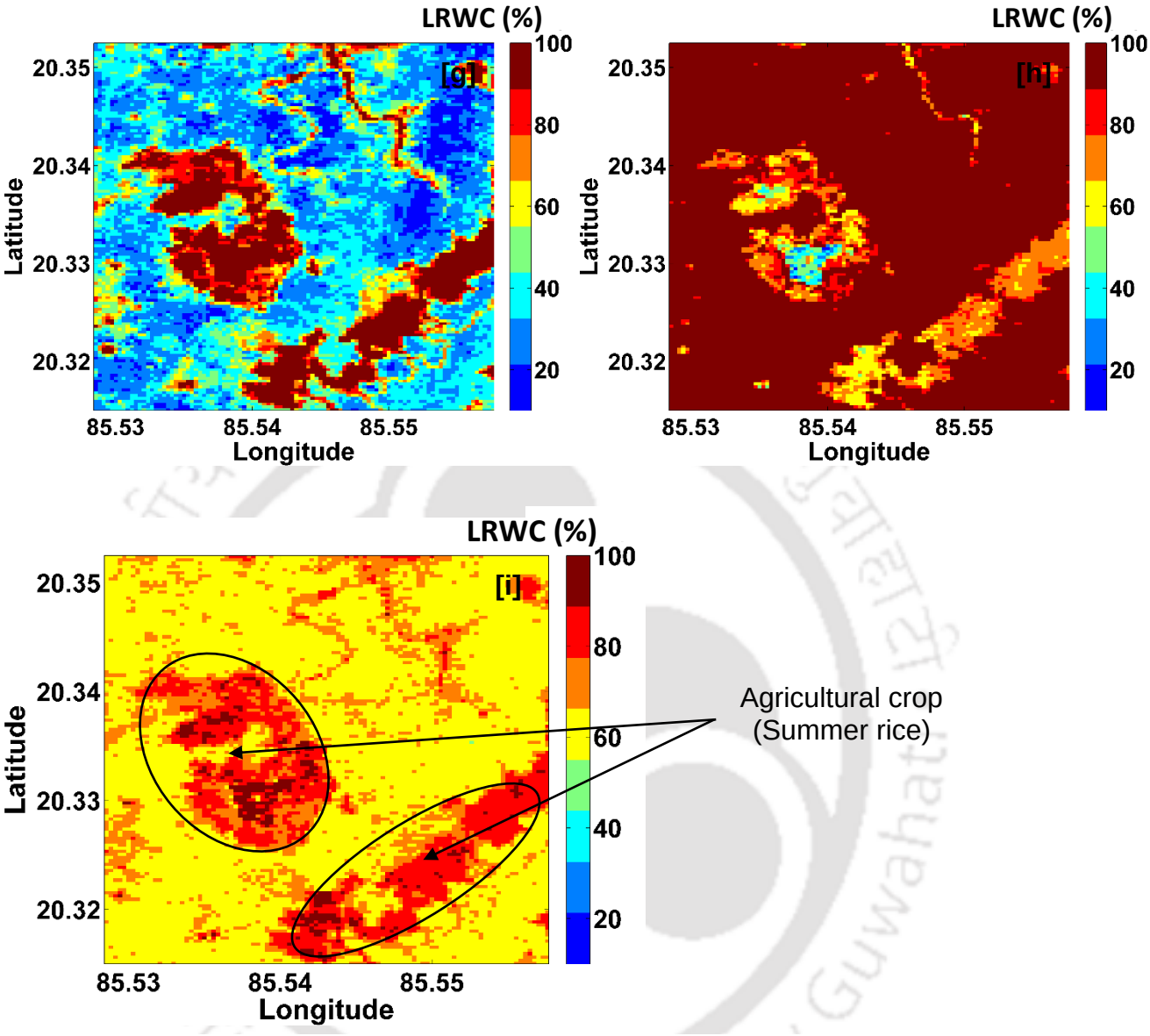

Figure 7.7 : Variability mapping of LRWC in a summer rice agriculture system derived from different narrow band index models during pre-monsoon period ((a): NDWI-1, (b): NDWI-2, (c): MSI, (d): NMDI, (e): SRWI, (f): NDII, (g): SAWI-1, (h): SAWI-2, (i): WI-Hyperion)

Additionally, mapping of LRWC from NDWI-2 regression model revealed that there is a wide variation of 50% to 83%, which is different from the previously established NDWI-2 model for winter rice LRWC prediction (Figure 7.7 (b)). This difference in variation may be attributed to the fact that the rice cultivated species in farmers' fields are different from the species studied in the experimental field (Assam) and the water availability during pre-

monsoon period may also be an influencing factor. Moreover, LRWC variation of summer rice agriculture system using MSI linear regression model derived from NWI-4 from Hyperion image ranged from 65 - 95% (Figure 7.7 (c)). This result ascertained that Hyperion imagery has the potential to extract the water content variation accurately, which can be an indicator of water stress in rice plant. On the other hand, interesting observations resulted from NMDI regression model (Figure 7.7 (d)) in LRWC mapping in a summer rice agriculture system. It is noticed that when the agriculture system varies from winter rice to summer rice where water is a major problem, LRWC variation is found very less, 10% to 30%. Under lower water content condition, the higher yielding summer rice species may be affected significantly. From Figure 7.7 (e), spatial distribution of LRWC from SRWI regression model derived from WBI model during pre-monsoon period also revealed satisfactory outcomes from hyperspectral imagery with a wide variation of 47 - 76%. Following similar guidelines, it is found that the seasonal variability under pre-monsoon period can be captured well under NDII regression model approach from hyperspectral imagery (Figure 7.7 (f)) with LRWC value varying from 57% to 83% in case of summer rice cultivation practice. The LRWC field variability is captured well by using this index model.

Once the narrow band vegetation index models are established, the heterogeneity of rice agriculture system is captured from Hyperion imagery to indicate the changes in LRWC from monsoon paddy crop to pre-monsoon paddy crop by using SAWI-1 (Figure 7 (g)) and SAWI-2 (Figure 7.7 (h)) proposed by Jin et al. (2013). Figures 7.7 (g) and 7.7 (h) show significant variation of LRWC from 62 - 94% and 47- 94% for SAWI-1 and SAWI-2 respectively under summer rice agriculture practices. The field variation is clearly observed from these index models. From Figure 7.7 (i), reasonable predictions are made for the paddy crop in pre-monsoon period that exhibited 67% to 92% variability in LRWC from WI–Hyperion regression model (Ustin et al., 2002). However, it could not attribute appreciable heterogeneity in LRWC for winter rice agriculture system.

The statistics of the above LRWC mapping of paddy crop obtained from different index regression models are reported in Table 7.5. It is found that mean value of LRWC in summer rice is quite less than that of winter rice. It is interesting to note that LRWC mapped from Hyperion image has a good agreement with the observed LRWC. The observed LRWC

obtained for the rice varieties grown in the rice agriculture system in Kamrup district of Assam varied from 61% to 92% and their standard deviation ranged from 0.638 to 1.095. From Table 7.5, it is inferred that, within the range of observed LRWC value, the narrow band index regression models (NDWI-1, NDWI-2, NDII, SAWI-1, SAWI-2) well predicted the LRWC for winter rice agriculture system from Hyperion imagery. However, it was not possible to synchronize Hyperion findings with ground measurements of the summer rice agriculture system. Considering the observed LRWC of 24 rice varieties in study area grown in a winter rice agriculture system, these index models (NDWI-2, MSI, SRWI, NDII, SAWI-1, WI-Hyperion) performed approximately in the same range of spatial distribution of LRWC for a summer rice agriculture system in a crop calendar from Hyperion imagery.

Table 7.5 : LRWC statistics derived from narrow band index maps

Index Model	**Winter Rice Agriculture System**		**Summer Rice Agriculture System**	
	Mean	Std Dev.	Mean	Std Dev.
NDWI-1	76	6.716	62.5	7.025
NDWI-2	72	12.65	66	7.812
MSI	80	12.951	78	6.551
NMDI	65	13.54	24	14.08
SRWI	70.5	8.332	59	6.256
NDII	75.5	7.05	59	8.518
SAWI-1	79	8.253	79	5.684
SAWI-2	73.5	5.521	71.5	6.215

7.8 Conclusions

Reproductive phase is clearly identified as the most sensitive phase in evaluating leaf water content of paddy crop through narrow band water indices. Hyperspectral indices particularly WBI, NWI-3 and NWI-4 showed strong correlation with LRWC at this phase. As collection of hyperspectral observations through spectroradiometers with high wavelength ranges are

too expensive, regression method is adopted to investigate how well the selected best three VNIR water indices -WBI, NWI-3 and NWI-4 correlate with that of the water indices in SWIR region. Significantly, it confirmed that there is a strong correlation between WBI and NDWI-1, NDWI-2, SRWI, NDII, SAWI-1 (only for winter rice agriculture), WI–Hyperion. Similarly, NWI-4 exhibited strong correlation with MSI, SAWI-1 (only for summer rice agriculture), SAWI-2, and NWI-3 exhibited correlation with NMDI.

The best estimates of LRWC at the reproductive phase for summer rice agriculture system is achieved from NDWI-2, MSI, SRWI, NDII, SAWI-1, WI-Hyperion index regression models. It revealed that the spatial distribution of LRWC which widely varied from 47% to 94% in summer rice agriculture system is likely close to *in-situ* LRWC variation. It is observed that the narrow band water index regression models - NDWI-1, NDWI-2, NDII, SAWI-1, SAWI-2 performed well in mapping of LRWC in an Indian winter rice agriculture system in a crop calendar from space platform via Hyperion L1R data with a very high accuracy. The index models effectively performed in predicting the LRWC variation that ranged from 60% to 93% in winter rice agriculture system. It is in good agreement with the observed LRWC. Moreover, a strong linkage between QTL and drought-tolerant genes was ascertained for the paddy crop LRWC and hence drought tolerant species can be developed for different environmental conditions (Venuprasad et al., 2012). Additionally, it is found that the predicted LRWC by using the narrow band water indices more closely followed the observed LRWC data for an Indian rice agriculture system. However, these index based predictive models need to be tested in different agro-climatic regions for more reliability and better acceptance.

8 Fusion of Multispectral and Hyperspectral Data to Retrieve Plot Scale Variability of Crop Parameters

8.1 Introduction

In field-scale variability management, implementation of conventional sampling methods are not sufficient to manage the crop-yield influencing factors like biophysical, biochemical and soil characteristics. The most essential paddy crop parameters, chlorophyll and nitrogen content, that measure crop growth should be determined, so that they can be further used to identify the complex nature of field variability. To boost productivity and profitability of rice production, understanding the heterogeneous nature of chlorophyll and nitrogen content of paddy crop over spatial domain is imperative for farmers to apply fertilizers and farm inputs in selected rice plots rather than following the general practice of applying fertilizer homogenously over the entire field**.**

Moreover, Gianelle and Guastella (2007) reported that most of the crop parameters have a spectral signature at a certain wavelength of the spectrum that can be captured and identified by satellite sensors with finer spectral bandwidths (Marshall and Thenkabail, 2015; Verrelst et al., 2015). Past studies have demonstrated that satellite sensors, in particular hyperspectral sensors due to their contiguous narrow wave bands, have the potential to retrieve detailed information of crop parameters in the field of agricultural studies (Bannari et al., 2015; Daughtry et al., 2004; Nidamanuri and Zbell, 2011; Pena-Barragan et al., 2011; Thenkabail, 2000). However, investigations have also been carried out on agricultural applications by

using multispectral broad band satellite-based measurements. Few such applications are derivation of crop radiometric and biophysical performance from MODIS data (Huete et al., 2002; Ozdogan, 2010), crop identification (Schmedtmann and Campagnolo, 2015; Yang et al., 2011) and monitoring agricultural crop growth from SPOT time series data (El Hajj et al., 2009), and crop field extraction from temporal web enabled Landsat data (Yan and Roy, 2014). Due to lack of narrow bands, narrow band vegetation indices could not be established from these sensors to estimate crop biophysical parameters for agricultural studies (Song et al., 2011). Additionally, there are some limitations of hyperspectral sensor like EO-1 Hyperion. It has a very low temporal and spatial resolution. Furthermore, hyperspectral data needs a very careful pre-processing as it contains hundreds of hyperspectral narrow bands at a spectral resolution of 10 nm, which is a very complex and time-consuming process.

To overcome these difficulties, an effort has been made to develop a new methodology to introduce hyperspectral narrow bands into multispectral high spatial resolution data through index-based fusion approach. Two different new approaches were incorporated in the methodology to obtain the fused product. Based on the proposed methodology, spatial variability maps of chlorophyll and nitrogen at plot scale within the field for both the study sites were developed from multispectral LISS IV. Finally, their performance was evaluated using statistical analysis.

8.2 Study Area and Satellite Data required

For the fulfilment of this objective, study was carried out in farmers' agricultural fields in Cuttack, Odisha (Study site 2). Details of the study site is described in Chapter 3. Both kharif and rabi rice are grown in this area.

The Hyperion satellite image data, covering the Study site 2 in Cuttack, Odisha acquired on 8th March, 2016, was used for hyperspectral resolution simulation to generate spatial distribution of paddy crop parameters from multispectral data. Crop studies, using optical satellite data, is generally not possible during monsoon season (July-November) due to the presence of cloud cover in the sky. Therefore, Resourcesat-2 (IRS-P6) completely cloud free images were not available during this period. Hence, IRS-P6, LISS IV sensor data passing

through the study site, acquired on 22nd February 2016, the details of which is provided in Chapter 3, was ordered for this work from National Remote Sensing Centre, India (https://www.nrsc.gov.in).

8.3 Methodology to derive the Crop Parameters from high spatial Multispectral data

8.3.1 Index based fusion approach for hyperspectral and multispectral data

An effort has been made to derive narrow band vegetation indices by adopting fusion of Hyperion narrow band with LISS IV broad band. The hyperspectral bands of Hyperion L1R Hyperion data are of 10 nm bandwidth, whereas LISS IV data has three bands: b2 (0.52-0.59 µm, green), b3 (0.62-0.68 µm, red) and b4 (0.77-0.86 µm, NIR). This fusion approach will be further implemented to retrieve chlorophyll and nitrogen content at plot scale within the rice field.

8.3.2 Derivation of multispectral bands (Synthetic bands) from Hyperion data

8.3.2.1 Band Average Concept

The critical bands, sensitive to paddy crop, were selected for different narrow band vegetation indices such as Simple Ratio (SR), Leaf Nitrogen concentration (LNC), Optimised Soil-Adjusted Vegetation Index (OSAVI), Gitelson, modified Simple Ratio (mSR) and MERIS Terrestrial chlorophyll Index (MTCI), which are discussed in Chapter 6. All the broad band equivalents were expressed in terms of narrow bands of the Hyperion image of the study site acquired on 8th March, 2016. These broad band equivalents were tested for the existence of relationship with that of critical narrow bands.

The relationship is stated in the following expressions.

$$\rho_{GC} = \beta_1 . G\rho_{IH} + \alpha_1 \quad (8.1)$$

$$\rho_{RC} = \beta_2 . R\rho_{IH} + \alpha_2 \quad (8.2)$$

$$\rho_{NC} = \beta_3 . N\rho_{IH} + \alpha_3 \quad (8.3)$$

where, $\rho_{IH} = \frac{1}{n}\sum_{i=1}^{n}\rho_i$

ρ_{IH} = broad band equivalent to integrated narrow bands of Hyperion image

ρ_i = broad band reflectance at *i* (*i* at a step size of 10 nm)

α , β = linear coefficients

and $G\rho_{IH}$, $R\rho_{IH}$, $N\rho_{IH}$ are the three spectral (LISS IV) broad bands equivalent to integrated Hyperion narrow bands calculated for green, red and NIR regions of the spectrum, respectively, and ρ_{GC}, ρ_{RC}, ρ_{NC} are the critical narrow bands of green, red and NIR regions of the spectrum, respectively.

It was found that some of the critical bands were highly correlated to the broad bands equivalent to the integrated narrow bands, whereas others failed to reciprocate much. Therefore, a higher linear coefficient of determination ($R^2 > 0.95$) between critical bands and broad bands equivalent to integrated narrow bands derived from Hyperion bands was considered (Figure 8.1). By adopting band average concept method, bands like 533 nm, 565 nm, 681 nm, 705 nm, 717 nm, 750 nm and 800 nm were found to be significant amongst all the critical bands. Furthermore, the multispectral bands of LISS IV image were converted into three synthetic multispectral bands, which were derived as a function of Hyperion narrow bands sensitive to paddy crop.

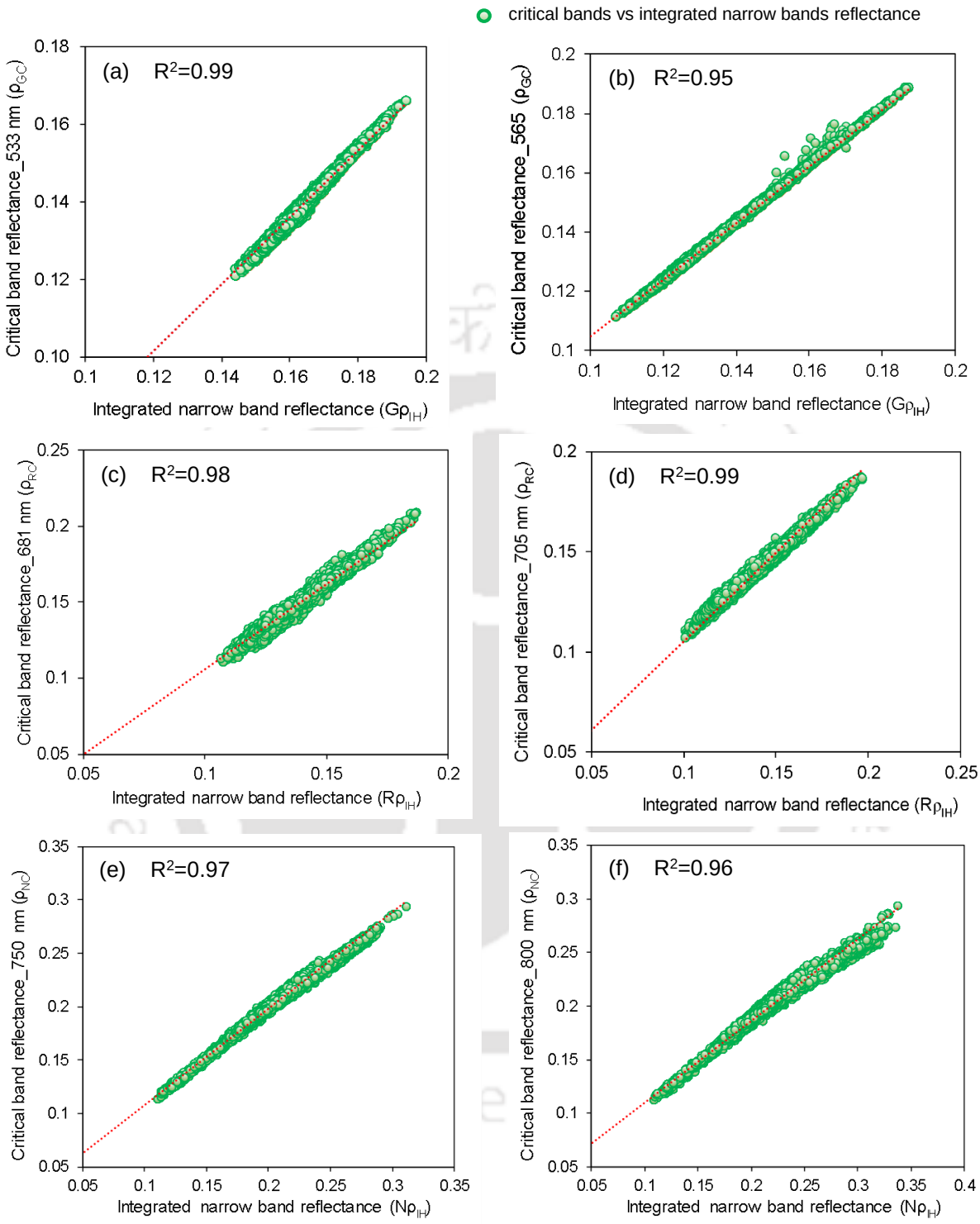

Figure 8.1 : Correlation between critical bands and broad bands equivalent to integrated narrow bands, green: (a)-(b), red: (c)-(d), NIR: (e)-(f).

For this LISS IV image representing the study area dominated with paddy crop cultivation, a linear relationship was established between multispectral broad band (so called synthetic band; $S\rho_{LISS\ IV}$) and broad band equivalent to integrated narrow bands of Hyperion image (ρ_{IH}).

The relationship is represented in the following expressions.

$$GS\rho_{LISS\ IV} = \beta_G \cdot G\rho_{IH} + \alpha_G \quad (8.4)$$

$$RS\rho_{LISS\ IV} = \beta_R \cdot R\rho_{IH} + \alpha_R \quad (8.5)$$

$$NS\rho_{LISS\ IV} = \beta_N \cdot N\rho_{IH} + \alpha_N \quad (8.6)$$

where,

α and β are linear coefficients, and $GS\rho_{LISS\ IV}$, $RS\rho_{LISS\ IV}$, $NS\rho_{LISS\ IV}$ are the three multispectral synthetic bands derived for Hyperion narrow bands and $G\rho_{IH}$, $R\rho_{IH}$, $N\rho_{IH}$ are the three broad bands equivalent to integrated narrow bands in green, red and NIR regions of the spectrum, respectively.

8.3.2.2 Spectral Shape Function Concept

The hyperspectral narrow bands are nothing but integration of measurements of the spectrum. The bands illustrate the shape of the spectrum over a certain spectral region (Fensholt and Sandholt, 2003; Khanna et al., 2007), and this is used as a major source of information. In this context, the reflectance of the narrow bands, that capture spectral information of paddy crop, were used to fit a spectral shape, in order to add a new dimension to the biophysical parameter studies in case of paddy crop. The spectral shape function can be further used to get the critical wavelengths, which will provide more detailed information on paddy crop parameters in the field level. To identify the sensitive bands for establishing the spectral shape function, band to band correlation (Figure 8.2) was done for all the critical bands (533 nm, 565 nm, 574 nm, 681 nm, 695 nm, 705 nm, 709 nm, 717 nm, 740 nm, 750 nm, 800 nm) as per findings from Chapter 6. By considering the coefficient of determination, $R^2 > 0.95$, significant wavelengths were selected. An interesting result was achieved showing that the wavelengths 533 nm, 681 nm, 705 nm, 717 nm, 750 nm and 800 nm wave bands were found critical from band to band correlation analysis.

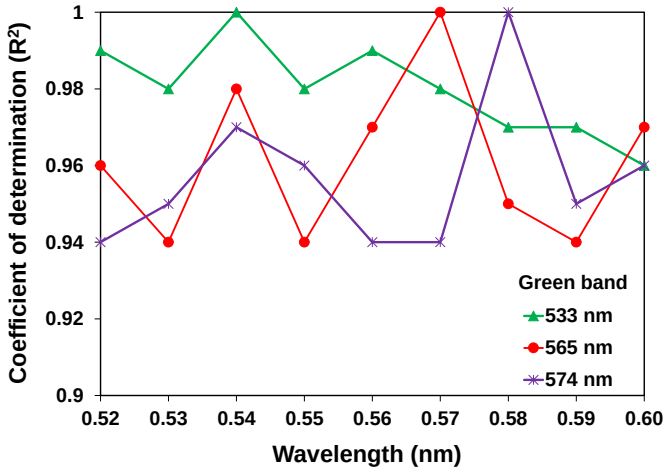

(a)

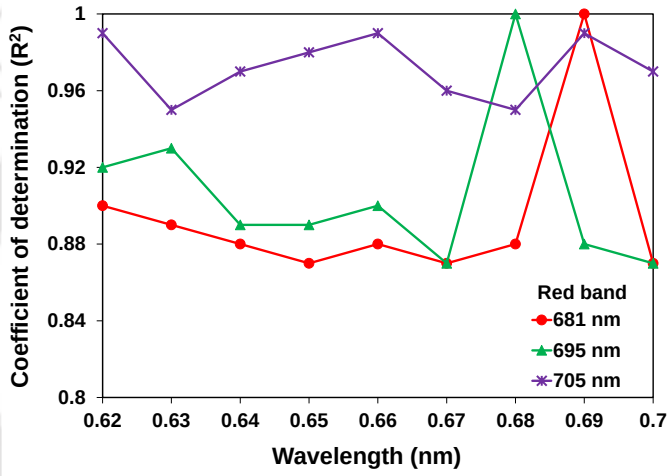

(b)

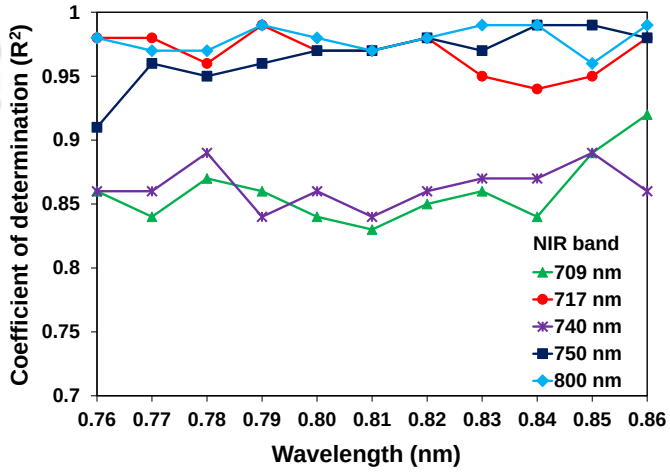

(c)

Figure 8.2 : Band to band correlation analysis to get the critical bands from spectral shape function method, (a) green, (b) red, (c) NIR

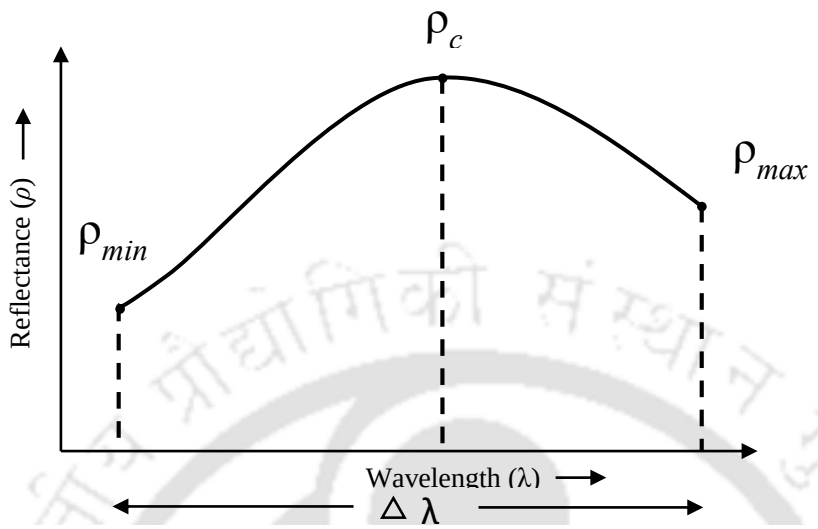

Figure 8.3 : Sketch describing the spectral shape fit for broad band of multispectral data

8.4 Results and Discussion

Due to non-availability of Hyperion data with good temporal resolution, predominantly it is not possible to monitor the rice crop parameters covering all the stages of rice crop age period. Secondly, it is a difficult task to find the paddy crop parameters like chlorophyll and nitrogen at field level from space platform. Therefore, an earnest effort has been made to estimate the parameters from multispectral data at plot scale within the crop field. To do so, index based fusion approach for multispectral and hyperspectral data was adopted by incorporating band average method and spectral shape function method. For the present study, estimation of paddy crop parameters from LISS IV imagery (of the Study site 2) acquired on 22nd February 2016 was carried out by using narrow band index regression models. These index models were specifically derived for paddy crop in Indian rice agriculture system from hyperspectral data.

8.4.1 Performance of band average method

The critical multispectral wavelengths were well picked up from Hyperion narrow bands by

adopting band average concept method. The functional relationship between multispectral band and hyperspectral band was derived (Table 8.1). It may be noted that the LISS IV and Hyperion images acquired for the study site in the year 2016 were used to develop the relationship. The multispectral and hyperspectral index fusion approach has a great advantage over spatial resolution of 5.8 m, which retained the significant information of rice crop parameters through critical bands. Therefore, it was specially attained to extract the paddy crop variability such as chlorophyll and nitrogen at plot level within the agricultural field. However, the foremost concern is that by adopting this index fusion approach, all the chlorophyll and nitrogen related vegetation indices could not be used to estimate chlorophyll and nitrogen. Thus, solely those indices in which significant critical bands resulted from band average methodology were implemented. In this context, only two indices, OSAVI and LNC were ascertained for the estimation of chlorophyll, whereas LNC and SR indices were confirmed for nitrogen prediction.

Table 8.1 : Coefficient of determination and model parameters from linear models established between multispectral broad band (Synthetic band; $S\rho_{LISS\ IV}$) and broad band equivalent to integrated narrow bands (ρ_{IH})

Multispectral band (LISS IV)	Slope	Intercept	Coefficient of determination (R^2)
Green	0.0319	17.2958	0.981
Red	0.0716	16.0248	0.917
NIR	0.0869	24.9234	0.930

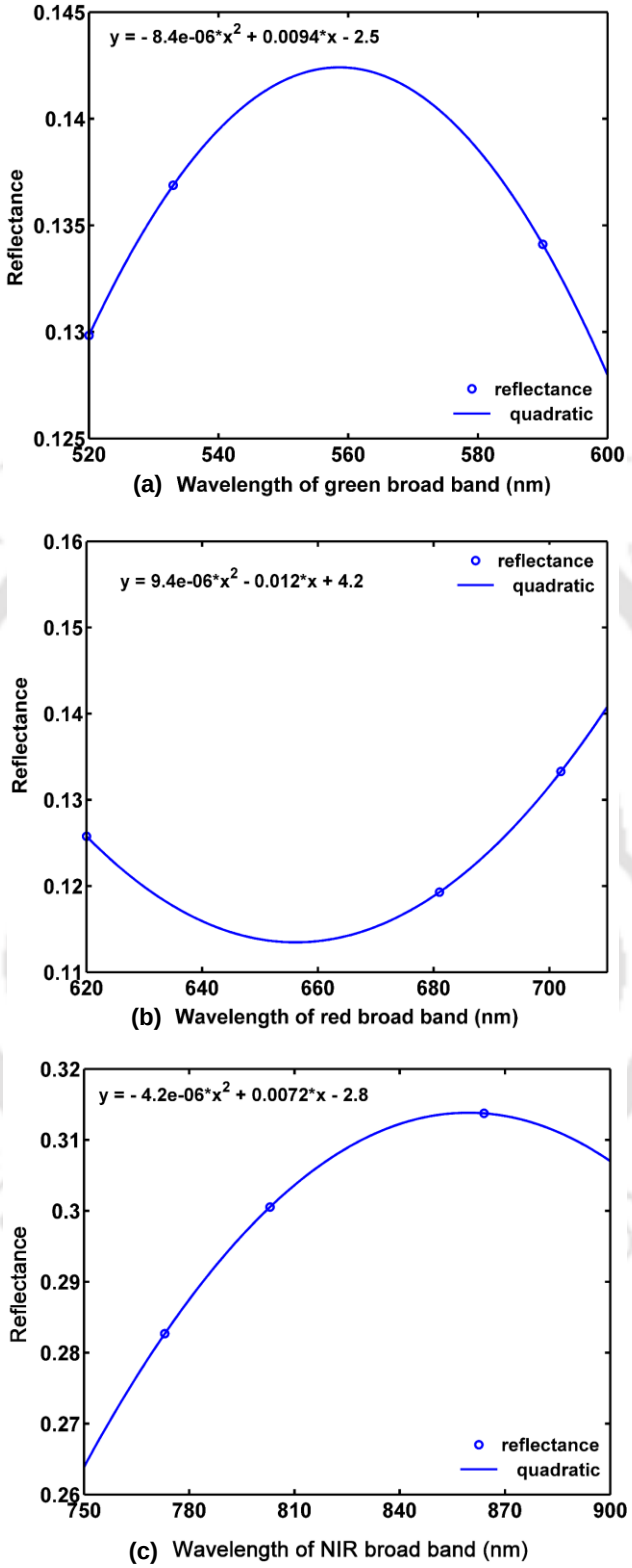

Figure 8.4 : Spectral shape function established for different broad bands of multispectral data - (a) green (b) red (c) NIR

8.4.2 Performance of spectral shape function method

The spectral shape functions were established for broad bands (green, red and NIR regions) of the multispectral LISS IV data. It may be noted that the paddy crop spectral shape was produced using Hyperion image of the study site acquired on 8th March, 2016. It was found that the predicted shapes exhibited different non-linear relationships over three wider ranges of the spectrum (Figure 8.4). Further interesting observations were made from the scatter plots of critical wavelengths with the minimum and maximum wavelengths of the broad bands (Figure 8.5).

$$\rho_{\min} = a_1 \cdot \rho_c + b_1 \tag{8.7}$$

$$\rho_{\max} = a_2 \cdot \rho_c + b_2 \tag{8.8}$$

where $\rho_{\min}$ = Lower minimum spectral band of the broad band

$\rho_{\max}$ = Upper maximum spectral band of the broad band

ρ_c = Critical band of the spectrum

a, b = Linear coefficients

The scatter plots indicated that the critical wavelengths, which were found significant from band to band correlation, have significant correlation with coefficient of determination (R^2) greater than 0.85. Figure 8.5 (a)-(b) demonstrates that the critical wavelength at 565 nm exhibited very low correlation with wider scattered data points for both the minimum as well as the maximum wavelength. This low correlation between the critical and the minimum or maximum band may have been caused due to its insensitivity towards the rice crop phenological metric at this wavelength. Thus, the reflectance magnitude of the spectral feature has poor performance in the scatter plot and this has also been confirmed from the redundancy in band to band correlation plot. Therefore, by employing index based fusion approach, only a few chlorophyll and nitrogen based indices were able to predict the chlorophyll and nitrogen variability within the field. This spectral shape method revealed that both, LNC and OSAVI, indices can be used for chlorophyll estimation, whereas only LNC index can be employed for nitrogen estimation at the plot level within the crop field from multispectral LISS IV data. These findings were completely different from that of the band average method.

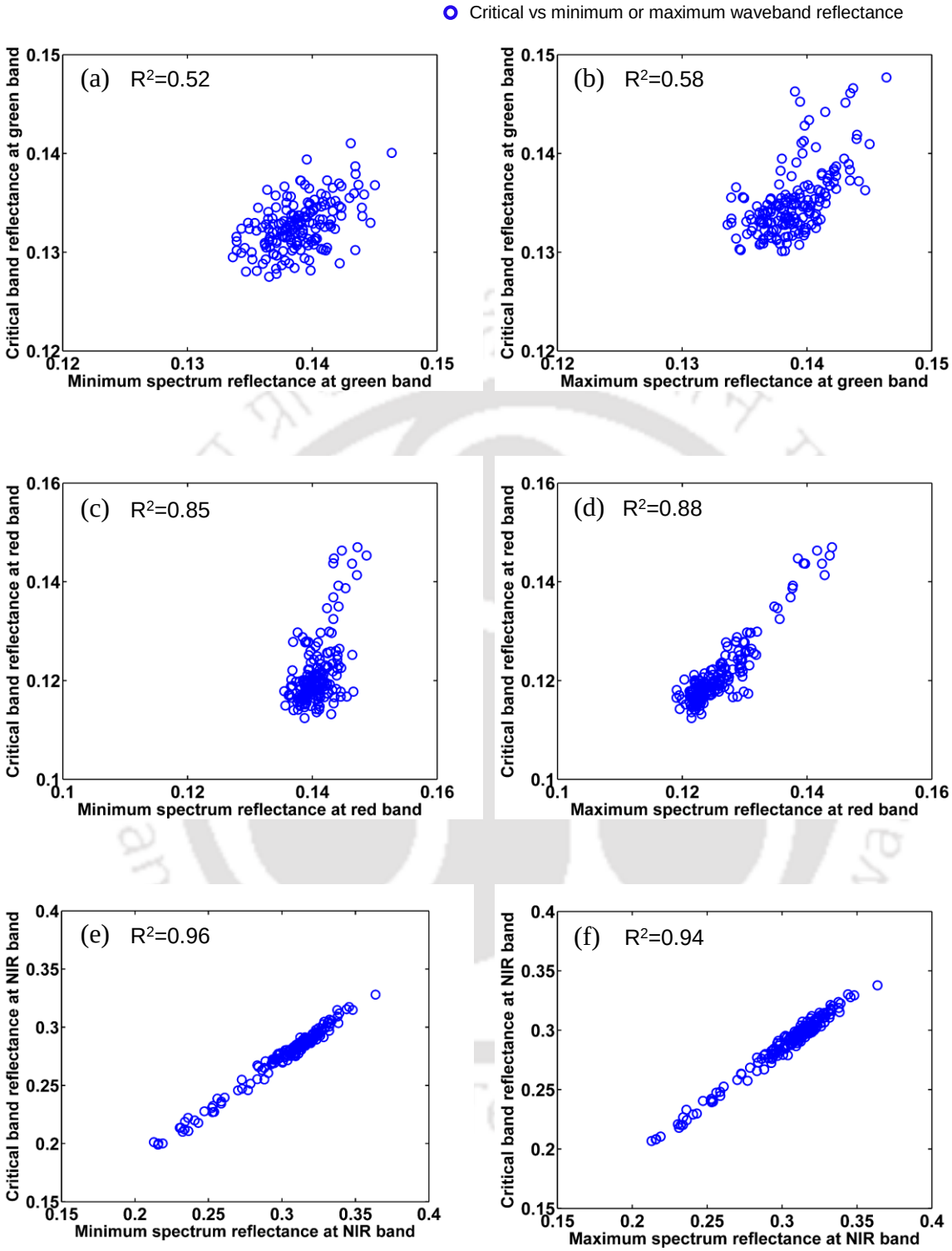

Figure 8.5 : Scatter plots of reflectance of critical band with minimum and maximum wavebands of the broad band spectrum of LISS IV data, green: (a)-(b), red: (c)-(d), NIR: (e)-(f).

8.4.3 Variability mapping of chlorophyll at plot scale from space platform

By using the index based fusion approach, the above discussed indices were derived from the multispectral LISS IV data and applied to estimate the rice chlorophyll at plot scale within the field. An interesting observation was made from the OSAVI and LNC index models, achieved through band average and spectral shape function methods. The regression models are summarized in Table 8.2. The chlorophyll content was estimated using OSAVI index model for both band average method (Figure 8.6 (b, c)) and spectral shape function method (Figure 8.6 (d, e)). Here, chlorophyll variation is shown in typical five plots within the field. It exhibited chlorophyll variation that ranged from 7.22 – 8.86% (Figure 8.6 (b, c)) in the plot level from band average method, whereas the variation obtained from spectral shape function method ranged from 3.06% to 9.01% (Figure 8.6 (d, e)). The plot scale variation of chlorophyll was found to be in good agreement with the observed chlorophyll content of rice leaves (1.13 - 7.26%). It represented how well the field variability has captured the spatial distribution of leaf pigment chlorophyll content especially within each rice plot. It can be seen that the variability in the five plots was found to be significant in case of spectral shape function method as compared to band average method.

Table 8.2 : Presently developed regression models for rice crop parameters estimation

Index	Fit-equation	Related to	Tested species
OSAVI	$y = 20.003x - 3.4824$	Chl	Rice (*Oryza sativa* L.)
LNC	$y = -226.05x^2 + 313.56x - 100.14$	Chl	Rice (*Oryza sativa* L.)
SR	$y = 29.178x - 25.294$	N	Rice (*Oryza sativa* L.)
LNC	$y = -306.34x^2 + 372.74x - 109.56$	N	Rice (*Oryza sativa* L.)

Moreover, considerable spatial variability of chlorophyll resulted from multispectral LISS IV image through LNC regression model by using band average method (Figure 8.7 (b, c)) and spectral shape function method (Figure 8.7 (d, e)). From Figure 8.7 (b, c), it is observed that

by using band average method, the chlorophyll content varied from 4.58% to 8.78% for the rice plots within the field. While on the other hand, Figure 8.7 (d, e) indicates a wide variation of 2.84% to 8.93% was achieved in chlorophyll content for rice in case of spectral shape function method. This variability was found significantly different and it provided more detailed information at each plot scale than the band average method. It can be further visualised that though there was a distinct variation of chlorophyll content by applying different narrow band indices, however, a superior degree of spatial variability in the paddy crop plots within the fields was obtained from multispectral LISS IV data.

This indicated that spatial distribution may have been affected by many integrative factors such as climate, parent material, seasonal variation, soil type, cultivation method, cropping system, irrigation and most importantly topography. Similar finding was reported by Vrindts et al. (2003) that winter wheat yields were affected by spatial variability of winter wheat related to topographic variations.

8.4.4 Variability mapping of nitrogen at plot scale from space platform

The spatial variability of nitrogen content of rice agriculture system was determined by employing index based fusion approach for hyperspectral and multispectral images. While, both the LNC and SR index models were obtained from band average method, only LNC model was found to be significant in estimating nitrogen content from shape function concept. In this respect, it was clear that by adopting fusion index approach method all the indices sensitive to nitrogen could not be employed. Based on the critical bands obtained from the above mentioned concepts, vegetation indices were selected for better estimation of crop parameter. With the implementation of band average method, LNC index model exhibited nitrogen content variation from 3.37% to 6.04% (Figure 8.8 (b, c)). It illustrates considerable spatial variability of nitrogen content at plot scale within the field for the rice crop shown in five plots. Furthermore, LNC index model clearly realized spatial distribution of nitrogen content of rice from spectral shape function method (Figure 8.8 (d, e)). It can be seen that the variability is significantly different in each of the five rice plots (Figure 8.8 (e)).

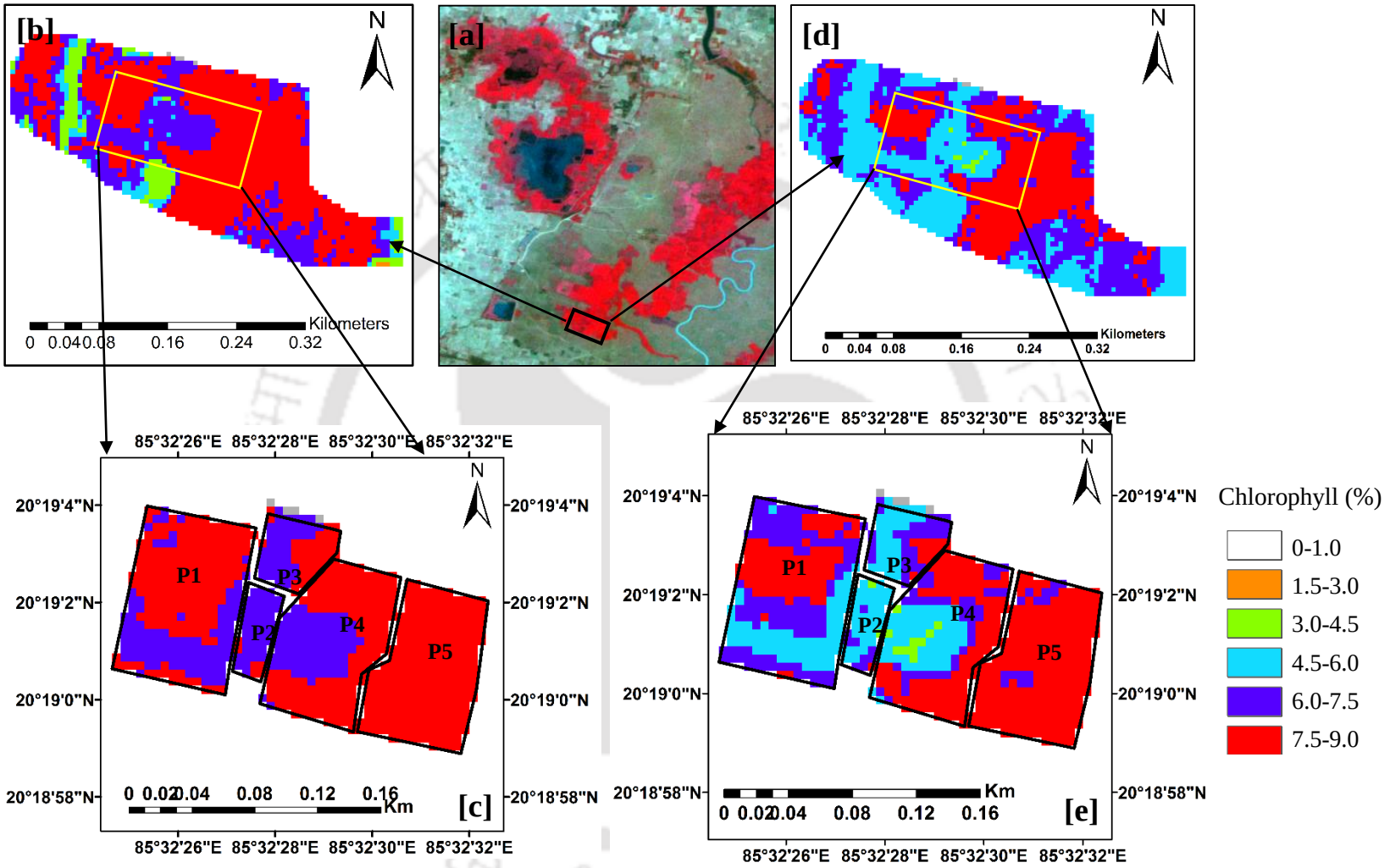

Figure 8.6 : Spatial variability of chlorophyll at plot scale from OSAVI model using (b, c) Band average method (d, e) and Spectral shape function method

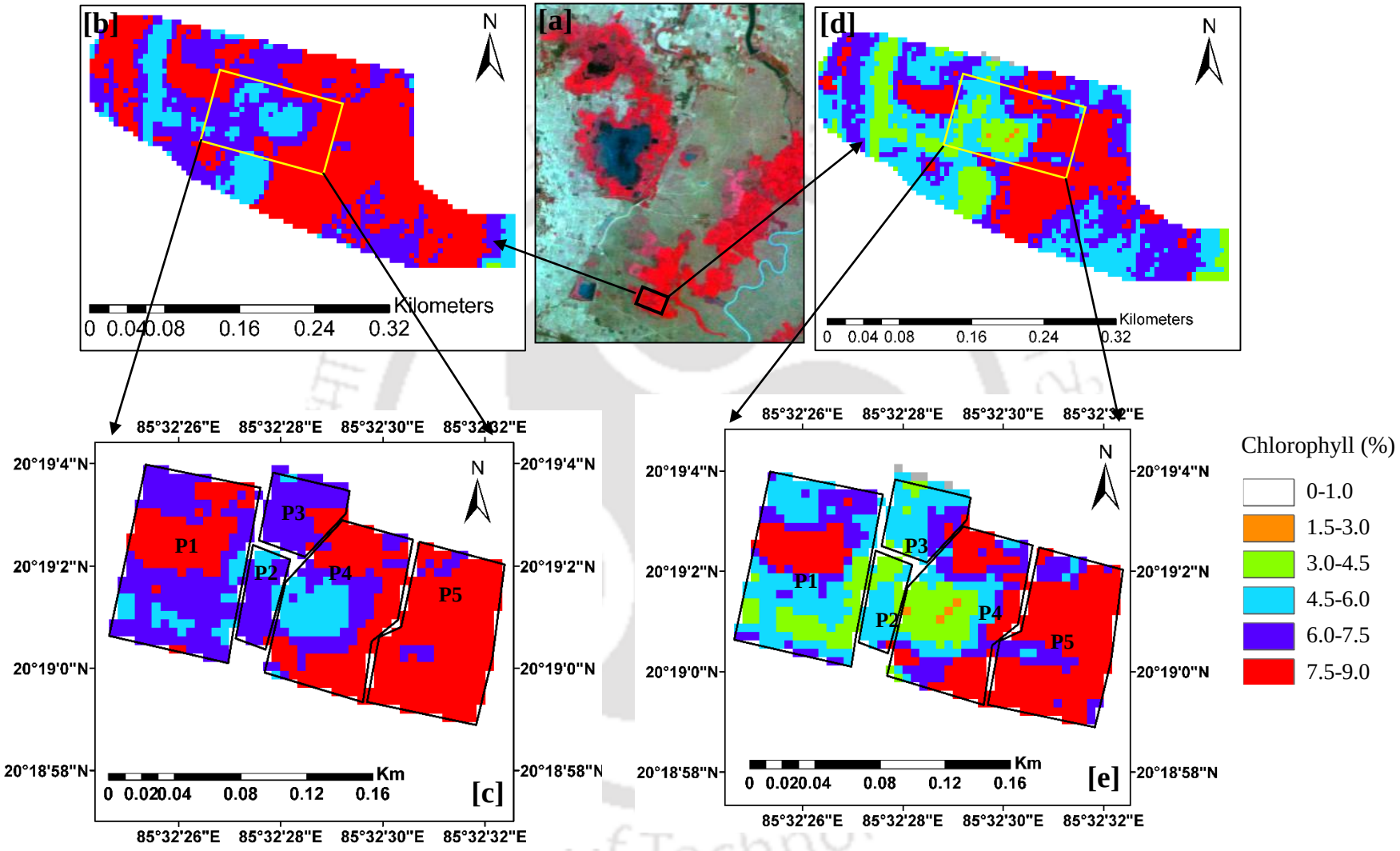

Figure 8.7 : Spatial variability of chlorophyll at plot scale from LNC model using (b, c) Band average method and (d, e) Spectral shape function method

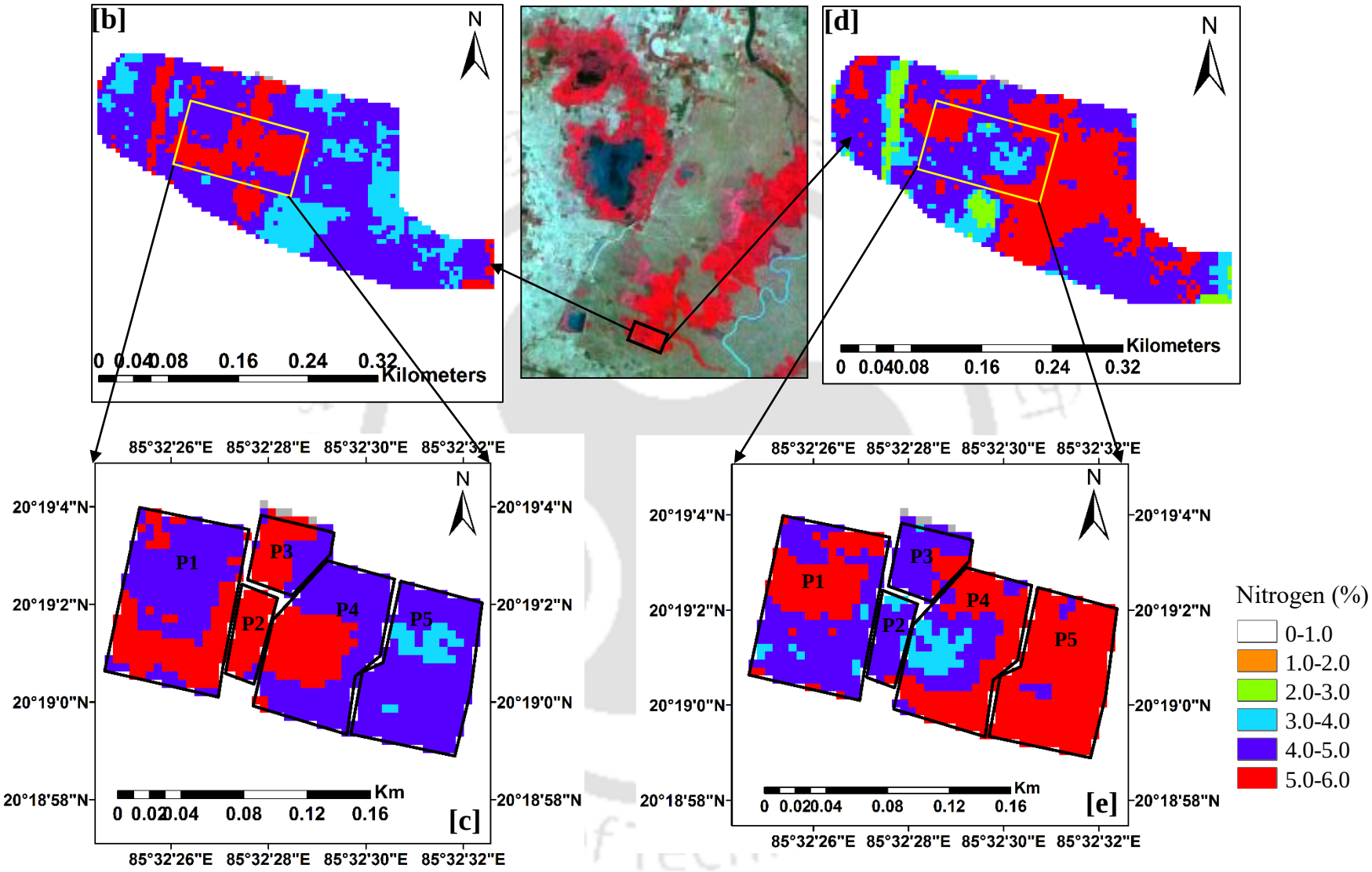

Figure 8.8 : Spatial variability of nitrogen at plot scale from LNC model using (b, c) Band average method and (d, e) Spectral shape function method.

Here the variability of nitrogen content was more as compared to the band average method. The nitrogen content was found to be widely varying from 3.1% to 5.85% at plot scale within the field. It was observed that the variation obtained from LNC index model has a good agreement with observed nitrogen content that ranged from 1.12% to 3.92%.

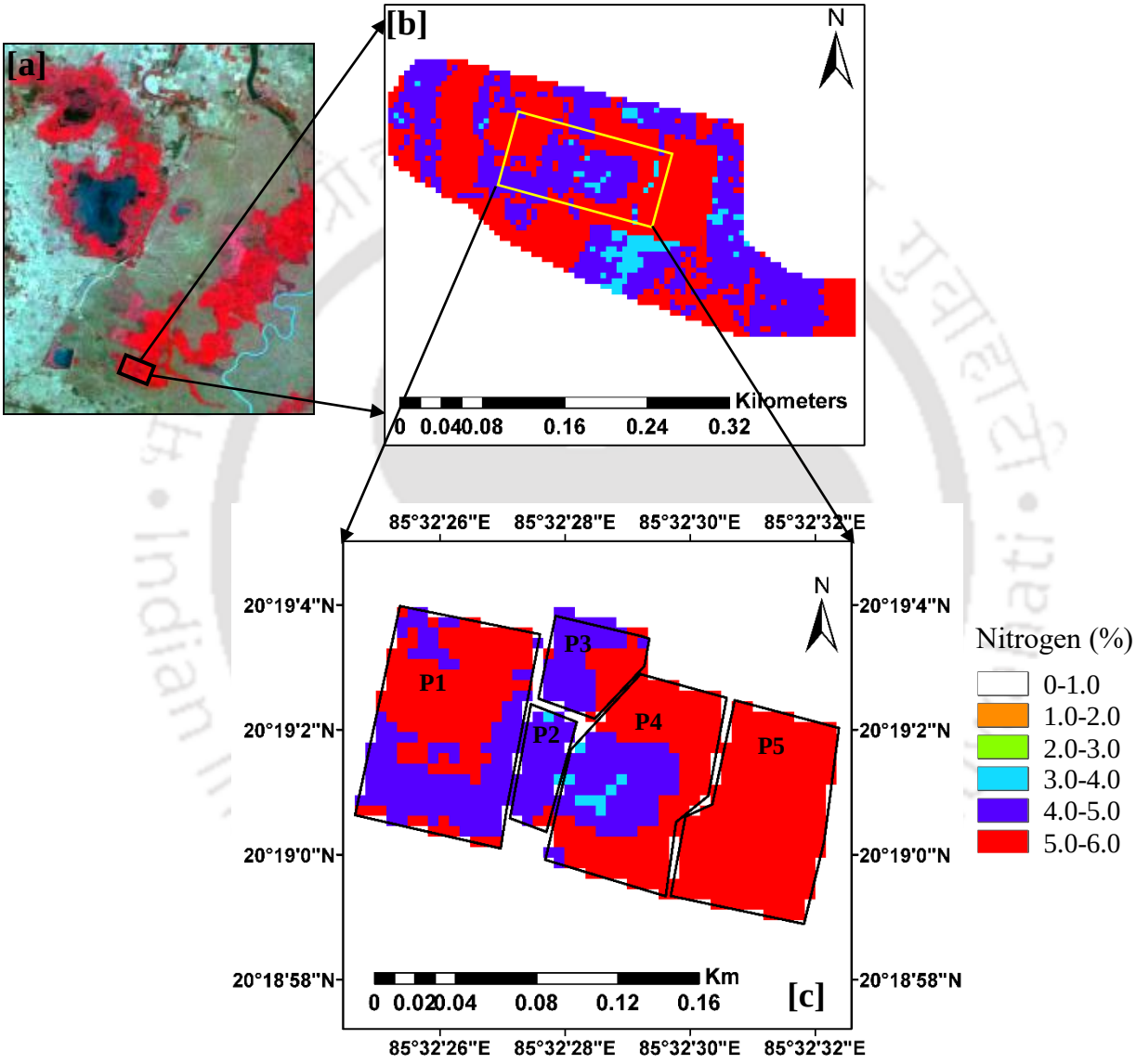

Figure 8.9 : Spatial variability of nitrogen at plot scale from SR model using (b, c) Band average method

Furthermore, SR index model was also found to be significant in estimating nitrogen content from band average method. Nitrogen content variability was tried to be mapped from LISS

IV image (Figure 8.9 (b, c)). Figure 8.9 (b) exhibits the nitrogen variability indicating the spatial distribution of crop field from space platform. The rice nitrogen content was distributed spatially over rice plots ranging from 3.82 – 5.96%. An interesting feature was noticed that there was no variability in the fifth rice plot compared to the other four plots. However, the the LNC index model was able to predict the spatial variability of paddy crop nitrogen in that plot. This index model exhibited a non-significant spatial distribution of nitrogen content at the rice plot level. This may have happened because the combinations of green narrow bands in the SR index only may not be sufficient to find out the induced variability during pre-monsoon period for summer rice crop.

Additionally, the degree of spatial variability of nitrogen derived from LNC index model was found to be more significant as compared to SR index model in summer rice. This behaviour may be attributed to the long-term basic stability of farm management, fertilization, tillage, planting method, cropping systems, irrigation application and spatial structure of soil characteristics of the study area that had led to a large spatial distribution pattern. The above findings indicated that the properties concerning the spatial variability of rice nitrogen content at plot scale within the paddy fields derived from LISS IV image reflect the heterogeneity in rice agriculture system and provide a better choice of fertilizer inputs by taking variability into account for precision rice farming.

8.4.5 Statistical analysis of the index based fusion approach for multispectral and hyperspectral data

The overall functional range of chlorophyll was categorized into several classes between 0% to 9.0%, and their plot-wise spatial distribution (% of total area) was compared between band average concept method and spectral shape function method (Figure 8.10). The distribution of classes achieved from OSAVI model using band average method was found to be less in comparison to spectral shape function method. Further, in case of LNC model, the chlorophyll content derived from band average method exhibited improved results, and it was found to be well distributed spatially over the rice plots from shape function method (Figure 8.11). Table 8.3 summarizes the mean and standard deviation of chlorophyll content for each of the rice plots derived from both the methods, which illustrates almost similar variability at plot scale.

The OSAVI model predicted mean chlorophyll variation of 7.26 - 8.36% (band average method) and 5.564 - 8.279% (shape function method) at plot scale, whereas the LNC model predicted variation that ranged from 6.52 - 8.631% (band average method) and 6.13 - 8.456% (shape function method).

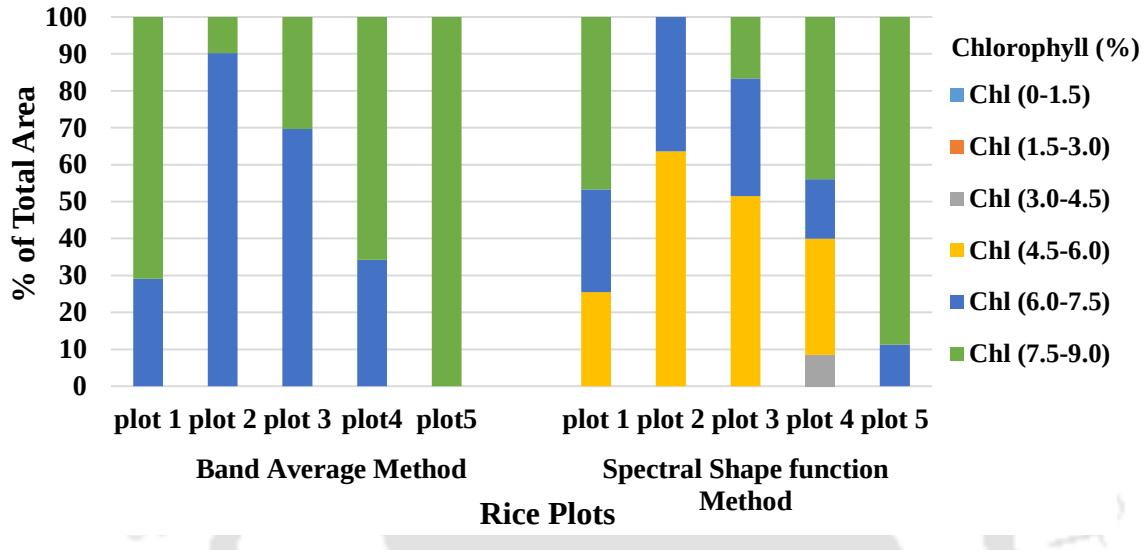

Figure 8.10 : Distribution of area under different classes of chlorophyll (Chl) derived from fused product of OSAVI model using band average and spectral shape function methods

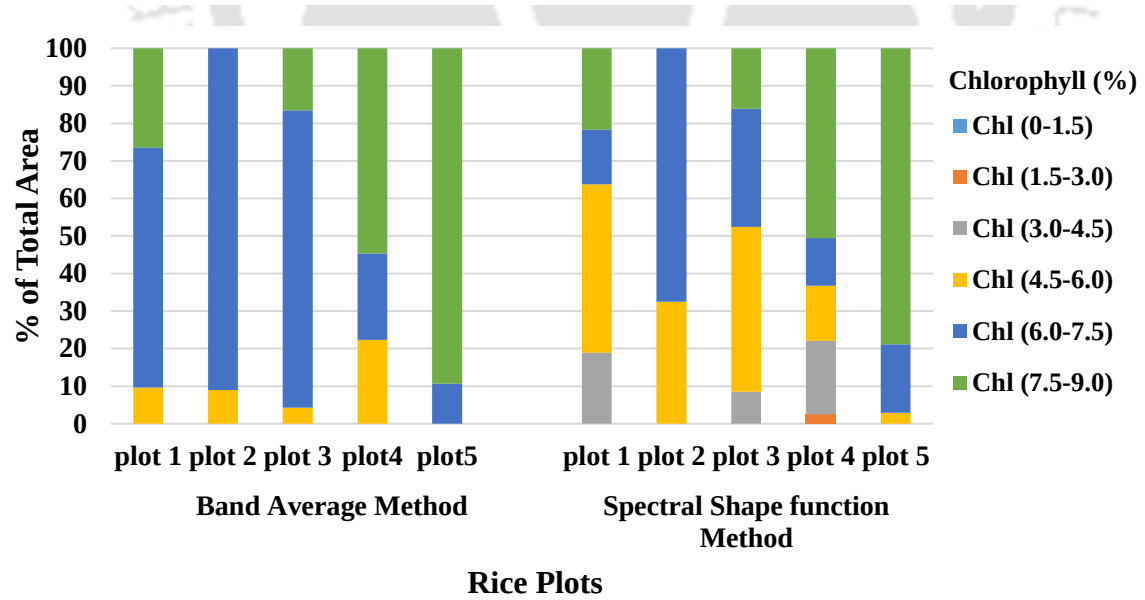

Figure 8.11 : Distribution of area under different classes of chlorophyll (Chl) derived from fused product of LNC model using band average and spectral shape function methods

Table 8.3 : Plot-wise statistics of chlorophyll derived from (a) OSAVI, (b) LNC models employing Band average method and Spectral shape function method

		Chlorophyll Content (%)				
		plot1	plot2	plot3	plot4	plot5
(a) OSAVI						
Band Average method	Mean	7.686	7.26	7.39	7.688	8.36
	SD	0.427	0.303	0.348	0.581	0.304
Spectral Shape Function method	Mean	7.163	5.948	5.654	7.031	8.279
	SD	0.467	0.875	0.521	0.346	0.335
(b) LNC						
Band Average method	Mean	8.56	6.52	7.53	8.245	8.631
	SD	0.313	0.464	0.671	0.317	0.267
Spectral Shape Function method	Mean	7.43	6.13	6.58	7.67	8.456
	SD	0.542	0.575	0.487	0.489	0.432

Similarly, the class distribution of nitrogen, derived from the image of the study site acquired on 22nd February 2016, was categorized between 0 – 6% to visualize their plot-wise spatial distribution (% of total area) obtained from band average concept method and spectral shape function method. Here, LNC and SR models were found to be functional in predicting nitrogen content from band average method, whereas only LNC model performed satisfactorily for spectral shape function method. This may be due to the phenological behavior of paddy crop in the particular region of the spectrum. The spatial distribution of LNC model at plot scale is represented in Figure 8.12 for both the methods. On the other hand, Figure 8.13 illustrates the spatial distribution of nitrogen content predicted from SR index model using band average method. Here, similar observation was made, where spectral shape function method exhibited more variability as compared to band average method in case of LNC model. However, overall result of the SR index model did not exhibit satisfactory variation of nitrogen within the rice plots. Besides these, plot-wise mean and standard deviation of nitrogen content for each of the rice plots was also compared for different methods and index models (Table 8.4). It indicates that mean value of nitrogen content of each plot was around 4.34% to 5.6% and 4.56% to 5.64% for band average method and spectral shape function method respectively. In case of

SR index model, plot wise mean value of nitrogen content was found to be high, mostly greater than 5%, representing a minor spatial variability in comparison to LNC model.

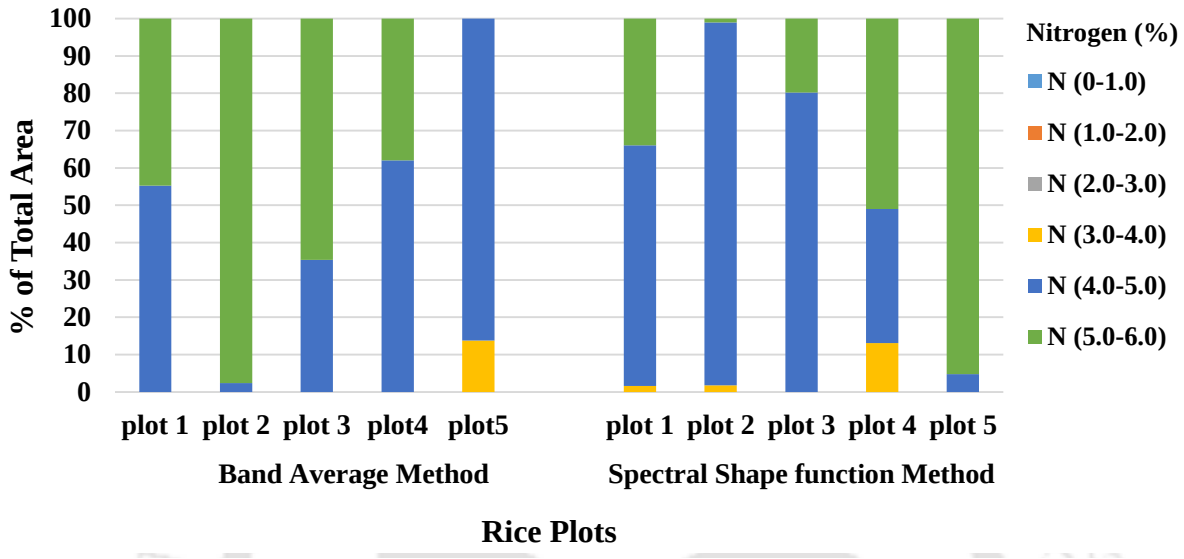

Figure 8.12 : Distribution of area under different classes of nitrogen (N) derived from fused product of LNC model using band average and spectral shape function methods

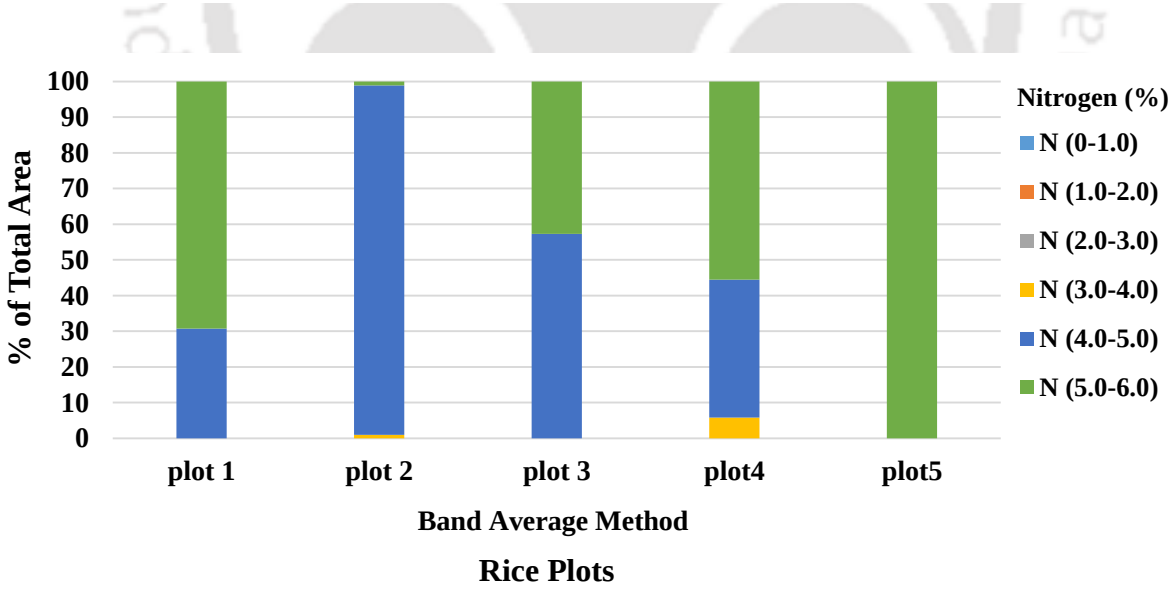

Figure 8.13 : Distribution of area under different classes of nitrogen (N) derived from fused product of SR model using band average method

Table 8.4 : Plot-wise statistics of nitrogen derived from (a) LNC (b) SR models employing Band average method and Spectral shape function method

		Nitrogen Content (%)				
		plot1	plot2	plot3	plot4	plot5
(a)LNC						
Band Average method	Mean	5.35	5.6	5.24	4.58	4.34
	SD	0.112	0.103	0.12	0.206	0.158
Spectral Shape Function method	Mean	4.74	4.56	4.82	5.32	5.64
	SD	0.242	0.261	0.197	0.175	0.107
(b) SR						
Band Average method	Mean	5.48	4.52	5.12	5.43	5.6
	SD	0.121	0.182	0.157	0.126	0.101

Hence, it can be inferred that proposed methodology can be applied for the variability mapping of crop parameters at plot scale level within the field to overcome the limitations of Hyperion image. It can also be further used for operational precision farming more efficiently

8.5 Conclusions

The spatial variability of paddy crop parameters such as chlorophyll and nitrogen were retrieved at plot scale within the field. The utilization of the narrow band index fusion technique can provide the field heterogeneity at plot level that can aid in implementing precision farming more effectively. The hyperspectral data from Hyperion sensor, which is very difficult to obtain and has very low temporal resolution for a specified location around the globe, cannot be used for operational crop parameter prediction from space platform. Therefore, in the present study, an effort has been made towards spatial distribution mapping of chlorophyll and nitrogen from multispectral image using narrow band index fusion method. The critical bands were identified from narrow band Hyperion image by establishing regression methods between critical band and Hyperion bands lying in the broad band spectrum. Bands were selected based on very high coefficient of determination ($R^2 > 0.95$). Further, the synthetic multispectral critical bands were derived by adopting band average and

spectral shape function approaches. By using the band average method, spectral narrow bands like 533 nm, 565 nm, 681 nm, 705 nm, 717 nm, 750 nm and 800 nm were found significant amongst all the critical bands. Hence, combination of these bands comprising OSAVI, LNC, SR indices could be employed rather than all the chlorophyll and nitrogen related vegetation indices sensitive to paddy crop discussed in Chapter 6. Further the spectral shape functions were established for broad bands (green, red and NIR) of multispectral LISS IV data to get the equivalent critical bands.

It was revealed that OSAVI, LNC index models could be used for the prediction of chlorophyll content at plot scale within the field using both the band average and spectral shape function approaches. In case of OSAVI model, the chlorophyll content varied from 7.22 – 8.86% and 3.06 - 9.01% for band average method and spectral shape function method respectively, whereas LNC model produced a variation of 4.58 - 8.78% and 2.84 - 8.93% for band average and spectral shape methods respectively. By employing LNC model, the band average method exhibited improved spatial distribution results for chlorophyll content as compared to OSAVI model. The chlorophyll content derived from shape function method was found to be well distributed spatially over the rice plots within the field. Similarly, LNC and SR index models could be used for assessment of nitrogen content. In case of LNC index model, the nitrogen content varied from 3.37 - 6.04% and 3.1 - 5.85% for band average and spectral shape methods respectively, whereas SR index exhibited a variation of 3.82 - 5.96% only for band average method. The index models had good agreement with the observed nitrogen content that ranged from 1.12% to 3.92%. The degree of spatial variability of nitrogen derived from LNC index model was found to be more significant as compared to SR index model in summer rice cultivation. It was also ascertained that the spatial distribution of nitrogen content of rice was better achieved through spectral shape function method. Further, statistical analysis of index based fusion approach for multispectral and hyperspectral data was also carried out that demonstrated plot-wise spatial distribution of chlorophyll and nitrogen. It confirmed that the proposed methodology can be applied for the variability mapping of crop parameters at plot scale level within the fields from space platform, which can be beneficial in achieving operational precision farming more efficiently.

9 Conclusions and Future Recommendations

9.1 A brief Overview of the study

Rice is the most important food crop in India, which occupies the largest area of cultivation in the world. Researchers, scientists and planners throughout the world have been working on increasing crop productivity to safeguard food security for the growing population of the world. Precision agriculture is an integrated information and production based farming system, which is mainly centred around site specific crop management established on field variability concept. Plot scale variability mapping from space platform was a difficult task due to rapid variation in biophysical parameter within the field. Estimation of paddy crop biophysical parameters, a prerequisite for precision rice farming, was a very challenging task for an Indian rice agriculture system, where small scale farming are predominant. The advantages of hyperspectral remote sensing techniques have made it possible to identify the critical wavelengths sensitive to paddy crop characteristics. Based on these critical wavelengths, different fertilizer treatments and irrigation scheduling could be implemented by employing improved vegetation indices. Significant narrow wave bands have shown that the rice varieties can be discriminated well with different nitrogen treatments as well as with no nitrogen treatment at all. The crop biophysical parameters such as total chlorophyll, nitrogen, leaf water content were quantified. It was found that the incorporation of critical wavelengths into development of vegetation index models have demonstrated the field variability from Hyperion satellite imagery. Different index models were investigated in mapping of total chlorophyll and nitrogen content of paddy crop at field scale from satellite

images. They have shown good agreement with the observed values of the crop parameters. Furthermore, reproductive phase was found to be the most critical stage to find the leaf water content variability. It was found that water indices in the visible near-infrared (VNIR) region have good relations with the short-wave infrared (SWIR) region. Hence, VNIR index models can be directly mapped to SWIR indices to map the leaf water content at field scale. Additionally, fusion of multispectral LISS IV image and Hyperion image was successful in capturing the plot scale variability within the paddy field, attributed to the rapid variation in topography for small scale farms in an Indian rice agriculture system.

9.1.1 Literature review

Review of literatures on worldwide applications of precision rice farming with advanced remote sensing techniques is discussed in Chapter 2. Precision agriculture studies contributing to nutrient management in paddy cropping systems by different researchers was also summarized. The importance and need of precision rice farming in a developing country like India, where small scale farming is predominant, was reported. The paddy crop characteristics, prediction of biophysical parameters, crop yield and field variability in an Indian rice agriculture system were studied in combination with ground and satellite based measurements. Employment of recent advanced remote sensing technologies have provided insight into field variability mapping for a complicated heterogeneous agricultural system like the Indian rice agriculture system.

9.1.2 Study site and data acquisition

The study area comprises of two sites in India where paddy crop was grown as discussed in Chapter 3. Paddy crop was grown under controlled environment to understand the different characteristics of crop parameters. Field campaigns were conducted at two agriculture sites during two different seasons in a crop calendar to study the various inputs and cropping management system. The *in-situ* data was collected using a sophisticated instrument, spectroradiometer, from the paddy field. Moreover, satellite images were acquired from Hyperion (EO-1) and LISS IV (IRS-P6) satellite sensors passing over these study sites. Further, laboratory chemical analysis for leaf samples of study site was done to measure crop

biophysical parameters.

9.1.3 Plant growth monitoring via proposed improved vegetation indices

Time to time monitoring of paddy crop growth is an important task for predicting crop yield. The crop behaviour is mainly governed by spectral signatures in which narrow bands at specific wavelengths contribute to different crop features. The hyperspectral data has the potential to retrieve vital information on agricultural crop characteristics throughout its developmental stage. To identify the wavelengths sensitive to paddy crop growth monitoring, a proper methodology needs to be adopted. To determine the critical wavelengths, difference contour plots were developed by using spectroradiometric measurements observed from eight rice varieties under three nitrogen levels: N_1 (50 kg/ha), N_2 (100 kg/ha) and N_3 (150 kg/ha). From the difference plots of nitrogen applications, it is revealed that the crop growth has started earlier with N_3 (150 kg/ha) application than N_2 (100 kg/ha) application in most of the rice varieties. The critical wavelengths, at which the effects of nitrogen applications on spectral reflectance response for the rice varieties were found significant, werev $\rho_{550}, \rho_{560}, \rho_{655}, \rho_{750}, \rho_{755}, \rho_{780}, \rho_{810}, \rho_{840}, \rho_{900}, \rho_{920}, \rho_{1000}, \rho_{1010}, \rho_{1020}$. Additionally, difference contour plots were generated for different rice varieties, which exhibited no significant difference in their growth level. Furthermore, based on wavelengths, two indices focused on water content and three vegetation indices aimed to discriminate nitrogen treatments were proposed and compared with established vegetation index (VI) green ratio index (GRI) (Inoue et al., 2008). The proposed advanced indices include $\rho_{560}, \rho_{840}, \rho_{920}, \rho_{1020}$ that efficiently differentiated between nitrogen levels in all rice varieties, but the existing indices sensitive to nitrogen including $\rho_{550}, \rho_{560}, \rho_{810}, \rho_{830}$ were not able to differentiate properly between nitrogen treatments. It was found that the proposed indices VI_1 and VI_2 were effectively able to differentiate the level of nitrogen treatments for most of the varieties except for one or two rice varieties, whereas the existing indices were not able differentiate between the rice varieties except two or three varieties. It was observed from the quantitative analysis of rice genotypes that VI_2 could be functionally used for the assessment of nitrogen stress in a rice agriculture system. Chapter 4 describes the improved

methodology focused on obtaining the critical wavelengths and the development of advanced vegetation indices for monitoring rice growth under different nitrogen treatments in Indian climatic conditions.

9.1.4 Discrimination of paddy crop species using advanced clustering technique

Discrimination of rice species with very fine differences among the varieties is difficult to be determined. However, application of advanced algorithm based on waveform classification followed by clustering technique on acquired hyperspectral data performed well in discriminating the rice genotypes with three different levels of nitrogen treatments as well as with no nitrogen treatment. Embedded noise in the spectra was well captured during the spectra data collection from field, which can be eliminated to obtain a pure spectral signature. Thus, a better spectral library for the rice genotypes under different nitrogen treatments was developed. It was found that rice genotypes were well discriminated showing independent clusters towards each of rice genotypes, whereas some of varieties were mixed representing one cluster in which fine difference between the rice varieties could not be identified. It was because the reflectance properties were significant at certain wavelengths for a specific crop. The significant wavelengths for this discrimination were identified in green (519, 549, 559 nm), red (649 nm), red edge (729 nm) and NIR (789, 799, 809, 819 nm) regions of the spectrum. The potential of optimal narrow bands retrieved from ground based hyperspectral data using a spectroradiometer in the discrimination of rice species is discussed in Chapter 5. This information can be used to develop three band or four band indices especially for paddy crop, which can deliver vital information in regards to precision rice farming. However, it needs validation with more number of ground based hyperspectral data sets.

9.1.5 Estimation and variability study of crop parameters of rice from hyperspectral imagery

It is very important to improve rice productivity for augmenting growth, while at the same time minimizing adverse environmental impacts through precision nitrogen fertilizer management practices. Moreover, leaf nitrogen content is a strong influencing factor in crop growth and canopy photosynthesis rate which leads to production of leaf chlorophyll content

(Chl) through photosynthesis. In this Chapter 6, paddy crop nitrogen and chlorophyll contents were estimated from field observations. Furthermore, these most important crop parameters were predicted from space-borne hyperspectral satellite imagery through the establishment of different narrow band index models. The spatial distribution of total chlorophyll content and nitrogen content are presented in this chapter. It was found that the simple ratio (SR) index model produced satisfactory result in the estimation of nitrogen content from spectroradiometric hyperspectral data than satellite based Hyperion imagery. It was observed that another index i.e. modified LNC index model established a nonlinear relationship showing, nitrogen content performed better than that of the established Tian et al. (2011) model as far as the estimated nitrogen content from Hyperion imagery was concerned. It was observed that the nitrogen content spatially varied from 2.35 - 3.82%, which had a good agreement with the observed nitrogen content (1.12 - 3.92%) and it was 2.36 - 2.51% in case of Tian et al. (2011). Within the observed chlorophyll range obtained from the studied rice varieties grown in the rice agriculture system, LNC, OSAVI, Gitelson, mSR and MTCI index models agreeably predicted the chlorophyll content of paddy crop from Hyperion imagery. Total chlorophyll content had a wide spatial coverage ranging from 1.77-5.81 mg/g (LNC index), 3.0-13 mg/g (OSAVI index), 0.5-10.43 mg/g (Gitelson index), 2.18-10.61 mg/g (mSR index) and 2.90-5.40 mg/g (MTCI index). The proposed index models were more convincing in estimation of rice chlorophyll content spatially over an agricultural system from Hyperion imagery. Moreover, spatial variation of chlorophyll and nitrogen mapping of paddy crop from Hyperion imagery could be used to develop an informative system for field heterogeneity identification. The rice field heterogeneity was captured well through clustering algorithm from Hyperion imagery for an Indian rice agriculture system. It was confirmed that the variability attributed to small scale farming system in India is a function of slope of the field. The major sources of field heterogeneity were large scale variation in soil moisture and water availability due to rapid change in topography within a very small field scale in an Indian rice agriculture system.

9.1.6 Water stress variability mapping in rice agriculture system

To study water stress in a rice agriculture field, Hyperion images were processed and analyzed

over two different seasonal periods in a crop calendar and the details of study are described in Chapter 7. Reproductive phase was found to be the most sensitive phase amongst the crop developmental stages in evaluating leaf water content of paddy crop through narrow band water indices. Hyperspectral indices particularly WBI, NWI-3 and NWI-4 showed strong correlation with LRWC at the reproductive phase. Collection of hyperspectral observations through spectroradiometers with high wavelength ranges are too expensive, thus this study was carried out to investigate how VNIR water indices were correlated with SWIR band water indices. The three VNIR water indices (WBI, NWI-3 and NWI-4) best correlated with water indices in the SWIR region. The WBI established good correlationship with SWIR band indices - NDWI-1, NDWI-2, SRWI, NDII, SAWI-1 (only for winter rice agriculture), WI–Hyperion. Likewise, NWI-3 showed correlationship with NMDI and NWI-4 responded to MSI, SAWI-1(only for summer rice agriculture), and SAWI-2.

The NDWI-2, MSI, SRWI, NDII, SAWI-1, WI-Hyperion index regression models ascertained that the spatial distribution of LRWC which widely varied from 47% to 94% in a summer rice agriculture system. Whereas, the NDWI-1, NDWI-2, NDII, SAWI-1, SAWI-2 index regression models performed well in mapping of LRWC in an Indian winter rice agriculture system in a crop calendar from space platform via Hyperion L1R data with a very high accuracy. The analysis effectively showed the LRWC variation from 60% to 93% in winter rice agriculture system. The predicted LRWC variation from space platform represented a close agreement with that of the field observation values. Moreover, a strong linkage between QTL and drought-tolerant genes was ascertained for the paddy crop LRWC and hence drought tolerant species can be developed for different environmental conditions (Venuprasad et al., 2012). Development of various index models, utilization of these models in obtaining the spatial distribution of water stress and comparison between the developed and established models are described in detail in Chapter 7.

9.1.7 Fusion of multispectral and hyperspectral data to retrieve plot scale variability of crop parameters.

To study the spatial variability of paddy crop parameters such as chlorophyll and nitrogen at plot scale within the field, utilization of narrow band index fusion technique has become

helpful in providing the field heterogeneity at plot level to improve precision farming effectively. The temporal resolution of hyperspectral satellite is very poor, making it difficult for the non-destructive estimation of crop parameters from space platform. Here, Chapter 8 emphasized on the spatial distribution mapping of chlorophyll and nitrogen at plot scale by adopting narrow band index fusion approach using multispectral LISS IV image and hyperspectral Hyperion image. Additionally, the synthetic multispectral critical bands were derived by adopting band average and spectral shape function approaches. With the utilization of band average method, spectral narrow bands like 533 nm, 565 nm, 681 nm, 705 nm, 717 nm, 750 nm and 800 nm were found significant amongst all the critical bands. Therefore, only the OSAVI, LNC and SR index models concerning the combination of the obtained significant bands could be employed rather than all the chlorophyll and nitrogen related vegetation indices described in Chapter 6. It was revealed that OSAVI, LNC index models could be used for the prediction of chlorophyll content at plot scale within the field using both the band average and spectral shape function approaches. In case of OSAVI model, the chlorophyll content varied from 7.22 – 8.86% and 3.06 - 9.01% for band average method and spectral shape function method respectively, whereas LNC model produced a variation of 4.58 - 8.78% and 2.84 - 8.93% for band average and spectral shape methods respectively. Similarly, LNC and SR index models could be used for assessment of nitrogen content. In case of LNC index model, the nitrogen content varied from 3.37 - 6.04% and 3.1 - 5.85% for band average and spectral shape methods respectively, whereas SR index exhibited a variation of 3.82 - 5.96% only for band average method. The index models had a good agreement with the observed nitrogen content that ranged from 1.12% to 3.92%. The degree of spatial variability of nitrogen derived from LNC index model was found to be more significant as compared to SR index model in summer rice cultivation. The above findings indicated that the properties concerning the spatial variability of rice nitrogen content at plot scale within the paddy fields derived from LISS IV image may reflect the heterogeneity in a rice agriculture system and provide a better choice for fertilizer inputs by taking variability into account for precision rice farming. Statistical analysis of the index based fusion approach for multispectral and hyperspectral data was carried out for assessment of the degree of variability at plot scale within the paddy field. These findings are well represented and discussed more in detail in Chapter 8. This chapter

described about variability mapping of crop parameters at plot scale level within the field from space platform which can help in attaining operational precision farming more efficiently.

9.2 Recommendations for Future work

The present study provides an insight towards the precision agriculture to map the field scale variability using remote sensing techniques. This study leaves wide scope for future investigation to explore more in this direction, which may yield fruitful outcomes. The future scope of the study are discussed as follows.

1. The proposed index models can be further studied for understanding more about temporal and spatial variability mapping of crop parameters over an agricultural system with the help of airborne flights over other parts of India from AVIRIS platform, currently being carried out by ISRO-NASA HySI programme.
2. The retrieved critical bands could be assimilated into a sensor carried in a drone to monitor the paddy crop variables at plot scale for the advancement in precision rice agriculture in a most economic and effective way.
3. Crop growth models can be developed by integrating the most important information like crop variety, nutrient, fertilizer and water variability to understand the crop dynamics at plot scale within the field.
4. Non-destructive estimation of other paddy crop parameters are needed to be investigated further to increase the rice yield, in regards to improving precision rice agriculture further.
5. Additionally, more research studies are needed to be carried out in other parts of India during different seasonal periods under various topographic conditions in order to apply suitable site-specific field crop management schemes.

Bibliography

Aaron, R.S., John, F.S., Mark, A.L., James, S.S., Sven, H.J., Ariovaldo L.J., 2004. Appropriateness of management zones for characterizing spatial variability of soil properties and irrigated corn yields across years. Agronomy Journal, 96(1), pp.195-203.

Asner, G.P., 1998. Biophysical and biochemical sources of variability in canopy reflectance. Remote Sensing of Environment, 64(3), pp.234-253.

Aubert, M., Baghdadi, N., Zribi, M., Douaoui, A., Loumagne, C., Baup, F., El Hajj, M. and Garrigues, S., 2011. Analysis of TerraSAR-X data sensitivity to bare soil moisture, roughness, composition and soil crust. Remote Sensing of Environment, 115(8), pp.1801-1810.

Auernhammer, H., 2001. Precision farming—the environmental challenge. Computers and Electronics in Agriculture, 30(1), pp.31-43.

Auernhammer, H., Demmel, M., Maidl, F.X., Schmidhalter, U., Schneider, T., Wagner, P., 1999. An On-farm communication system for precision farming with nitrogen real-time application. American Society of Agricultural Engineers, USA, (99), pp.11.

Babar, M.A., Reynolds, M.P., Van Ginkel, M., Klatt, A.R., Raun, W.R. and Stone, M.L., 2006. Spectral reflectance indices as a potential indirect selection criteria for wheat yield under irrigation. Crop Science, 46(2), pp.578-588.

Babu, R.C., Nguyen, B.D., Chamarerk, V., Shanmugasundaram, P., Chezhian, P., Jeyaprakash, P., Ganesh, S.K., Palchamy, A., Sadasivam, S., Sarkarung, S. and Wade, L.J., 2003. Genetic analysis of drought resistance in rice by molecular markers. Crop Science, 43(4), pp.1457-1469.

Baez-Gonzalez, A.D., Kiniry, J.R., Maas, S.J., Tiscareno, M.L., Macias, C.J.J.L., Mendoza, J.L., Richardson, C.W., Salinas, G. and Manjarrez, J.R., 2005. Large-area maize yield forecasting using leaf area index based yield model. Agronomy Journal, 97(2), pp.418-425.

Bailey, J.S., Wang, K., Jordan, C. and Higgins, A., 2001. Use of precision agriculture technology to investigate spatial variability in nitrogen yields in cut grassland. Chemosphere, 42(2), pp.131-140.

Balasundram, S.K., Memarian, H. and Khosla, R., 2013. Estimating oil palm yields using vegetation indices derived from Quickbird. Life Science Journal, 10(4), pp.851-860.

Bannari, A., Khurshid, K.S., Staenz, K. and Schwarz, J., 2008. Potential of Hyperion EO-1 hyperspectral data for wheat crop chlorophyll content estimation. Canadian Journal of Remote Sensing, 34(S1), pp.S139-S157.

Bannari, A., Staenz, K., Champagne, C. and Khurshid, K.S., 2015. Spatial variability mapping of crop residue using Hyperion (EO-1) hyperspectral data. Remote Sensing, 7(6), pp.8107-8127.

Basso, B., Ritchie, J.T., Pierce, F.J., Braga, R.P. and Jones, J.W., 2001. Spatial validation of crop models for precision agriculture. Agricultural Systems, 68(2), pp.97-112.

Bauer, M.E., 1985. Spectral inputs to crop identification and condition assessment. Proceedings of the IEEE, 73(6), pp.1071-1085.

Bausch, W.C. and Khosla, R., 2010. QuickBird satellite versus ground-based multi-spectral data for estimating nitrogen status of irrigated maize. Precision Agriculture, 11(3), pp.274-290.

Bausch, W.C., 1993. Soil background effects on reflectance-based crop coefficients for corn. Remote Sensing of Environment, 46(2), pp.213-222.

Becker, E. and Schmidhalter, U., 2017. Evaluation of yield and drought using active and passive spectral sensing systems at the reproductive stage in wheat. Frontiers in Plant Science, 8, pp.1-15.

Berjon, A.J., Cachorro, V.E., Zarco-Tejada, P.J. and de Frutos, A., 2013. Retrieval of biophysical vegetation parameters using simultaneous inversion of high resolution remote sensing imagery constrained by a vegetation index. Precision Agriculture, 14(5), pp.541-557.

Bhuyan, M.H.M., Ferdousi, M.R. and Iqbal, M.T., 2012. Foliar spray of nitrogen fertilizer on raised bed increases yield of transplanted aman rice over conventional method. ISRN Agronomy, pp.1-8.

Blackmer, T.M. and Schepers, J.S., 1995. Use of a chlorophyll meter to monitor nitrogen status and schedule fertigation for corn. Journal of Production Agriculture, 8(1), pp.56-60.

Blackmer, T.M., Schepers, J.S. and Varvel, G.E., 1994. Light reflectance compared with other nitrogen stress measurements in corn leaves. Agronomy Journal, 86(6), pp.934-938.

Boegh, E., Soegaard, H., Broge, N., Hasager, C.B., Jensen, N.O., Schelde, K. and Thomsen, A., 2002. Airborne multispectral data for quantifying leaf area index, nitrogen concentration, and photosynthetic efficiency in agriculture. Remote Sensing of Environment, 81(2), pp.179-193.

Boitt, M., Ndegwa, C. and Pellikka, P., 2014. Using Hyperspectral Data to Identify Crops in a Cultivated Agricultural Landscape-A Case Study of Taita Hills, Kenya. Journal of Earth Science & Climatic Change, 5(9), pp.1-4.

Bolton, D.K. and Friedl, M.A., 2013. Forecasting crop yield using remotely sensed vegetation indices and crop phenology metrics. Agricultural and Forest Meteorology, 173, pp.74-84.

Borregaard, T., Nielsen, H., Nørgaard, L. and Have, H., 2000. Crop–weed discrimination by line imaging spectroscopy. Journal of Agricultural Engineering Research, 75(4), pp.389-400.

Broge, N.H. and Mortensen, J.V., 2002. Deriving green crop area index and canopy chlorophyll density of winter wheat from spectral reflectance data. Remote Sensing of Environment, 81(1), pp.45-57.

Brown, L., Chen, J.M., Leblanc, S.G. and Cihlar, J., 2000. A shortwave infrared modification to the simple ratio for LAI retrieval in boreal forests: An image and model analysis. Remote Sensing of Environment, 71(1), pp.16-25.

Bunting, P. and Lucas, R., 2006. The delineation of tree crowns in Australian mixed species forests using hyperspectral Compact Airborne Spectrographic Imager (CASI) data. Remote Sensing of Environment, 101(2), pp.230-248.

Cammarano, D., Fitzgerald, G.J., Casa, R. and Basso, B., 2014. Assessing the robustness of vegetation indices to estimate wheat N in Mediterranean environments. Remote Sensing, 6(4), pp.2827-2844.

Campbell, J.B. 1996. Introduction to Remote Sensing. Taylor & Francis, London.

Carlson, T.N. and Ripley, D.A., 1997. On the relation between NDVI, fractional vegetation cover, and leaf area index. Remote Sensing of Environment, 62(3), pp.241-252.

Carrijo, D.R., Lundy, M.E. and Linquist, B.A., 2017. Rice yields and water use under alternate wetting and drying irrigation: A meta-analysis. Field Crops Research, 203, pp.173-180.

Casanova, D., Epema, G.F. and Goudriaan, J., 1998. Monitoring rice reflectance at field level for estimating biomass and LAI. Field Crops Research, 55(1-2), pp.83-92.

Cetin, H., Pafford, J.T. and Mueller, T.G., 2005. Precision agriculture using hyperspectral remote sensing and GIS. In Recent Advances in Space Technologies Proceedings, IEEE, pp. 70-77.

Chakraborty, M., Manjunath, K.R., Panigrahy, S., Kundu, N. and Parihar, J.S., 2005. Rice crop parameter retrieval using multi-temporal, multi-incidence angle Radarsat SAR data. ISPRS Journal of Photogrammetry and Remote Sensing, 59(5), pp.310-322.

Chappelle, E.W., Kim, M.S. and McMurtrey, J.E., 1992. Ratio analysis of reflectance spectra (RARS): an algorithm for the remote estimation of the concentrations of chlorophyll a, chlorophyll b, and carotenoids in soybean leaves. Remote Sensing of Environment, 39(3), pp.239-247.

Chavarria, G. and dos Santos, H.P., 2012. Plant water relations: Absorption, transport and control mechanisms. In Advances in Selected Plant Physiology Aspects. InTech, pp.105-132.

Chen, D., Huang, J. and Jackson, T.J., 2005. Vegetation water content estimation for corn and soybeans using spectral indices derived from MODIS near-and short-wave infrared bands. Remote Sensing of Environment, 98(2), pp.225-236.

Chen, J.M., 1996. Evaluation of vegetation indices and a modified simple ratio for boreal applications. Canadian Journal of Remote Sensing, 22(3), pp.229-242.

Chen, L.S., and Wang. K., 2014. Diagnosing of rice nitrogen stress based on static scanning technology and image information extraction. Journal of soil science and plant nutrition, 14(2), pp.1–9.

Chen, P., Haboudane, D., Tremblay, N., Wang, J., Vigneault, P. and Li, B., 2010. New spectral indicator assessing the efficiency of crop nitrogen treatment in corn and wheat. Remote Sensing of Environment, 114(9), pp.1987-1997.

Chen, X., Cui, Z., Fan, M., Vitousek, P., Zhao, M., Ma, W., Wang, Z., Zhang, W., Yan, X., Yang, J. and Deng, X., 2014. Producing more grain with lower environmental costs. Nature, 514(7523), pp.486-489.

Cheng, T., Riano, D. and Ustin, S.L., 2014. Detecting diurnal and seasonal variation in canopy water content of nut tree orchards from airborne imaging spectroscopy data using continuous wavelet analysis. Remote Sensing of Environment, 143, pp.39-53.

Cheng, Y.B., Zarco-Tejada, P.J., Riaño, D., Rueda, C.A. and Ustin, S.L., 2006. Estimating vegetation water content with hyperspectral data for different canopy scenarios: Relationships between AVIRIS and MODIS indexes. Remote Sensing of Environment, 105(4), pp.354-366.

Chhabra, A., Manjunath, K.R. and Panigrahy, S., 2010. Non-point source pollution in Indian agriculture: Estimation of nitrogen losses from rice crop using remote sensing and GIS. International Journal of Applied Earth Observation and Geoinformation, 12(3), pp.190-200.

Cho, M.A. and Skidmore, A.K., 2006. A new technique for extracting the red edge position from hyperspectral data: The linear extrapolation method. Remote Sensing of Environment, 101(2), pp.181-193.

Cho, M.A., Skidmore, A., Corsi, F., Van Wieren, S.E. and Sobhan, I., 2007. Estimation of green grass/herb biomass from airborne hyperspectral imagery using spectral indices and partial least squares regression. International Journal of Applied Earth Observation and Geoinformation, 9(4), pp.414-424.

Cho, M.A., Sobhan, I., Skidmore, A.K. and De Leeuw, J., 2008. Discriminating species using hyperspectral indices at leaf and canopy scales. The International Archives of the Photogrammetry, Remote Sensing and Spatial Information Sciences, 37(B7), pp.369-376.

Choudhury, B., Khan, M.L. and Dayanandan, S., 2013. Genetic structure and diversity of indigenous rice (Oryza sativa) varieties in the Eastern Himalayan region of Northeast India. SpringerPlus, 2(1), pp.1-10.

Choudhury, I. and Chakraborty, M., 2006. SAR signature investigation of rice crop using RADARSAT data. International Journal of Remote Sensing, 27(3), pp.519-534.

Chung, S.O., Sudduth, K.A. and Drummond, S.T., 2002. Determining yield monitoring system delay time with geostatistical and data segmentation approaches. Transactions of the American Society of Agricultural Engineers, 45(4), pp.915-926.

Claverie, M., Demarez, V., Duchemin, B., Hagolle, O., Ducrot, D., Marais-Sicre, C., Dejoux, J.F., Huc, M., Keravec, P., Beziat, P. and Fieuzal, R., 2012. Maize and sunflower biomass estimation in southwest France using high spatial and temporal resolution remote sensing data. Remote Sensing of Environment, 124, pp.844-857.

Clevers, J.G. and Kooistra, L., 2012. Using hyperspectral remote sensing data for retrieving canopy chlorophyll and nitrogen content. Journal of Selected Topics in Applied Earth Observations and Remote Sensing, IEEE, 5(2), pp.574-583.

Clevers, J.G., Kooistra, L. and Schaepman, M.E., 2010. Estimating canopy water content using hyperspectral remote sensing data. International Journal of Applied Earth Observation and Geoinformation, 12(2), pp.119-125.

Clevers, J.G.P.W., 1989. Application of a weighted infrared-red vegetation index for estimating leaf area index by correcting for soil moisture. Remote Sensing of Environment, 29(1), pp.25-37.

Cochrane, M.A., 2000. Using vegetation reflectance variability for species level classification of hyperspectral data. International Journal of Remote Sensing, 21(10), pp.2075-2087.

Collins, W., 1978. Remote sensing of crop type and maturity. Engineering, 44(1), pp.43-55.

Colombo, R., Bellingeri, D., Fasolini, D. and Marino, C.M., 2003. Retrieval of leaf area index in different vegetation types using high resolution satellite data. Remote Sensing of Environment, 86(1), pp.120-131.

Croft, H., Chen, J.M., Zhang, Y. and Simic, A., 2013. Modelling leaf chlorophyll content in broadleaf and needle leaf canopies from ground, CASI, Landsat TM 5 and MERIS reflectance data. Remote Sensing of Environment, 133, pp.128-140.

Crutzen, P.J., Aselmann, I. and Seiler, W., 1986. Methane production by domestic animals, wild ruminants, other herbivorous fauna, and humans. Tellus B: Chemical and Physical Meteorology, 38(3-4), pp.271-284.

Curran, P.J. 1985. Principles of Remote Sensing. Longman Group Limited, London.

Curran, P.J., Dungan, J.L. and Gholz, H.L., 1990. Exploring the relationship between reflectance red edge and chlorophyll content in slash pine. Tree Physiology, 7(1-2-3-4), pp.33-48.

Dadhwal, V.K. 1986. Remote sensing studies for wheat inventory assessment. Proceedings of the Fifth Asian Agriculture Symposium, Kumomoto, Japan, pp.1-16.

Dadhwal, V.K. 1999. Remote sensing applications for agriculture. Retrospective and perspective. In Proceedings National Symposium on Remote Sensing Applications for Natural Resources: Retrospective and Perspective, Indian Society of Remote Sensing, Dehradun, pp.11-22.

Dadhwal, V.K. and Ray, S.S., 2000. Crop Assessment using remote sensing-Part-II: Crop condition and yield assessment. Indian Journal of Agricultural Economics, 55(2), p.55-67.

Darvishzadeh, R., Skidmore, A., Schlerf, M., Atzberger, C., Corsi, F. and Cho, M., 2008. LAI and chlorophyll estimation for a heterogeneous grassland using hyperspectral measurements. ISPRS Journal of Photogrammetry and Remote Sensing, 63(4), pp.409-426.

Das, D.K., Maiti, D. and Pathak, H., 2009. Site-specific nutrient management in rice in Eastern India using a modeling approach. Nutrient Cycling in Agroecosystems, 83(1), pp.85-94.

Das, P.K. and Seshasai, M.V.R., 2015. Multispectral sensor spectral resolution simulations for generation of hyperspectral vegetation indices from Hyperion data. Geocarto International, 30(6), pp.686-700.

Das, P.K. and Seshasai, M.V.R., 2015. Multispectral sensor spectral resolution simulations for generation of hyperspectral vegetation indices from Hyperion data. Geocarto International, 30(6), pp.686-700.

Dash, J., Curran, P.J., 2004. The MERIS terrestrial chlorophyll index. International Journal of Remote Sensing, 25, pp.5403–5413.

Datt, B., 1999. Remote sensing of water content in Eucalyptus leaves. Australian Journal of Botany, 47(6), pp.909-923.

Datt, B., McVicar, T.R., Van Niel, T.G., Jupp, D.L. and Pearlman, J.S., 2003. Preprocessing EO-1 Hyperion hyperspectral data to support the application of agricultural indexes. Transactions on Geoscience and Remote Sensing, IEEE, 41(6), pp.1246-1259.

Daughtry, C.S.T., Hunt, E.R. and McMurtrey, J.E., 2004. Assessing crop residue cover using shortwave infrared reflectance. Remote Sensing of Environment, 90(1), pp.126-134.

Daughtry, C.S.T., Walthall, C.L., Kim, M.S., De Colstoun, E.B. and McMurtrey, J.E., 2000. Estimating corn leaf chlorophyll concentration from leaf and canopy reflectance. Remote Sensing of Environment, 74(2), pp.229-239.

de Castro, A.I., Jurado-Expósito, M., Penja-Barragán, J.M. and Lopez-Granados, F., 2012. Airborne multi-spectral imagery for mapping cruciferous weeds in cereal and legume crops. Precision Agriculture, 13(3), pp.302-321.

de Jong, S.M., Addink, E.A. and Doelman, J.C., 2014. Detecting leaf-water content in Mediterranean trees using high-resolution spectrometry. International Journal of Applied Earth Observation and Geoinformation, 27, pp.128-136.

Dobermann, A. and White, P.F., 1999. Strategies for nutrient management in irrigated and rainfed lowland rice systems. In Resource Management in Rice Systems: Nutrients, Springer Netherlands, pp.1-26.

Dobermann, A., 2000. Rice: Nutrient disorders & nutrient management (Vol. 1). International Rice Research Institute.

Doraiswamy, P.C., Hatfield, J.L., Jackson, T.J., Akhmedov, B., Prueger, J. and Stern, A., 2004. Crop condition and yield simulations using Landsat and MODIS. Remote Sensing of Environment, 92(4), pp.548-559.

Dwyer, L.M., Tollenaar, M. and Houwing, L., 1991. A nondestructive method to monitor leaf greenness in corn. Canadian Journal of Plant Science, 71(2), pp.505-509.

Eitel, J.U.H., Long, D.S., Gessler, P.E. and Smith, A.M.S., 2007. Using in-situ measurements to evaluate the new RapidEye™ satellite series for prediction of wheat nitrogen status. International Journal of Remote Sensing, 28(18), pp.4183-4190.

Eklundh, L., Harrie, L. and Kuusk, A., 2001. Investigating relationships between Landsat ETM+ sensor data and leaf area index in a boreal conifer forest. Remote Sensing of Environment, 78(3), pp.239-251.

El Hajj, M., Begue, A., Guillaume, S. and Martine, J.F., 2009. Integrating SPOT-5 time series, crop growth modeling and expert knowledge for monitoring agricultural practices—The case of sugarcane harvest on Reunion Island. Remote Sensing of Environment, 113(10), pp.2052-2061.

Elvidge, C.D. and Chen, Z., 1995. Comparison of broad-band and narrow-band red and near-infrared vegetation indices. Remote Sensing of Environment, 54(1), pp.38-48.

Fang, H., Liang, S. and Kuusk, A., 2003. Retrieving leaf area index using a genetic algorithm with a canopy radiative transfer model. Remote Sensing of Environment, 85(3), pp.257-270.

Fang, H., Wu, B., Liu, H. and Huang, X., 1998. Using NOAA AVHRR and Landsat TM to estimate rice area year-by-year. International Journal of Remote Sensing, 19(3), pp.521-525.

Feder, G., Just, R.E. and Zilberman, D., 1985. Adoption of agricultural innovations in developing countries: A survey. Economic development and cultural change, 33(2), pp.255-298.

Feng, W., Yao, X., Zhu, Y., Tian, Y.C. and Cao, W.X., 2008. Monitoring leaf nitrogen status with hyperspectral reflectance in wheat. European Journal of Agronomy, 28(3), pp.394-404.

Fensholt, R. and Sandholt, I., 2003. Derivation of a shortwave infrared water stress index from MODIS near-and shortwave infrared data in a semiarid environment. Remote Sensing of Environment, 87(1), pp.111-121.

Feret, J.B., François, C., Gitelson, A., Asner, G.P., Barry, K.M., Panigada, C., Richardson, A.D. and Jacquemoud, S., 2011. Optimizing spectral indices and chemometric analysis of leaf chemical properties using radiative transfer modeling. Remote Sensing of Environment, 115(10), pp.2742-2750.

Filella, I., Serrano, L., Serra, J. and Penuelas, J., 1995. Evaluating wheat nitrogen status with canopy reflectance indices and discriminant analysis. Crop Science, 35(5), pp.1400-1405.

Fleming, K.L., Westfall, D.G., Wiens, D.W. and Brodahl, M.C., 2000. Evaluating farmer defined management zone maps for variable rate fertilizer application. Precision Agriculture, 2(2), pp.201-215.

Fontanelli, G., Paloscia, S., Pampaloni, P., Pettinato, S., Santi, E., Montomoli, F., Brogioni, M. and Macelloni, G., 2013. HydroCosmo: The monitoring of hydrological parameters on agricultural areas by using Cosmo-SkyMed images. European Journal of Remote Sensing, 46(1), pp.875-889.

Franz, E., Gebhardt, M.R. and Unklesbay, K.B., 1991. The use of local spectral properties of leaves as an aid for identifying weed seedlings in digital images. Transactions of the American Society of Agricultural Engineers, 34(2), pp.682-0687.

Frazier, A.E., Wang, L. and Chen, J., 2014. Two new hyperspectral indices for comparing vegetation chlorophyll content. Geo-spatial Information Science, 17(1), pp.17-25.

Gallo, K.P., Daughtry, C.S.T. and Bauer, M.E., 1985. Spectral estimation of absorbed photosynthetically active radiation in corn canopies. Remote Sensing of Environment, 17(3), pp.221-232.

Galloza, M.S. and Crawford, M., 2011. Exploiting multisensor spectral data to improve crop residue cover estimates for management of agricultural water quality. Geoscience and Remote Sensing Symposium IGARSS, IEEE, pp.3668-3671.

Galvao, L.S., Roberts, D.A., Formaggio, A.R., Numata, I. and Breunig, F.M., 2009. View angle effects on the discrimination of soybean varieties and on the relationships between vegetation indices and yield using off-nadir Hyperion data. Remote Sensing of Environment, 113(4), pp.846-856.

Gamon, J.A., Penuelas, J. and Field, C.B., 1992. A narrow-waveband spectral index that tracks diurnal changes in photosynthetic efficiency. Remote Sensing of Environment, 41(1), pp.35-44.

Gao, B.C., 1996. NDWI—A normalized difference water index for remote sensing of vegetation liquid water from space. Remote Sensing of Environment, 58(3), pp.257-266.

Gao, X., Huete, A.R., Ni, W. and Miura, T., 2000. Optical–biophysical relationships of vegetation spectra without background contamination. Remote Sensing of Environment, 74(3), pp.609-620.

Gianelle, D.A.M.I.A.N.O. and Guastella, F., 2007. Nadir and off-nadir hyperspectral field data: Strengths and limitations in estimating grassland biophysical characteristics. International Journal of Remote Sensing, 28(7), pp.1547-1560.

Gitelson, A.A., 2011. Nondestructive estimation of foliar pigment (chlorophylls, carotenoids, and anthocyanins) contents: Evaluating a semianalytical three-band model. Hyperspectral Remote Sensing of Vegetation, pp.141-166.

Gitelson, A.A., Gritz, Y. and Merzlyak, M.N., 2003. Relationships between leaf chlorophyll content and spectral reflectance and algorithms for non-destructive chlorophyll assessment in higher plant leaves. Journal of Plant Physiology, 160(3), pp.271-282.

Gitelson, A.A., Vina, A., Ciganda, V., Rundquist, D.C. and Arkebauer, T.J., 2005. Remote estimation of canopy chlorophyll content in crops. Geophysical Research Letters, 32(8), pp.1-4.

Godwin, R.J. and Miller, P.C.H., 2003. A review of the technologies for mapping within-field variability. Biosystems engineering, 84(4), pp.393-407.

Goel, P.K., Prasher, S.O., Landry, J.A., Patel, R.M., Viau, A.A. and Miller, J.R., 2003. Estimation of crop biophysical parameters through airborne and field hyperspectral remote sensing. Transactions of the American Society of Agricultural Engineers, 46(4), pp.1235-1246.

Guo, C. and Guo, X., 2016. Estimating leaf chlorophyll and nitrogen content of wetland emergent plants using hyperspectral data in the visible domain. Spectroscopy Letters, 49(3), pp.180-187.

Gutierrez, M., Reynolds, M.P. and Klatt, A.R., 2010. Association of water spectral indices with plant and soil water relations in contrasting wheat genotypes. Journal of Experimental Botany, 61(12), pp.3291-3303.

Haboudane, D., Miller, J.R., Tremblay, N., Zarco-Tejada, P.J. and Dextraze, L., 2002. Integrated narrow-band vegetation indices for prediction of crop chlorophyll content for application to precision agriculture. Remote Sensing of Environment, 81(2), pp.416-426.

Haboudane, D., Tremblay, N., Miller, J.R. and Vigneault, P., 2008. Remote estimation of crop chlorophyll content using spectral indices derived from hyperspectral data. IEEE Transactions on Geoscience and Remote Sensing, 46(2), pp.423-437.

Han, J., Pei, J. and Kamber, M., 2011. Data mining: concepts and techniques. Elsevier.

Hansen, P.M. and Schjoerring, J.K., 2003. Reflectance measurement of canopy biomass and nitrogen status in wheat crops using normalized difference vegetation indices and partial least squares regression. Remote Sensing of Environment, 86(4), pp.542-553.

Hardisky, M. A., V. Klemas, and R. M. Smart., 1983. The influence of soil salinity, growth form, and leaf moisture on the spectral radiance of Spartina alterniflora canopies. Photogrammetric Engineering and Remote Sensing, 49, pp.77 – 83.

Hatfield, J.L. and Prueger, J.H., 2010. Value of using different vegetative indices to quantify agricultural crop characteristics at different growth stages under varying management practices. Remote Sensing, 2(2), pp.562-578.

Hauk, S., Skibbe, K., Röhle, H., Schröder, J., Wittkopf, S. and Knoke, T., 2015. Nondestructive estimation of biomass yield for short-rotation woody crops is reliable and shows high yields for commercial stands in bavaria. BioEnergy Research, 8(3), pp.1401-1413.

Heiskanen, J., Rautiainen, M., Stenberg, P., Mottus, M. and Vesanto, V.H., 2013. Sensitivity of narrowband vegetation indices to boreal forest LAI, reflectance seasonality and species composition. ISPRS journal of Photogrammetry and Remote Sensing, 78, pp.1-14.

Hill, M.J., Román, M.O. and Schaaf, C.B., 2012. Dynamics of vegetation indices in tropical and subtropical savannas defined by ecoregions and Moderate Resolution Imaging Spectroradiometer (MODIS) land cover. Geocarto International, 27(2), pp.153-191.

Horler, D.N.H., Dockray, M. and Barber, J., 1983. The red edge of plant leaf reflectance. International Journal of Remote Sensing, 4(2), pp.273-288.

Houborg, R., Anderson, M. and Daughtry, C., 2009. Utility of an image-based canopy reflectance modeling tool for remote estimation of LAI and leaf chlorophyll content at the field scale. Remote Sensing of Environment, 113(1), pp.259-274.

Houborg, R., Soegaard, H. and Boegh, E., 2007. Combining vegetation index and model inversion methods for the extraction of key vegetation biophysical parameters using Terra and Aqua MODIS reflectance data. Remote Sensing of Environment, 106(1), pp.39-58.

Houborg, R., Soegaard, H. and Boegh, E., 2007. Combining vegetation index and model inversion methods for the extraction of key vegetation biophysical parameters using Terra and Aqua MODIS reflectance data. Remote Sensing of Environment, 106(1), pp.39-58.

Huang, W., Wang, Z., Huang, L., Lamb, D.W., Ma, Z., Zhang, J., Wang, J. and Zhao, C., 2011. Estimation of vertical distribution of chlorophyll concentration by bi-directional canopy reflectance spectra in winter wheat. Precision agriculture, 12(2), pp.165-178.

Huete, A., Didan, K., Miura, T., Rodriguez, E.P., Gao, X. and Ferreira, L.G., 2002. Overview of the radiometric and biophysical performance of the MODIS vegetation indices. Remote Sensing of Environment, 83(1), pp.195-213.

Huete, A.R., Liu, H.Q., Batchily, K. and Van Leeuwen, W.J.D.A., 1997. A comparison of vegetation indices over a global set of TM images for EOS-MODIS. Remote Sensing of Environment, 59(3), pp.440-451.

Hunt, E.R. and Rock, B.N., 1989. Detection of changes in leaf water content using near-and middle-infrared reflectances. Remote Sensing of Environment, 30(1), pp.43-54.

Hunt, E.R. Jr., 1991. Airborne remote sensing of canopy water thickness scaled from leaf spectrometer data. International Journal of Remote Sensing, 12(3), pp.643-649.

Hunt, E.R., Doraiswamy, P.C., McMurtrey, J.E., Daughtry, C.S., Perry, E.M. and Akhmedov, B., 2013. A visible band index for remote sensing leaf chlorophyll content at the canopy scale. International Journal of Applied Earth Observation and Geoinformation, 21, pp.103-112.

Hunt, E.R., Rock, B.N. and Nobel, P.S., 1987. Measurement of leaf relative water content by infrared reflectance. Remote Sensing of Environment, 22(3), pp.429-435.

Inoue, Y., Penuelas, J., Miyata, A. and Mano, M., 2008. Normalized difference spectral indices for estimating photosynthetic efficiency and capacity at a canopy scale derived from hyperspectral and CO 2 flux measurements in rice. Remote Sensing of Environment, 112(1), pp.156-172.

Inoue, Y., Sakaiya, E., Zhu, Y. and Takahashi, W., 2012. Diagnostic mapping of canopy nitrogen content in rice based on hyperspectral measurements. Remote Sensing of Environment, 126, pp.210-221.

Jain, N., Ray, S.S., Singh, J.P. and Panigrahy, S., 2007. Use of hyperspectral data to assess the effects of different nitrogen applications on a potato crop. Precision Agriculture, 8(4-5), pp.225-239.

Janssen, B.H., 1998. Efficient use of nutrients: an art of balancing. Field Crops Research, 56(1-2), pp.197-201.

Janssen, B.H., Guiking, F.C.T. Van der Eijk, D., Smaling, E.M.A., Wolf, J. and Van Reuler, H., 1990. A system for quantitative evaluation of the fertility of tropical soils (QUEFTS). Geoderma, 46, pp.299-318.

Jaynes, D.B., Colvin, T.S., Karlen, D.L., Cambardella, C.A. and Meek, D.W., 2001. Nitrate loss in subsurface drainage as affected by nitrogen fertilizer rate. Journal of Environmental Quality, 30(4), pp.1305-1314.

Jiang, Z., Huete, A.R., Didan, K. and Miura, T., 2008. Development of a two-band enhanced vegetation index without a blue band. Remote Sensing of Environment, 112(10), pp.3833-3845.

Jiao, Q., Zhang, B., Liu, J. and Liu, L., 2014. A novel two-step method for winter wheat-leaf chlorophyll content estimation using a hyperspectral vegetation index. International Journal of Remote Sensing, 35(21), pp.7363-7375.

Jiao, X., McNairn, H., Shang, J., Pattey, E., Liu, J., & Champagne, C., 2009. The sensitivity of RADARSAT-2 polarimetric SAR data to corn and soybean leaf area index. Canadian Journal of Remote Sensing, 37(1), pp.69–81.

Jin, X., Xu, X., Song, X., Li, Z., Wang, J. and Guo, W., 2013. Estimation of leaf water content in winter wheat using grey relational analysis–Partial least squares modeling with hyperspectral data. Agronomy Journal, 105(5), pp.1385-1392.

Jorgensen, R.N., Hansen, P.M. and Bro, R., 2006. Exploratory study of winter wheat reflectance during vegetative growth using three-mode component analysis. International Journal of Remote Sensing, 27(05), pp.919-937.

Joseph, G., 2005. Fundamentals of remote sensing. Universities Press.

Kar, S., Rathore, V.S., Sharma, R. and Swain, S.K., 2016. Classification of river water pollution using Hyperion data. Journal of Hydrology, 537, pp.221-233.

Karuppaiah, V. and Sujayanad, G.K., 2012. Impact of climate change on population dynamics of insect pests. World Journal of Agricultural Sciences, 8 (3), pp. 240-246.

Kashyap, P.S. and Panda, R.K., 2003. Effect of irrigation scheduling on potato crop parameters under water stressed conditions. Agricultural Water Management, 59(1), pp.49-66.

Kergoat, L., Lafont, S., Arneth, A., Le Dantec, V., Saugier, B., 2008. Nitrogen controls plant canopy light-use efficiency in temperate and boreal ecosystems. Journal of Geophysical Research: Biogeosciences, 113(G4), pp.1-19.

Khanna, S., Palacios-Orueta, A., Whiting, M.L., Ustin, S.L., Riano, D. and Litago, J., 2007. Development of angle indexes for soil moisture estimation, dry matter detection and land-cover discrimination. Remote Sensing of Environment, 109(2), pp.154-165.

Kim, D.M., Zhang, H., Zhou, H., Du, T., Wu, Q., Mockler, T.C. and Berezin, M.Y., 2015. Highly sensitive image-derived indices of water-stressed plants using hyperspectral imaging in SWIR and histogram analysis. Scientific Reports, 5, pp.1-11.

Kiritani, K., 2007. The impact of global warming and land- use change on the pest status of rice and fruit bugs (Heteroptera) in Japan. Global Change Biology, 13(8), pp.1586-1595.

Kneubuehler, M., Schaepman, M.E. and Kellenberger, T.W., 1998, July. Comparison of different approaches of selecting endmembers to classify agricultural land by means of hyperspectral data (DAIS7915). Geoscience and Remote Sensing Symposium Proceedings, IGARSS, IEEE, 2, pp. 888-890.

Koetz, B., Baret, F., Poilvé, H. and Hill, J., 2005. Use of coupled canopy structure dynamic and radiative transfer models to estimate biophysical canopy characteristics. Remote Sensing of Environment, 95(1), pp.115-124.

Kokaly, R.F., 2001. Investigating a physical basis for spectroscopic estimates of leaf nitrogen concentration. Remote Sensing of Environment, 75(2), pp.153-161.

Kong, W., Zhang, C., Liu, F., Nie, P. and He, Y., 2013. Rice seed cultivar identification using near-infrared hyperspectral imaging and multivariate data analysis. Sensors, 13(7), pp.8916-8927.

Kumar, A., Bernier, J., Verulkar, S., Lafitte, H.R. and Atlin, G.N., 2008. Breeding for drought tolerance: direct selection for yield, response to selection and use of drought-tolerant donors in upland and lowland-adapted populations. Field Crops Research, 107(3), pp.221-231.

Kumar, A., Manjunath, K.R., Bala, R., Sud, R.K., Singh, R.D. and Panigrahy, S., 2013. Field hyperspectral data analysis for discriminating spectral behavior of tea plantations under various management practices. International Journal of Applied Earth Observation and Geoinformation, 23, pp.352-359.

Kumar, R., Venuprasad, R. and Atlin, G.N., 2007. Genetic analysis of rainfed lowland rice drought tolerance under naturally-occurring stress in eastern India: heritability and QTL effects. Field Crops Research, 103(1), pp.42-52.

Lafitte, H.R., Yongsheng, G., Yan, S. and Li, Z.K., 2007. Whole plant responses, key processes, and adaptation to drought stress: the case of rice. Journal of Experimental Botany, 58(2), pp.169-175.

Law, B.E., Falge, E., Gu, L.V., Baldocchi, D.D., Bakwin, P., Berbigier, P., Davis, K., Dolman, A.J., Falk, M., Fuentes, J.D. and Goldstein, A., 2002. Environmental controls over carbon dioxide and water vapor exchange of terrestrial vegetation. Agricultural and Forest Meteorology, 113(1), pp.97-120.

Le Maire, G., Francois, C. and Dufrene, E., 2004. Towards universal broad leaf chlorophyll indices using PROSPECT simulated database and hyperspectral reflectance measurements. Remote Sensing of Environment, 89(1), pp.1-28.

Ledgard, S.F., 2001. Nitrogen cycling in low input legume-based agriculture, with emphasis on legume/grass pastures. Plant and Soil, 228(1), pp.43-59.

Lee, K.S., Cohen, W.B., Kennedy, R.E., Maiersperger, T.K. and Gower, S.T., 2004. Hyperspectral versus multispectral data for estimating leaf area index in four different biomes. Remote Sensing of Environment, 91(3), pp.508-520.

Lee, Y.J., Chang, K.W., Shen, Y., Huang, T.M. and Tsay, H.L., 2007. A handy imaging system for precision agriculture studies. International Journal of Remote Sensing, 28(21), pp.4867-4876.

Lee, Y.J., Yang, C.M., Chang, K.W. and Shen, Y., 2008. A simple spectral index using reflectance of 735 nm to assess nitrogen status of rice canopy. Agronomy Journal, 100(1), pp.205-212.

Li, H., Zheng, L., Lei, Y., Li, C., Liu, Z. and Zhang, S., 2008. Estimation of water consumption and crop water productivity of winter wheat in North China Plain using remote sensing technology. Agricultural Water Management, 95(11), pp.1271-1278.

Li, T., Feng, Y. and Li, X., 2009. Predicting crop growth under different cropping and fertilizing management practices. Agricultural and Forest Meteorology, 149(6-7), pp.985-998.

Liang, K., Zhong, X., Huang, N., Lampayan, R.M., Liu, Y., Pan, J., Peng, B., Hu, X. and Fu, Y., 2017. Nitrogen losses and greenhouse gas emissions under different N and water management in a subtropical double-season rice cropping system. Science of The Total Environment, 609, pp.46-57.

Liang, L., Qin, Z., Zhao, S., Di, L., Zhang, C., Deng, M., Lin, H., Zhang, L., Wang, L. and Liu, Z., 2016. Estimating crop chlorophyll content with hyperspectral vegetation indices and the hybrid inversion method. International Journal of Remote Sensing, 37(13), pp.2923-2949.

Ling, B., Goodin, D.G., Mohler, R.L., Laws, A.N. and Joern, A., 2014. Estimating canopy nitrogen content in a heterogeneous grassland with varying fire and grazing treatments: Konza Prairie, Kansas, USA. Remote Sensing, 6(5), pp.4430-4453.

Liu, S., Peng, Y., Du, W., Le, Y. and Li, L., 2015. Remote estimation of leaf and canopy water content in winter wheat with different vertical distribution of water-related properties. Remote Sensing, 7(4), pp.4626-4650.

Liu, X. and Bo, Y., 2015. Object-based crop species classification based on the combination of airborne hyperspectral images and LiDAR data. Remote Sensing, 7(1), pp.922-950.

Liu, X., Wang, H., Zhou, J., Hu, F., Zhu, D., Chen, Z. and Liu, Y., 2016. Effect of N fertilization pattern on rice yield, N use efficiency and fertilizer–N fate in the Yangtze river basin, China. PloS One, 11(11), pp.1-20.

Liu, X., Zhang, Y., Han, W., Tang, A., Shen, J., Cui, Z., Vitousek, P., Erisman, J.W., Goulding, K., Christie, P. and Fangmeier, A., 2013. Enhanced nitrogen deposition over China. Nature, 494(7438), pp.459-462.

Liu, Z.Y., Wu, H.F. and Huang, J.F., 2010. Application of neural networks to discriminate fungal infection levels in rice panicles using hyperspectral reflectance and principal components analysis. Computers and Electronics in Agriculture, 72(2), pp.99-106.

Lobell, D.B., Ortiz-Monasterio, J.I., Asner, G.P., Naylor, R.L. and Falcon, W.P., 2005. Combining field surveys, remote sensing, and regression trees to understand yield variations in an irrigated wheat landscape. Agronomy Journal, 97(1), pp.241-249.

Long, S.P., Farage, P.K. and Garcia, R.L., 1996. Measurement of leaf and canopy photosynthetic CO_2 exchange in the field. Journal of Experimental Botany, 47(11), pp.1629-1642.

Maccioni, A., Agati, G., Mazzinghi, P., 2001. New vegetation indices for remote measurement of chlorophylls based on leaf directional reflectance spectra. Journal of Photochemistry and Photobiology 61, pp.52–61.

Magney, T.S., Eitel, J.U., Huggins, D.R. and Vierling, L.A., 2016. Proximal NDVI derived phenology improves in-season predictions of wheat quantity and quality. Agricultural and Forest Meteorology, 217, pp.46-60.

Magri, A., Van Es, H.M., Glos, M.A. and Cox, W.J., 2005. Soil test, aerial image and yield data as inputs for site-specific fertility and hybrid management under maize. Precision Agriculture, 6(1), pp.87-110.

Main, R., Cho, M.A., Mathieu, R., O'Kennedy, M.M., Ramoelo, A. and Koch, S., 2011. An investigation into robust spectral indices for leaf chlorophyll estimation. ISPRS Journal of Photogrammetry and Remote Sensing, 66(6), pp.751-761.

Major, D.J., Baret, F. and Guyot, G., 1990. A ratio vegetation index adjusted for soil brightness. International Journal of Remote Sensing, 11(5), pp.727-740.

Manjunath, K.R., Panigrahy, S., Kumari, K., Adhya, T.K., Parihar, J.S., 2006. Spatiotemporal modelling of methane flux from the rice fields of India using remote sensing and GIS. International Journal of Remote Sensing, 27, pp.4701–4707.

Mariotto, I., Thenkabail, P.S., Huete, A., Slonecker, E.T. and Platonov, A., 2013. Hyperspectral versus multispectral crop-productivity modeling and type discrimination for the HyspIRI mission. Remote Sensing of Environment, 139, pp.291-305.

Marshall, M. and Thenkabail, P., 2015. Advantage of hyperspectral EO-1 Hyperion over multispectral IKONOS, GeoEye-1, WorldView-2, Landsat ETM+, and MODIS vegetation indices in crop biomass estimation. ISPRS Journal of Photogrammetry and Remote Sensing, 108, pp.205-218.

McCloy, K.R., Smith, F.R. and Robinson, M.R., 1987. Monitoring rice areas using Landsat MSS data. International Journal of remote sensing, 8(5), pp.741-749.

Miao, Y., Mulla, D.J., Randall, G.W., Vetsch, J.A. and Vintila, R., 2009. Combining chlorophyll meter readings and high spatial resolution remote sensing images for in-season site-specific nitrogen management of corn. Precision Agriculture, 10(1), pp.45-62.

Milton, E.J. and Rollin, E.M., 2006. Estimating the irradiance spectrum from measurements in a limited number of spectral bands. Remote Sensing of Environment, 100(3), pp.348-355.

Moran, M.S., Hymer, D.C., Qi, J. and Kerr, Y., 2002. Comparison of ERS-2 SAR and Landsat TM imagery for monitoring agricultural crop and soil conditions. Remote Sensing of Environment, 79(2), pp.243-252.

Muchovej, R.M. and Newman, P.R., 2004. Nitrogen fertilization of sugarcane on a sandy soil: I. Yield and leaf nutrient composition. Journal American Society Sugar Cane Technologists, 24, pp.210-224.

Mulla, D.J., 2013. Twenty five years of remote sensing in precision agriculture: Key advances and remaining knowledge gaps. Biosystems engineering, 114(4), pp.358-371.

Mutanga, O. and Skidmore, A.K., 2004. Narrow band vegetation indices overcome the saturation problem in biomass estimation. International Journal of Remote Sensing, 25(19), pp.3999-4014.

Muthayya, S., Sugimoto, J.D., Montgomery, S. and Maberly, G.F., 2014. An overview of global rice production, supply, trade, and consumption. Annals of the new york Academy of Sciences, 1324(1), pp.7-14.

Nagendra, H., 2001. Using remote sensing to assess biodiversity. International Journal of Remote Sensing, 22(12), pp.2377-2400.

Navarro-Cerrillo, R.M., Trujillo, J., de la Orden, M.S. and Hernández-Clemente, R., 2014. Hyperspectral and multispectral satellite sensors for mapping chlorophyll content in a Mediterranean Pinus sylvestris L. plantation. International Journal of Applied Earth Observation and Geoinformation, 26, pp.88-96.

Neue, H.U., 1993. Methane emission from rice fields. Bioscience, 43(7), pp.466-474.

Nguyen, H.T. and Lee, B.W., 2006. Assessment of rice leaf growth and nitrogen status by hyperspectral canopy reflectance and partial least square regression. European Journal of Agronomy, 24(4), pp.349-356.

Nidamanuri, R.R. and Zbell, B., 2011. Transferring spectral libraries of canopy reflectance for crop classification using hyperspectral remote sensing data. Biosystems Engineering, 110(3), pp.231-246.

Noori, O. and Panda, S.S., 2016. Site-specific management of common olive: Remote sensing, geospatial, and advanced image processing applications. Computers and Electronics in Agriculture, 127, pp.680-689.

Nuarsa, I.W., Nishio, F. and Hongo, C., 2011. Relationship between rice spectral and rice yield using MODIS data. Journal of Agricultural Science, 3(2), pp.80-88.

Okamoto, K. and Fukuhara, M., 1996. Estimation of paddy field area using the area ratio of categories in each mixel of Landsat TM. International Journal of Remote Sensing, 17(9), pp.1735-1749.

Onder, S., Caliskan, M.E., Onder, D. and Caliskan, S., 2005. Different irrigation methods and water stress effects on potato yield and yield components. Agricultural Water Management, 73(1), pp.73-86.

O'Neal, M.R., Frankenberger, J.R., Ess, D.R., 2000. Spatial precipitation variability in the choice of nitrogen fertilization rates. Proceedings of Fifth International Conference on Precision Agriculture (CD), Bloomington, MN, USA, American Society of Agronomy, pp.1-15.

Osborne, S.L., Schepers, J.S., Francis, D.D. and Schlemmer, M.R., 2002. Detection of phosphorus and nitrogen deficiencies in corn using spectral radiance measurements. Agronomy Journal, 94(6), pp.1215-1221.

Otter-Nacke, S., Godwin, D.C. and Richie, J.T., 1986. Testing and validating the CERES-Wheat model in diverse environments. US Department of Agriculture, Washington, D.C.

Ozdogan, M., 2010. The spatial distribution of crop types from MODIS data: Temporal unmixing using Independent Component Analysis. Remote Sensing of Environment, 114(6), pp.1190-1204.

Pampolino, M.F., Manguiat, I.J., Ramanathan, S., Gines, H.C., Tan, P.S., Chi, T.T.N., Rajendran, R. and Buresh, R.J., 2007. Environmental impact and economic benefits of site-specific nutrient management (SSNM) in irrigated rice systems. Agricultural Systems, 93(1), pp.1-24.

Panda, S.S., 2004. Data Mining Application in Production Management of Crop (Paper 1). Ph.D. Dissertation, North Dakota State University, Fargo, ND, USA.

Panda, S.S., Ames, D.P. and Panigrahi, S., 2010. Application of vegetation indices for agricultural crop yield prediction using neural network techniques. Remote Sensing, 2(3), pp.673-696.

Panda, S.S., Hoogenboom, G. and Paz, J.O., 2010. Remote sensing and geospatial technological applications for site-specific management of fruit and nut crops: a review. Remote Sensing, 2(8), pp.1973-1997.

Panda, S.S., M. Rao, P.S., Thenkabail, and J. Fitzgerald, 2015. Remote Sensing Satellites and Sensors: Optical, Radar, LiDAR, Microwave, Hyperspectral, and UAVs. 1st Chapter in Remote Sensing Handbook: Vol. I, II, and III, Ed P. S. Thenkabail. CRC Press: New York.

Panda, S.S., Panigrahi, S. and Ames, D.P., 2010. Crop yield forecasting from remotely sensed aerial images with self-organizing maps. Transactions of the ASABE, 53(2), pp.323-338.

Panda, S.S., Steele, D.D., Panigrahi, S. and Ames, D.P., 2011. Precision water management in corn using automated crop yield modeling and remotely sensed data. International Journal of Remote Sensing Applications, 1(1), pp.11-21.

Pask, A.J.D., Pietragalla, J., Mullan, D.M. and Reynolds, M.P., 2012. Physiological breeding II: a field guide to wheat phenotyping. Cimmyt, pp.1-131.

Pena-Barragan, J.M., Ngugi, M.K., Plant, R.E. and Six, J., 2011. Object-based crop identification using multiple vegetation indices, textural features and crop phenology. Remote Sensing of Environment, 115(6), pp.1301-1316.

Peng, S., Buresh, R.J., Huang, J., Zhong, X., Zou, Y., Yang, J., Wang, G., Liu, Y., Hu, R., Tang, Q. and Cui, K., 2010. Improving nitrogen fertilization in rice by site-specific N management. A review. Agronomy for Sustainable Development, 30(3), pp.649-656.

Peng, Y. and Gitelson, A.A., 2012. Remote estimation of gross primary productivity in soybean and maize based on total crop chlorophyll content. Remote Sensing of Environment, 117, pp.440-448.

Penuelas, J., Filella, I., Biel, C., Serrano, L. and Save, R., 1993. The reflectance at the 950–970 nm region as an indicator of plant water status. International Journal of Remote Sensing, 14(10), pp.1887-1905.

Penuelas, J., Filella, I., Serrano, L. and Save, R., 1996. Cell wall elasticity and water index (R970 nm/R900 nm) in wheat under different nitrogen availabilities. International Journal of Remote Sensing, 17(2), pp.373-382.

Penuelas, J., Pinol, J., Ogaya, R. and Filella, I., 1997. Estimation of plant water concentration by the reflectance water index WI (R900/R970). International Journal of Remote Sensing, 18(13), pp.2869-2875.

Porporato, A., Laio, F., Ridolfi, L. and Rodriguez-Iturbe, I., 2001. Plants in water-controlled ecosystems: active role in hydrologic processes and response to water stress: III. Vegetation water stress. Advances in Water Resources, 24(7), pp.725-744.

Prasad, A.K., Singh, R.P., Tare, V. and Kafatos, M., 2007. Use of vegetation index and meteorological parameters for the prediction of crop yield in India. International Journal of Remote Sensing, 28(23), pp.5207-5235.

Prasad, B., Carver, B.F., Stone, M.L., Babar, M.A., Raun, W.R. and Klatt, A.R., 2007. Genetic analysis of indirect selection for winter wheat grain yield using spectral reflectance indices. Crop science, 47(4), pp.1416-1425.

Prasad, K.A., Gnanappazham, L., Selvam, V., Ramasubramanian, R. and Kar, C.S., 2015. Developing a spectral library of mangrove species of Indian east coast using field spectroscopy. Geocarto International, 30(5), pp.580-599.

Prasannakumar, N.R., Chander, S. and Sahoo, R.N., 2014. Characterization of brown planthopper damage on rice crops through hyperspectral remote sensing under field conditions. Phytoparasitica, 42(3), pp.387-395.

Pu, R. and Gong, P., 2004. Wavelet transform applied to EO-1 hyperspectral data for forest LAI and crown closure mapping. Remote Sensing of Environment, 91(2), pp.212-224.

Ranjan, R., Sahoo, R.N., Chopra, U.K., Pramanik, M., Singh, A.K. and Pradhan, S., 2015. Assessment of water status in Wheat (Triticum aestivum L.) using ground based hyperspectral reflectance. Proceedings of the National Academy of Sciences, India Section B: Biological Sciences, pp.1-12

Rao, P.N. and Rao, V.R., 1987. Rice crop identification and area estimation using remotely-sensed data from Indian cropping patterns. International Journal of Remote Sensing, 8(4), pp.639-650.

Ray, S.S., Das, G., Singh, J.P. and Panigrahy, S., 2006. Evaluation of hyperspectral indices for LAI estimation and discrimination of potato crop under different irrigation treatments. International Journal of Remote Sensing, 27(24), pp.5373-5387.

Roberts, D.A., Smith, M.O. and Adams, J.B., 1993. Green vegetation, nonphotosynthetic vegetation, and soils in AVIRIS data. Remote Sensing of Environment, 44(2-3), pp.255-269.

Rokach, L. and Maimon, O., 2005. Clustering methods. In Data mining and knowledge discovery handbook, Springer US, pp. 321-352.

Rosenzweig, C., Iglesias, A., Yang, X.B., Epstein, P.R. and Chivian, E., 2001. Climate change and extreme weather events; implications for food production, plant diseases, and pests. Global change and human health, 2(2), pp.90-104.

Rumpf, T., Mahlein, A.K., Steiner, U., Oerke, E.C., Dehne, H.W. and Plümer, L., 2010. Early detection and classification of plant diseases with Support Vector Machines based on hyperspectral reflectance. Computers and Electronics in Agriculture, 74(1), pp.91-99.

Rumpf, T., Romer, C., Weis, M., Sökefeld, M., Gerhards, R. and Plümer, L., 2012. Sequential support vector machine classification for small-grain weed species discrimination with special regard to Cirsium arvense and Galium aparine. Computers and Electronics in Agriculture, 80, pp.89-96.

Sahu, G.C. and Mishra, A., 2005. Soil of Orissa and its management. Orissa Review, pp.56-60.

Sankaran, S., Mishra, A., Ehsani, R. and Davis, C., 2010. A review of advanced techniques for detecting plant diseases. Computers and Electronics in Agriculture, 72(1), pp.1-13.

Santi, E., Fontanelli, G., Montomoli, F., Brogioni, M., Macelloni, G., Paloscia, S., Pettinato, S. and Pampaloni, P., 2012. The retrieval and monitoring of vegetation parameters from COSMO-SkyMed images. Geoscience and Remote Sensing Symposium, IGARSS, IEEE, pp.7031-7034.

Sasao, A. and Shibusawa, S., 2000. Prospects and strategies for precision farming in Japan. JARQ, Japan Agricultural Research Quarterly, 34(4), pp.233-238.

Scharf, P.C., Kitchen, N.R., Sudduth, K.A., Davis, J.G., Hubbard, V.C. and Lory, J.A., 2005. Field-scale variability in optimal nitrogen fertilizer rate for corn. Agronomy Journal, 97(2), pp.452-461.

Scherr, S.J. and Satya Yadav, I.F.P.R.I., 1995. Land Degradation in the Developing World: Implications for Food, Agriculture, and the Environment to the Year 2020. International Food Policy Research Institute.

Schlemmer, M., Schepers, J.S., Ferguson, R.B., Peng, Y., and Shanahan, J., 2013. Remote estimation of nitrogen and chlorophyll contents in maize at leaf and canopy levels. International Journal of Applied Earth Observation and Geoinformation, 25, pp. 47–54.

Schmedtmann, J. and Campagnolo, M.L., 2015. Reliable crop identification with satellite imagery in the context of common agriculture policy subsidy control. Remote Sensing, 7(7), pp.9325-9346.

Schmidhalter, U., Maidl, F.X., Heuwinkel, H., Demmel, M., Auernhammer, H., Noack, P.O. and Rothmund, M., 2008. Precision farming–adaptation of land use management to small scale heterogeneity. In Perspectives for agroecosystem management (pp. 121-199).

Schmitter, P., Steinrücken, J., Römer, C., Ballvora, A., Léon, J., Rascher, U. and Plümer, L., 2017. Unsupervised domain adaptation for early detection of drought stress in hyperspectral images. ISPRS Journal of Photogrammetry and Remote Sensing, 131, pp.65-76.

Serrano, L., Filella, I. and Penuelas, J., 2000. Remote sensing of biomass and yield of winter wheat under different nitrogen supplies. Crop Science, 40(3), pp.723-731.

Shibusawa, S., 1998. Precision farming and terra-mechanics. Fifth ISTVS Asia-Pacific Regional Conference in Korea,

Shiu, Y.S., Lin, M.L., Huang, C.H. and Chu, T.H., 2012. Mapping paddy rice agriculture in a highly fragmented area using a geographic information system object-based post classification process. Journal of Applied Remote Sensing, 6(1), pp.55-67.

Sikuku, P.A., Netondo, G.W., Musyimi, D.M. and Onyango, J.C., 2010. Effects of water deficit on days to maturity and yield of three NERICA rainfed rice varieties. Journal of Agricultural and Biological Science, 5(3), pp.1-9.

Sims, D.A. and Gamon, J.A., 2002. Relationships between leaf pigment content and spectral reflectance across a wide range of species, leaf structures and developmental stages. Remote Sensing of Environment, 81(2), pp.337-354.

Song, S., Gong, W., Zhu, B. and Huang, X., 2011. Wavelength selection and spectral discrimination for paddy rice, with laboratory measurements of hyperspectral leaf reflectance. ISPRS Journal of Photogrammetry and Remote Sensing, 66(5), pp.672-682.

Srinivasan, A., 2006. Handbook of precision agriculture: principles and applications. New York, NY, USA, Food Products Press.

Stimson, H.C., Breshears, D.D., Ustin, S.L. and Kefauver, S.C., 2005. Spectral sensing of foliar water conditions in two co-occurring conifer species: Pinus edulis and Juniperus monosperma. Remote Sensing of Environment, 96(1), pp.108-118.

Stott, B.L., Borgelt, S.C. and Sudduth, K.A., 1993. Yield determination using an instrumented Claas combine. In American Society of Agricultural Engineers. Meeting (USA).

Strachan, I.B., Pattey, E. and Boisvert, J.B., 2002. Impact of nitrogen and environmental conditions on corn as detected by hyperspectral reflectance. Remote Sensing of Environment, 80(2), pp.213-224.

Stroppiana, D., Boschetti, M., Brivio, P.A. and Bocchi, S., 2009. Plant nitrogen concentration in paddy rice from field canopy hyperspectral radiometry. Field crops research, 111(1), pp.119-129.

Stroppiana, D., Boschetti, M., Confalonieri, R., Bocchi, S. and Brivio, P.A., 2006. Evaluation of LAI-2000 for leaf area index monitoring in paddy rice. Field Crops Research, 99(2), pp.167-170.

Suarez, L., Zarco-Tejada, P.J., Berni, J.A.J., Gonzalez-Dugo, V. and Fereres, E., 2009. Modelling PRI for water stress detection using radiative transfer models. Remote Sensing of Environment, 113(4), pp.730-744.

Suarez, L., Zarco-Tejada, P.J., González-Dugo, V., Berni, J.A.J., Sagardoy, R., Morales, F. and Fereres, E., 2010. Detecting water stress effects on fruit quality in orchards with time-series PRI airborne imagery. Remote Sensing of Environment, 114(2), pp.286-298.

Swain, K.C. and Zaman, Q.U., 2012. Rice crop monitoring with unmanned helicopter remote sensing images. In Remote Sensing of Biomass-Principles and Applications. InTech.

Tackenberg, O., 2007. A new method for non-destructive measurement of biomass, growth rates, vertical biomass distribution and dry matter content based on digital image analysis. Annals of Botany, 99(4), pp.777-783.

Tang, Y.L., Huang, J.F., Cai, S.H. and Wang, R.C., 2007. Nitrogen contents of rice panicle and paddy by hyperspectral remote sensing. Pakistan journal of biological sciences: PJBS, 10(24), pp.4420-4425.

Tennakoon, S.B., Murty, V.V.N. and Eiumnoh, A., 1992. Estimation of cropped area and grain yield of rice using remote sensing data. International Journal of Remote Sensing, 13(3), pp.427-439.

Thenkabail, P.S., Enclona, E.A., Ashton, M.S. and Van Der Meer, B., 2004. Accuracy assessments of hyperspectral waveband performance for vegetation analysis applications. Remote Sensing of Environment, 91(3), pp.354-376.

Thenkabail, P.S., Smith, R.B. and De Pauw, E., 2000. Hyperspectral vegetation indices and their relationships with agricultural crop characteristics. Remote Sensing of Environment, 71(2), pp.158-182.

Thomas, J.R. and Gausman, H.W., 1977. Leaf reflectance vs. leaf chlorophyll and carotenoid concentrations for eight crops. Agronomy Journal, 69(5), pp.799-802.

Tian, G., Gao, L., Kong, Y., Hu, X., Xie, K., Zhang, R., Ling, N., Shen, Q. and Guo, S., 2017. Improving rice population productivity by reducing nitrogen rate and increasing plant density. PLOS One, 12(8), pp.1-18.

Tian, L., J.F. Reid, and J.W. Hummel, 1999. Development of a precision sprayer for site-specific weed management, Transactions of the American Society of Agricultural Engineers, 42(4), pp.893–900.

Tian, Y., Zhu, Y. and Cao, W., 2004. Relationship between canopy reflectance and plant water status of wheat. The Journal of Applied Ecology, 15(11), pp.2072-2076.

Tian, Y.C., Yao, X., Yang, J., Cao, W.X., Hannaway, D.B. and Zhu, Y., 2011. Assessing newly developed and published vegetation indices for estimating rice leaf nitrogen concentration with ground-and space-based hyperspectral reflectance. Field Crops Research, 120(2), pp.299-310.

Tilling, A.K., O'Leary, G.J., Ferwerda, J.G., Jones, S.D., Fitzgerald, G.J., Rodriguez, D. and Belford, R., 2007. Remote sensing of nitrogen and water stress in wheat. Field Crops Research, 104(1), pp.77-85.

Tripathi, R., Sahoo, R.N., Gupta, V.K., Sehgal, V.K. and Sahoo, P.M., 2013. Developing Vegetation Health Index from biophysical variables derived using MODIS satellite data in the Trans-Gangetic plains of India. Emirates Journal of Food and Agriculture, 25(5), pp.376-384.

Tucker C. J., 1978. A comparison of satellite sensors for monitoring vegetation. Photogrammetric Engineering and Remote Sensing, 44, pp.1369–1380.

Tucker, C.J., 1980. Remote sensing of leaf water content in the near infrared. Remote Sensing of Environment, 10(1), pp.23-32.

Tucker, C.J., Holben, B.N., Elgin Jr, J.H. and McMurtrey III, J.E., 1980. Relationship of spectral data to grain yield variation. Photogrammetric Engineering and Remote Sensing, 46(5), pp.657-666.

Ullah, S., Schlerf, M., Skidmore, A.K. and Hecker, C., 2012. Identifying plant species using mid-wave infrared (2.5–6μm) and thermal infrared (8–14μm) emissivity spectra. Remote Sensing of Environment, 118, pp.95-102.

Ustin, S.L., Riano, D. and Hunt, E.R., 2012. Estimating canopy water content from spectroscopy. Israel Journal of Plant Sciences, 60(1-2), pp.9-23.

Ustin, S.L., Roberts, D.A., Gardner, M. and Dennison, P., 2002. Evaluation of the potential of Hyperion data to estimate wildfire hazard in the Santa Ynez Front Range, Santa Barbara, California. Geoscience and Remote Sensing Symposium, IEEE, 2, pp.796-798. .

Venuprasad, R., Bool, M.E., Quiatchon, L., Cruz, M.S., Amante, M. and Atlin, G.N., 2012. A large-effect QTL for rice grain yield under upland drought stress on chromosome 1. Molecular Breeding, 30(1), pp.535-547.

Verrelst, J., Camps-Valls, G., Muñoz-Marí, J., Rivera, J.P., Veroustraete, F., Clevers, J.G. and Moreno, J., 2015. Optical remote sensing and the retrieval of terrestrial vegetation bio-geophysical properties–A review. ISPRS Journal of Photogrammetry and Remote Sensing, 108, pp.273-290.

Vohland, M., Mader, S. and Dorigo, W., 2010. Applying different inversion techniques to retrieve stand variables of summer barley with PROSPECT+ SAIL. International Journal of Applied Earth Observation and Geoinformation, 12(2), pp.71-80.

Vrindts, E., Reyniers, M., Darius, P., Gilot, M., Sadaoui, Y., Frankinet, M., Hanquet, B. and Destain, M.F., 2003. Analysis of soil and crop properties for precision agriculture for winter wheat. Biosystems engineering, 85(2), pp.141-152.

Vyas, D., Christian, B. and Krishnayya, N.S.R., 2013. Canopy level estimations of chlorophyll and LAI for two tropical species (teak and bamboo) from Hyperion (EO-1) data. International Journal of Remote Sensing, 34(5), pp.1676-1690.

Vyas, D., Krishnayya, N.S.R., Manjunath, K.R., Ray, S.S. and Panigrahy, S., 2011. Evaluation of classifiers for processing Hyperion (EO-1) data of tropical vegetation. International Journal of Applied Earth Observation and Geoinformation, 13(2), pp.228-235.

Wade, L.J., McLaren, C.G., Quintana, L., Harnpichitvitaya, D., Rajatasereekul, S., Sarawgi, A.K., Kumar, A., Ahmed, H.U., Singh, A.K., Rodriguez, R. and Siopongco, J., 1999. Genotype by environment interactions across diverse rainfed lowland rice environments. Field Crops Research, 64(1), pp.35-50.

Wang, D., Wang, J. and Liang, S., 2010. Retrieving crop leaf area index by assimilation of MODIS data into a crop growth model. Science China Earth Sciences, 53(5), pp.721-730.

Wang, G., Zhang, Q.C., Witt, C. and Buresh, R.J., 2007. Opportunities for yield increases and environmental benefits through site-specific nutrient management in rice systems of Zhejiang province, China. Agricultural Systems, 94(3), pp.801-806.

Wang, L. and Qu, J.J., 2007. NMDI: A normalized multi-band drought index for monitoring soil and vegetation moisture with satellite remote sensing. Geophysical Research Letters, 34(20), pp.1-5.

Wang, W., Yao, X., Yao, X., Tian, Y., Liu, X., Ni, J., Cao, W. and Zhu, Y., 2012. Estimating leaf nitrogen concentration with three-band vegetation indices in rice and wheat. Field Crops Research, 129, pp.90-98.

Wang, X., Zhao, C., Guo, N., Li, Y., Jian, S. and Yu, K., 2015. Determining the canopy water stress for spring wheat using canopy hyperspectral reflectance data in loess plateau semiarid regions. Spectroscopy Letters, 48(7), pp.492-498.

Wang, Z., Skidmore, A.K., Wang, T., Darvishzadeh, R., Heiden, U., Heurich, M., Latifi, H. and Hearne, J., 2017. Canopy foliar nitrogen retrieved from airborne hyperspectral imagery by correcting for canopy structure effects. International Journal of Applied Earth Observation and Geoinformation, 54, pp.84-94.

Wardlow, B.D., Egbert, S.L. and Kastens, J.H., 2007. Analysis of time-series MODIS 250 m vegetation index data for crop classification in the US Central Great Plains. Remote Sensing of Environment, 108(3), pp.290-310.

Whelan, B.M. and McBratney, A.B., 2002. A parametric transfer function for grain-flow within a conventional combine harvester. Precision Agriculture, 3(2), pp.123-134.

Whelan, B.M., mcbratney, A.B., Boydell, B.C., 1997. The Impact of Precision Agriculture. Proceedings of the ABARE Outlook Conference, The Future of Cropping in NW NSW, Moree, UK, pp.5

Wiegand, C., Anderson, G., Lingle, S. and Escobar, D., 1996. Soil salinity effects on crop growth and yield-Illustration of an analysis and mapping methodology for sugarcane. Journal of Plant Physiology, 148(3-4), pp.418-424.

Wiegand, C.L., Rhoades, J.D., Escobar, D.E. and Everitt, J.H., 1994. Photographic and videographic observations for determining and mapping the response of cotton to soil salinity. Remote Sensing of Environment, 49(3), pp.212-223.

Wiseman, G., McNairn, H., Homayouni, S. and Shang, J., 2014. RADARSAT-2 polarimetric SAR response to crop biomass for agricultural production monitoring. Journal of Selected Topics in Applied Earth Observations and Remote Sensing, IEEE, 7(11), pp.4461-4471.

Wu, C., Niu, Z., Tang, Q. and Huang, W., 2008. Estimating chlorophyll content from hyperspectral vegetation indices: Modeling and validation. Agricultural and Forest Meteorology, 148(8), pp.1230-1241.

Wu, W.B., Peng, Y., Tang, H.J., Zhou, Q.B., Chen, Z.X. and Shibasaki, R., 2010. Characterizing spatial patterns of phenology in cropland of China based on remotely sensed data. Agricultural Sciences in China, 9(1), pp.101-112.

Xiao, X., Boles, S., Frolking, S., Li, C., Babu, J.Y., Salas, W. and Moore, B., 2006. Mapping paddy rice agriculture in South and Southeast Asia using multi-temporal MODIS images. Remote Sensing of Environment, 100(1), pp.95-113.

Xie, G.D., Chen, S.B., Qi, W.H., Lu, Y., Yang, X.W. and Liu, C.L., 2003. A multidisciplinary and integrated study of rice precision farming. Chinese Geographical Science, 13(1), pp.9-14.

Xu, H.R., Ying, Y.B., Fu, X.P. and Zhu, S.P., 2007. Near-infrared spectroscopy in detecting leaf miner damage on tomato leaf. Biosystems Engineering, 96(4), pp.447-454.

Xu, X., Gu, X., Song, X., Li, C. and Huang, W., 2010. Assessing rice chlorophyll content with vegetation indices from hyperspectral data. In International Conference on Computer and Computing Technologies in Agriculture, Springer, Berlin, Heidelberg, pp.296-303.

Yan, L. and Roy, D.P., 2014. Automated crop field extraction from multi-temporal Web Enabled Landsat Data. Remote Sensing of Environment, 144, pp.42-64.

Yang, C., Everitt, J.H. and Murden, D., 2011. Evaluating high resolution SPOT 5 satellite imagery for crop identification. Computers and Electronics in Agriculture, 75(2), pp.347-354.

Yang, C.M. and Chen, R.K., 2004. Modeling rice growth with hyperspectral reflectance data. Crop Science, 44(4), pp.1283-1290.

Yang, H., Chen, E., Li, Z., Yang, G., Xu, X., Yuan, L., Feng, Q. and Zhao, L., 2014, August. Capability of multi-temporal Radarsat-2 data in monitoring canola crop and its plant height. Agro-geoinformatic, Third International Conference, IEEE, pp. 1-5.

Yang, X., Yu, Y. and Fan, W., 2015. Chlorophyll content retrieval from hyperspectral remote sensing imagery. Environmental Monitoring and Assessment, 187(7), pp.1-13.

Yi, Q.X., Huang, J.F., Wang, F.M., Wang, X.Z. and Liu, Z.Y., 2007. Monitoring rice nitrogen status using hyperspectral reflectance and artificial neural network. Environmental science and Technology, 41(19), pp.6770-6775.

Yim, O. and Ramdeen, K.T., 2015. Hierarchical cluster analysis: comparison of three linkage measures and application to psychological data. Quant. Methods. Psychol, 11, pp.8-21.

Zarco-Tejada, P.J., Berjon, A., López-Lozano, R., Miller, J.R., Martín, P., Cachorro, V., González, M.R. and De Frutos, A., 2005. Assessing vineyard condition with hyperspectral indices: Leaf and canopy reflectance simulation in a row-structured discontinuous canopy. Remote Sensing of Environment, 99(3), pp.271-287.

Zarco-Tejada, P.J., González-Dugo, V. and Berni, J.A., 2012. Fluorescence, temperature and narrow-band indices acquired from a UAV platform for water stress detection using a micro-hyperspectral imager and a thermal camera. Remote Sensing of Environment, 117, pp.322-337.

Zarco-Tejada, P.J., Miller, J.R., Morales, A., Berjon, A. and Agüera, J., 2004. Hyperspectral indices and model simulation for chlorophyll estimation in open-canopy tree crops. Remote Sensing of Environment, 90(4), pp.463-476.

Zarco-Tejada, P.J., Miller, J.R., Noland, T.L., Mohammed, G.H. and Sampson, P.H., 2001. Scaling-up and model inversion methods with narrowband optical indices for chlorophyll content estimation in closed forest canopies with hyperspectral data. Transactions on Geoscience and Remote Sensing, IEEE, 39(7), pp.1491-1507.

Zarco-Tejada, P.J., Rueda, C.A. and Ustin, S.L., 2003. Water content estimation in vegetation with MODIS reflectance data and model inversion methods. Remote Sensing of Environment, 85(1), pp.109-124.

Zhang, C. and Kovacs, J.M., 2012. The application of small unmanned aerial systems for precision agriculture: a review. Precision agriculture, 13(6), pp.693-712.

Zhang, H., Han, M., Chávez, J.L. and Lan, Y., 2017. Improvement in estimation of soil water deficit by integrating airborne imagery data into a soil water balance model. International Journal of Agricultural and Biological Engineering, 10(3), pp.37-46.

Zhang, N., Wang, M. and Wang, N., 2002. Precision agriculture—a worldwide overview. Computers and electronics in agriculture, 36(2-3), pp.113-132.

Zhang, Q., Li, Q. and Zhang, G., 2012. Rapid determination of leaf water content using VIS/NIR spectroscopy analysis with wavelength selection. Journal of Spectroscopy, 27(2), pp.93-105.

Zhang, Y., Chen, J.M., Miller, J.R. and Noland, T.L., 2008. Leaf chlorophyll content retrieval from airborne hyperspectral remote sensing imagery. Remote Sensing of Environment, 112(7), pp.3234-3247.

Zhao, D., Huang, L., Li, J. and Qi, J., 2007. A comparative analysis of broadband and narrowband derived vegetation indices in predicting LAI and CCD of a cotton canopy. ISPRS Journal of Photogrammetry and Remote Sensing, 62(1), pp.25-33.

Zhao, D., Reddy, K.R., Kakani, V.G. and Reddy, V.R., 2005. Nitrogen deficiency effects on plant growth, leaf photosynthesis, and hyperspectral reflectance properties of sorghum. European Journal of Agronomy, 22(4), pp.391-403.

Zhao, G., Miao, Y., Wang, H., Su, M., Fan, M., Zhang, F., Jiang, R., Zhang, Z., Liu, C., Liu, P. and Ma, D., 2013. A preliminary precision rice management system for increasing both grain yield and nitrogen use efficiency. Field crops research, 154, pp.23-30.

Zhu, Y., Yao, X., Tian, Y., Liu, X. and Cao, W., 2008. Analysis of common canopy vegetation indices for indicating leaf nitrogen accumulations in wheat and rice. International Journal of Applied Earth Observation and Geoinformation, 10(1), pp.1-10.

Zhu, Y., Zhou, D., Yao, X., Tian, Y. and Cao, W., 2007. Quantitative relationships of leaf nitrogen status to canopy spectral reflectance in rice. Australian Journal of Agricultural Research, 58(11), pp.1077-1085.

Zygielbaum, A.I., Gitelson, A.A., Arkebauer, T.J. and Rundquist, D.C., 2009. Non-destructive detection of water stress and estimation of relative water content in maize. Geophysical Research Letters, 36(12), pp.1-4.

Publications

Journals

- Moharana S., and Dutta S. (2018) 'Estimation of water stress variability for a rice agriculture system from space-borne hyperion imagery', Agricultural Water Management, 213:260-269.
- Moharana, S., and Dutta S. (2016) 'Spatial variability of chlorophyll and nitrogen content of rice from hyperspectral imagery', ISPRS Journal of Photogrammetry and Remote Sensing, 122:17-29.
- Moharana S., Medhi H., and Dutta S. (2016) 'Advanced vegetation indices for sensing paddy growth via hyperspectral measurements', Geocarto International, 1:1-18.
- Moharana S., and Dutta S. (2014) 'Hyperspectral remote sensing of paddy crop using in-situ measurement and clustering technique', International Archives of the Photogrammetry, Remote Sensing and Spatial Information Sciences, 8:845-851.
- Moharana S., and Dutta S. (2018) 'Fusion of hyperspectral and high spatial resolution multispectral imagery for paddy crop parameters variability mapping at plot scale', Remote Sensing of Environment, (Under Review).
- Moharana S., and Dutta S. (2017) 'Estimating chlorophyll content of paddy crop through hyperspectral techniques, Journal of Spatial Science, (Under Review).
- Moharana S., and Dutta S. (2017) 'A Review on Hyperspectral Remote Sensing Applications to retrieve crop nutrient and pigments for major crops in India. (In preparation).

Conferences

- Moharana S., Dutta S., Chandna P.K., (2018). 'Assessing the spatial variability of crop nitrogen and water content using advanced techniques of hyperspectral remote sensing', 5th International Rice Congress (IRC-2018), October 14–17, Marina Bay Sands, Singapore.

- Moharana S., and Dutta S. (2017). 'Mapping of biophysical parameters of rice agriculture system from hyperspectral imagery', European Geosciences Union (EGU)-General Assembly 2017, April 23–28, Vienna, Austria.

- Moharana S., and Dutta S. (2017). 'Non-destructive measurement of nitrogen and chlorophyll content in Indian rice varieties', International Symposium on Plant Biotechnology for Crop Improvement, January 20-21, IIT Guwahati, India.

- Moharana S., and Dutta S. (2016). 'Capability of Hyperspectral data in Spatial Variability Distribution of Chlorophyll and Water Stress in Rice Agriculture System', American Geophysical Union (AGU) Fall Meeting- 2016, December 12-16, San Francisco, California, USA.

- Moharana S., and Dutta S. (2016). 'Mapping of chlorophyll and nitrogen of paddy crop from hyperspectral imagery', National Symposium on Recent Advances in Remote Sensing and GIS with Special Emphasis on Mountain Ecosystems and Annual conventions of & Indian Society of Remote Sensing & Indian Society of Geomatics, Dec 7-9, Dehradun, India.

- Moharana S., and Dutta S. (2015). 'Application of hyperspectral data in spatial variability distribution of paddy field', National Symposium on Geomatics for Digital India and Annual conventions of Indian Society of Geomatics & Indian Society of Remote Sensing Engineering, Dec 16-18, JK Lakshmipat University, Jaipur, Rajasthan,India.

- Moharana S., and Dutta S. (2015). 'Field variation mapping of paddy crop from space borne hyperspectral data using clustering technique', International Conference on Hydraulics and water resources, HYDRO-2015, Dec 17-19, IIT Roorkee, India.

- Moharana S., and Dutta S. (2014). 'Hyperspectral remote sensing of paddy crop using in-situ measurement and clustering technique', ISPRS Technical Commission VIII Symposium, (ISPRS-2014) Dec 9-12, Hyderabad, India.

- Moharana S., and Dutta S. (2014). 'Waveform classification approach on hyperspectral measurements of paddy crop', National Conference on Emerging technology trends in Agricultural Engineering (ETTAE-2014), Nov 7-8, NERIST, Nirjuli, Arunachal Pradesh.

- Moharana S., and Dutta S. (2013). 'New vegetation indices for monitoring paddy growth using hyperspectral measurements', National Symposium on remote sensing and GIS for environment with special emphasis on marine and coastal dynamics, Dec 4-6, Andhra University, Visakhapatnam.